

Dissertation ETH No. 15529

# **Generic Approaches to Risk Based Inspection Planning for Steel Structures**

A dissertation submitted to the  
SWISS FEDERAL INSTITUTE OF TECHNOLOGY ZÜRICH  
for the degree of  
Doctor of Technical Sciences

presented by

Daniel Straub  
Dipl. Bau-Ing. ETH  
born 30 November 1975  
citizen of Egnach TG

accepted on the recommendation of

Prof. Dr. Michael Havbro Faber, examiner  
Prof. Ton Vrouwenvelder, co-examiner

2004



## Preface

This work would not have been possible without the support of many individuals.

Prof. Dr. Michael H. Faber initiated this work and motivated me to conduct research in the area of risk and reliability. He has been a most inspiring teacher and motivating leader. His exceptional support throughout the project, both technically and personally, is highly appreciated.

In 2001, Dr. Jean Goyet offered me the opportunity to work for half a year in an industrial context at Bureau Veritas in Paris. I am especially thankful for his friendship and for him sharing his vast experience with me during extensive discussions over many lunches and coffees.

To Prof. Ton Vrouwenvelder of TU Delft I express my thanks for acting as a referee. He and many others I met professionally during this period provided important input to this work through common discussions; in particular the open atmosphere I encountered at most of the scientific meetings in which I participated was highly inspiring and motivating.

My colleagues at the university should not only take credit for their technical support, but moreover for providing a familiar, amicable atmosphere at the office. It is their achievement that working over these last years never became a mere duty.

Finally I want to thank all my friends and especially my family and Tina for their support and sympathy throughout the duration of this work and for their constant efforts to keep me from turning into a total recluse – especially in the later stages. This work is dedicated to them.

Daniel Straub

Zürich, April 2004



## Abstract

Steel structures are subject to deterioration processes such as fatigue crack growth or corrosion. The models describing these processes often contain major uncertainties, which can be reduced through inspections. By providing information on the actual state of the structure, inspections facilitate the purposeful application of repair actions. In doing so, inspections represent an effective risk mitigation measure, for existing structures often the only feasible one.

Risk based inspection planning (RBI) provides the means for quantifying the effect of inspections on the risk and thus for identifying cost optimal inspection strategies. By combining the Bayesian decision analysis with structural reliability analysis, RBI uses the available probabilistic models of the deterioration processes and the inspection performances to present a consistent decision basis. Although the principles of RBI were formulated for fatigue deterioration in the early 1990s, its application has in the past been limited to relatively few industrial projects. The complexity of the approach, combined with the required numerical efforts, has hindered its implementation in an efficient software tool and thus its integration into the general asset integrity management procedures of the owners and operators of structures. These drawbacks have motivated the development of generic approaches to RBI.

The main idea of the generic approaches is to perform the demanding probability calculations for generic representations of structural details. Based on these “generic inspection plans”, the optimal inspection plans for a particular structure are obtained by means of an interpolation algorithm from simple indicators of the considered deterioration process. Because these indicators are obtained from standard design calculations and specifications, the application of RBI is greatly simplified once the generic inspection plans are calculated.

In this work, the generic approaches to RBI are developed together with the tools required for their implementation in an industrial context. This includes a presentation of the general RBI methodology, a review of the probabilistic deterioration models for fatigue and corrosion of steel structures and the description of inspection performance models. Whereas most of these aspects are well established for fatigue subjected structures, new concepts are introduced for the treatment of corrosion deterioration. A framework for the generic modelling is developed and the application is demonstrated on two examples for fatigue and corrosion. Various aspects of the implementation are presented, including the development of a software tool.

The generic approaches, due to their computational efficiency, facilitate the integral treatment of structural systems, as opposed to the traditional RBI approaches which focus on individual details. These “system effects” are investigated and it is demonstrated how the inspection efforts can be optimised for entire systems. Additionally a consistent framework is established for the determination of risk acceptance criteria related to inspection planning for structural systems. These system orientated developments ensure that the generic approaches to RBI, which have already demonstrated their efficiency in practical applications, are fully consistent with the objectives of the owners and operators of structures.

# Zusammenfassung

Stahlbauten unterliegen Schädigungsprozessen wie Ermüdung oder Korrosion. Modelle, die diese Prozesse beschreiben, beinhalten oft grosse Unsicherheiten, welche nur durch Inspektionen reduziert werden können. Diese liefern Informationen über den wirklichen Zustand des Bauwerks und erleichtern so die zielgerichtete Anwendung von Unterhaltmassnahmen. Auf diese Weise stellen Inspektionen eine wirksame Massnahme zur Risikoreduktion dar, für bestehende Bauwerke sogar oft die einzig mögliche.

Risikobasierte Inspektionsplanung (RBI) ermöglicht es, den Einfluss von Inspektionen auf das Risiko zu quantifizieren und damit kostenoptimale Inspektionsstrategien zu identifizieren. RBI kombiniert die Bayes'sche Entscheidungstheorie mit den Methoden der strukturellen Zuverlässigkeitsanalyse. Dadurch erlaubt sie es, probabilistische Modelle von Schädigungsprozessen und der Qualität von Inspektionen zu verwenden, um eine konsistente Entscheidungsbasis zu schaffen. Obschon die Grundlagen von RBI für ermüdungsbeanspruchte Bauwerke bereits vor 15 Jahren formuliert wurden, war ihre Verbreitung in der Praxis stark eingeschränkt, was hauptsächlich auf die Komplexität der Methode und numerische Schwierigkeiten zurückzuführen ist. Diese haben die effiziente Umsetzung der Methode in eine Software verhindert und damit auch die Integration in das Unterhaltsmanagement der Bauwerksbetreiber. Diese Nachteile der bestehenden Methoden haben die Entwicklung von generischen Ansätzen zu RBI motiviert.

Die Grundidee der generischen Ansätze ist, die aufwendigen Zuverlässigkeitsberechnungen für generische Bauteile durchzuführen. Basierend auf diesen „generischen Inspektionsplänen“ werden die Inspektionspläne für spezifische Bauteile mit Hilfe eines Interpolationsverfahrens bestimmt. Weil die Bauteile dabei mit einfachen Indikatoren beschrieben werden, welche aus normalen Bemessungsverfahren resultieren, wird die Anwendung von RBI stark vereinfacht.

In dieser Arbeit werden die generischen Ansätze zu RBI ausgearbeitet und die für eine Umsetzung benötigten Hilfsmittel und Regeln entwickelt. Dies beinhaltet eine Darstellung der allgemeinen RBI Methodik, eine Zusammenfassung der probabilistischen Schädigungsmodelle für Stahlbauwerke und die Beschreibung von Modellen für die Insektionsqualität. Während für Ermüdungsbeanspruchung viele dieser Ansätze bereits etabliert sind, werden für korrosionsbeanspruchte Bauwerke neue Modelle entwickelt. Die generische Modellierung wird eingeführt und an zwei Beispielen demonstriert. Verschiedene Aspekte der Umsetzung werden behandelt, unter anderen die Entwicklung einer Software.

Aufgrund ihrer Recheneffizienz erleichtern die generischen Ansätze die gesamtheitliche Betrachtung von Bauwerkssystemen, im Gegensatz zu den traditionellen RBI Ansätzen, welche sich auf einzelne Bauteile beschränken. Diese „System-Effekte“ werden untersucht und es wird gezeigt, wie der Inspektionsaufwand für Systeme optimiert werden kann. Zudem wird eine konsistente Grundlage entwickelt für die Bestimmung von akzeptierbaren Risiken im Zusammenhang mit der Planung von Inspektionen. Diese Erweiterungen der Methodik in Richtung Systeme stellt sicher, dass die generischen Ansätze zu RBI, welche ihre Effizienz in der Praxis bereits bewiesen haben, vollständig konsistent mit den Zielen der Bauwerksbetreiber sind.

# Table of Contents

<b>1</b>	<b>Introduction</b>	
1.1	Relevance .....	1
1.2	Outline .....	2
1.3	Scope of work .....	4
1.4	Thesis overview .....	5
<b>2</b>	<b>Risk based inspection planning</b>	
2.1	Introduction .....	7
2.2	Probabilities of events and structural reliability analysis .....	7
2.2.1	Probability of failure .....	7
2.2.2	Probabilities of inspection outcomes .....	9
2.2.3	Intersection of probabilities .....	9
2.2.4	Probability updating .....	10
2.2.5	Time-dependent reliability problems .....	11
2.2.6	Computation of probabilities .....	13
2.3	Decision analysis .....	13
2.3.1	Decisions under uncertainty .....	13
2.3.2	Utility theory .....	14
2.3.3	Bayesian decision analysis .....	15
2.3.4	Classical Bayesian prior and posterior decision analysis .....	15
2.3.5	Classical Bayesian pre-posterior analysis .....	16
2.4	Maintenance and inspection optimisation .....	20
2.4.1	Expected cost of an inspection strategy .....	22
2.4.2	Optimisation procedure .....	27
2.5	Reliability based inspection planning .....	30
2.6	RBI for corrosion subjected structures .....	30
<b>3</b>	<b>Deterioration modelling</b>	
3.1	Introduction .....	33
3.2	Fatigue (SN model) .....	33
3.2.1	Introduction .....	33
3.2.2	Hot spots .....	34
3.2.3	SN curves .....	35
3.2.4	Damage accumulation (Palmgren-Miner) .....	39
3.2.5	Fatigue loading .....	40
3.2.6	Uncertainties in design fatigue calculations .....	42

3.3	Modelling the fatigue crack growth (FM model)	45
3.3.1	Introduction	45
3.3.2	Crack initiation	46
3.3.3	Crack propagation	51
3.3.4	Failure and fracture	55
3.4	Calibration of the FM to the SN model	57
3.4.1	Applied calibration algorithm	59
3.5	Corrosion	61
3.5.1	Introduction	61
3.5.2	Corrosion phenomena	61
3.5.3	Corrosion modelling	64
3.5.4	Uncertainties in corrosion modelling	70
3.5.5	Corrosion protection	71
3.5.6	Failure modes	73
3.6	Corrosion fatigue	75
3.6.1	Reliability analysis	76
<b>4</b>	<b>Inspection modelling</b>	
4.1	Introduction	77
4.2	Inspection performance models	78
4.2.1	Probability of detection ( <i>PoD</i> )	78
4.2.2	Probability of false indications	79
4.2.3	Probability of indication	79
4.2.4	Accuracy of defect sizing	80
4.2.5	Inspection performance models as likelihood functions	81
4.3	Derivation of inspection performance models	81
4.3.1	The ICON project	81
4.3.2	Statistical inference of the parameters	81
4.3.3	Numerical examples and investigations	81
4.4	Limit state functions for inspection modelling	84
4.4.1	Indication event	84
4.4.2	Crack size measurement	85
4.5	Uncertainty in the inspection performance models	85
4.5.1	Sources of uncertainty	85
4.5.2	Probabilistic <i>PoD</i> formulation	86
4.5.3	Influence of the <i>PoD</i> uncertainty on the reliability updating	87
4.6	Modelling the dependencies between individual inspections	87
4.7	Modelling inspections for corrosion control	88
4.7.1	Example inspection performance model for corrosion subjected structures	89
4.7.2	Reliability updating for structures subject to localised corrosion based on measurements	90



## 5 Generic modelling

5.1	Introduction .....	95
5.2	Definitions .....	97
5.3	Computational aspects .....	99
5.3.1	Calculation of the generic inspection plans .....	100
5.3.2	Format of the generic inspection plans .....	100
5.3.3	Application of the generic inspection plans using iPlan.xls .....	102
5.3.4	Interpolation procedure .....	102
5.4	Determination of the generic representations .....	102
5.5	Generic modelling for fatigue .....	103
5.5.1	Generic parameters in the SN fatigue analysis .....	104
5.5.2	Generic parameters in the crack growth model .....	109
5.5.3	Summary of the model .....	110
5.5.4	Inspection model for the numerical investigations .....	112
5.5.5	Cost model for the numerical investigations .....	113
5.5.6	Results for the reference case .....	114
5.5.7	Results of the sensitivity analysis and determination of the generic representations .....	116
5.5.8	Derivation of the generic database .....	130
5.5.9	Verification of the generic database .....	131
5.5.10	Actualisation of inspection plans .....	135
5.5.11	Accounting for modifications in the fatigue loading .....	136
5.6	Generic modelling for corrosion .....	140
5.6.1	Generic approach to RBI for pipelines subject to CO <sub>2</sub> corrosion .....	141
5.6.2	Example results .....	144
5.6.3	Actualisation of inspection plans .....	150
5.6.4	Conclusions on the generic approach to RBI for corrosion subjected structures ...	153

## 6 Risk based inspection planning for structural systems

6.1	Introduction .....	155
6.2	System effects in RBI .....	155
6.2.1	Types of dependencies between hot spots .....	155
6.2.2	Interference from inspection results at other hot spots .....	158
6.3	RBI for systems .....	158
6.4	RBI for systems based on the generic approach .....	161
6.5	Considering system effects through the system PoD .....	164
6.6	Implementation of RBI for systems in practical applications .....	166
6.6.1	Comments on the proposed approach .....	169
6.7	Discussion .....	169

**7 Risk acceptance criteria**

7.1 Introduction .....	171
7.2 Acceptance criteria derived directly for individual hot spots .....	172
7.2.1 Risk acceptance criteria explicitly specified .....	172
7.2.2 Risk acceptance criteria derived directly from codes .....	173
7.3 System approach to acceptance criteria for individual hot spots .....	174
7.3.1 Risk acceptance criteria for collapse of the structure .....	175
7.3.2 Risk acceptance criteria for the individual hot spots based on a system model ....	177
7.4 Integration of the different approaches .....	181
7.4.1 Calibration of the system approach to the code requirements .....	182
7.5 Conclusions .....	184

**8 Conclusions and outlook**

8.1 Conclusions .....	187
8.1.1 Originality of work .....	188
8.1.2 Limitations .....	189
8.2 Outlook .....	190
8.2.1 On the probabilistic models .....	190
8.2.2 On the RBI procedures .....	191
8.2.3 On the application and validation .....	192

**Annexes**

A Analytical solutions for the expected SN damage when the stress ranges are represented by a Weibull distribution .....	193
B Comparing different crack propagation models .....	195
C Accuracy of the Monte Carlo simulation .....	207
D iPlan.xls .....	213
E Interpolation of inspection plans .....	219
F Nomenclature .....	223

<b>References</b> .....	229
-------------------------	-----

# 1 Introduction

## 1.1 Relevance

The deterioration of steel structures is a major source of cost to the public. Uhlig (1949) estimated the annual cost of corrosion (a large part of which is attributed to steel structures) in the US as 5.5 billion US\$. Half a century later, the direct annual cost of corrosion in the US is assessed in Koch et al. (2001) as 276 billion US\$, which represents 3.1% of the gross national product (GNP); 121 billion US\$ thereof is attributed to corrosion control. It is estimated that the indirect costs are in the same order of magnitude. The part of the cost that can be reduced by optimisation of design, operation and maintenance is difficult to quantify, but both references conclude that the economy and the government are still far from implementing optimal corrosion control practices. A similar study, published in 1983, indicates that the total cost of fatigue and fracture to the US economy is about 4 percent of the GNP, see Stephens et al. (2001). It is again stated that these costs could be significantly reduced by proper design and maintenance.

To reduce the cost of deterioration or, in other words, to optimise the life-cycle cost of structures, a balance must be achieved between the benefit of risk reduction (through improved design and maintenance, including inspections) and the cost associated with these measures. For structures in service, the design is often fixed and maintenance is the only feasible risk reduction measure. This optimisation problem is illustrated in Figure 1.1. For new-built structures a balance between design and the inspection-maintenance efforts must also be envisaged to arrive at the minimum risk reduction cost for a specific level of reliability. This (two-dimensional) optimisation is depicted in Figure 1.2.

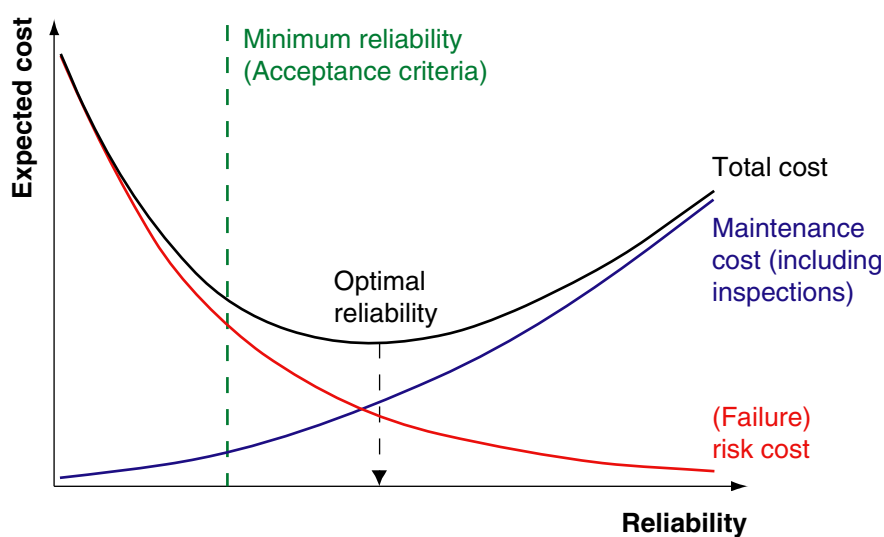


Figure 1.1 – The optimisation problem for structures in service.

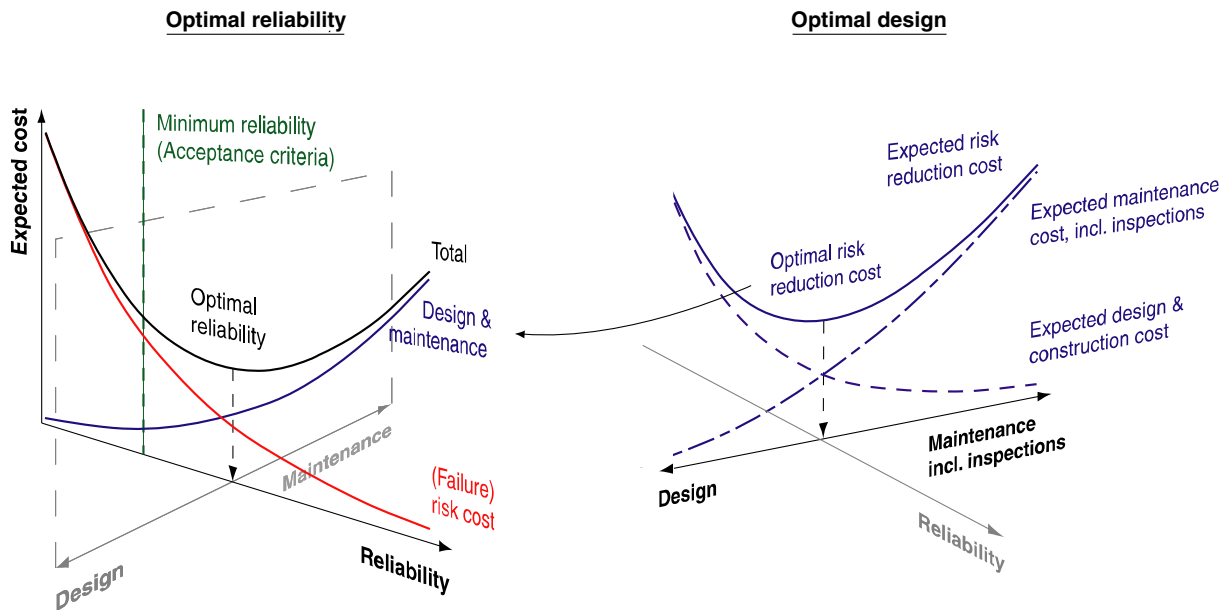


Figure 1.2 – The general optimisation problem for new-built structures.

Most deterioration phenomena on structures are of a highly stochastic nature; the models describing these processes consequently involve large variations and uncertainties. Inspections can reduce the uncertainty which is related to the incomplete knowledge of the state of nature (the epistemic uncertainties); in doing so, they facilitate the purposeful application of mitigation actions. For new-built structures inspections are thus in many cases a cost-effective risk reducing measure; for existing structures (where the design is fixed) they are often the only practical one. Risk based inspection planning (RBI) provides the means to evaluate the optimal inspection efforts based on the total available information and models, in accordance with Figure 1.1 and Figure 1.2.

## 1.2 Outline

Risk based inspection planning (RBI) is concerned with the optimal allocation of deterioration control. In practice, the term RBI is used to denote substantially different procedures, from fully quantitative to fully qualitative ones, yet all procedures are based on the basic concept of risk prioritising, i.e. the inspection efforts are planned in view of the risk associated with the failure of the components. Quantitative procedures vary substantially, often depending on the industry where they are applied. Whereas published RBI procedures for structures are based on fully quantitative probabilistic deterioration and inspection models which are combined using Bayesian updating, RBI in the process industry is generally based on frequency data and accounts for inspection quality in a qualitative manner<sup>a</sup>. Such a semi-quantitative

<sup>a</sup> Koppen (1998) presents an outline of the RBI methodology according to the API 580 document, which is a standard approach in the process industry.

approach is generally not appropriate for deteriorating structures. For these, empirical statistics are not available as most structures are unique and experience with structural failures is sparse. For the same reasons, qualitative estimations of the impact of inspections on the probability of failure are not suitable for structural systems.

Because structural systems are considered, within this thesis the term RBI is applied to denote fully quantitative methods of inspection optimisation, which are based on Bayesian decision theory; other approaches are not considered further. In Goyet et al. (2002a) an overall working procedure for inspection optimisation is described; therein the RBI procedures presented in the present work are termed *Detailed RBI* to emphasise that they form only one step in the total asset integrity management process. This process comprises a general, more qualitative analysis, a detailed analysis for the most critical parts of the system and an implementation strategy. This general strategy and process, although indispensable for any practical application, is not the subject of this work and the reader is therefore referred to the aforementioned reference for a broader view on the total process. It is just pointed out here that the methodology presented in this thesis addresses only identified deterioration and failure modes. The identification of the potential failure modes and locations must be performed at an earlier stage during a qualitative risk analysis procedure. Especially the problem of so-called gross errors must be covered by such procedures.

RBI has its origins in the early 1970's when quantitative inspection models were for the first time considered for the updating of deterioration models by means of Bayes' rule, Tang (1973). In their fundamental study, Yang and Trapp (1974) presented a sophisticated procedure that allows the computation of the probability of fatigue failure for aircraft under periodic inspections, taking into account the uncertainty in the inspection performance. Their procedure, which takes basis in the Bayesian updating of the probability distributions describing the crack size, is computationally very efficient due to its closed form solution, but has the disadvantage of not being flexible with regard to changes of the stochastic deterioration model. Based on the previous study, Yang and Trapp (1975) introduced a procedure for the optimisation of inspection frequencies, which represents the first published RBI methodology. This procedure was later further developed (e.g. to include the uncertainty of the crack propagation phase), but the limited flexibility with regard to the applicable limit state functions was not overcome. Yang (1994) provides an overview on these developments. In the offshore industry, optimisation of inspection efforts on structures was first considered in Skjong (1985), using a discrete (Markov chain) fatigue model.

The mathematical limitations of the first approaches to RBI were finally overcome in the mid 1980's with the development of structural reliability analysis (SRA), enabling the updating of the probability of events, see e.g. Madsen (1987). This makes it possible to update, in principle, any possible stochastic model that describes the events, although at the cost of increased computational effort. The introduction of SRA thus lead to new advances in inspection optimisation, mainly in the field of offshore engineering, where epistemic uncertainties are often prevailing and consequently a more flexible probability calculation is preferable. In Madsen et al. (1987) the application of SRA for the updating of the fatigue reliability of offshore structures is demonstrated, based on a calibration of a crack growth model to the SN fatigue model. In Thoft-Christensen and Sørensen (1987) an inspection optimisation strategy based fully on SRA is presented. Further developments are published in Fujita et al. (1989), Madsen et al. (1989) and Sørensen et al. (1991). At that time, first

applications were reported, see Aker (1990)<sup>a</sup>, Faber et al. (1992b) Pedersen et al. (1992), Sørensen et al. (1992) or Goyet et al. (1994). Since then the general RBI methodology has essentially remained the same; a state-of-the-art procedure is described in Chapter 2. Additional efforts were directed towards the consideration of RBI for systems, e.g. Faber et al. (1992a), Moan and Song (1998) and Faber and Sorensen (1999), and the integration of experiences and observations in the models, Moan et al. (2000a, b). Applications of the methodology to areas other than to fixed offshore structures subject to fatigue include: RBI for fatigue deterioration in ship structures presented in Sindel and Rackwitz (1996), RBI for pipelines subject to corrosion as reported in e.g. Hellevik et al. (1999), RBI for mooring chains, Mathiesen and Larsen (2002), RBI for fatigue deterioration on FPSO, Lotsberg et al. (1999), as well as fatigue reliability updating on bridges, Zhao and Haldar (1996), and ship structures, Guedes Soares and Garbatov (1996a).

To date the application of RBI in practice is still limited. To a large extent this is due to the substantial numerical efforts required by the SRA methods which make it difficult to perform the calculations in an automatic way and, in addition, require specialised knowledge by the engineer. This problem was the motivation for the introduction of the generic approach to RBI in Faber et al. (2000). The basic idea is to perform the inspection planning for generic representations of structural details which are specified by characteristics commonly used in fatigue design, such as the Fatigue Design Factor (*FDF*) and the applied SN curve. Inspection plans for the specific details can then be obtained from the pre-fabricated generic inspection plans by the use of simple interpolation schemes.

### 1.3 Scope of work

The main subject of the thesis is the elaboration of the generic approach to RBI for fatigue as first introduced in Faber et al. (2000), with the objective of developing, investigating and describing all aspects of the methodology as required for application in practice. This includes:

- A consistent description of the decision problems in inspection planning.
- A summary and investigation of appropriate deterioration models.
- A description of the consistent modelling of inspection performance, as well as the derivation of the model parameters.
- The development of methodologies and software tools for the evaluation of the generic plans.
- The determination and investigation of appropriate interpolation schemes for the inspection plans.
- Software tools for the application of the generic inspection plans to structures.
- The provision of appropriate methods for the determination of risk acceptance criteria.

---

<sup>a</sup> The inspection planning tool presented by Aker (1990) is later reviewed by Moan et al. (2000b), who analyse the effect of the tool on the maintenance efforts and compare its predictions to observations from offshore platforms.

In addition to providing the tools for the practical application of RBI on deteriorating components, the potential of the approach for future integral application on entire structures is investigated. This requires modelling the effect of inter-dependencies between the deterioration at different locations in the structure as well as the effect of inter-dependencies in the inspection performance over the structure. The development of practical approaches that account for these effects is based on new concepts in the decision modelling. Furthermore, the application to deterioration modes other than fatigue, such as corrosion, is studied, the differences between these applications are studied and examples are presented to demonstrate the feasibility of RBI for structures subject to corrosion.

Whereas parts of the results are directly applicable, others require further development before they can be implemented; however, all research performed in the framework of this thesis is a prerequisite for an integral RBI approach to a total installation as outlined in Faber et al. (2003a).

## 1.4 Thesis overview

Corresponding to the two major directions pointed out above, the present thesis can be read along two lines: One part of the thesis comprises a reference work that develops an efficient and therefore highly practical state-of-the-art RBI methodology. It should provide all the means required for the application of RBI on structures subject to fatigue, such as presented by Faber et al. (2003b). The second part of the thesis consists of more fundamental research which will require additional investigation before the methods reach the state of applicability. This part includes new concepts and developments of problems previously treated, (such as RBI for structures subject to corrosion, inspection modelling, risk acceptance criteria) but also essentially new research on problems not investigated previously (RBI for systems in particular). The originality of the work is discussed in Chapter 8.

Figure 1.3 provides a graphical overview of the entire thesis; rectangular boxes indicate the applied reference work, oval boxes represent new fields of development and research.

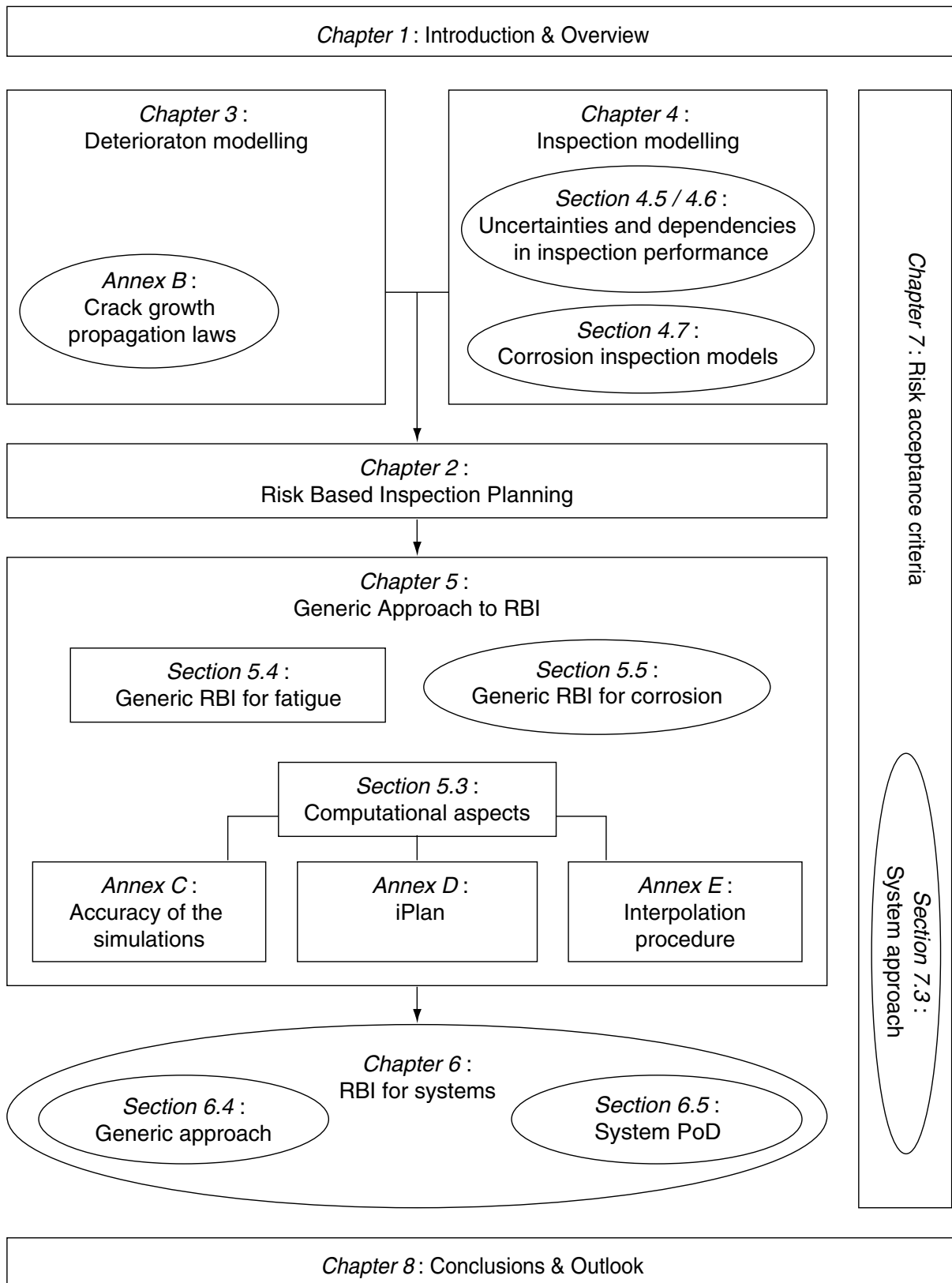


Figure 1.3 – Graphical overview of the thesis.



## 2 Risk based inspection planning

### 2.1 Introduction

This chapter presents a state-of-the-art risk based inspection planning (RBI) methodology in accordance with the basic references introduced in Section 1.2. RBI is based on reliability analysis, whose basics are briefly introduced in Section 2.2, and on Bayesian pre-posterior decision analysis, outlined in Section 2.3. Sections 2.4 and 2.5 finally demonstrate how these are combined to arrive at a consistent and practical RBI methodology. Although the presentation of RBI is as general as possible, part of the approach is specific for fatigue subjected structural elements<sup>a</sup>. This is considered in Section 2.6 where RBI for elements and components susceptible to corrosion is discussed in view of the specifics of this deterioration mode. The stochastic deterioration and inspection performance models required for practical applications are presented later in Chapters 3 and 4 with a focus on their application in RBI.

The basic theories in both reliability analysis and decision analysis are provided in a very condensed form. The reader who is not familiar with these theories is required to take up the stated references; due to the maturity of these fields good reference books are available. The applied mathematical notation follows the standard conventions to the extent possible, exceptions are indicated. A summary of the applied nomenclature is provided in Annex F .

### 2.2 Probabilities of events and structural reliability analysis

In RBI, the main events that are random outcomes are the failure event (denoted by  $F$ ) and the events describing the inspection outcomes. In the following the methods for calculating the probability of occurrence of these events are outlined.

#### 2.2.1 Probability of failure

In Tait (1993) it is described how by the end of the 1930s both loads  $S$  and resistance  $R$  of engineering structures were being commonly expressed as statistical distributions. He also quotes a report by Pugsley (1942)<sup>b</sup> where the application of these distributions to the calculation of the failure probability is described, Equation (2-1):

---

<sup>a</sup> The term element is used in this chapter to denote the individual locations of possible failure. In chapter 5 the term hot spot is introduced which is then used equivalently.

<sup>b</sup> In civil engineering, the need for statistical concepts and probability measures in the determination of safety factors in order to arrive at consistent levels of safety is pointed out in Freudenthal (1947).

$$P(F) = P(R \leq S) = \int_0^{\infty} f_R(r) \int_r^{\infty} f_S(s) ds dr \quad (2-1)$$

Equation (2-1) describes the basic structural reliability problem when  $S$  and  $R$  are independent and non-negative. A more general description of the event of failure is made possible by the use of a limit state function  $g(\mathbf{X})$ , where  $\mathbf{X}$  is a vector of all basic random variables<sup>a</sup> involved in the problem. The limit state function defines the border between the safe domain where  $g > 0$  and the failure domain where  $g \leq 0$ <sup>b</sup>. The probability of failure is then determined by integration over the failure domain:

$$P(F) = P(g(\mathbf{X}) \leq 0) = \int_{g(\mathbf{x}) \leq 0} f_{\mathbf{X}}(\mathbf{x}) d\mathbf{x} \quad (2-2)$$

Only in special cases an analytical solution to Equation (2-2) exists. However, different numerical and approximation techniques are available for its solution, such as numerical integration, Monte Carlo simulation (MCS) and importance sampling. Melchers (1999b) provides an overview on these methods.

A different approach to the solution of Equation (2-2) is to simplify the probability density function  $f_{\mathbf{X}}(\mathbf{x})$ . In Structural Reliability Analysis (SRA) this is pursued by the concept of the reliability index  $\beta$  introduced in Hasofer and Lind (1974), which is related to the probability of failure by the relation

$$\beta = -\Phi^{-1}(p_F) \quad (2-3)$$

$\Phi(\cdot)$  is the standard normal distribution function. The expression  $p_F$  is equivalent to  $P(F)$ . The approach is based on transformations of  $f_{\mathbf{X}}(\mathbf{x})$  to independent standard normal probability density functions  $\varphi(u_i)$ , such as the Rosenblatt transformation according to Hohenbichler and Rackwitz (1981) or the Nataf transformation, Der Kiureghian and Liu (1986). The reliability index  $\beta$  is then equal to the minimal distance in the  $u$ -space of the failure surface (where  $g(\mathbf{u}) = 0$ )<sup>c</sup> from the origin.

The detailed meaning and significance of the reliability index as well as the techniques for its calculation (such as the First Order Reliability Method (FORM)) can be found in Melchers (1999b) and Ditlevsen and Madsen (1996).

---

<sup>a</sup> The basic random variables include all uncertain input parameters in the limit state function.

<sup>b</sup> Limit state functions for failure are given for the different specific deterioration and failure mechanisms in the respective sections of this thesis.

<sup>c</sup> The failure surface is transformed into the  $u$ -space by transforming all the basic random variables in the limit state function.

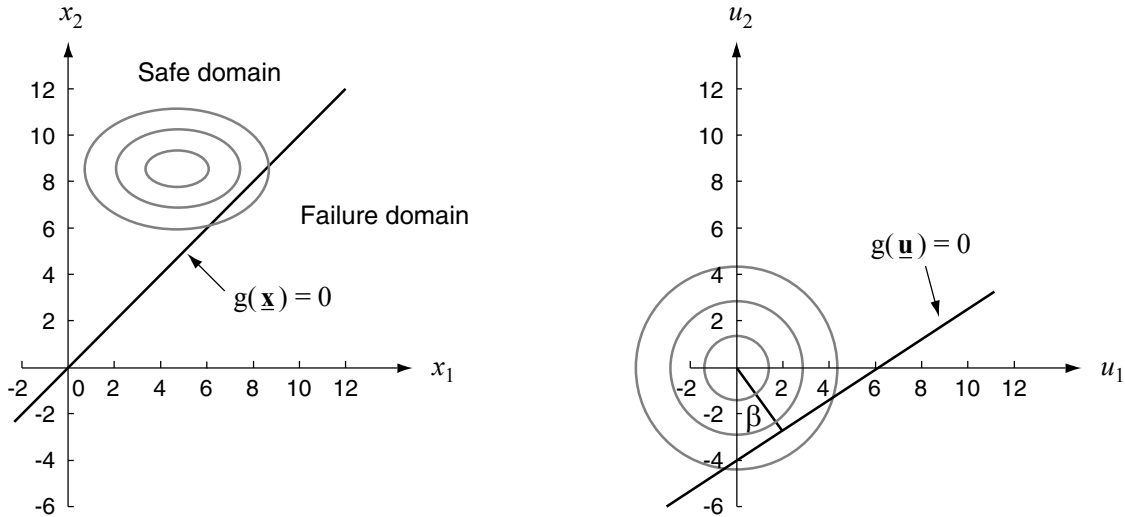


Figure 2.1 – The transformation to the standard normal space, after Faber (2003a).

## 2.2.2 Probabilities of inspection outcomes

The different possible inspection outcomes, which are triggering different maintenance actions, are also described by limit state functions (LSF), see Madsen et al. (1986) or Madsen (1987). These inspection outcomes include the event of indication of a defect  $I$ , the event of detection of a defect  $D$ , the event of false indication  $FI$  or the event of a defect measurement with measured size  $s_m$ . The specific LSF applied for these events are described in Chapter 4. The probability of the different inspection outcomes are then evaluated in accordance with the previous section; as an example the probability of an indication of a defect at the inspection (where the event of indication  $I$  is described by the LSF  $g_I(\underline{\mathbf{X}})$ ) is, in analogy to Equation (2-2), written as

$$P(I) = P(g_I(\underline{\mathbf{X}}) \leq 0) = \int_{g_I(\underline{\mathbf{x}}) \leq 0} f_{\underline{\mathbf{x}}}(\underline{\mathbf{x}}) d\underline{\mathbf{x}} \quad (2-4)$$

Most measurement events  $M$  are fundamentally different because they are equality events, for which the probability of occurrence is given as  $P(g(\underline{\mathbf{X}}) = 0)$ . Consequently, for measurement events, Equation (2-4) is altered accordingly:

$$P(s_m) = P(g_M(\underline{\mathbf{X}}) = 0) = \int_{g_M(\underline{\mathbf{x}}) = 0} f_{\underline{\mathbf{x}}}(\underline{\mathbf{x}}) d\underline{\mathbf{x}} \quad (2-5)$$

## 2.2.3 Intersection of probabilities

RBI and decision analysis in general is based on the construct of so-called decision trees which are introduced in Sections 2.3 and 2.4. Most of the branches in these decision trees represent intersections of events (e.g. the event of failure combined with no indication of a defect at the previous inspection). It is thus necessary that the probability of the intersection of

different events can be computed. In analogy to Equation (2-2), the probability that event  $E_1$  occurs together with the event  $E_2$  is written as

$$P(E_1 \cap E_2) = P(g_1(\mathbf{X}) \leq 0 \cap g_2(\mathbf{X}) \leq 0) = \int_{g_1(\mathbf{x}) \leq 0 \cap g_2(\mathbf{x}) \leq 0} f_{\mathbf{x}}(\mathbf{x}) d\mathbf{x} \quad (2-6)$$

In principle the same techniques that are used for the computation of probabilities of single events are also applied for the calculation of intersection of probabilities, although with additional complexity; see Melchers (1999b) for details.

### 2.2.4 Probability updating

In many situations the conditional probability is of interest, i.e. the probability of occurrence of an event  $E_2$  given the occurrence of another event  $E_1$ . The solution to this problem is the classical Bayes' rule, Equation (2-7).

$$P(E_2|E_1) = \frac{P(E_1 \cap E_2)}{P(E_1)} = \frac{P(E_1|E_2)P(E_2)}{P(E_1)} \quad (2-7)$$

From the middle expression in Equation (2-7) it is seen that the conditional probability can be evaluated by combining Equations (2-2) and (2-6).  $P(E_1|E_2)$  on the right hand side of Bayes' rule is known as the likelihood and is a measure for the amount of information on  $E_2$  gained by knowledge of  $E_1$ , it is also denoted by  $L(E_1|E_2)$ . The likelihood is typically used to describe the quality of an inspection, as will be shown in Chapter 4.  $P(E_2|E_1)$  is known as the posterior probability of occurrence of  $E_2$  or equivalently its updated occurrence probability. Different examples of the updating of probabilities of events are given by Madsen (1987); the updating of the probability of fatigue failure after an inspection, as presented in Figure 2.2, is a typical operation in RBI.

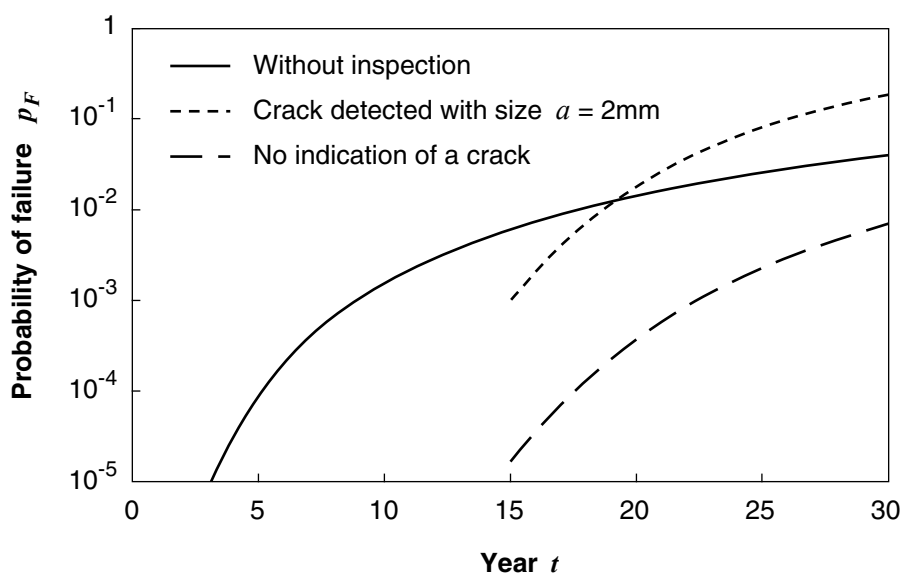


Figure 2.2 – The updating of the probability of fatigue failure using the knowledge of an inspection result at the time  $t = 15y$ .

If Bayes' rule is applied to update a probability density function (pdf) based on the observation of an event  $E_1$ , this is written as

$$f_x''(x|E_1) = L(E_1|x) \cdot f_x'(x) \cdot const \quad (2-8)$$

$f_x''(x)$  is known as the posterior pdf of  $x$ ,  $f_x'(x)$  as the prior pdf. The constant in Equation (2-8) is determined by the condition that the integration of  $f_x''(x)$  over the total domain of  $X$  must result in unity, it corresponds to the denominator  $P(E_1)$  in Equation (2-7). As an example consider the case where the depth  $a$  of the largest crack in a weld is described by  $f_a'(a) \sim \text{LN}[1\text{mm}, 0.4\text{mm}]$ <sup>a</sup> a-priori (before any measurements, but from experience on similar welds). Additionally an inspection is performed resulting in the measurement of a crack with depth  $a_m = 3\text{mm}$ . The uncertainty associated with the measurements can be modelled by an error  $\varepsilon_m$  distributed as  $\text{N}[0, 0.5\text{mm}]$ ; N indicates a Normal distribution. The likelihood function of this measurement is then described by  $L(a_m|a) \sim \text{N}[3\text{mm}, 0.5\text{mm}]$ . The posterior pdf of the crack size after this measurement,  $f_a''(a|a_m)$ , evaluated by means of Equation (2-8), is shown in Figure 2.3.

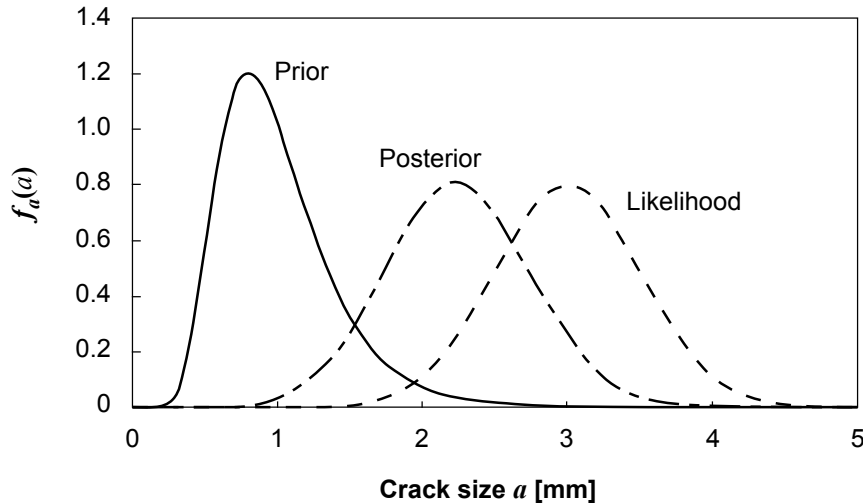


Figure 2.3 – Illustration of the updating of a probability density function.

More details on probability updating in view of engineering applications are provided in JCSS (2001).

### 2.2.5 Time-dependent reliability problems

All deterioration is time-dependent and consequently also all reliability problems related to deterioration are time-dependent, see also JCSS (2002). The failure event of a deteriorating structure can in general be modelled as a first-passage problem, i.e. failure occurs when the limit state function, which is now additionally a function of time, becomes zero for the first

<sup>a</sup> LN stands for the Lognormal distribution. The values given in square brackets following the distribution symbol are the mean value  $\mu$  and the standard deviation  $\sigma$  of the distribution.

time given that it was positive at  $t = 0$ . The probability of failure between time 0 and  $T$  is then

$$p_F(T) = 1 - P(g(\underline{\mathbf{X}}(t)) > 0, \quad \forall t \in [0, T]) \quad (2-9)$$

For most deterioration the problem is simplified by the fact the damage is monotonically increasing with time, but still only approximate solutions exist for the general case. Different approaches to the evaluation of the time-dependent reliability are given by Madsen et al. (1986) and Melchers (1999b), but most of these methods are numerically cumbersome and hardly applicable to the development of the generic inspection plans. Thus, in the following, first a special case is described, which due to its simplicity is important in practical applications; finally some aspects of the more general problem are discussed.

### 2.2.5.1 Deterioration problems with a fixed damage limit

If failure occurs when the deterioration reaches a constant limit then the problem can be solved as time-independent with the time  $t$  being a simple parameter of the model. This is because the deterioration is monotonically increasing and thus if failure has not occurred at time  $t_1$ , it has not occurred at  $t < t_1$ . When the failure rate (in this work denoted by annual probability of failure) is of interest, the reliability problem is simply evaluated at  $t = t_1, t_2, \text{ etc.}$  whereby  $t_i = t_{i-1} + 1\text{yr}$ . The annual probability of failure in year  $t_i$  is then

$$\Delta p_F(t_i) = \frac{p_F(t_i) - p_F(t_{i-1})}{1 - p_F(t_{i-1})} \quad (2-10)$$

A typical case of such a problem is the SN fatigue modelling, where failure occurs given that the accumulated damage has reached 1 (or an uncertain damage limit  $\Delta$ ), see Section 3.2.

### 2.2.5.2 Deterioration problems with varying loading

It is often convenient to represent reliability problems with varying loads in the classical form of a resistance  $R(t)$  and a load  $S(t)$ . Such a situation with deteriorating resistance is illustrated in Figure 2.4:

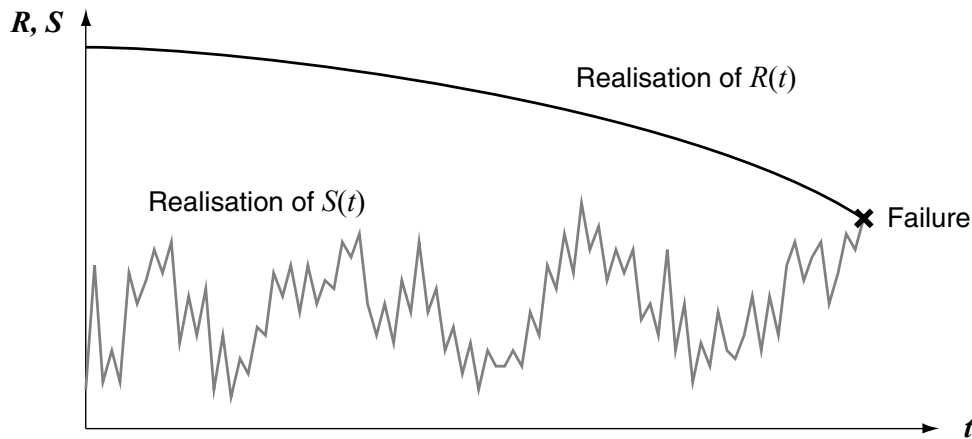


Figure 2.4 – One realisation of the time-dependent problem.

This is a classical first-passage problem. The applicable solution strategy depends very much on the nature of the two processes  $R(t)$  and  $S(t)$  and no general method is available. A widely applied solution to the problem is based on the construct of a Poisson process for the out-crossings from the safe to the failure domain, see Englund et al (1995) for a review of the theory. Given the expected number of out-crossings  $E[N^+(T)]$ , the probability of failure has to be determined by time integration. This is based on the assumption of independence between the individual out-crossings. However, many of the basic random variables in  $R(t)$  and, to a lesser extent, in  $S(t)$  have non-ergodic characteristics (e.g. all the deterioration models applied in this thesis consist completely of time-independent random variables). Out-crossing events are thus no longer independent, which leads to the following solution, in accordance with Schall et al. (1991): Let  $\underline{\mathbf{Q}}$  be the vector containing all the slowly varying ergodic processes,  $\underline{\mathbf{R}}$  a vector of all time invariant random variables. The probability of failure must then be evaluated by integrating the conditional  $P_F(t|\underline{\mathbf{q}}, \underline{\mathbf{r}})$  over the total domains of  $\underline{\mathbf{Q}}$  and  $\underline{\mathbf{R}}$ , see Schall et al. (1991) for the detailed formulations.

In some cases it is convenient to discretise the problem in time intervals, e.g. yearly periods, and to approximate the resistance during each interval by a constant value  $R_i$ . Under special conditions, the loading can furthermore be approximated by the extreme value distribution  $f_{S_{max}}(s)$  for that period, so that the problem can be reduced to a time-invariant problem. However, it is very important to realise that in all cases due attention must be paid to the assumptions regarding the ergodicity of the processes, as discussed above, and consequently the validity of assumptions regarding independency between the failure events in two different time periods.

## 2.2.6 Computation of probabilities

For the examples presented in this thesis, all probability calculations are performed using either Monte Carlo simulation (MCS) or FORM. Tailor made software modules are used for this purpose, as these allow the automated integration of the calculations in the decision analysis. However, commercial software packages like Strurel (1999) allow the computation of Equations (2-2) and (2-6) using all the different aforementioned techniques.

## 2.3 Decision analysis

### 2.3.1 Decisions under uncertainty

The final objective of RBI is the identification of the optimal decisions on maintenance actions for deteriorating structures. Thereby, the modelling and the analysis of deterioration and maintenance actions are typically subject to uncertainties in the following aspects:

- Uncertainty on the state of the system (deterioration)
- Uncertainty on the performance of the inspection and repair actions
- Uncertainty on the consequences of failure

Optimisation of the maintenance actions must thus account for these uncertainties. Bayesian decision analysis, as introduced in this section, provides the technique to perform such an optimisation and builds the basis for the methods presented in this thesis.

### 2.3.2 Utility theory

Utility theory is a cornerstone of the classical decision theory (and consequently the Bayesian decision theory), as it provides the means for the formalisation of the preferences of the decision maker. It was developed in Von Neuman and Morgenstern (1947); a good introduction is presented in Luce and Raiffa (1957), whereas in Ditlevsen (2003) the theory and its axioms are introduced in view of engineering problems. Here only a very short and consequently incomplete overview is provided.

Basically there is a set of possible events  $E_1$  to  $E_n$  (e.g. different outcomes of a game). An index is assigned to all events so that a larger index signifies that this event is preferred over another. The decision maker can now choose between different actions (also called lotteries). Each action will lead to probabilities of occurrence for the different events, i.e. action  $a$  will lead to event  $E_1$  with probability  $p_1^{(a)}$ , to event  $E_2$  with probability  $p_2^{(a)}$  and so on. Equivalently action  $b$  will lead to event  $E_1$  with probability  $p_1^{(b)}$  and so on for all other alternatives. The probabilities thereby must fulfil the condition

$$p_1^{(i)} + p_2^{(i)} + \dots + p_n^{(i)} = 1 \quad (2-11)$$

If the preferences fulfil a set of axioms<sup>a</sup> (consistency requirements) as defined by Von Neumann and Morgenstern (1947), or in slightly different form by Luce and Raiffa (1957), then a numerical index called utility  $u$  can be assigned to the basic events  $E_1$  to  $E_n$  in such a way that one decision (on which action to take) is preferred to another if and only if the expected utility of the former is larger than the utility of the latter.

Considering the maintenance of individual structures, the utility  $u$  can be assumed linear with respect to monetary units for the considered range of events<sup>b</sup>. Therefore it can be stated that the optimisation criterion to be applied in the RBI is the expected cost criterion (respectively expected benefit, if the benefits of the activity are also included in the analysis). This conclusion is in accordance with Benjamin and Cornell (1970).

It should be noted that the expected cost criterion demands that all the consequences of an event are expressed in monetary terms. Regarding the valuation of fatalities due to an accident, this has for a long time been controversial among structural engineers (although accepted by other professions). On the other hand it has been argued by decision analysts that not assigning a value to human life may lead to inconsistent decisions, Benjamin and Cornell

---

<sup>a</sup> One of the axioms states that the ordering of preferences among different events is transitive. Formally if  $\succ$  means “preferred to” then transitivity demands that if  $E_i \succ E_j$  and  $E_j \succ E_k$  then also  $E_i \succ E_k$  for any events.

<sup>b</sup> This assumes that the indirect costs associated with the event failure, of repair and inspection are included in the modelling. For extreme events (e.g. the loss of several installations) the quantification of the indirect costs becomes very difficult, e.g. if the owner faces bankruptcy due to the event, but this is of little relevance to the considered applications.



(1970). Furthermore, recent work on the Life Quality Index (LQI) reported in Nathwani et al. (1997) and Rackwitz (2002) does now provide a philosophical and theoretical framework for the valuation of human life and its application in decision theory; see also JCSS (2001) for further considerations on this topic.

### 2.3.3 Bayesian decision analysis

The classical decision theory developed by Von Neumann and Morgenstern (1947), which is based on the utility theory as sketched in the previous section, builds the fundamental basis for the optimisation procedures as presented in this work. The Bayesian decision analysis, as presented by Raiffa and Schlaifer (1961), additionally provides the formal mechanism for taking into account the preferences and judgements of the decision maker. The fundamental assumptions are that the decision maker is capable of

- a) assigning a (subjective) probability distribution to all the uncertain variables in the problem
- b) assigning a unique utility  $u$  to all combinations of realisations of the involved variables and decisions (i.e. the preferences of the decision maker can be formalised)

These assumptions are controversial among engineers (and even more so with other professions). However, in accordance with Savage (1972) and Raiffa and Schleifer (1961), the author believes that only by quantification of the subjective (but based on objective information) preferences and judgements it is possible to arrive at consistent decisions. Without this formalisation decisions under uncertainty will be essentially arbitrary, although in many practical situations the optimal decision is intuitively clear, due to the limited amount of possible events. It is to be noted that although the fundamental assumptions are controversial, the theory has been (implicitly or explicitly) applied to many engineering problems, often without much consideration of its fundamental basis. Faber (2003b) discusses the relevance of the Bayesian decision analysis for engineering applications and clarifies the uncertainty modelling, which often leads to a misunderstanding of the analysis.

The classical reference for the application of Bayesian decision analysis to civil engineering problems is the monograph by Benjamin and Cornell (1970). They notice that “this approach recognizes not only that the ultimate use of probabilistic methods is decision making but also that the individual, subjective elements of the analysis are inseparable from the more objective aspects. [This theory] provides a mathematical model for making engineering decisions in the face of uncertainty.”

### 2.3.4 Classical Bayesian prior and posterior decision analysis

Benjamin and Cornell (1970) name the prior decision analysis “decisions with given information”. It is applied when an action  $a$  is to be planned and all the relevant information on the true state  $\Theta$  is available. This does not signify that the true state is a deterministic

value<sup>a</sup>, but that it is not possible to learn more on  $\Theta$  before  $a$  is performed<sup>b</sup>. The true state is described by a prior probability density function (pdf)  $f'_{\Theta}(\theta)$ . Prior decision analysis aims at identifying the action  $a$  that maximises the expected utility  $E[u]$ , where the utility is a function of  $a$  and  $\Theta$ , Equation (2-12).

$$\max_a u(a) = \max_a E_{\Theta}[u(a, \theta)] = \max_a \int_{\Theta} u(a, \theta) f'_{\Theta}(\theta) d\theta \quad (2-12)$$

The analysis is trivial once the problem is properly modelled in the form of a decision tree, see Benjamin and Cornell (1970) for examples.

Posterior decision analysis is in principle identical to the prior analysis, except that new information, as e.g. obtained by inspections, is available and taken into account. Based on the additional information, the prior pdf  $f'_{\Theta}(\theta)$  is updated to the posterior  $f''_{\Theta}(\theta)$ , in accordance with section 2.2.4. The final optimisation of the action  $a$  then follows Equation (2-12) where the prior pdf is replaced with the posterior pdf.

### 2.3.5 Classical Bayesian pre-posterior analysis

The following section summarises the pre-posterior analysis from Bayesian decision theory, following the classical book by Raiffa and Schlaifer (1961). Pre-posterior analysis aims at identifying the optimal decision on inspections (or experiments).

Generally, the inspection and maintenance planning decision problem can be described in terms of the following decision and events<sup>c</sup>:

- $e$ , the possible inspections or experiments, i.e. number, time, location and type of inspections
- $Z$ , the sample outcomes, i.e. inspection results such as no-detections, detections, observed crack length, observed crack depth.
- $a$ , the terminal acts, i.e. the possible actions after the inspection such as do nothing, repairs, change of inspection and maintenance strategy.
- $\Theta$ , the true but unknown “state of the nature” such as non-failure, failure, degree of deterioration.
- $u(e, z, a, \theta)$ , the utility assigned, by consideration of the preferences of the decision maker, to any combination of the above given decisions and events. Utilities are often, but not necessarily, expressed in monetary terms.

---

<sup>a</sup> If  $\Theta$ , and consequently the total decision problem, is purely deterministic, then the identification of the optimal action is straightforward and is not considered further.

<sup>b</sup> A typical example of such a case is the decision on whether to bet or not on the outcome of the rolling of a dice, the true state being a number between 1 and 6.

<sup>c</sup> In contrast to the notation in Raiffa and Schlaifer (1961) the capital letters  $Z$  and  $\Theta$  indicate random variables and not the spaces of these variables.

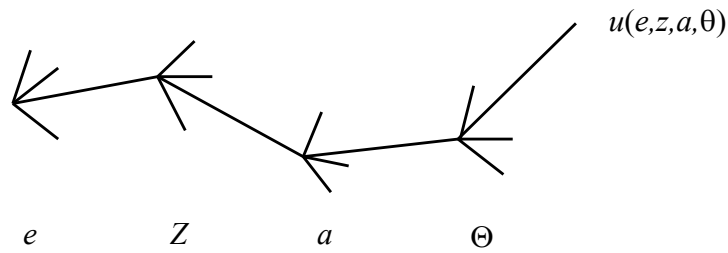


Figure 2.5 – Classical decision tree of the pre-posterior analysis, after Raiffa and Schlaifer (1961).

By means of pre-posterior analysis it is possible to determine the expected utility resulting from the inspection decision  $e$  by assigning to the possible inspection results  $z$  a decision rule  $d$  on the actions in regard to repairs and/or changes in future inspection and maintenance plans, such that

$$a = d(e, z) \quad (2-13)$$

An inspection or maintenance strategy is defined by a particular set of the variables  $e$  and  $d$ . Its corresponding expected utility is <sup>a</sup>

$$E[u(e, d)] = E_{\Theta, Z|e, d} [u(e, Z, d(e, Z), \Theta)] \quad (2-14)$$

Note that the utility function  $u(\cdot)$  is a deterministic function. However, the determination of this function can include other uncertain variables and the utility function then represents the expectation with respect to these variables. In other words, all random variables (rv) that are not included in either  $Z$  or  $\Theta$  are integrated out for the determination of  $u(\cdot)$ . As an example, the consequence of a failure depends (among other factors) on the number of people present at the location of occurrence, which is uncertain. The cost of a failure for a particular combination of  $(e, z, a, \theta)$  is thus determined by integration over the pdf of the number of people present at the location.

The optimal inspection strategy is found by maximising Equation (2-14).

### 2.3.5.1 Value of information

The value of information (VOI) concept forms an important part of the pre-posterior analysis. Often, direct maximisation of Equation (2-14) is not possible and the VOI may then prove useful for the optimisation of the maintenance actions. Such a case is presented by Straub and Faber (2002b) for the optimisation of inspection efforts in structural systems. The theory of the VOI is extensively described by Raiffa and Schlaifer (1961); it is in the following introduced by means of an example.

<sup>a</sup> Equation (2-14) corresponds to the normal form of the Bayesian decision analysis. The difference to the extensive form of the analysis (which renders the same results) consists in the use of an explicit decision rule  $d$ .

The VOI theory is valid when sample utilities  $u_s$  (which are related directly to the inspections and their outcomes) and the terminal utilities  $u_t$  (a function of the terminal action and the state of nature) are additive, i.e. when

$$u(e, z, a, \theta) = u_s(e, z) + u_t(a, \theta) \quad (2-15)$$

This condition is in general fulfilled for the envisaged applications.

Consider the following situation: A weld is susceptible to initial defects in the form of flaws, quantified by their size  $\Theta$  (the uncertain state of nature). If the maximal flaw in the weld exceeds a certain depth  $\theta_R$ , it is economical to repair the weld, which is denoted by  $a_1$ . A-priori (meaning without any additional information) the weld is not repaired<sup>a</sup>, denoted by  $a_0$ . Given that the crack has a specific size  $\theta$ , either  $a_0$  or  $a_1$  is the optimal action to take. If perfect information were available (i.e. if  $\theta$  were known), the optimal action would be taken, resulting in the gains of  $v_t(\theta)$  as compared to the a-priori action, Equation (2-16):

$$v_t(\theta) = \max[0, u_t(a_1, \theta) - u_t(a_0, \theta)] \quad (2-16)$$

$v_t(\theta)$  is known as the Conditional Value of Perfect Information (CVPI), conditional on  $\theta$ , and is illustrated in Figure 2.6:

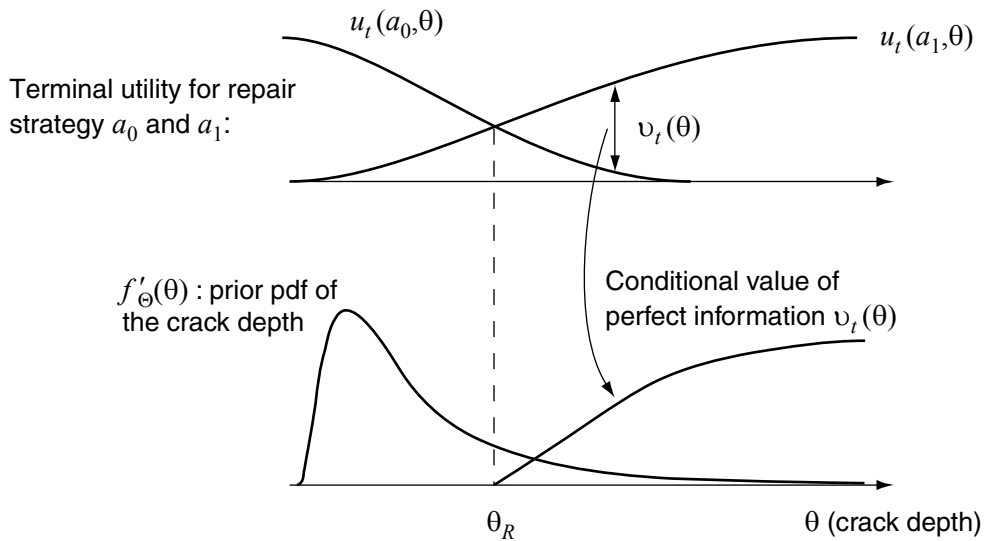


Figure 2.6 - Conditional value of perfect information.

Assume now that it is possible to perform a perfect initial inspection, where perfect means that after the inspection the crack size is known with certainty. After the inspection is carried out, the value of the information gained by the inspection is calculated by means of Equation

<sup>a</sup> It is assumed that this is the optimal action based on the prior distribution of  $\Theta$ . If the standard procedure were to repair the weld a-priori, then probably the design would not be optimal, as could be seen by a prior decision analysis.

(2-16), but before the inspection, it is only possible to compute the expected value of the information that can be obtained. This is named Expected Value of Perfect Information (EVPI) and is defined as

$$EVPI = E_{\Theta}[CVPI(\theta)] = \int_{\Theta} v_i(\theta) f'_{\Theta}(\theta) d\theta \quad (2-)$$

In reality, if an inspection  $e$  is performed, only imperfect information is obtained. As an example, a Magnetic Particle Inspection (MPI) of the weld results in either indication or no-indication of a defect, but does not provide any information about the size of the crack; the outcome may furthermore be erroneous. This is taken into account by the likelihood  $L(z|e, \theta)$ , which models the uncertainties in the inspection performance. Based on the inspection result and the likelihood, the prior pdf of  $\Theta$  is updated to the posterior pdf  $f_{\Theta}''(\theta|z)$ . Then, by means of posterior decision analysis, the optimal repair action can be evaluated as a function of the inspection outcome  $z$  in analogy to Equation (2-12). For the considered example, the expected utilities of both alternative actions are evaluated as

$$E''_{\Theta|z}[u_i(a_i, \theta)] = \int_{\Theta} u_i(a_i, \theta) f_{\Theta}''(\theta|z) d\theta, \quad i = 1, 2 \quad (2-18)$$

$E''_{\Theta|z}$  denotes the expectation with respect to the posterior pdf of  $\Theta$ . If the optimal action given the outcome  $z$  is  $a_0$ , i.e. equal to the optimal action before the inspection, then the inspection does not alter the terminal utility and has thus no value. However, if the optimal action given  $z$  is  $a_1$ , then the inspection has a value which is equal to the difference in the expected utility. The information obtained by the inspection has therefore the value

$$v_{iz}(z) = \max\left[0, E''_{\Theta|z}[u_i(a_1, \theta)] - E''_{\Theta|z}[u_i(a_0, \theta)]\right] \quad (2-19)$$

$v_{iz}(z)$  is known as the Conditional Value of Sample Information (CVSI), conditional on the inspection outcome  $z$ . Note the analogy between the Equations (2-16) and (2-19).

In addition, based on the prior pdf of  $\Theta$  and the inspection model, the probability of occurrence of the possible inspection outcomes can be evaluated as

$$f_z(z|e) = E_{\Theta}[f_z(z|e, \theta)] = \int_{\Theta} L(z|e, \theta) f_{\Theta}(\theta) \cdot d\theta \quad (2-20)$$

Finally, by combining Equations (2-19) and (2-20), the Expected Value of Sample Information (EVSI) is obtained as

$$EVSI(e) = E_z[CVSI(z)] = \int_z v_{iz}(z) f_z(z|e) dz \quad (2-21)$$

The EVSI is the expected utility gained from performing the inspection  $e$ . This may now be used to evaluate and compare different inspection techniques. Note that with increasing quality of the inspection, the EVSI asymptotically approaches the EVPI.

The EVSI for the MPI inspection of the weld is thus evaluated as follows: Given an indication of a crack at the inspection, a posterior analysis reveals that the optimal action is to repair the

weld ( $a_1$ ). This is based on the evaluation of Equation (2-18), which is assumed to result in  $E''_{\Theta|\{z=I\}}[u_t(a_0, \theta)] = 50\text{€}$  and  $E''_{\Theta|\{z=I\}}[u_t(a_1, \theta)] = 150\text{€}$ .

The CVSI is now determined based on Equation (2-19). Given an indication it is  $v_{tz}(z=I) = 100\text{€}$ , given no-indication the CVSI is  $v_{tz}(z=\bar{I}) = 0\text{€}$  because the mitigation action is not altered. If the probability of having an indication is evaluated by means of Equation (2-20) as  $P(I|e) = 0.1$ , the EVSI (which is the expected value of the information gained by the inspection) is calculated as  $EVSI = 0.9 \cdot 0\text{€} + 0.1 \cdot 100\text{€} = 10\text{€}$ . This value can now be compared to the cost of the inspection; if the inspection is more expensive than 10€, it should not be performed.

## 2.4 Maintenance and inspection optimisation

Risk based inspection planning (RBI) is an application of the pre-posterior analysis from the Bayesian decision analysis, as presented in Section 2.3.4. The analysis is based on the inspection decisions  $e$ , the inspection outcomes  $z$ , the repair and mitigation actions  $a$  (or alternatively the decision rule  $d$ ), the condition of the structure  $\theta$  and the utility (cost or benefit) associated with each set of these variables. The problem is best represented in the form of a decision tree. Because several inspection decisions must be modelled at different points in time, the resulting decision tree is different from the general tree shown in Figure 2.5; it is presented in Figure 2.7. Whereas the general one incorporates all possible inspection decisions, the RBI decision tree shows only one possible strategy, with a specific set of inspection times, and it only allows computing the expected cost for this specific strategy. To perform the optimisation, the decision tree must be established and evaluated for all different strategies whose total expected cost can then be compared.

Note that the decision tree as a simple approximation assumes that the failure event is a terminal event, no reconstruction after failure is considered in the event tree. In principle it is possible to extend the model by including the rebuilding of the element or structure after failure. These so-called renewal models are studied in the literature, see e.g. Streicher and Rackwitz (2003). However, for any practical application presented in this thesis, the computation effort becomes too large. Because the service-life is generally assumed to be finite and because the structural elements generally have a high reliability, detailed modelling of the behaviour after failure will change the final results only slightly, if at all, as can be seen from Kübler and Faber (2002). The applied simplification is thus reasonable, especially because all the events and actions after failure can be included in the expected consequences of failure.

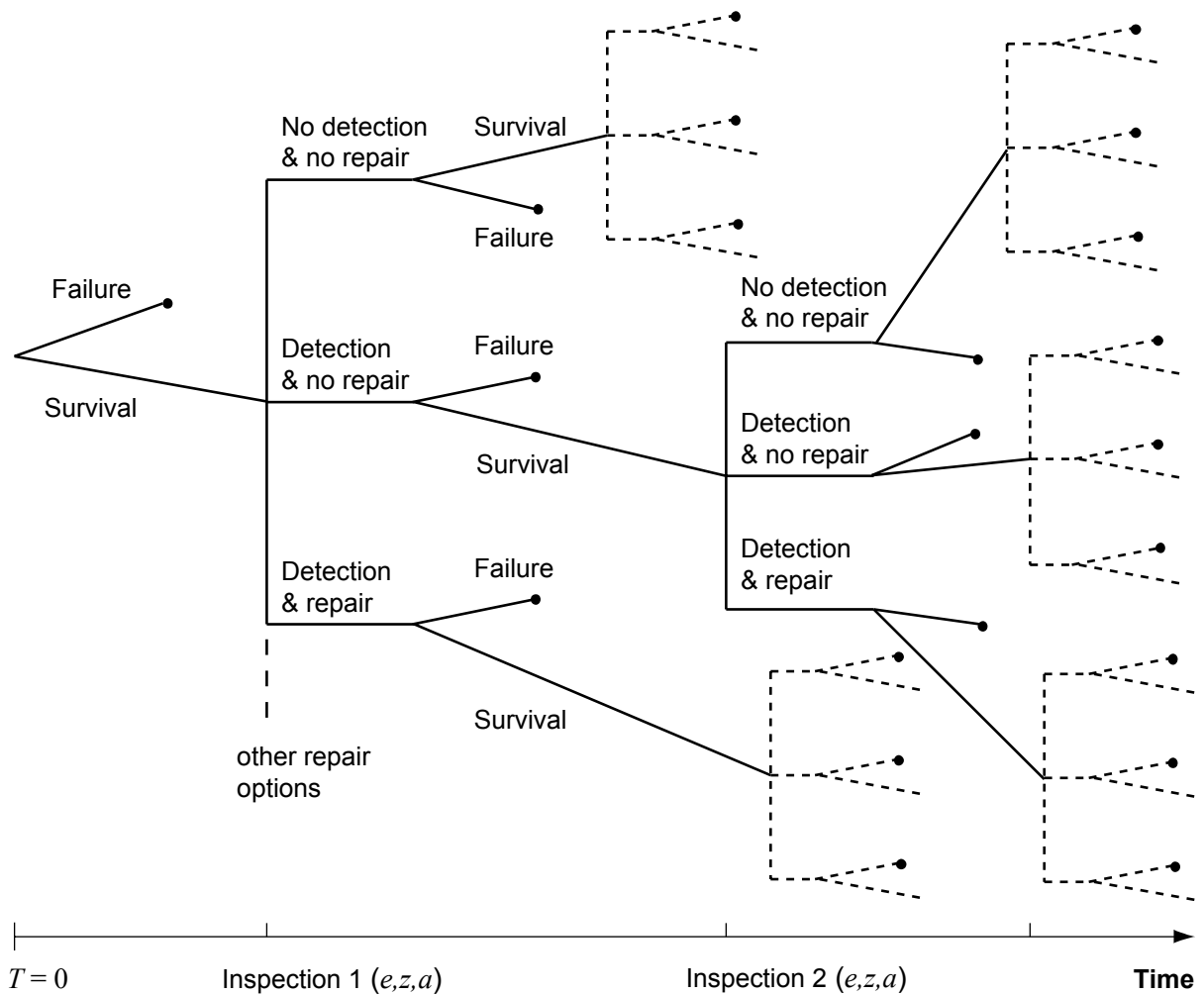


Figure 2.7 - The classical decision tree in RBI.

The ultimate goal of RBI is to determine the optimal decisions in regard to inspection and maintenance actions. Concerning the inspections, it has to be determined

- where to inspect (location in the structure)
- what to inspect for (indicator of the system state)
- how to inspect (inspection technique)
- when to inspect (time of inspections)

Regarding repair and mitigation actions, the goal is the identification of the optimal decision rule, that defines the type of repair to perform based on the inspection outcome.

The optimisation procedure as presented, the classical RBI procedure, is restricted to the consideration of single elements. The determination of *where to inspect*, however, must consider the system as a whole. This is accounted for in Chapter 6, where the interdependencies between the individual elements are addressed. *What to inspect for* depends mainly on the deterioration mechanism under consideration, respectively the available inspection techniques. *How to inspect* and *when to inspect*, described by the inspection

parameters  $e$ , as well as the optimal decision rule  $d$  on the mitigation actions to perform, is typically determined by the classical RBI procedures.

### 2.4.1 Expected cost of an inspection strategy

The optimisation objective, in accordance with Section 2.3.2, is the minimisation of the expected cost (respectively the expected benefits<sup>a</sup>) of the inspection plan. Figure 2.7 shows the full decision tree, that allows to compute the expected cost of a specific inspection strategy as a function of the cost of the basic events and decisions  $e$ ,  $z$ ,  $a$ ,  $\theta$ . The full decision tree consists of a large number of individual branches, which are prohibitive for the direct evaluation of the expected cost by calculation of the probabilities of occurrence of all branches. If after each inspection  $n_a$  different mitigation alternatives are available<sup>b</sup>, then the number of branches to consider is, as a function of the number of inspections  $n_{Insp}$ ,

$$n_b = n_a^{n_{Insp}} + \sum_{i=0}^{n_{Insp}} n_a^i \quad (2-22)$$

E.g for  $n_{Insp} = 5$  inspections and  $n_a = 3$  different possible mitigation actions, the number of branches becomes  $n_b = 607$ ; if  $n_{Insp} = 9$  and  $n_a = 2$  then  $n_b = 1535$ . Thus, to reduce the number of probability evaluations the following two alternative simplifications concerning the behaviour of the repaired element are considered:

- (a) A repaired element behaves like a new element
- (b) A repaired element behaves like an element that has no indication at the inspection

The second assumption is generally applied in the literature, e.g. Thoft-Christensen and Sorensen (1987), Madsen et al. (1989) or Faber et al. (2000). Both simplifications additionally assume statistical independence of the repaired element to the element before the repair. This is clearly not fulfilled in many cases, e.g. when the loading is the same before and after the repair. The simplification also makes an assumption about the number and times of inspections that are performed after the repair. In reality, the repaired element may be subject to additional inspections (which is reasonable if the element does not behave independently before and after the repair). Although the simplifications are not totally realistic, their influence is limited as generally the probability of repairing is low for the structures and deterioration modes under consideration. For elements with low reliability, the simplifications have to be reconsidered.

---

<sup>a</sup> Here the benefits of the structure under consideration are not directly included in the analysis, only the influence (cost) of the maintenance actions and events on the benefits (which in decision analysis is denoted *opportunity loss*).

<sup>b</sup> It is only the number of possible mitigation actions and not the number of different inspection outcomes that is of concern. This follows from the theorems of the Bayesian decision theory. The branches “Detection & no repair” and the “No detection & no repair” as shown in Figure 2.7 do consequently not require a separate computation.



By application of each of the two alternatives, only the probabilities of the branches as illustrated in Figure 2.8 have to be evaluated. Therein the first alternative is indicated, namely the consideration of repaired elements as equivalent to new elements.

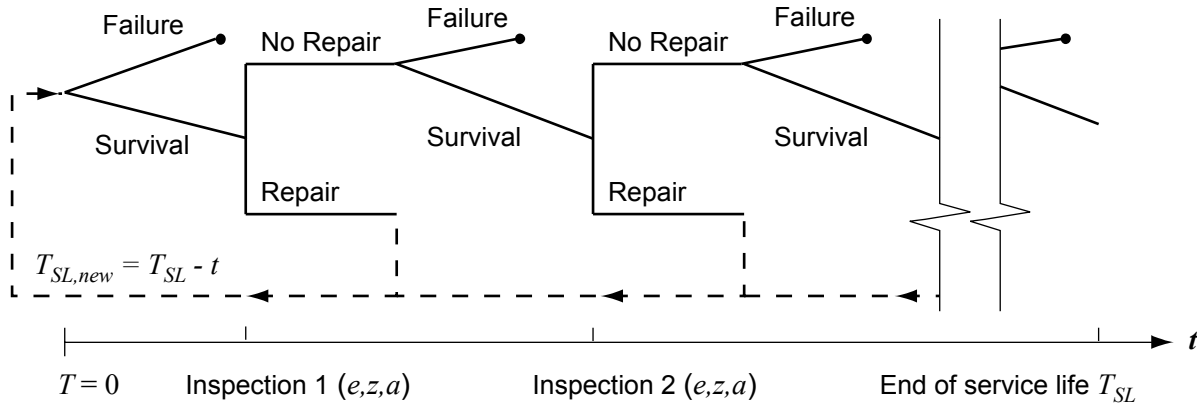


Figure 2.8 – Simplified RBI decision tree corresponding to simplification (a).

The applied simplifications render the optimisation of the repair technique superfluous, as no differentiation between different repair methods is made<sup>a</sup>. This is also justified by the fact that repair solutions are commonly tailor-made and not prescribed already in the inspection planning phase.

Discretising the time axis in yearly intervals ( $\Delta t = 1\text{yr}$ ), the probability of occurrence of all branches is now determined by computation of:

- $p_F(\underline{e}, d, T)$ , the probability of failure in the period  $T$ , given no repair in the period. It is dependent on the inspection parameters  $\underline{e}$  as well as the repair policy  $d$ .
- $\Delta p_F(\underline{e}, d, t_i)$ , the annual probability of failure in year  $t_i$  given no repair before  $t_i$  and given no failure before  $t_i$ <sup>b</sup>, evaluated from

$$\Delta p_F(\underline{e}, d, t_i) = \frac{p_F(\underline{e}, d, T_i) - p_F(\underline{e}, d, T_{i-1})}{\Delta t(1 - p_F(\underline{e}, d, T_{i-1}))} \quad (2-23)$$

- $p_I(\underline{e}, d, t)$ , the probability of indication at time  $t$  given no repair before  $t$ , as a function of the inspection parameters  $\underline{e}$  and the repair policy  $d$ .
- $p_R(\underline{e}, d, t)$ , the probability of repair given no repair at all inspections before  $t$  as a function of the decision rule  $d$  and the inspection parameters  $\underline{e}$ .

<sup>a</sup> This does not prevent from performing an optimisation of the repair technique, *once* a defect is identified. Given that a defect is present, this optimisation, which is a posterior decision analysis, becomes more important than it is in the inspection planning stage.

<sup>b</sup> The annual probability of failure as defined here is often referred to as failure rate or failure intensity. Note that the calculations of the expected cost are based on the probability that the failure falls in a specific interval, i.e. only the nominator in Equation (2-23) is required. However, the use of the present format ensures consistency with the acceptance criteria, which must be defined in terms of the annual failure rate, see Rackwitz (2000).

The expected cost of an inspection plan is now computed based on the cost model, which consists of:

- Expected cost of failure  $C_F$  (expected with respect to the possible impacts of the failure on the structure).
- Cost of inspection as a function of the inspection technique  $e_t$  applied at time  $t$ ,  $C_{Insp}(e_t, t)$ . If no inspection is planned at time  $t$  then  $C_{Insp}(e_t, t) = 0$ .
- Cost of repair,  $C_R$ .
- The interest rate  $r$ . It has to be determined based on the financial strategy of the operator or the owner of the structure.

The decision maker must be able to quantify the costs and interest rate. Thereby it is sufficient to operate with the ratio of failure to inspection / repair costs, no absolute values are required. It is furthermore observed that the results are in general not very sensitive to changes in the costs. In Chapter 5 an illustrative comparison between two different cost models as well as different interest rates is provided.

The total expected costs during the service life period  $T_{SL}$  can be computed as the summation of the expected failure cost, the expected inspection cost and the expected repair cost, Equation (2-24). All these are expressed by their present values.

$$E[C_T(\underline{e}, d, T_{SL})] = E[C_F(\underline{e}, d, T_{SL})] + E[C_I(\underline{e}, d, T_{SL})] + E[C_R(\underline{e}, d, T_{SL})] \quad (2-24)$$

Using simplification rule (a) the expected cost of inspections is defined by

$$E[C_{Insp}(\underline{e}, d, T_{SL})] = \sum_{t=t_1}^{t_{n_{Insp}}} \left[ (1 - p_F(\underline{e}, d, t)) \left( 1 - \sum_{i=1}^{t-1} p_R(\underline{e}, d, i) \right) \cdot \left( C_{Insp}(e_t, t) + p_R(\underline{e}, d, t) E[C_{Insp}(\underline{e}, d, T_{SL} - t)] \right) \frac{1}{(1+r)^t} \right] \quad (2-25)$$

$t_1$  is the time of the first inspection,  $t_{n_{Insp}}$  that of the last. Using simplification rule (b) the expected cost of inspections is, in accordance with Faber et al. (2000),

$$E[C_{Insp}(T_{SL}, \underline{e}, d)] = \sum_{t=t_1}^{t_{n_{Insp}}} C_{Insp}(e_t, t) (1 - p_F(\underline{e}, d, t)) \frac{1}{(1+r)^t} \quad (2-26)$$

The expected repair cost is, by use of simplification rule (a), given as

$$E[C_R(\underline{e}, d, T_{SL})] = \sum_{t=t_1}^{t_{n_{Insp}}} \left[ (1 - p_F(\underline{e}, d, t)) \left( 1 - \sum_{i=1}^{t-1} p_R(\underline{e}, d, i) \right) \cdot \left[ p_R(\underline{e}, d, t) (C_R + E[C_R(\underline{e}, d, T_{SL} - t)]) \right] \frac{1}{(1+r)^t} \right] \quad (2-27)$$

Using simplification rule (b) the expected cost of repair is, in accordance with Faber et al. (2000),

$$E[C_R(\underline{e}, d, T_{SL})] = \sum_{t=t_1}^{t_{Insp}} C_R p_R(\underline{e}, d, t) (1 - p_F(\underline{e}, d, t)) \frac{1}{(1+r)^t} \quad (2-28)$$

Using simplification rule (a), the expected cost of failure are computed as

$$E[C_F(\underline{e}, d, T_{SL})] = \sum_{t=1}^{T_{SL}} \left[ \left( 1 - \sum_{i=1}^{t-1} p_R(\underline{e}, d, i) \right) \frac{1}{(1+r)^t} \cdot \left( \Delta p_F(\underline{e}, d, t) (1 - p_F(\underline{e}, d, t-1yr)) C_F + p_R(\underline{e}, d, t) E[C_F(\underline{e}, d, T_{SL} - t)] \right) \right] \quad (2-29)$$

Using simplification rule (b) the expected cost of failure is, Faber et al. (2000),

$$E[C_F(\underline{e}, d, T_{SL})] = \sum_{t=1}^{T_{SL}} C_F \Delta p_F(\underline{e}, d, t) (1 - p_F(\underline{e}, d, t-1yr)) \frac{1}{(1+r)^t} \quad (2-30)$$

In this thesis the simplification rule (a) is applied, but Figure 2.9 shows the difference of applying rule (b) instead of (a) on the reference case presented in Chapter 5. The difference is small for this case but may be larger for other cases, e.g. when applying a smaller interest rate. The inspection strategies in Figure 2.9 are calculated as a function of the maximum annual probability of failure, the threshold  $\Delta p_F^T$ ; this concept is introduced in Section 2.4.2.2.

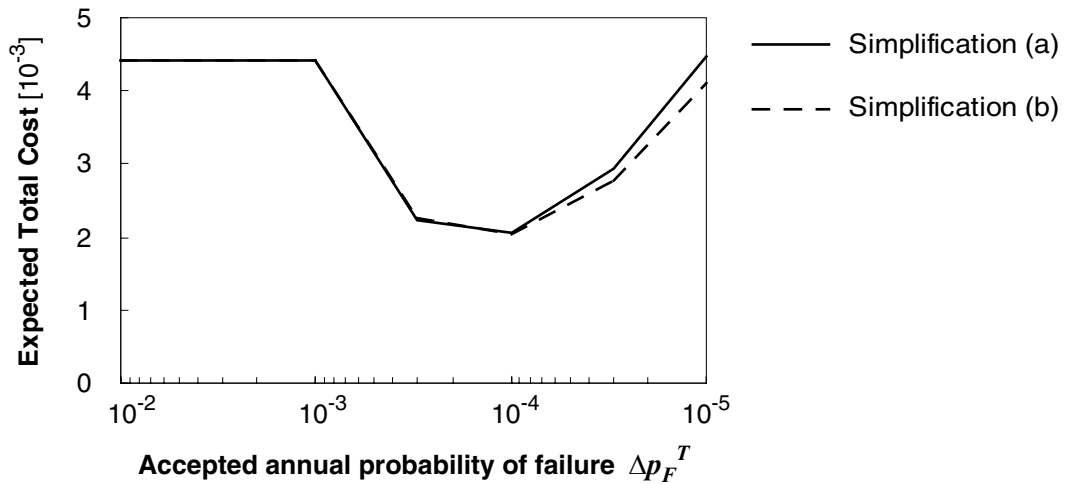


Figure 2.9 – Influence of the two different simplification rules in the evaluation of the total expected cost (applying the reference case from Chapter 5).

#### 2.4.1.1 Influence of the decision rule $d$

The decision rule prescribes the mitigation action that is performed, dependent on the inspection outcome. In the following three different decision rules are presented and subsequently discussed. These are

- a) Repair all defects indicated at the inspection
- b) After an indication perform a measurement and repair only cracks deeper than  $a_R$
- c) After an indication all cracks up to a depth of  $a_R$  are repaired by grinding (whose cost are assumed to be negligible), all cracks deeper than  $a_R$  are repaired by a more sophisticated technique with cost  $C_R$

In principle the decision rule is an optimisation parameter, i.e. the inspection plans should be evaluated for the different alternatives and the cost optimal alternative should be identified. However, in practice the decision rule is often given by the owner or the operator of the structure. Therefore the decision rule c) is prescribed in this thesis and no optimisation is performed<sup>a</sup>. To investigate the influence of the decision rule, the three alternatives are applied to the reference case described in Chapter 5, the results are given in Table 2.1. Thereby the repair limit was set to  $a_R = 1\text{mm}$  and the evaluation of the crack size is associated with an uncertainty described by  $\varepsilon_m \sim N[0,0.5\text{mm}]$ .

Table 2.1 – Expected cost as a function of the threshold on the annual probability of failure  $\Delta p_F^T$  for different decision rules [in  $10^{-3}$ ].

Accepted $\Delta p_F$ [ $\text{yr}^{-1}$ ] (Threshold)	Decision rule a)				Decision rule b)				Decision rule c)			
	E[ $C_T$ ]	E[ $C_F$ ]	E[ $C_I$ ]	E[ $C_R$ ]	E[ $C_T$ ]	E[ $C_F$ ]	E[ $C_I$ ]	E[ $C_R$ ]	E[ $C_T$ ]	E[ $C_F$ ]	E[ $C_I$ ]	E[ $C_R$ ]
$10^{-2}$	4.4	4.4	0	0	4.4	4.4	0	0	4.4	4.4	0	0
$10^{-3}$	4.4	4.4	0	0	4.4	4.4	0	0	4.4	4.4	0	0
$3 \cdot 10^{-4}$	3.2	1.5	0.6	1.1	2.2	1.4	0.7	0.1	2.2	1.5	0.6	0.1
$10^{-4}$	4.3	0.5	1.5	2.3	2.3	0.4	1.7	0.2	2.1	0.5	1.4	0.1
$3 \cdot 10^{-5}$	6.4	0.2	2.6	3.6	3.2	0.2	2.8	0.3	2.9	0.2	2.6	0.2
$10^{-5}$	9.6	0.1	4.1	5.5	4.6	0.1	4.2	0.3	4.5	0.1	4.1	0.3

Decision rule a) leads to the largest cost due to the large repair cost associated with repairing after every indication of a defect. This strategy, which is also not very realistic, is by far the less economical one. Little difference is observed between decision rule b) and c), indicating that the repair of detected defects less than 1mm has not a large influence on the reliability of the elements. This indicates that the choice of  $a_R = 1\text{mm}$  is reasonable<sup>b</sup>. The small difference between b) and c) justifies the prescription of decision rule c).

<sup>a</sup> Among the three presented alternatives c) will always be the most economical one, because it is assumed that the repair of small defects does not lead to additional cost. An optimisation is thus not reasonable for the presented alternatives.

<sup>b</sup> In principle the optimal  $a_R$  can be evaluated by application of decision rule b), the optimal  $a_R$  being the one leading to minimal total expected cost.

## 2.4.2 Optimisation procedure

In accordance with the previous section and accounting for a maximum acceptable annual failure probability  $\Delta p_F^{max}$  (the acceptance criteria as discussed in Chapter 7), the optimisation problem is written as

$$\begin{aligned} \min_{\mathbf{e}, d} E[C_T(\mathbf{e}, d, T_{SL})] \\ \text{s.t.} \quad \Delta p_F(\mathbf{e}, d, t) \leq \Delta p_F^{max}, \quad t = 0, \dots, T_{SL} \end{aligned} \quad (2-31)$$

Here the (operational) constraints on the optimisation variables  $\mathbf{e}$  and  $d$  are not explicitly stated, but have to be considered in the optimisation.

The inspection parameters  $\mathbf{e}$  are a set of different inspection methods and times when they are applied. If  $e_i$  represents the inspection method at the  $i^{\text{th}}$  inspection, which is planned at  $t_i$ , then  $\mathbf{e} = (e_1, t_1, \dots, e_{n_{insp}}, t_{n_{insp}})^T$ .

### 2.4.2.1 Restrictions to the general optimisation problem

As a first restriction to the general optimisation procedure it is required that the minimal interval of inspections is one year, consequently the possible inspection times can be discretised in yearly intervals<sup>a</sup>. A second restriction, which could for special cases be relaxed, is to demand that the same inspection technique is applied over the whole service life period, i.e.  $e_1 = e_2 = \dots = e_{n_{insp}} = e$ .

Because the evaluation of the total expected cost requires great computational efforts (due to the involved probability calculations), direct optimisation is not possible even with the above restrictions, as the possible number of different combinations of inspection times is prohibitive. For an element with service life  $T_{SL}$  it becomes  $2^{T_{SL}}$ , i.e. if  $T_{SL} = 30\text{yr}$  then there are  $1.07 \cdot 10^9$  possible number of different combinations of inspection times. To overcome this problem, two approaches are presented in the following sections that derive the inspection times as a function of a single parameter, which is then subject to optimisation. These are the

- Constant threshold approach
- Equidistant inspection times approach

Both approaches are described by Faber et al. (2000), a comparison between the two and a full optimisation is described by Bloch et al. (2000).

### 2.4.2.2 Constant threshold approach

The optimisation parameter is the threshold on the annual probability of failure,  $\Delta p_F^T$ . The inspection times are determined so that an inspection is always performed in the year before  $\Delta p_F^T$  is exceeded, as is illustrated in Figure 2.10.

---

<sup>a</sup> The case where the standard procedure is to perform two different inspections at the same time can be modelled as with single inspections when applying the inspection performance model for the combined effect of the two inspections, see Yang and Donath (1983).

As the inspection times are now a function of the threshold  $\Delta p_F^T$  and the inspection technique  $e$ , the optimisation problem can be rewritten as

$$\begin{aligned} \min_{e, \Delta p_F^T, d} & E[C_T(e, \Delta p_F^T, d, T_{SL})] \\ \text{s.t.} & \Delta p_F^T \leq \Delta p_F^{\max} \end{aligned} \quad (2-32)$$

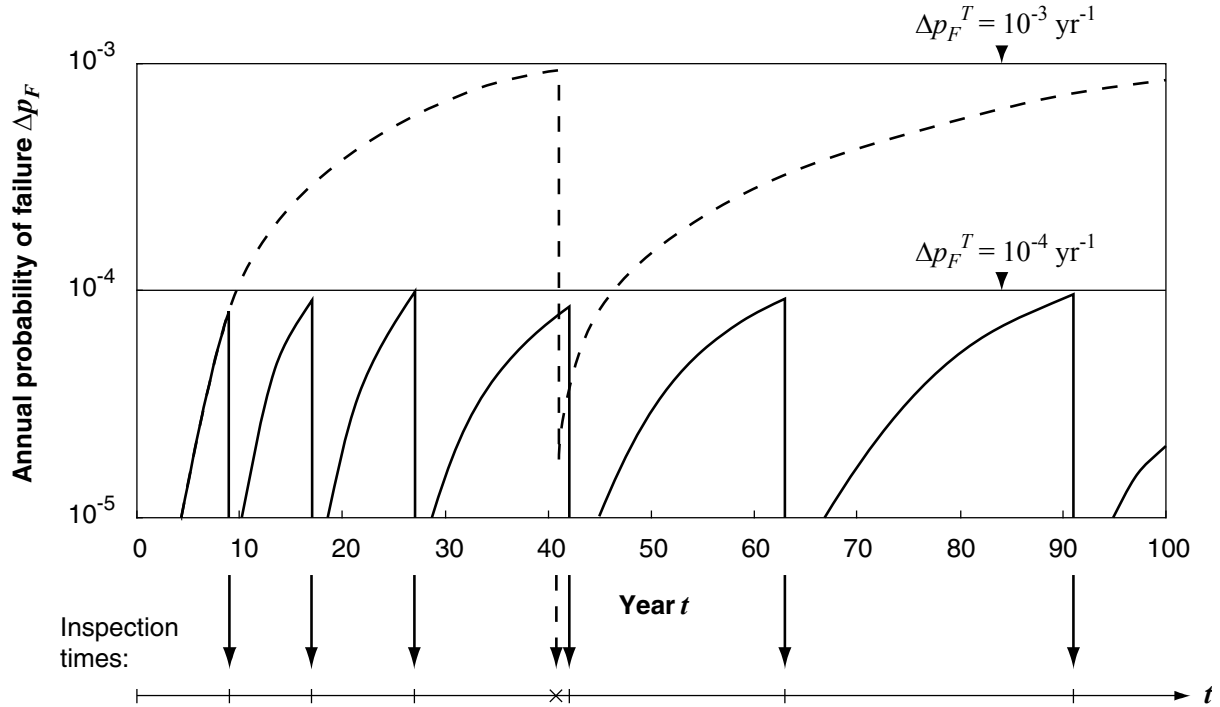


Figure 2.10 - Illustration of the threshold approach (from the reference case introduced in Chapter 5).

### 2.4.2.3 Equidistant inspection times

The optimisation parameter is the number of inspections to perform,  $n_{Insp}$ , or the constant interval between inspection times. In the former case the individual inspection times are determined by the requirement of equal intervals between inspections. The optimisation problem can then be written as

$$\begin{aligned} \min_{e, n_{Insp}, d} & E[C_T(e, n_{Insp}, d, T_{SL})] \\ \text{s.t.} & \Delta p_F(e, n_{Insp}, d, t) \leq \Delta p_F^{\max}, \quad t = 0, \dots, T_{SL} \end{aligned} \quad (2-33)$$

### 2.4.2.4 Optimisation

The final optimisation is performed by simply evaluating the total expected costs for different values of  $\Delta p_F^T$  or  $n_{Insp}$ . For the equidistant approach, the optimisation parameter is an integer variable, so the optimisation renders the exact optimal solution. In contrast,  $\Delta p_F^T$  is a

continuous variable, and the optimisation is thus only approximate for the threshold approach. Because the inspection plans are not very sensitive to small changes in  $\Delta p_F^T$ , this is not crucial. Figure 2.11 shows the optimisation for the reference case from Chapter 5 using both the threshold and the equidistant approach.

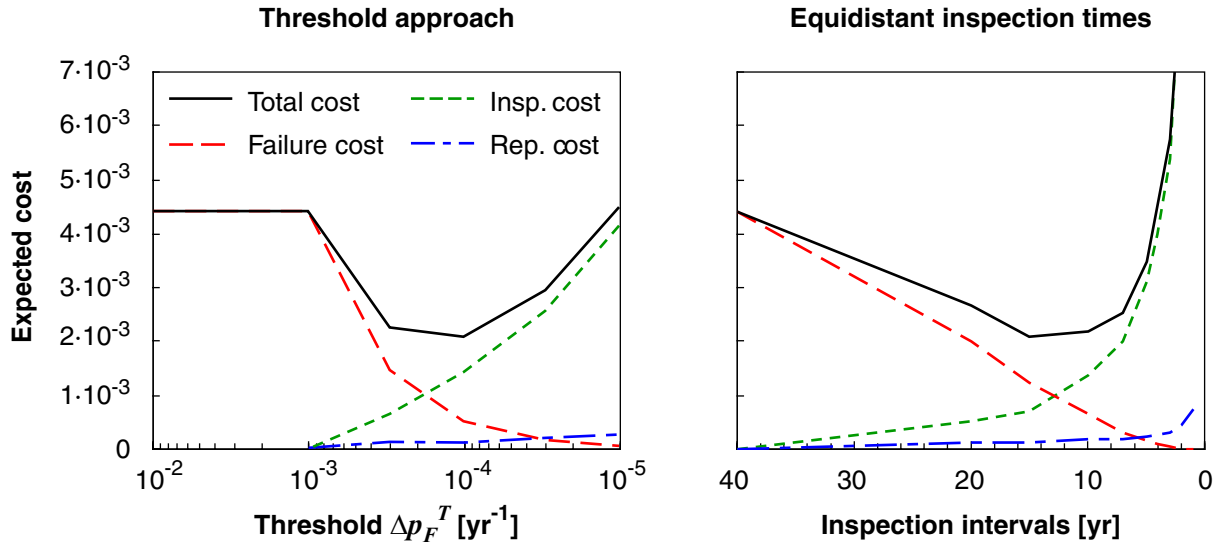


Figure 2.11 – Optimisation using the threshold and the equidistant approach for the fatigue reference case from Chapter 5.

For the case presented in Figure 2.11, both approaches lead to similar expected cost. Whereas the minimal total expected cost is  $\min E[C_T] = 2.07 \cdot 10^{-3}$  for the optimal threshold, it is  $\min E[C_T] = 2.08 \cdot 10^{-3}$  for the optimal equidistant case. However, a difference in the corresponding optimal inspection times is observed, they are  $t_{insp} = 9, 17, 27$  yr for the threshold approach and  $t_{insp} = 15, 30$  yr for the equidistant approach. For all thresholds larger than  $\Delta p_F^T = 10^{-3}$  yr<sup>-1</sup> no inspections are required, which explains the constant expected costs for these thresholds.

#### 2.4.2.5 Conclusions

It is generally observed that the total expected cost is not very sensitive to small changes of the optimisation parameters around the optimal value. This may also explain why both approaches render similar total expected cost, an observation that is in accordance with similar investigations by Bloch et al. (2000) on an example case. Regarding the resulting inspection times, their solutions demand more inspections for the optimal equidistant plan than for the threshold plan, which is in contrast to the presented results. It is consequently concluded that no general tendency exists as to which approach leads to more inspections.

These observations support the experience made by the author that, from the mathematical point of view, no approach is superior to the other. It should thus be determined by the owner or the operator of the structure which approach to pursue, in accordance with his practice and constraints: If constant inspection intervals are required due to operational reasons, then the equidistant plans will be preferable. If this is not essential, then the threshold approach is

advantageous, because the optimisation parameter allows the direct documentation of compliance with given acceptance criteria, Equation (2-32).

## 2.5 Reliability based inspection planning

In many situations the decision maker is not able to quantify the different cost factors involved in the inspection decisions. Although the optimisation of the risk is not applicable in such situations, the methodologies presented in this chapter can still be applied for the determination of the minimal inspection efforts required to comply with given acceptance criteria. These are typically specified in terms of acceptable annual probabilities of failure  $\Delta p_F^{max}$ , Chapter 7. The outcome of a reliability based inspection planning are the required inspection times and techniques for all structural elements in the structure. An application of reliability based inspection planning is described by Faber et al. (2003b).

The determination of the inspection times for a given inspection technique follows the procedure illustrated in Figure 2.10, i.e. an inspection is demanded before  $\Delta p_F$  exceeds the threshold  $\Delta p_F^{max}$  specified by the code or the operator. Although this methodology is named reliability based inspection planning it does not prevent a risk prioritisation: If the acceptance criteria  $\Delta p_F^{max}$  is given as a function of the redundancy, as discussed by Straub and Faber (2003b) and applied in Faber et al. (2003b), then the resulting inspection plans will demand more inspections for the more critical elements and are thus based on risk considerations. However, no optimisation is performed and the resulting inspection plan is only optimal if the acceptance criteria are optimal<sup>a</sup>. If they are optimal, then the reliability based is equivalent to the risk based inspection planning.

The inspection plans derived by means of reliability based inspection planning are only valid as long as inspections result in no-indication, as this is the basic assumption made for the determination of the inspection times according to Figure 2.10. However, the generic approach to RBI provides the means for adopting the inspection plans to the situations where a defect is indicated. This is treated in Section 5.5.10.

## 2.6 RBI for corrosion subjected structures

When considering RBI for the purpose of corrosion control, the same basic theory as utilised for fatigue subjected structures is applicable, as illustrated by Hellevik et al. (1999) or Straub and Faber (2000). However, because corrosion generally is of a less discrete nature and the evolution of the damage with time is different, the decision rules to apply are less obvious:

---

<sup>a</sup> This is generally not the case, because, apart from the practical problems involved, the acceptance criteria derived from the specifications in codes and regulations are ideally optimised from a societal point of view and not from that of the operator. In activities where structural failure can lead to large economical consequences the optimal inspection efforts can be much larger than the minimum required efforts, see also Chapter 7 for further considerations.



Whereas for fatigue the repair decision is based on the indication of a defect, this rule is generally not applicable to steel structures subject to corrosion. Steel structures subject to corrosion are often designed with a corrosion allowance, i.e. some corrosive wear is accounted for by the design and does not require a repair. Consequently, for most of these structures the event of indication is not relevant for decisions on the mitigation actions (as expressed by the decision rule  $d$ ); instead some corrosion depth  $d_R$  at which a repair is performed, has to be defined. Different approaches can be found in the literature: Whereas in Sydberger et al. (1995) it is assumed that this criterion is a fixed value, it is considered as a constant optimisation parameter in Hellevik et al. (1999).

It is noted that  $d_R$  should be a time dependent variable, taking into account that a certain corrosion depth is more critical if observed at an earlier stage: A corrosion depth equal to 10% of the wall thickness is generally not a serious problem if observed two years before the end of service life. However, if it is observed after the first two years in service, the updated corrosion model will predict a fast deterioration progress. The probability of failure after the inspection will then be very large and it may be economical to implement a risk mitigation action.

Unfortunately, it appears that all published approaches ignore the fact that an inspection plan, which is based on the assumption of a measured corrosion depth  $d_m$  smaller than  $d_R$ , is no longer valid as soon as  $d_m$  is observed, even if  $d_m < d_R$ . This is because the probability of failure is not the same if it is updated with the event  $\{d_m\}$  as if it is updated with  $\{d_m < d_R\}$ . A full model would thus require including any possible measurement result as a separate branch in the decision tree (which is not possible due to practical reasons). A solution to this problem is proposed in Section 5.6, based on the specifics of the inspection performance model for corrosion control, which is introduced in Chapter 4.



## **3 Deterioration Modelling**

### **3.1 Introduction**

This chapter introduces the probabilistic modelling of fatigue and corrosion degradation. These phenomena are by far the most important deterioration mechanisms occurring in steel structures. The Committee on Fatigue and Fracture Reliability (1982) notes that some 80-90% of the failures in metallic structures are related to fatigue and fracture; however, for many steel structures corrosion is the most costly deterioration mechanism, especially if the installed corrosion protection systems are included. Other deterioration mechanisms like steel erosion, including abrasion and cavitation, are not considered here.

The chapter presents only little original work, its importance consists in the fact that the models are presented in the view of their application in RBI. The emphasis is different from that in common textbooks on the subjects. Aspects which in the author's opinion are often not given sufficient attention in publications on RBI are treated in more details, such as the crack initiation models for fatigue.

### **3.2 Fatigue (SN model)**

#### **3.2.1 Introduction**

Fatigue of metals is a complex process that occurs in cyclic loaded structures such as ships, offshore structures, bridges, planes, pressure vessels, pipelines, cranes, vehicles, rail tracks and machinery. The awareness for and the modelling of fatigue started in the mid 19<sup>th</sup> century with the occurrence of fatigue failures in the railway industry. Since then tremendous research efforts have been directed towards the understanding and prediction of fatigue mechanisms and failures, see Stephens et al. (2001) for a historical overview. The brittle fractures in the welded Liberty ships during World War II resulting in the loss of large number of these vessels initiated a widespread research on these phenomena. Fatigue failures of both civil and military aircraft after 1950 has given rise to the understanding of the importance of inspection and maintenance in the treatment of fatigue. This has also motivated the first approaches to RBI, as outlined in Chapter 1. The catastrophic collapse of the semi-submersible platform "Alexander L. Kielland" in 1980 due to a fatigue failure, see Hobbacher (1983), has led to increased sensibility for fatigue in the offshore industry and motivated the developments of RBI in that area. An overview on the fatigue problems (and their treatment) in railroad bridges, highway bridges and offshore structures is presented in Byers et al. (1997b).

Fatigue cracks arise generally at locations with local stress concentrations, typically welds and other connection types (e.g. rivets, bolts) as well as cut outs. Welds are especially vulnerable due to inhomogeneities, imperfections and high stress concentrations caused by the

geometry, as discussed in Fricke (2003). In addition, the high tensile residual stresses in welded connections lead to the fact that compressive stresses are as damaging as tensile stresses, Maddox (1991). Consequently, if not stated otherwise, the considerations in this thesis are directed towards dealing with and modelling of fatigue in welds, although most observations apply also to other fatigue problems. The framework is further restricted to high-cycle fatigue, which is more common than low-cycle fatigue for many types of steel structures.

The SN fatigue model consists of a combination of the SN curves (due to Wöhler) with the Palmgren-Miner damage accumulation law. It is the common approach to fatigue in the structural design.

### 3.2.1.1 The aim of SN fatigue modelling

The basic idea presented in this thesis is to base the inspection planning on performance indicators obtained from normal design procedures. It is thus required to evaluate the reliability related to the design specifications and on this basis infer the influence of the design parameters on the optimal inspection planning. Because typical design calculations are based on SN models, it is necessary to evaluate the reliability according to these models.

In order to evaluate the influence of inspections on the fatigue reliability, a damage indicator which is directly observable is required. Because the SN damage indicator  $D_{tot}$  cannot be measured, an inspection does not give any direct information on this value, but only on the size of the crack. A model which predicts the crack size at any time  $t$  is thus required, Madsen et al. (1986). This is provided in the two subsequent Sections 3.3 and 3.4, where the crack growth modelling of fatigue deterioration is introduced and calibrated to the SN model.

### 3.2.1.2 Organisation of the chapter

In the following first the main concepts of design fatigue modelling are introduced, such as the SN curve and the Palmgren-Miner damage accumulation law. The determination of stresses, equivalent stress ranges and number of stress cycles is shortly outlined and factors influencing the fatigue life are outlined. The main focus lies on the evaluation of fatigue reliability related to the design specifications. This issue is treated at the end of the fatigue section.

## 3.2.2 Hot spots

In accordance with Straub and Faber (2002b), hot spots are defined as *identified possible locations of fatigue failures*. They are the areas in the structure that are subjected to high fatigue loading due to local stress concentrations. Typical welded connections, such as illustrated in Figure 3.1 and Figure 3.2, often contain more than one hot spot. It is assumed that fatigue occurs only at the hot spots. The RBI procedure is based on this assumption and violations thereof must be accounted for by adequate means, such as general visual inspections. This particular aspect forms part of the general asset integrity management procedure, see Goyet et al. (2002a), and is not considered in the present work.

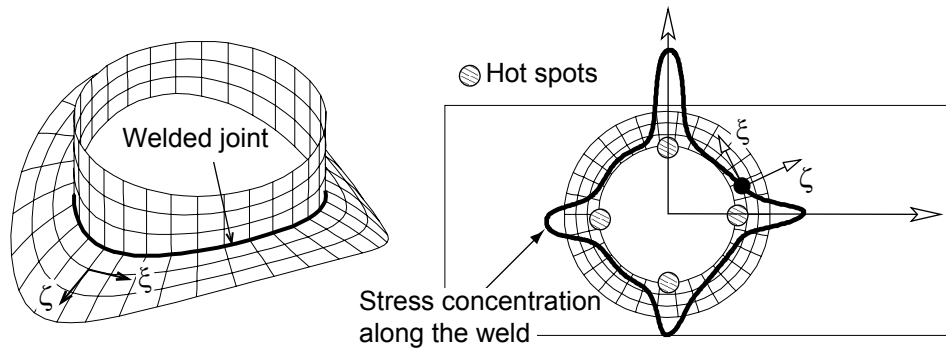


Figure 3.1 – Tubular joint with four hot spots, after Rouhan and Schoefs (2003).

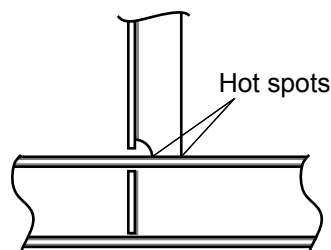


Figure 3.2 – Typical connection in a ship structure with two hot spots, from Bureau Veritas rules (2000).

### 3.2.3 SN curves

The SN curves are empirical models relating the number of cycles to failure ( $N_F$ ) to different (constant) stress ranges or amplitudes ( $\Delta S$ ). The classical experiment for the evaluation of  $N_F$ , as described in Radaj (1995), was introduced by Wöhler around 1860. Unfortunately, the definition of failure in the literature is ambiguous, two common definitions are:

- Failure occurs when the fatigue crack becomes a through-thickness crack.
- Failure is reached with the initiation of a crack, where the initiated crack is often defined as the visible crack.

Different formulations of  $\Delta S - N_F$  relationships are collected by the Committee on Fatigue and Fracture Reliability (1982), the classical is the Basquin Equation, assuming a linear relationship between  $\ln(N_F)$  and  $\ln(\Delta S)$ :

$$N_F = C_1 \cdot \Delta S^{-m_1} \quad (3-1)$$

$C_1$  and  $m_1$  are parameters that are determined by experiments. Alternatively a multi-linear curve, as illustrated in Figure 3.3 and defined in Equation 3-2, is often applied.

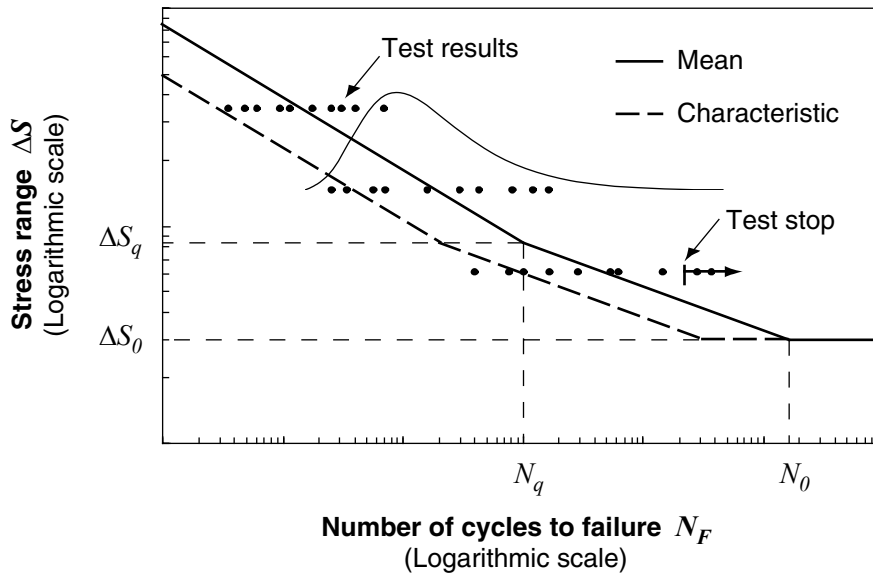


Figure 3.3 – Illustration of the bi-linear SN curve with cut off  $\Delta S_0$ .

For the SN curve in Figure 3.3 the definition consists additionally of the parameters  $m_2$ ,  $\Delta S_q$  and the so-called cut off  $\Delta S_0$  (also referred to as endurance limit or fatigue threshold), below which no failure occurs. The SN curve in Figure 3.3 is defined in Equation (3-2):

$$\begin{aligned}
 N_F &= C_1 \cdot \Delta S^{-m_1}, & \Delta S &\geq \Delta S_q \\
 N_F &= C_1 \cdot \Delta S_q^{(m_2-m_1)} \cdot \Delta S^{-m_2}, & \Delta S_q &\geq \Delta S \geq \Delta S_0 \\
 N_F &= \infty, & \Delta S_0 &\geq \Delta S
 \end{aligned}
 \tag{3-2}$$

Some guidelines and codes define  $N_q$  instead of  $\Delta S_q$ . However, because in experiments  $\Delta S$  is the free variable and  $N_F$  the dependent variable,  $\Delta S_q$  is the logical choice.<sup>a</sup>

SN curves are purely empirical models, thus no parametrical form of the curve has general advantages over another. It is to be noted that the use of a multi-linear curve and the application of a cut-off is controversial, IIW (1996). Figure 3.3 also illustrates the typical scatter in fatigue testing, which is the reason for the necessity for a statistical approach to the description of the SN curve.

### 3.2.3.1 Stresses in the SN analysis

Different approaches to the SN analysis are applied, distinguished by the level at which the stresses are evaluated and compared. A review is given in Fricke (2003), here only short definitions are stated for three important levels of analysis as illustrated in Figure 3.4:

<sup>a</sup> This is of relevance to the probabilistic description of the SN curve, as can be seen from Figure 3.3: If  $N_q$  were fixed, the change of slope in the characteristic curve would be at  $N = N_q$  instead of  $\Delta S = \Delta S_q$ . The same applies to the cut-off level.

- **Nominal stress approach:** SN curves are given for specific types of details, where  $S = S_n$  is the nominal stress, determined by external and internal loads and the cross section properties.
- **Hot spot stress approach** (also structural or geometrical stress approach): SN curves are given for specific types of materials and environments (typically corrosive/non-corrosive).  $S = S_{HS}$  is the hot spot stress, evaluated by consideration of the local geometry, but excluding the effect of the welds.  $S_{HS}$  is calculated by extrapolation of the stresses on the surface at some distance of the weld. However, no general agreement on the calculation of the hot spots stresses exists to date, Radaj and Sonsino (2000).
- **Notch stress approach:** Notch stresses  $S = S_N$  are the peak stresses at e.g. the root of a weld or the edge of a cut-out.

Other levels of stress analysis are applied in practice, see also Van Wingerde et al. (1995). In design procedures  $\Delta S_{HS}$  or  $\Delta S_N$  are often obtained by combination of the nominal stress with stress concentration factors SCF given for specific connection types. In this thesis, if not stated otherwise, fatigue stresses are hot spot stresses.

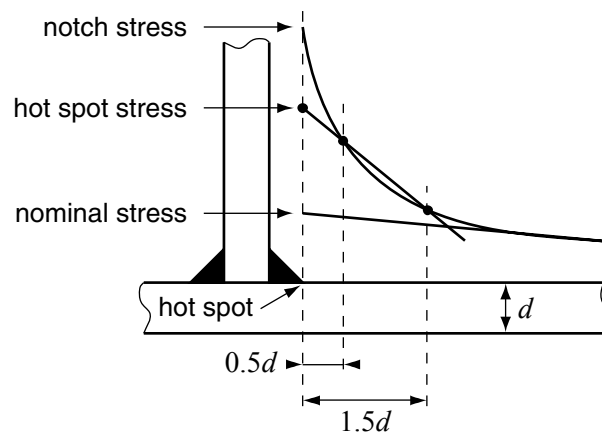


Figure 3.4 – Illustration of the different stress levels from Bureau Veritas rules (2000).

The SN curves are generally derived from test with uniaxial loading<sup>a</sup>. On the other hand, in most real structures multiaxial stresses occur. It is therefore required to relate these multiaxial stress states to fatigue equivalent stresses. As reported in Stephens et al. (2001), for materials with a ductile behaviour the stress ranges are best described by the von Mises equivalent stresses. For materials with brittle behaviour the use of the largest principal stress range is more appropriate. For specific applications the approach to apply depends on the definitions of the SCF's and the SN curves, as well as on whether the different stress components are in-

<sup>a</sup> This does not signify that the notch stresses or hot spot stresses are also uniaxial. This depends on the local geometry and the consideration of multiaxial fatigue is thus often included in the SCF; i.e. even if the nominal stresses are uniaxial, the hot spot or the notch stresses are often multiaxial.

phase or not. More details on the subject of multiaxial loading, including out-of-phase loading, are provided in Stephens et al. (2001).

### 3.2.3.2 Factors influencing fatigue performance

Aside from the stress range  $\Delta S$  the fatigue performance depends on many other factors which are illustrated in Figure 3.5. Some of these factors are explicitly accounted for by the design SN curves. Many codes include e.g. a thickness correction. Other factors which are not explicitly addressed introduce additional scatter in the SN curves.

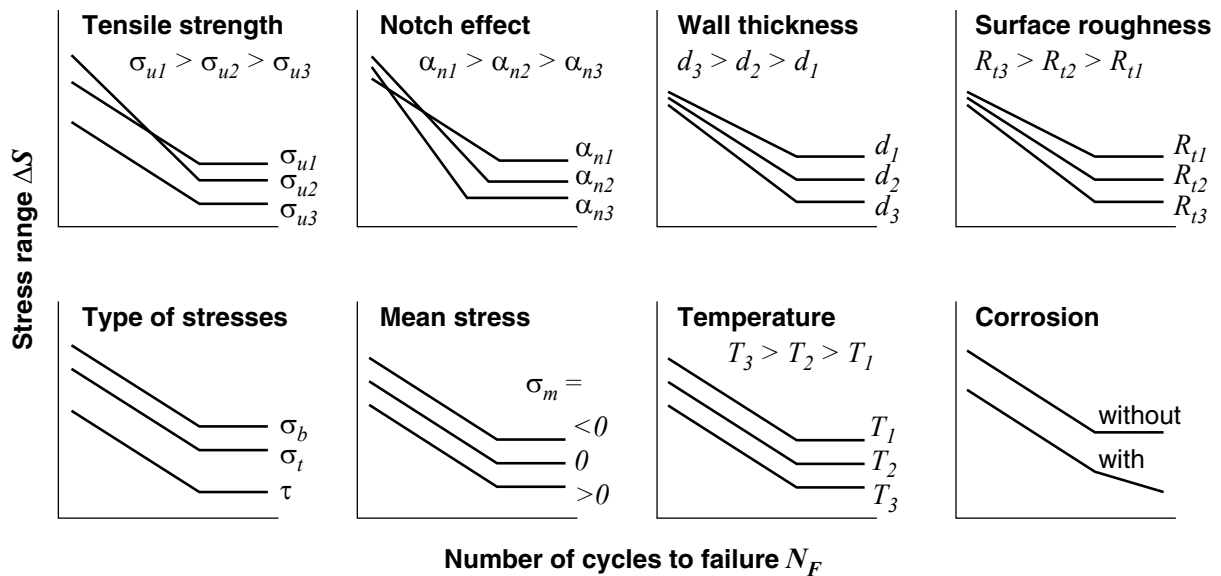


Figure 3.5 – Factors influencing the fatigue performance, after Radaj (1995).

### 3.2.3.3 Fatigue design SN curves

Most design SN curves are characteristic curves with a 95% survival probability. Some of the factors influencing fatigue life are directly addressed by the design rules, such as the thickness. Others are generally neglected, such as the stress ratio  $R_s$  (or equivalently the mean stress), which is difficult to determine in practice considering the residual stresses in welds.

Different fatigue design rules and SN curves from offshore related codes and standards, as well as from the Eurocode 3 (1992), are reviewed in HSE (2001). Different fatigue guidelines are discussed in Van Wingerde et al. (1995). The approaches vary between the different types of stresses, e.g. Eurocode 3 (1992) and SIA 161 (1990) give SN curves which are based on nominal stresses for a set of structural details in a non-corrosive environment. Eurocode 3 (1992) additionally allows for a hot spot stress approach. Most structural codes for offshore applications are based on a hot spot approach.



### 3.2.4 Damage accumulation (Palmgren-Miner)

By referring to the SN model, in general the linear damage accumulation law by Palmgren and Miner is implied together with the SN curve. It is an interaction-free theory, i.e. the damage accumulation after  $N$  cycles is independent of the order in which these cycles occur, Madsen et al. (1986). The damage increment is for each cycle with stress range  $\Delta S_i$  defined as

$$\Delta D_i = \frac{1}{N_{F,i}} \quad (3-3)$$

where  $N_{F,i}$  is the number of cycles to failure for  $\Delta S_i$  as given by the associated SN curve, Equations 3-1 and 3-2. This relationship dates back to Palmgren (1924). The total accumulated damage after  $N$  cycles is given by

$$D_{tot} = \sum_{i=1}^N \Delta D_i \quad (3-4)$$

Failure<sup>a</sup> is reached when  $D_{tot}$  reaches  $\Delta$ , the damage criteria which is generally modelled with mean value 1 and standard deviation  $\sigma_{\Delta}$ <sup>b</sup>. The SN limit state function is thus

$$g_{SN} = \Delta - D_{tot} \quad (3-5)$$

When the stress is a stationary stochastic process then the Palmgren-Miner model is a consistent description if the damage accumulates linearly with time. In Lutes et al. (1984) it is shown that it is also consistent with a fairly broad class of theoretical models that predict non-linear damage growth, including the Paris-Erdogan crack growth law<sup>c</sup>.

When the stresses are not a stationary process, such as the situations illustrated in Figure 3.6, then the Palmgren-Miner model is generally not consistent with observations. So-called sequence effects, which lead to non-stationary of the stress processes, may be due to modifications in the structure or the loading. Additionally many structures undergo completely different loadings during the construction process. At the design stage this is seldom accounted for, either because the loading history is not known beforehand or because no appropriate design procedure is available, such as SN curves for variable-amplitude loading.

---

<sup>a</sup> Miner (1945) defines failure as “the inception of a crack, when observed”. As discussed earlier, the failure criteria is different for different test series and not always clearly defined.

<sup>b</sup> Miner (1945) originally defined that failure occurs when the damage reaches 1. Thus, strictly speaking, the stochastic description of  $\Delta$  is in contradiction to Miner’s rule.

<sup>c</sup> If the damage indicator in the Paris-Erdogan law (see Section 3.3.3) is the ratio of the crack depth  $a$  to the critical crack size  $a_0$ , then the damage in general increases non-linearly with the number of stress cycles. However, it can be shown that an alternative damage indicator can be formulated from the Paris-Erdogan law which does increase linearly with the number of stress cycles, see also Madsen et al. (1986).

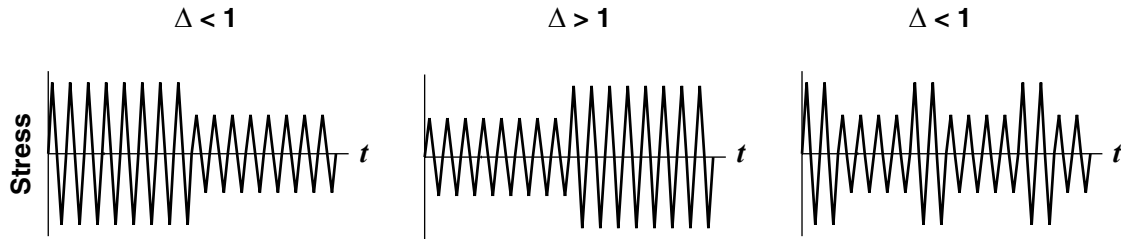


Figure 3.6 – Sequence effects due to crack initiation, after Dowling (1972).

### 3.2.5 Fatigue loading

If the SN model is assumed valid, then for the purpose of fatigue evaluation a stress process can be described by the distribution of stress ranges  $f_{\Delta S}(\Delta S)$ , the stress cycle rate  $\nu$  and (simplifying) the mean stress ratio  $R_S$ . For a profound description and discussion on the characterisation of fatigue loading see e.g. Madsen et al. (1986) or Dowling (1972). There different cycling counting methodologies are considered, whereof all those investigated by Madsen et al. (1986) give the same result for an ideal narrow-band stress history. For general loadings it is concluded that the rain-flow counting method generally gives the best results. This is also the method specified in Eurocode 3 (1992) together with the (for large numbers of cycles asymptotically equivalent) reservoir method.

The derivation of the probability density function (pdf) of the stress ranges  $f_{\Delta S}(\Delta S)$  and the stress cycle rate  $\nu$  is application specific. Byers et al. (1997b) discuss different application areas and their respective way of evaluating these parameters. Apart from the derivation from rainflow-counting of a realisation of the stress process,  $f_{\Delta S}(\Delta S)$  is often approximated by the Raleigh or the Weibull distribution. The Raleigh distribution is generally used when the stress process is both normal and narrow-band, see e.g. Lutes et al. (1984). It is also proposed in the literature to use the Raleigh approximation for broadband processes together with a correction factor accounting for the bandwidth of the stochastic process, Wirsching and Light (1980) or Lutes et al. (1984). In addition, an approximate solution for non-normal stress processes is suggested in Winterstein (1984).

Due to the cumulative nature of the Palmgren-Miner law (Equation 3-4), for high-cycle fatigue, the stress range distribution can be replaced by the expected value of the  $m_1^{\text{th}}$  order of the stress range,  $E[\Delta S^{m_1}]$ , if the material parameters  $C_1$  and  $m_1$  are constant with time. The total damage in the time period  $T$  is thus

$$D_{tot}(T) = \sum_{i=1}^{N(T)} \Delta D_i \approx N(T) \cdot E[\Delta D_i] = N(T) \cdot \frac{1}{C_1} \cdot E[\Delta S^{m_1}] \quad (3-6)$$

The number of stress cycles in the time interval  $T$  is

$$N(T) = \nu \cdot T \quad (3-7)$$

Equation 3-6 is valid for the single slope SN curve only. If an SN curve including a cut off  $\Delta S_0$  is applied, this is valid if the cut off is included in the distribution of  $\Delta S$  (a censored distribution or a truncated distribution with respective number of stress cycles). If a SN curve with multiple slopes is used, then an analytical solution as in Equation 3-6 is not generally available; however, for the case where the stress ranges  $\Delta S$  are Weibull distributed, a solution is given in Annex A.

The Weibull distribution occurs very commonly in natural processes related to dynamic response of elastic systems. In addition, the Weibull distribution is quite flexible in representing random variables with lower bounds, regardless of whether it is physically justified or not, Winterstein and Veers (2000). For marine structures, the long term stress ranges due to wave loads are often modelled by a Weibull distribution, Almar-Næss (1984); for fatigue loads on wind turbines, it is shown in Winterstein and Lange (1996) that the Weibull distribution provides a reasonable fit to observed data; for road bridges, Waarts and Vrouwenvelder (1992) observe that the fatigue loading can be approximated by a Raleigh distribution (which is a special case of the Weibull distribution). However, for some load types a parametrical description of the stress range distribution appears not appropriate, e.g. for railroad bridges as evaluated by Stadelmann (2003).

### 3.2.5.1 Equivalent stress range

As follows from Equation (3-6), the full stress range distribution can, for the single slope SN curve, be replaced by the constant  $\Delta S_e = (E[\Delta S^{m_1}])^{1/m_1}$ .  $\Delta S_e$  denotes the equivalent stress range, see Eurocode 3 (1992). The equivalent stress range is of importance in crack growth analysis, when, for computational reasons, it is not possible to account for the full stress range distribution  $f_{\Delta S}(\Delta S)$ . For the general case the definition is as follows:  $\Delta S_e$  leads (applying the (design) SN model) to the same total damage as the true distribution of  $\Delta S$ . It should be noted that  $\Delta S_e$ , as illustrated in Figure 3.7, is not necessarily representative for the stress ranges where the largest damage occurs.

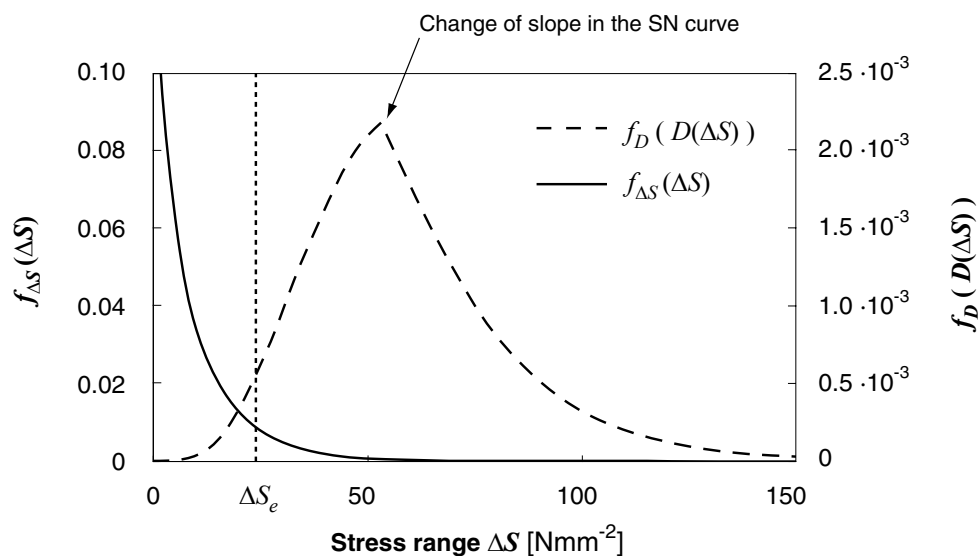


Figure 3.7 – Probability density function (pdf) of the Weibull distributed stress ranges and pdf of the corresponding damage, together with the equivalent stress range  $\Delta S_e$ . The model is that of the reference case defined in Section 5.5.

If the SN curve contains a cut off  $S_0$  then all cycles with stress ranges below  $S_0$  do not contribute to the fatigue damage. In that case an equivalent number of stress cycles,  $\nu_e$ , should be evaluated and  $\Delta S_e$  must then be calculated with  $\nu_e$ .

### 3.2.6 Uncertainties in design fatigue calculations

Uncertainty in fatigue analysis is related to

- 1) the fatigue modelling (uncertainty on the validity of the SN model)
- 2) the fatigue resistance (uncertainty on the applied SN curve)
- 3) the loading (natural variability and uncertainty in the environmental modelling and stress calculations)

These three sources of uncertainties should be modelled by corresponding random variables. However, due to the empirical nature of the SN model (parameters can only be determined by experiments) the different random variables cannot all be estimated individually. Because the parameters are interrelated, care is needed when models are taken from the literature for individual random variables separately.

The uncertainty in the SN model is related to a) the use of Miner's damage accumulation rule and b) the empirical nature of the SN curves (Its parametrical form is not physically justified and is thus a source of uncertainty. In addition not all influencing parameters are directly addressed and this increases the scatter in the observations). Whereas b) must be considered by introducing an uncertainty on the SN curve, a) is generally modelled by treating the damage at failure,  $\Delta$ , as a random variable, as discussed by the Committee on Fatigue and Fracture Reliability (1982) and Folsø et al. (2002).

#### a) Uncertainty on Miner's rule

The random properties of  $\Delta$  can account for the deviations of the real loading and conditions to those in SN fatigue tests. These deviations include especially the effect of variable-amplitude loading, illustrated in Figure 3.6.  $\Delta$  must thus be evaluated by comparison between the fatigue life as determined from variable amplitude loading in tests and as calculated based on Miner's rule (which includes tests with constant amplitude loading to determine the SN curves). It is noted that this requires a large number of tests. An overview of performed experiments is given in Schütz (1979), where it is pointed to the enormous cost of such test programs. It is concluded that it is generally not possible to predict if Miner's rule will be on the non-conservative or on the conservative side. The Committee on Fatigue and Fracture Reliability (1982) merges results from various experimental investigations; based on all available data it is suggested that a model of  $\Delta$  having a lognormal distribution with median equal to 1.0 and a coefficient of variation ( $CoV$ ) equal to 0.65 is reasonable. A survey of published test results for details from Marine structures is given in Wirsching and Chen (1988). There it is concluded that because fatigue behaviour is influenced by so many factors, it is difficult to interpret the meaning of each of the results. Although the given figures also "contain variability inherent in the material", some coherence is observed in the published values and the final statement is that "a slight non-conservative bias is suggested by recent tests on welded details, and uncertainties of 30-60% seem to be typical". The most commonly

applied model dates back to Wirsching (1984) and is based on unspecified “results of random fatigue testing”. Wirsching (1984) proposes a lognormal distribution with median equal to 1.0 and  $CoV$  equal to 0.3. To date, this model has become the standard model, e.g. Folsø et al. (2002) and SSC (1996), but it should be kept in mind that in the original publication it was noted that “this value reflects the application of professional judgement in reviewing the evidence [the data]”. Lacking alternatives, this model is however recommended if no specific information on the fatigue problem at hand is available.

#### b) Uncertainty on the SN curves

The uncertainty on the constant amplitude fatigue resistance as modelled by the SN curve is commonly accounted for by randomising the parameter  $C_1$  in Equations 3-1 and 3-2, where  $\log(C_1)$  is assumed to follow a normal distribution (implying a lognormal distribution for  $C_1$ ). The other parameters are then modelled by deterministic values. The distribution parameters of  $C_1$  must be evaluated by statistical analysis of the SN (Wöhler) tests; it is thereby of importance that tests are performed for a representative group of details and conditions (representative for the details and conditions on which the SN curve is applied). Although the design SN curves are defined by a characteristic value of  $C_1$  and are thus based on the distribution of  $C_1$ , published data on the scatter in  $C_1$  are sparse. For the SN curves of the Department of Energy (DoE), UK, the uncertainty is stated in e.g. SSC (1996) and BV NI 393. Ranges of uncertainties for  $C_1$  in Eurocode 3 (1992) are given in ECCS (1985) for special cases. For the SN curves in the API RP2A code the uncertainties are presented by Wirsching (1984).

Other parameters in the SN curves, especially  $m_1$  and  $m_2$ , are generally modeled as deterministic, mainly due to the limited amount of underlying experimental data; a probabilistic description of other parameters than  $C_1$  would increase the statistical uncertainty and introduce a correlation between the parameters.

As noted earlier, the modelling of SN curves in the high cycle regime is subject to large uncertainties. Especially the use of a cut off limit is controversial, but also the change of slope in the SN curves for higher numbers of cycles. It consequently appears reasonable to introduce an uncertainty also on the parameters  $\Delta S_q$  and  $\Delta S_0$  (respectively  $N_q$  and  $N_0$ ), however, this uncertainty must be based on engineering judgement due to the lack of such models. In Skjong et al. (1995) the cut off level  $N_0$  is modeled as a Normal distributed random variable with  $CoV_{N_0} = 0.1$ . This model is adopted in the present work.

#### c) Uncertainty on the stress ranges

The uncertainty modelling of stress ranges is, by nature, very much depending on the applied stress calculation methods and must thus be considered specifically for the individual cases. In the following, some literature on the subject is reviewed and general models are collected in Table 3.1 as published for structures subjected to wave loads. The uncertainties on the calculated stresses are expressed in terms of an error factor  $B_S$  which is multiplied on the calculated stress ranges  $\Delta S_{calc}$ :

$$\Delta S = \Delta S_{calc} \cdot B_S \quad (3-8)$$

Only values for standard design calculations are given in Table 3.1, values for other, more accurate methods may be found in the stated references. Uncertainties arising from the different steps of the calculation procedure are here integrated to one overall value.

*Table 3.1 – Different published models of the uncertainty on the stress,  $B_s$ , for a standard design procedure.*

Application area	Source	Stress level	Median $\tilde{m}_{B_s}$	$CoV_{B_s}$	Distribution
Ship structures	SSC (1996), Level 2	Hot spot	1	0.25	LN
	Folsø et al. (2002)	Notch stress	0.85 <sup>a</sup> 0.81 <sup>b</sup>	0.44	?, LN assumed <sup>c</sup>
FPSO	Francois et al. (2000)	Nominal	?	0.25	?
Offshore structures	Wirsching (1984)	Hot spot	0.7	0.5	LN

For ship structures, SSC (1996) proposes four different  $CoV$ 's on the calculated stress, depending on the level of refinement of the stress analysis. These values range from 0.15 to 0.3. In Folsø et al. (2002) the uncertainty on the stress calculation is divided in uncertainties in a) load calculation, b) nominal stress calculation, c) hot spot stress calculation and d) quality of the detail. A stochastic model for these factors is provided for two different levels of accuracy in the fatigue calculations. A similar study is described in Fricke et al. (2002) where the fatigue life of a ship hull detail with well-defined loading is compared, evaluated according to approaches of eight different classification societies. Calculated fatigue lives range thereby from 1.8 years to 20.7 years. The  $CoV$  of the calculated design fatigue lives is  $CoV_{T_{FL}} \approx 0.55$ ; this scatter can be attributed to assumptions regarding loads, local stress analysis and SN curves. Due to the different approaches, it is not possible to directly conclude on the scatter in the individual parameters. An additional direct calculation of the loading resulted in a fatigue life shorter than the fatigue life determined by most of the rule based calculations. In Fricke et al. (2002) it is noted that designers regard the considered details as unproblematic with respect to fatigue and conclude that this indicates overly conservative results of the calculation procedures used by the classification societies.

For Floating Production Storage and Offloading systems (FPSO), a comparative study of the fatigue analysis methods of five classification societies is reported in Francois et al. (2000). Therein nominal stresses obtained from the different methods are compared by means of the evaluated equivalent nominal stresses. This allows estimating the scatter in fatigue design stress calculations, but no comparison to measured stresses is made, thus no statement on calculation bias is possible. For offshore structures, the different contributions of the

<sup>a</sup> For calculations according to Registro Italiano Navale or Bureau Veritas rules.

<sup>b</sup> For calculations according to Germanischer Lloyds rules.

<sup>c</sup> The lognormal distribution is assumed for the calculation of the values presented here, no distribution type is stated in the reference.

individual steps in fatigue stress calculations are assessed in Wirsching (1984). These estimations are based on “the experience of several companies” involved in a study of the American Petroleum Institute.

### 3.3 Modelling the fatigue crack growth

#### 3.3.1 Introduction

The aim of this section is the definition and discussion of models describing the fatigue crack dimensions  $\underline{s}$  at any time  $t$ .  $\underline{s}(t)$  is a vector that, depending on the applied model, either consists only of the crack depth  $a(t)$ , the crack length  $2c(t)$  or of both depth  $a(t)$  and length  $2c(t)$ <sup>a</sup>. The presentation of the subject in the following is not aiming to provide a detailed understanding of the processes causing fatigue crack growth, but to identify a model for  $\underline{s}(t)$  that is suitable and tractable in the RBI framework. In addition, limitations and shortcomings of the applied models will be outlined.

The models describing  $\underline{s}(t)$  are embraced by the term *fracture mechanics* (FM) approach in the following (as opposed to the SN approach), because the models are mainly based on the linear elastic fracture mechanics (LEFM) theory. Readers interested in fracture mechanics are referred to Broek (1986), Anderson (1995), Newman (1998) and Schindler (2002), on which this section is based.

Considering crack growth due to fatigue, the lifetime of a crack can be divided in three stages, as illustrated in Figure 3.8:

- Initiation (Nucleation)
- Propagation (Crack growth)
- Failure (Such as fracture, exceedance of critical crack size, loss of stiffness)

The number of cycles spent in the initiation phase is denoted by  $N_I$ , the number of cycles in the propagation phase is  $N_P$  and the total number of cycles  $N_F$  (which is in analogy to the SN approach). These parameters are related by Equation (3-9):

$$N_F = N_I + N_P \quad (3-9)$$

The three stages are considered separately in the next three sections.

---

<sup>a</sup> This implies a model geometry. Whereas a true crack can have any possible geometry, the model assumes a geometry that is easy to describe analytically. The engineering models include the semi-elliptical surface crack, the elliptical interior crack and the 1-dimensional models. The crack geometry is then fully described by the two parameters  $a$  and  $c$ .

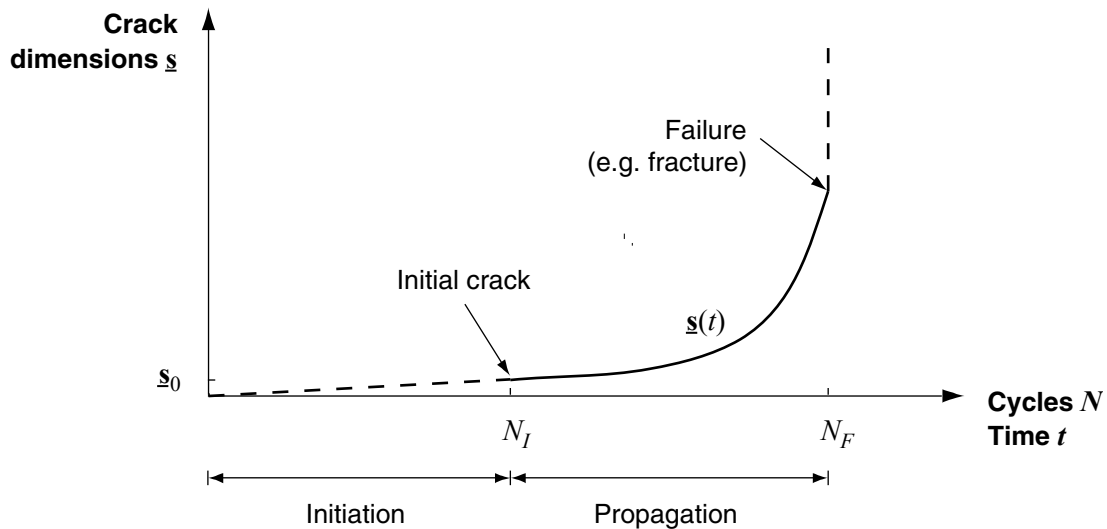


Figure 3.8- The three stages of fatigue crack growth schematically.

### 3.3.2 Crack initiation

The possible mechanisms leading to crack initiation are many, including inclusions in welds and other imperfections resulting from the manufacturing process, as well as micro-voids that develop to larger cracks by coalescence. Newman (1998) lists

- The slip-band cracking
- Inclusions or voids
- Service-induced or manufacturing defects

These three mechanisms are in accordance with the different crack growth cases given in Schijve (1979) as depicted in Figure 3.9. The first two phenomena, the growth of cracks from inclusions, voids or slip bands, are referred to as *small crack growth* in the following.

The different possible crack initiation mechanisms make it difficult to apply a general phenomenological model for fatigue crack initiation. A common engineering solution is the introduction of an initiation phase, which is defined by the number of cycles  $N_I$  to the development of a so-called initial crack with dimensions  $s_0$ , as illustrated in Figure 3.8. Because the underlying mechanics are not thoroughly understood,  $s_0$  is generally an empirical measure. Traditionally  $s_0$  is (imprecisely) defined as the size of the visible or detectable crack. Here the use of a stricter definition is advocated:  $s_0$  is chosen so that for this size the empirical crack growth relations used for describing the crack propagation phase are valid with sufficient accuracy. This definition is in accordance with Schijve (1979), where the following definition is proposed: “A crack is a macro-crack [in the propagation phase] as soon as the stress intensity factor  $K$  has a real meaning for describing its growth.”



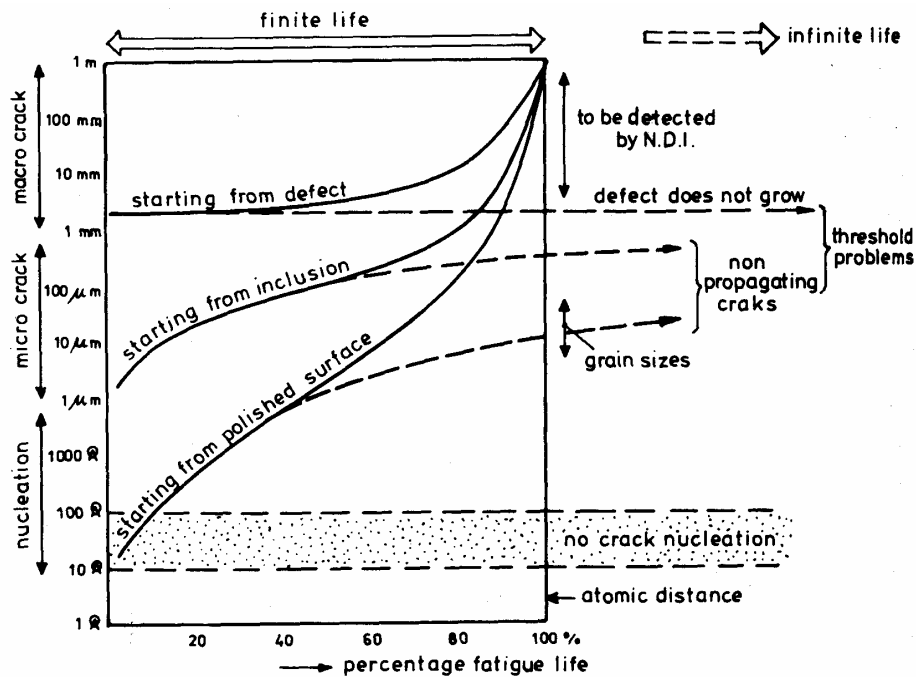


Figure 3.9 – Overview on the different crack initiation mechanisms and crack growth cases, from Schijve (1979).

According to Lassen (1997), the crack depth limit where LFM is applicable to the description of crack growth behaviour is  $a_0 = 100\mu\text{m}$ . Also, typical grain sizes in welded steel are in the order of 10–100 $\mu\text{m}$ . Because the application of LFM is not reasonable at crack sizes less than the size of the typical grain, the initial crack size should be larger than 0.1mm. In Phillips and Newman (1989) it is found that, for 2024-T3 aluminium alloy, accounting for small crack effects has only a small impact on the fatigue life analysis for cracks with initial depths of 0.1mm, but a large impact when assuming an initial depth of 0.01mm. This seems to indicate that 0.1mm is a reasonable choice for the lower boundary of the range where LFM is applicable.

For the purpose of fatigue crack growth modelling the main importance is to differ between cases where the initial crack is already present at the beginning (service-induced or manufacturing defects) and cases where a crack grows to the initial crack size  $s_0$  by short crack growth during  $N_i$  cycles. In a real structure generally both cases will be present; a pragmatic solution is to consider only the dominant mechanism.

### 3.3.2.1 Service-induced or manufacturing initial cracks

The causes of service-induced or manufacturing defects are many: poor workmanship, mechanical wear, corrosion<sup>a</sup>. The size and occurrence rate of such defects can only be found from measurements. In Bokalrud and Karlsen (1981) and Moan et al. (2000) this approach is pursued, deriving initial crack sizes from measurements on real structures. These studies are based on measurements at 827 randomly selected points on welds at various shipyards. The

<sup>a</sup> Cracks that initiate from corrosion defects are treated separately in Section 3.6 on corrosion fatigue.

depth of undercuts is found to follow an exponential distribution with mean  $E[a_0] = 0.11\text{mm}$ ; the occurrence rate of such undercuts is observed as  $325/20\text{m} = 16.2\text{m}^{-1}$ . In Moan et al. (2000) an extensive database of cracks detected on tubular joints in North Sea jacket structures is analysed. Results similar to those of Bokalrud and Karlsen (1981) are obtained, when accounting for the occurrence rate of the defects. Because inspection plans and SN curves generally consider failure of one hot spot, it is reasonable to take the distribution of the largest crack at the hot spot as the size of the initial crack. In Moan et al. (2000)  $E[a_0] = 0.38\text{mm}$  is found when assuming independency between the individual initial cracks, whereas the value given in Bokalrud and Karlsen (1981) changes to  $E[a_0] = 0.31\text{mm}$  based on 9.25 initial cracks per hot spot. Because these two studies base on a large amount of measurements from different structures, they are assumed to be representative for their type of structures from their specific building period. For modern weld qualities in steel, Lassen (1997) ascertains that the initial flaws are less than  $0.1\text{mm}$ . However, the distribution of the initial cracks clearly depends on the manufacturing process, the applied post-weld treatment and quality control. Additional references on distributions of initial crack sizes are given in Zhao and Stacey (2002).

If the service-induced or manufacturing defects are (on average) larger than the crack size limit for LEFM ( $\sim 0.1\text{mm}$ ), as discussed in the previous section, then the distribution found by measurements may directly be used as the distribution of the initial crack size. This neglects that in cases where no or only small manufacturing defects are present, the initial crack size may also be reached through micro-cracking. If the service-induced or manufacturing defects are generally smaller than the limit for LEFM, e.g. for grounded welds, then micro-cracking is the dominant mechanism and must be modelled as discussed in the next section.

### 3.3.2.2 Small crack growth

It has long been found that cracks also grow at stress intensity ranges well below the threshold  $\Delta K_{th}$ , used for describing the crack growth rate in the propagation phase together with Paris' law (this is introduced in Section 3.3.3). Figure 3.10 illustrates that these models are not valid for micro cracks; they underestimate the real crack growth rates.

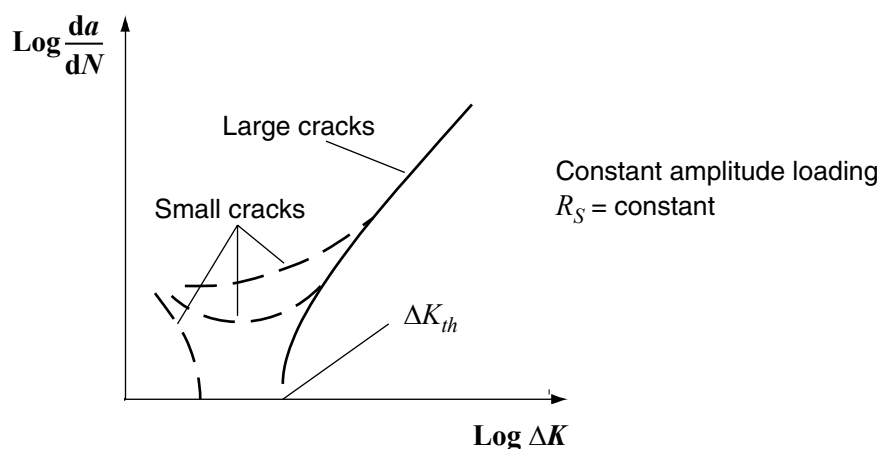


Figure 3.10 – Typical fatigue crack-growth behaviour of small cracks (micro-cracking) as opposed to large cracks (macro-cracks), from Phillips and Newman (1989).

Different approaches to the modelling of small crack growth can be found in the literature: The local stress-strain approach, as described in Lassen (1997), is first introduced by Lawrence (1978). A different approach, pursued by Phillips and Newman (1989), is to apply the  $\Delta K$  concept also to microcracks, assuming a relationship between  $\Delta K$  and  $da/dN$  as depicted in Figure 3.10. Bolotin et al. (1998) develop a simulation method where the damage accumulation in each grain is modelled separately. All these models demand for levels of model accuracy and parameters that are generally not available at the inspection planning stage. Because additionally the extrapolation of the models is crucial, these methodologies do not appear suitable for the application in RBI at the moment and are thus not treated further. It should also be noted that for the purpose of inspection planning no exact model of the crack behaviour below the initial crack size is necessary, because it is generally below the defect size that is detectable with non-destructive evaluation techniques applied in-service. It is thus sufficient to use a model that predicts the number of cycles to reach the initial crack size, as presented in Lassen (1997). The model introduced therein is given in Equation 3-10; it accounts for a dependency between the number of initial cycles and the applied stress ranges.

$$N_I = N_{I_0} \frac{(150 \text{ Nmm}^{-2})^{m_1}}{E[\Delta S^{m_1}]} \quad (3-10)$$

where  $N_{I_0}$  is the number of cycles to initiation at the normalising mean stress range,  $E[\Delta S] = 150 \text{ Nmm}^{-2}$ .  $N_0$  is modelled by a Weibull distribution with  $E[N_{I_0}] = 145 \cdot 10^3$  and  $\sigma_{N_{I_0}} = 50 \cdot 10^3$  and is assumed correlated to the crack propagation parameter  $C_p$ . Lassen's model assumes an analogue behaviour in the initiation phase to that in the propagation phase and the number of cycles to crack initiation is thus proportional to the stress range to the power of  $m_1$ , the exponential factor of the SN curve. It is noted that the model bases only on tests performed at constant amplitude loading with  $\Delta S = 150 \text{ Nmm}^{-2}$  and the extrapolation to other stress levels as performed by Equation 3-10 is not justified by experiments.

As outlined above, the initial crack size is highly dependent on the manufacturing process. In Lotsberg et al. (1999), where inspection planning on welded connections in a FPSO is described, it is assumed that for grounded welds the initiation time is equal to the propagation time (i.e. half of the fatigue life), whereas it is zero for as-welded joints. This simple solution is, however, in contradiction to the fact that the crack initiation life and the crack growth period are not necessarily related, Schijve (1994). Experiments reported in Lassen (1997) indicate a weak to medium correlation between the number of cycles in the propagation phase and the number of cycles in the initiation phase, depending on the local weld toe geometry.

### 3.3.2.3 Location and geometry of the initial crack

In engineering structures cracks generally initiate from inclusions, voids, service-induced or manufacturing defects. Newman (1998) notes that "crack initiation is primarily a surface phenomenon because: (1) local stresses are usually highest at the surface, (2) an inclusion particle of the same size has a higher stress concentration at the surface, (3) the surface is subjected to adverse environmental conditions, and (4) the surfaces are susceptible to inadvertent damage". Consequently the present work concentrates on surface defects.

Apart from the initial crack depth also the initial crack length is of interest. The crack length is generally considered by means of the initial aspect ratio, defined as  $r_{aspect} = a_0/c_0$ . In

Sigurdsson and Torhaug (1993) the influence of different  $r_{aspect}$  on the fatigue reliability is investigated and it is noted that for welded structures the ratio is usually small (in the interval 0.1 – 0.4). For corrosion fatigue, experiments described in Kondo (1989) show that for corrosion pits the aspect ratio is constant at all pit sizes,  $a_0 / c_0 = 0.7$ , see Section 3.6.

### 3.3.2.4 Summary

As mentioned, initial crack sizes depend on the material, environment, manufacturing process and quality and on the in-service conditions. Extrapolation of the values given above to other industries and applications is therefore critical. The different models for initial cracks are summarised in Table 3.2.

Table 3.2 Different published (engineering) models for initial surface cracks.

Source	Application	Depth <sup>a</sup>	Occurrence rate	Initiation time
Bokalrud and Karlsen (1981)	Butt welds in ship hulls	EXP <sup>b</sup> [0.11mm, 0.11mm]	16.2 m <sup>-1</sup> <sup>c</sup>	0
Moan et al. (2000)	Tubular joints in offshore jackets	EXP [0.38mm, 0.38mm]	per hot spot ( $\approx 0.47$ m)	0
Kountouris and Baker (1989) <sup>d</sup>	Welds in a TLP hull	LN [0.73, 0.78]	- *	0
Lotsberg et al. (1999)	Welds in a FPSO Hull	EXP [0.1mm, 0.1mm]	- *	0 if as-welded, half the propagation period if grounded
Lassen (1997)	Welded steel joints	Deterministic 0.1mm	- *	According to Equation 3-10

\* if no information on the occurrence rate is stated then it should be assumed that the implicit rate is one initial crack per hot spot or joint, respectively.

It is often noticed in the literature that crack initiation accounts for a large part of the fatigue life. Clearly this is highly dependent on the governing mechanism as illustrated in Figure 3.9 and is thus dependent on the weld quality, material and environment, as well as quality assurance procedures. No general relations are available in the literature and in general engineering judgement is needed to determine the model that applies in the specific case. It should be noted that the assumption of a short initiation time, as well as a large initial crack

<sup>a</sup> No information on the initial crack length is given in the stated references.

<sup>b</sup> EXP denotes the exponential distribution, LN the Lognormal distribution. Values in square brackets indicate the mean value and the standard deviation of the distribution.

<sup>c</sup> Corresponds to an expected value of the maximum crack size per hot spot equal to 0.31mm, Moan et al. (2000).

<sup>d</sup> As stated in Zhao and Stacey (2002).

size, is non-conservative in the context of the inspection planning methodology presented in this work, see Section 5.5.

Many (deterministic) approaches to inspection planning omit the modelling of crack initiation time. In principle these approaches account only for the time  $T_D$  that the crack spends between reaching a detectable crack size and final failure. The maximum inspection interval is then set equal to  $T_D$ , see also Section 5.5.7.2.

### 3.3.3 Crack propagation

Paris is the first to notice the relationship between the stress intensity factor range  $\Delta K^a$  and the crack growth rate  $da/dN$ , as described in Paris and Erdogan (1963). Figure 3.11 shows the typical fatigue crack growth behaviour.

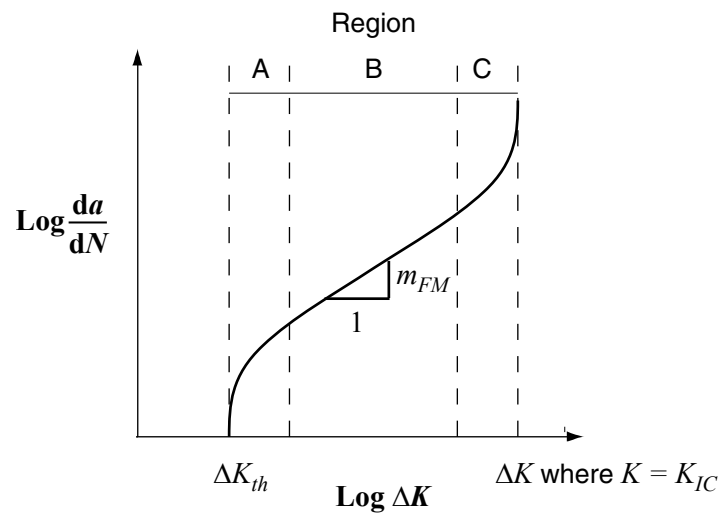


Figure 3.11 – Typical fatigue crack growth behaviour in metals.

The fatigue crack growth is generally divided in three different regions, in accordance with Figure 3.11. Paris' law (Equation 3-11) describes a linear relationship between  $\log \Delta K$  and  $\log(da/dN)$  in Region B. Therein  $C_P$  and  $m_{FM}$  are parameters to be determined by experiments.

$$\frac{da}{dN} = C_P \cdot \Delta K^{m_{FM}} \quad (3-11)$$

In Region A the crack growth process is governed by the threshold  $\Delta K_{th}$  below which no crack growth occurs. In Region C fatigue crack growth interferes with fracture, Paris' law thus underestimates the crack growth rate in this region.

<sup>a</sup> The index I on the stress intensity factor, indicating a crack opening mode I, is omitted, because a growing crack in general grows so that  $K_{II}$  (in-plane shear or sliding mode) or  $K_{III}$  (out-of-plane shear mode) disappear, Schindler (2002) or Stephens et al. (2001).

Equation (3-11) still forms the basis of most applied crack growth laws. However, many different modifications have been proposed to overcome the simplifications made by the expression and to include the crack growth behaviour during initiation and fracture. Newman (1998) lists some main directions. These modifications account explicitly for other factors, such as the maximal stress intensity factor  $K_{max}$  or, equivalently, the stress ratio  $R_s$ , defined as the ratio between minimal and maximal stresses:

$$R_s = \frac{S_{min}}{S_{max}} \quad (3-12)$$

The fracture toughness  $K_{IC}$  and Youngs' modulus  $E$  are other factors that are considered in crack growth laws. A widely applied law is given by Forman et al. (1967), where  $da/dN = f(\Delta K, R_s, K_{IC})$ .

In Elber (1971) it is shown that a crack closes before total unloading, i.e. a crack is closed when it is still in tension, and residual compressive stresses exist normal to the fracture surface at zero load. Because a crack cannot propagate while it is closed, Elber (1971) proposes to account for this so-called crack closure effect by replacing  $\Delta K$  in Equation (3-11) with  $\Delta K_{eff}$ , the effective stress intensity range:

$$\frac{da}{dN} = C_p \cdot \Delta K_{eff}^{m_{FM}} \quad (3-13)$$

$\Delta K_{eff}$  is determined from  $K_{max}$  and the stress intensity factor at which the crack is opened,  $K_{op}$ .

$$\Delta K_{eff} = \begin{cases} 0 & K_{op} \geq K_{max} \\ K_{max} - K_{op}, & K_{max} \geq K_{op} \geq K_{min} \\ K_{max} - K_{min}, & K_{min} \geq K_{op} \end{cases} \quad (3-14)$$

The threshold on the stress intensity factor,  $\Delta K_{th}$ , is at least partly explained by the effect of crack closure. If it is assumed that the crack closure effect is the only cause for  $\Delta K_{th}$ , it is possible to relate the threshold to  $K_{op}$  (in accordance with Equation (3-14) no crack growth takes place when  $K_{op} \geq K_{max}$ ). If alternatively  $\Delta K_{eff}$  is written as in Equation (3-15), it becomes apparent that the threshold is a function of the stress ratio  $R_s$ . This relation is also proposed in PD 6493 (1991).

$$\Delta K_{eff}(\Delta K, R_s, K_{op}) = \begin{cases} 0 & K_{op} \geq \frac{\Delta K}{1 - R_s} \text{ (Threshold)} \\ \frac{\Delta K}{1 - R_s} - K_{op}, & \text{else} \\ \Delta K, & K_{op} \leq \frac{\Delta K}{1 - R_s} \cdot R_s \end{cases} \quad (3-15)$$

The correlation between crack growth laws and experimentally assessed crack growth can be much improved by applying  $\Delta K_{eff}$  instead of  $\Delta K$ , Schindler (2002), yet the derivation of

$K_{op}$  from experiments or by calculations leads to new difficulties. Generally it can be concluded that more sophisticated laws may lead to a better prediction of the crack growth, *if* its parameters are known. Otherwise the application of simpler relationships (e.g. the classical Paris law) can be advocated for generic RBI, considering that the models are calibrated to the SN models, as described latter in Section 3.4. It is thus sufficient to use a parametric model that is able to represent the real behaviour of the crack growth. This is supported by Broeck (1986) who concludes that no particular expression based on  $da/dN$  will have significant advantages over another, because crack growth is influenced by so many uncontrollable factors and thus subject to large scatter. Different crack growth laws are applied and studied in Annex B where results from three different models are compared.

### 3.3.3.1 Parameters of the FM model

Because extrapolation of crack growth parameters to other materials (different steels) or environments is not appropriate, little information is generally available on these parameters for specific applications. In the following, some of the values presented in the literature are reviewed. Although some of the parameters are determined by calibration of the FM model to the SN model, according to Section 3.4 and demonstrated in Annex B, realistic estimates are required for all parameters. This allows validating the calibration procedure.

#### Paris parameters $m_{FM}$ and $C_P$

$m_{FM}$  and  $C_P$  are generally regarded as being interdependent. Using dimensional reasoning it has been argued that  $m_{FM}$  must be a linear function of  $\ln C_P$ , McCartney and Irving (1977). Lassen (1997) provides different values for the linear relationship, as found in the literature and from experiments, and finds good agreement between the different results. He states that a reference formula is given in Gurney (1978), which is

$$\ln C_P = -15.84 - 3.34m_{FM} \quad (3-16)$$

In addition, if the two parameters  $m_{FM}$  and  $C_P$  are determined empirically by curve-fitting, a dependency between the two variables is introduced through the analysis. Due to the dependency between  $m_{FM}$  and  $C_P$ , published values should only be referenced in pairs. Lassen (1997) argues that for the application of the FM model at stress ranges different from the test series in which the parameters where derived, it is better to use a model that assumes a fixed (deterministic)  $m_{FM}$ , independent of  $C_P$ . If the parameters are obtained from a calibration to the SN model for a specific stress range level, this objection is, however, not of concern; the relationship in Equation (3-16) is therefore applied in this work.

A collection of different parameter values given in the literature for structural steels are presented in Almar-Næss (1984). Theoretical considerations and published data reviewed in Irving and McCartney (1977) indicate that  $m_{FM}$  lies between 2 and 4. There it is furthermore noted that  $m_{FM}$  is considerably influenced by the environmental conditions. In addition, HSE (1998) collects and analyses published data on crack growth rates for different steels in different environments and compares those to the values given in PD 6493 (1991).

### Parameters $\Delta K_{th}$ and $K_{op}$

In Anderson (1995) it is concluded that the empirical relationships for the parameters given in the literature are not reliable for estimating  $\Delta K_{eff}$  (or  $K_{op}$ ), because empirical fits to a given set of data apply to a particular load regime (e.g. near-threshold behaviour) and should not be extrapolated to other regimes or other materials.

In PD 6493 (1991) equations for characteristic values of  $\Delta K_{th}$  are given based on a literature survey. There a strong dependency of  $\Delta K_{th}$  on  $R_S$  and the environment is found, which is in accordance with the crack closure effect, Equation (3-15). Due to large residual stresses (and therefore a large  $R_S$ ) for as-welded joints a value of  $\Delta K_{th} = 63 \text{ Nmm}^{-3/2}$  is recommended (this is, however, a characteristic value). Values are also reported in Almar-Næss (1984) for structural steels in air environment.

#### 3.3.3.2 Stress intensity factor range

Stress intensity factors  $K$  describing the crack propagation are evaluated according to the LEFM theory and have the generic form  $K = f(S, \sqrt{\underline{s}})$  where  $\underline{s}$  is a vector describing the crack dimensions.  $S$  is the von Mises effective stress; with respect to the notations in Section 3.2.3 it is approximately equivalent to the hot-spot stresses. Different approaches may be applied to evaluate the function  $f(S, \sqrt{\underline{s}})$ , the reader is referred to the literature referenced in Section 3.3.1 for details. Analytical solutions are generally not available for real structural details. On the other hand, finite element methods (FEM) are in general not appropriate for generic approaches because  $f(S, \sqrt{\underline{s}})$  should be available in an explicit form in order to be computationally efficient. Furthermore too much accuracy is not necessary regarding the simplifications made by the crack propagation models. Many empirical formulations for stress intensity factors of different structural details, as available in the literature, are, however, based on FEM. A widely applied equation of this type is presented in Newman and Raju (1981). There  $K = f(S, \sqrt{\underline{s}})$  is presented for surface cracks in a finite plate as a function of various geometrical parameters, assuming a semi-elliptical shape of the crack. Some modifications of the Newman and Raju (1981) modelling for stress intensity factors in welded tubular joints are reviewed in Etube et al. (2000). Such modifications account for the differences in the boundary conditions of the structural element to the finite plate (e.g. the effect of the weld geometry, Smith and Hurworth (1984), or the load shedding due to the statical indeterminacy in a tubular joint, Aaghaakouchak et al. (1989)). In Annex B the application of the Newman-Raju model together with the modifications is presented.

Considering a one-dimensional FM model, the stress intensity factors are often calculated by the use of a multiplying correction factor  $Y_G(a)$  that accounts for all the geometrical boundary conditions, Equation (3-17).

$$K = S \cdot \sqrt{\pi \cdot a} \cdot Y_G(a) \quad (3-17)$$

$Y_G(a)$  can be determined by a combination of different factors which describe the influence of the different boundary conditions individually, such a model is described in Hirt and Bez (1998).



### 3.3.3.3 Constant and variable amplitude loading

Although in contradiction to reality for most applications, generally a constant amplitude loading is assumed in the FM reliability analysis. If the loading is modelled as a stochastic process with variable stress ranges then, due to the dependency of the geometrical correction function on the crack size, the problem must be solved by time variant reliability analysis. Although standard software packages for reliability analysis, like Strurel (1999), in principle allow for the computation of such problems, their solution is numerically cumbersome and not suitable for application in RBI (where repetitive application of the algorithms including reliability updating is demanded). A discussion on the modelling of variable amplitude loading in fracture mechanics can be found e.g. in Schijve (1979) and Committee on Fatigue and Fracture Reliability (1982). A comparison of time variant and time invariant FM reliability analysis is provided in Marley and Moan (1992).

FM models including a lower threshold on the stress intensity factor range, such as Elbers model, should in principle be applied together with a variable-amplitude loading process. In reality a crack may stop to propagate for some time because  $\Delta K$  is below the threshold  $\Delta K_{th}$ , while suddenly propagating again due to few large stress cycles (the so-called sequence effects as already discussed in the SN modelling). These effects are neglected by the applied constant-amplitude load models, see Annex B for an illustration. Because they are also neglected by the SN model, the application of the constant-amplitude load models is consistent. However, this inaccuracy leads to an increased model uncertainty (in the SN model represented by the distribution of  $\Delta$ ).

### 3.3.3.4 Crack growth as a stochastic process

Crack growth can also be modelled as a stochastic process, see Yang (1994) for an overview. Thereby some of the parameters of the crack growth laws are modelled as random processes of time. A model with constant parameters, as used in the framework of this thesis, is equivalent to the special case of the stochastic process model where all parameters are fully correlated over time. It is concluded in Yang (1994) that this assumption has been found to be “quite reasonable”, although slightly conservative<sup>a</sup>. As noted in the previous section, in view of the calibration it is consistent to apply a simple model that corresponds to the SN model.

## 3.3.4 Failure and fracture

Two separate criteria are generally used in the FM analysis. The first criterion corresponds the situation where failure occurs when the crack exceeds a critical crack size, the second criterion represents brittle failure (fracture), e.g. Madsen et al. (1986). It is noted that in reality other failure modes may occur, such as yielding of the remaining cross section, and that these failure modes may interact, see also PD 6493 (1991). They are not considered in the following, in accordance with the general tradition in FM reliability analysis. However, other failure modes can sometimes be accounted for by setting the critical crack size accordingly.

---

<sup>a</sup> This does not hold for the applications as presented here, because the model is calibrated to the SN model.

The limit state functions corresponding to the two above criteria, if only crack depth is considered decisive, are given in Equations (3-18 and 3-19).

$$g_{a_c} = a_c - a \quad (3-18)$$

$$g_{fracture} = K_{IC} - K \quad (3-19)$$

$a_c$  is the critical crack depth used in the first failure criterion. It is normally chosen as the thickness of the structural element, so that failure is equivalent to a through-thickness crack. In many cases this is a conservative assumption due to the residual load carrying capacity. In principle  $a_c$  should correspond to

1. the failure criteria used in the SN tests.
2. the crack size which corresponds to the assumed consequences of failure.

Failure criteria in SN tests are not uniquely defined (different criteria are used), however, they are generally equal to or smaller than the through-thickness crack. Because consequences for most structural elements do not occur before the crack size has reached the thickness of the element, it is reasonable to set the critical crack size equal to the thickness. In addition, due to the highly non-linear characteristics of crack growth, the reliability is not very sensitive to  $a_c$ , so that this parameter can be determined by means of engineering judgement.

$K_{IC}$ , the (plane strain) fracture toughness, is the failure criterion for brittle failure. It is a temperature dependent material parameter which characterises the resistance to crack extension, evaluated by tests as described extensively by Broeck (1986). The fracture criterion corresponds to a first passage problem and time-variant reliability methods have to be applied for the evaluation of the associated failure probabilities.

Hagen and Sigurdsson (1994) compare the reliability calculated with each failure mode separately and combined on a hot spot in a tubular joint in an offshore jacket structure. They find that, when assuming that the stresses can be described by a Gaussian process, the contributions of both limit states to the total reliability are in the same order of magnitude. However, when they account for the non-Gaussian properties of the stress process (i.e. the higher order moments of the process as derived from the structural analysis), they observe that brittle fracture becomes the dominant failure mode. This is caused by the thicker tails of the non-Gaussian distributions, leading to a much larger outcrossing rate for high fracture thresholds.

The results from Hagen and Sigurdsson (1994) are in contradiction to the argument from Almar-Næss (1984), namely that “if region C crack growth [where fatigue and fracture interacts] becomes important, the cycle rate and the load spectra for most marine structures is such, that final failure will be imminent [when considering only the ductile failure mode]”. As a consequence, in spite of the results from Hagen and Sigurdsson (1994), fatigue reliability analysis generally concentrates on the critical crack size failure mode. The reason for this simplification is often the increased computational requirements when considering brittle fracture (the need for time variant reliability calculations and more accurate evaluation of stresses).

In the context of the generic approach to RBI, neglecting the fracture failure mode is justified by the fact that the FM model is calibrated to the SN model, which is representative for ductile failure. Furthermore, as the analysis is performed assuming constant amplitude loading, accounting for brittle failure does not change the results significantly. Because inspections are less effective for components that are subject to brittle failure, this simplification is, however, non-conservative. For structures with large load peaks with small occurrence probability (such as the non-Gaussian model from Hagen and Sigurdsson (1994)) fatigue problems have to be treated differently already during design calculations, as the SN concept in that case is no longer appropriate.

### 3.4 Calibration of the FM model to the SN model

Because design calculations are performed by means of the SN model and because inspection planning demands for FM models, the two models have to be related to each other. Such a link between the SN approach applied in design and the FM approach needed for RBI is the core of a generic approach to RBI based on design fatigue evaluations. Because the purely empirical SN model, which is based on experiments, contains all information available from the design, the semi-empirical FM model is calibrated to the SN model. Several RBI procedures are based on such a calibration, see e.g. Madsen et al. (1987), Pedersen et al. (1992), Lotsberg et al. (1999), Faber et al. (2000) and De Souza and Ayyub (2000). Three different calibration techniques from the literature are outlined in the following and subsequently the proposed calibration algorithm is presented.

When calibrating models, a measure of the goodness-of-fit has to be determined. The only information contained in the SN model is whether the hot spot has failed or survived, whereas the FM model gives the crack dimensions  $\underline{s}$  after any number of cycles  $N$ . When the model is deterministic, the FM model must thus be calibrated so that after  $N_F$  cycles the crack size reaches the critical crack dimensions  $\underline{s}_c$  (depending on the definition of failure in the SN model). The deterministic calibration is illustrated in Figure 3.12, assuming that also the initial crack size is known.

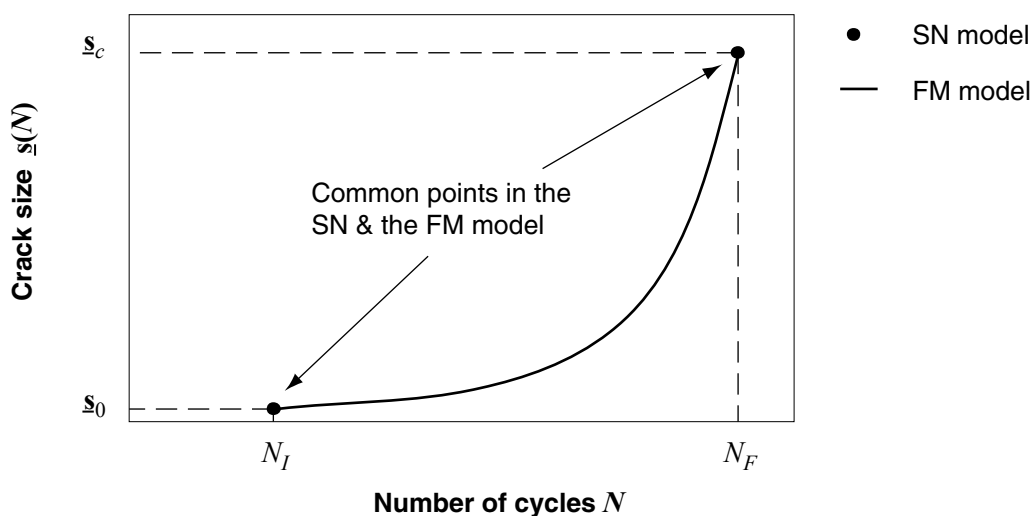


Figure 3.12 – The FM calibration principle for the deterministic case, from Straub (2001).

If a stochastic description of fatigue is considered, the calibration remains in principle as in Figure 3.12, but the parameters to which the FM model is fitted ( $N_F, \underline{s}_c, N_I, \underline{s}_0$ ) become random. The calibration methods presented in the literature use different strategies to account for the randomness of the fatigue phenomena. In Pedersen et al. (1992) and De Souza and Ayyub (2000) the FM model is calibrated so that the calculated number of cycles to failure  $N_F$  for different stress levels correspond to the SN curve. Whereas in De Souza and Ayyub (2000) only the mean SN curve is calibrated<sup>a</sup>, in Pedersen et al. (1992) additionally the characteristic curve is calibrated. In Faber et al. (2000) it is concentrated on the stress range under consideration. The FM model is calibrated so that the difference in the distribution of  $N_F$  between the SN and the FM approach is minimised for the considered  $\Delta S_e$ . These approaches are illustrated in Figure 3.13.

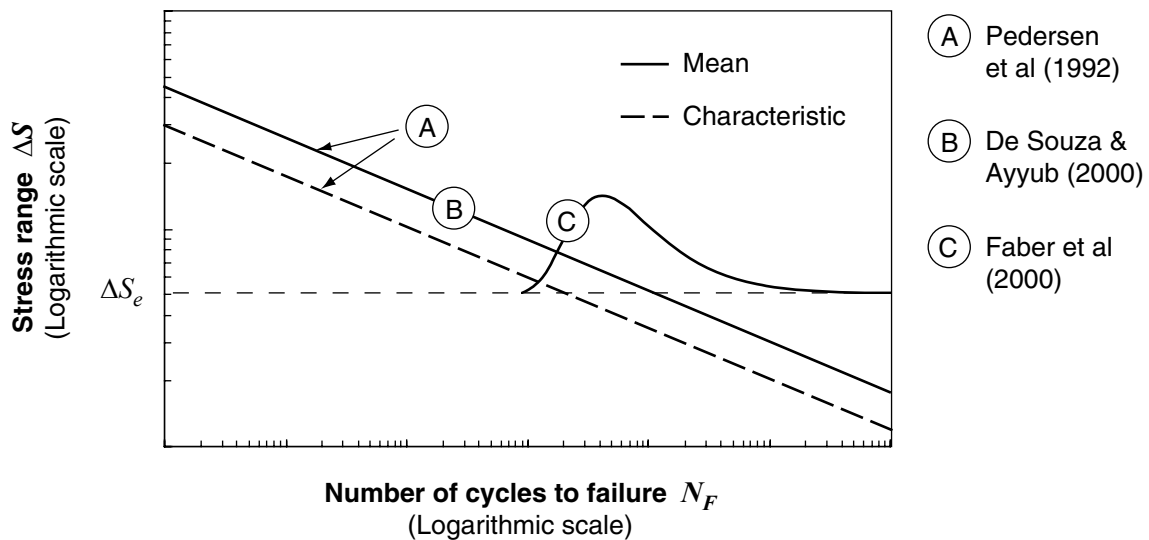


Figure 3.13 – Illustration of the different calibration approaches.

Clearly the calibration to the mean SN curve (approach B) does not account for the full stochastic information available from the SN model. Approach A, calibrating the FM model to the mean and the characteristic SN curve, accounts for the statistical nature of the SN curve and has the advantage that the calibration is valid for all stress range levels (i.e. for different *FDF*). It does however neglect the exact distribution at the considered stress range level. Because typical probabilities of failure that are dealt with in inspection planning are in the range of  $10^{-5}$  to  $10^{-3}$  per annum, it is the tail of the distribution (of  $N_F$ ) that is of interest. This tail is only accounted for by the method applied by Faber et al. (2000), which, on the other hand, has the disadvantage that it is numerically demanding and that it is valid only for the considered stress range. The calibrated parameters of the FM model are thus different for different stress ranges. This approach is applied within the framework of this thesis; the procedure is described in detail in the following section.

<sup>a</sup> This approach is a purely deterministic one, because for each stress range there is exactly one deterministic value of  $N_F$  to which the FM model is calibrated.

### 3.4.1 Applied calibration algorithm

The probability distribution of  $N_F$ ,  $F_{N_F}(N)$ , is equivalent to the probability of failure,  $p_F$ , as a function of the number of cycles (or time, when a constant stress cycle rate is assumed):

$$p_F(N) = F_{N_F}(N) \quad (3-20)$$

Because the reliability index  $\beta$  is uniquely related to  $p_F$  by means of Equation (2-3), the calibration can be performed based on  $\beta$ . Such a calibration is illustrated in Figure 3.14.

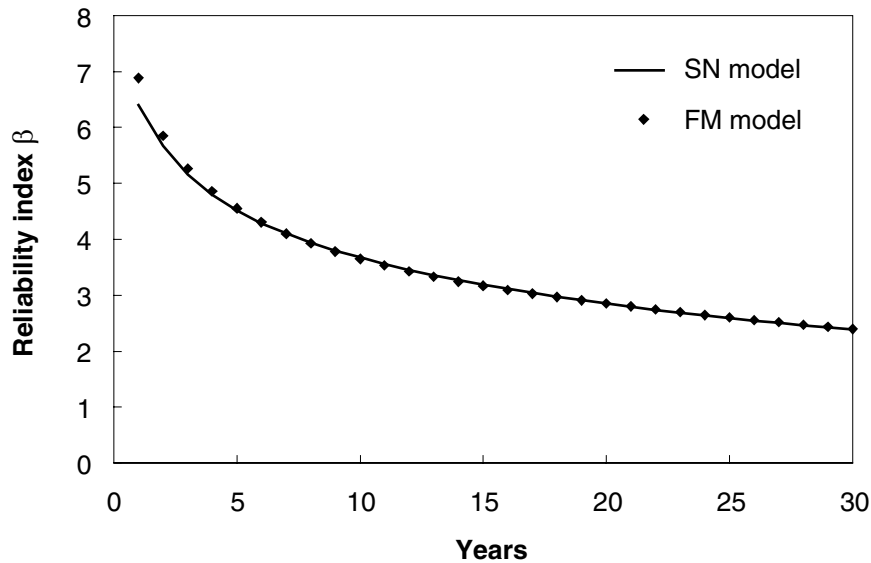


Figure 3.14 – Calibration of the FM model to the SN model, from Straub (2001).

The calibration is performed by a least-squares fitting in  $\beta$ -space, i.e. the following function is minimised with respect to the parameters of the FM model,  $x_1 \dots x_N$ :

$$\min_{x_1 \dots x_N} \sum_{t=1}^{T_{SL}} (\beta_{SN}(t) - \beta_{FM}(t; x_1 \dots x_N))^2 \quad (3-21)$$

$\beta_{SN}(t)$  is the reliability at time  $t$  as evaluated using the SN model,  $\beta_{FM}(t; x_1 \dots x_N)$  the reliability at time  $t$  as evaluated using the FM model with parameters  $x_1 \dots x_N$ .  $T_{SL}$  is the service life of the considered structures.

It could be argued that the minimisation should be performed in  $p_F$ -space instead of  $\beta$ -space because in general the expected cost is a linear function of the probability of failure and the calibration in  $\beta$ -space may thus over-emphasise the lower failure probabilities which have only minor influence on the total expected cost. However, as the FM model is used at different levels of maximum failure probabilities, it appears reasonable to focus equally on the different orders of magnitude. This is ensured by the calibration in  $\beta$ -space. An alternative would be to perform the calibration on  $\log(p_F)$ .

The minimisation in Equation (3-21) is performed by a quasi-Newton method with a finite-difference gradient evaluation<sup>a</sup>. The evaluation of the reliability indexes is performed by a FORM or SORM algorithm, because they give smooth results with respect to the minimisation variables. In the process it has to be ensured that these algorithms are sufficiently stable. Generally it can be stated that the calibration is numerically demanding.

#### 3.4.1.1 Calibrated parameters

The choice of the parameters to calibrate depends on the applied FM model. In general two parameters should be calibrated. Very often the crack growth rate parameter  $C_p$  is used, as for most models this is the parameter with the largest influence on the crack growth. The second parameter may be chosen as the parameter for which least information is available. It is of importance that the calibrated parameters have a certain influence on the evaluated reliability (as measured by the sensitivity factor  $\alpha$ ). Annex B shows the use of different parameters for the calibration of different models.

---

<sup>a</sup> The subroutine BCONF from the Fortran library IMSL (1997) is used.

## 3.5 Corrosion

### 3.5.1 Introduction

Although great efforts are spent on understanding, predicting and controlling corrosion, only relatively few research projects are concerned with the quantitative engineering models that are required for structural reliability analysis. As a consequence, for a wide range of engineering problems, the quantitative modelling of corrosion is still not satisfactory in view of an application in inspection and maintenance planning. Especially the modelling of spatial aspects is often not addressed at all and no engineering model is presented in the literature. This is reflected in this section, no readily applicable models for corrosion reliability are presented. Instead the different corrosion phenomena are very briefly introduced, followed by a review of the quantitative corrosion modeling for some specific applications and a short discussion of the uncertainty modeling. A section that considers the role of RBI on structural elements that are corrosion protected is included to account for the fact that in many applications the most critical structural elements will be protected. Finally the possible failure modes are presented in the form of limit state functions.

An application of the quantitative corrosion models in generic RBI is outlined in Section 5.6, conditional on the availability of suitable corrosion models.

### 3.5.2 Corrosion phenomena

The corrosion mechanisms are only very shortly treated in this chapter, but a wide range of literature is available on the subject. The general monograph on corrosion of steel by Kaesche (1990) provides the fundamental basis for this section and an extensive overview on the more practical aspects of corrosion can be found in Roberge (1999).

The complex corrosion problem is first approached by considering the geometrical characteristics of the defects, which facilitates a stochastic description of the defects. Then the driving mechanisms are briefly reviewed, mainly to illustrate the broad variety of existing corrosion processes, which renders the integral treatment of corrosion phenomena intractable.

#### 3.5.2.1 Geometrical description of corrosion defects

Corrosion phenomena can be differentiated by their geometrical characteristics without considering the driving mechanisms. In this spirit Figure 3.15 shows different possible forms of corrosion.

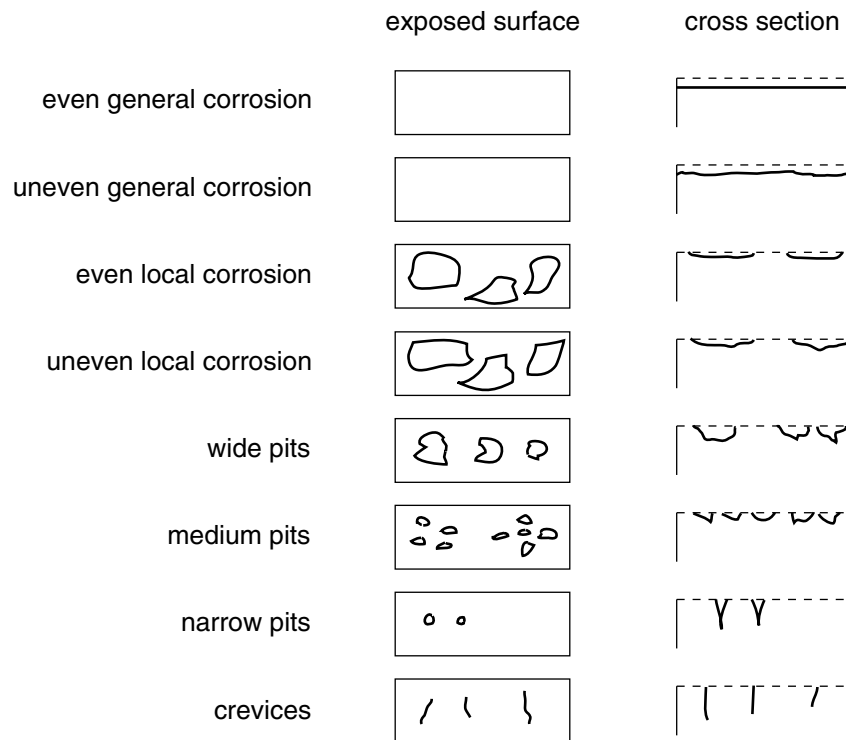


Figure 3.15 - Different corrosion types, after Melchers (1994).

The geometrical characteristics of the corrosion at a given point in time can be described by the stochastic characteristics of a spatial random field. If, simplifying, the corrosion geometry is described in the following by either uniform (general) corrosion or by localised corrosion, then most corrosion deterioration problems encountered in the real world are a combination of these two forms. Consequently the total corrosion depth at any location  $x$  and time  $t$  can be described by the sum of the two types, Equation (3-22).

$$d_c(x, t) = d_{uc}(t) + d_{lc}(x, t) \quad (3-22)$$

$d_c(x, t)$  is the total depth of the corrosion at the location  $x$  at time  $t$ ,  $d_{lc}(x, t)$  is the depth of the localised corrosion defect (depending on  $x$ ) and  $d_{uc}(t)$  is the depth of the uniform corrosion.

### 3.5.2.2 Uniform corrosion

Steel corrosion is a chemical process, where the iron molecules are transformed to different forms of ferrous hydroxides. The process can be split up in a cathodic and an anodic reaction, the latter being described by

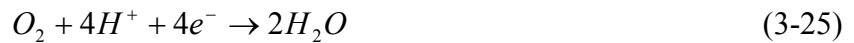


The cathodic reaction is dependent on the environment. As an example, the hydrogen evolution is characterised by





Another common cathodic reaction is the oxygen reduction:



It is noted that the simple Equations 3-23 to 3-25 can only provide a crude representation of the mechanisms involved and the different states occurring during the corrosion process, which will depend on different factors such as the chemical composition of the environment and the metal, the pH value of the environment and the temperature.

As corrosion is essentially an electric circuit with a flow of electrons between the anodic and the cathodic locations, it also requires an external conductive solution (electrolyte) in which both anode and cathode are immersed. The most common electrolyte is water. The different steps in the corrosion process are illustrated in Figure 3.16.

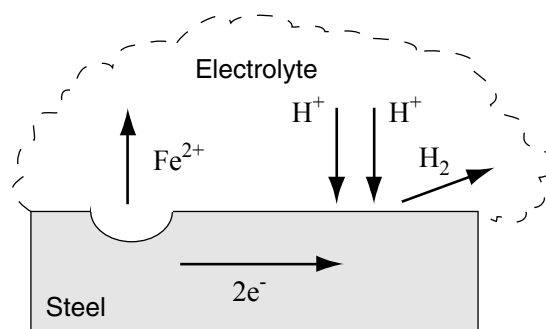


Figure 3.16 – Simplified scheme of the acid corrosion process.

Uniform corrosion is characterised by the fact that the electrochemical reactions proceed uniformly over the surface and no distinguishable macroscopic area which is solely anodic or cathodic exists.

### 3.5.2.3 Localised corrosion

Localised corrosion is based on the same basic principle of the corrosion cell as uniform corrosion, although the driving potential may be provided by different mechanisms. Localised corrosion is characterised by the fact that the anode and the cathode are positioned at different locations in the structure. Furthermore, the cathode may be orders of magnitude larger than the anode, thus greatly increasing the rate of corrosion at the anode.

Different types of localised corrosion mechanisms exist, including

- *Galvanic corrosion*: If two different metals are placed in contact with each other, a driving potential can exist and the less noble metal will then start to corrode. This can e.g. occur when a low-alloy steel is in contact with a (passive) stainless steel, which may then act as cathode.
- *Pitting corrosion*: In steels with a protection film (passive steels), a pit occurs when this film is damaged. The unprotected area starts to corrode and small pits form with a localised chemistry that supports the corrosion attack. Because pits (anodes) are small

compared to the surrounding passive area (cathode), corrosion rates in the pits can be orders of magnitude larger than for uniform corrosion.

- *Intergranular corrosion*: Corrosion at the grain boundaries of the steel crystals, caused by the physical and chemical differences between the centre and the edges of the grain.
- *Crevice corrosion*: An oxygen concentration cell forms when oxygen cannot penetrate a crevice (in sharp edges of the structure, e.g. at bolts). Due to the differences in oxygen concentration on the steel surface, a driving potential exists and corrosion starts in the area with less oxygen.
- *Stress corrosion cracking (SCC)*: Cracking of steel produced by the combined action of corrosion and tensile stress (external or residual stresses). Corrosion is caused by the fact that stressed areas have electrical potentials different from the neighbouring material and are also more likely to develop microscopic surface cracks. SCC is difficult to predict.<sup>a</sup>
- *Corrosion fatigue*: Surface quality influences the fatigue crack growth, because localised corrosion defects can serve as initial cracks from which crack growth starts. This phenomena is treated mainly by fracture mechanics, Section 3.6.
- *Stray current corrosion*: Occurs in soil and fluids, where stray currents are caused by external sources (e.g. electric railway systems or cathodic protection systems of nearby structures). The current flow through the steel structure causes anodic reactions at the location where the positive current exits the structure.
- *Microbiological corrosion*: Bacteria can change the environment at the steel surface, releasing acid products that cause corrosion. Furthermore, some bacteria interact directly with the metal surface (oxidising the iron). Microbiological corrosion can occur in both aerobic and anaerobic conditions.

To date, only few quantitative models have been identified which can predict corrosion degradation with a satisfactory accuracy. For galvanic corrosion, intergranular corrosion, crevice corrosion, SCC and stray current corrosion no such models are reported in the literature. Although they are important failure mechanisms they are not treated further in the present work, as the presented inspection planning methodology demands for predictive models of the deterioration process.

### 3.5.3 Corrosion modelling

As illustrated by Equation (3-22) a complete corrosion model includes the modelling of both temporal and spatial variability, i.e. it must predict the spatial distribution of corrosion depth at a specific point in time and the evolution of corrosion with time. However, most models available are restricted to the prediction of the temporal characteristics of the corrosion

---

<sup>a</sup> SCC caused one of the major structural collapses in Switzerland: In 1985, the suspended concrete ceiling of the Uster indoor swimming pool collapsed due to chloride-induced SCC of the stainless steel hangers, causing twelve fatalities, as described by Faller and Richner (2003).

process. On the other hand, the published models that consider the spatial aspects are mainly of a theoretical (mathematical) nature and are of little value in predicting corrosion for engineering purposes.

### 3.5.3.1 Temporal model - Empirical versus phenomenological (physical) modelling

When phenomenological modelling (also referred to as process, physical or mechanistic modelling) of the corrosion process is considered, the underlying mechanism must be understood in order to determine the limiting factors of the process and these must then be modelled. This is discussed in several publications, including Melchers (1999a and 2003a), Cole (2002) as well as Roberge et al. (2002) and is illustrated by an example in Figure 3.17, showing the different phases in corrosion development of steel immersed in sea water.

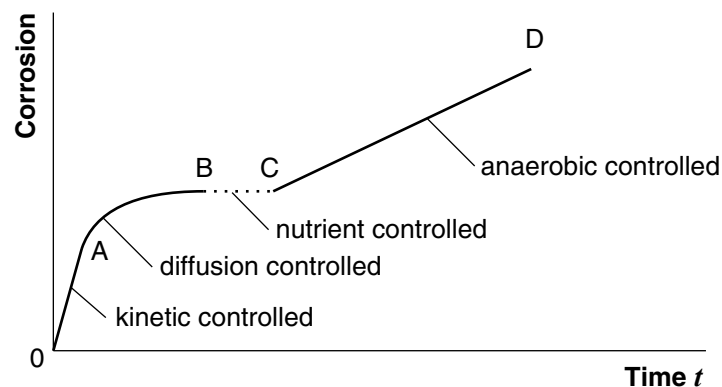


Figure 3.17 – Conceptual model for marine corrosion (immersion) from Melchers (1999a).

Each of the phases in Figure 3.17 have different limiting factors. When it is assumed that in each phase only one limiting factor is determining the corrosion degradation, the process can be modelled by this factor. As an example the diffusion controlled phase illustrated in Figure 3.17 is governed by the amount of oxygen available for the cathodic reaction. Corrosion products that accumulate on the surface will limit this amount. The amount of oxygen on the steel surface, and therefore the speed of the corrosion process, can thus be modelled by a diffusion model, and Melchers (1999a) shows that under special, simplifying assumptions the diffusion controlled corrosion phase can be described as

$$d_{UC}(T) = Const \cdot T^{1/2} \quad (3-26)$$

where  $T$  is the time spent in the diffusion controlled phase.

Equations like (3-26) are actually semi-empirical model, because its parameteres, like the constant in Equation (3-26), do not represent any physical quantities. Instead they must be fitted to measured corrosion degradation. Fully physical models would need e.g. knowledge on the concentration of  $O_2$  in the environment and the diffusion coefficient in the corrosion product. Clearly these input parameters are not generally available and fully physical models do not provide a satisfactory solution at present, see also Cole (2002). On the other hand, it is stated in Melchers (2003a) that “purely empirical models have little value”, because extrapolation of the models outside the range of data to which they were calibrated is not

possible. It is therefore argued that corrosion models for RBI must be based on consideration of the governing mechanisms and their driving or limiting factors; this is also supported by the small literature review presented in the following section.

### 3.5.3.2 Models for corrosion on low-alloy steel in different environments

#### Atmospheric corrosion

For atmospheric corrosion, extensive research was performed with the aim of deriving empirical models that are valid for different environmental conditions. Most empirical equations for the depth of uniform atmospheric corrosion  $d_{UC}$  are of the generic form

$$d_{UC}(t) = \alpha_{UC} \cdot t^{\beta_{UC}} \quad (3-27)$$

with the empirically deduced parameters  $\alpha_{UC}$  and  $\beta_{UC}$ . This model is also partly justified by phenomenological considerations, see also Equation (3-26). The derivation of such a model is described in Feliu et al. (1993a,b), using linear and non-linear regression analysis to determine the parameters from a large set of published data. Thereby  $\alpha_{UC}$  and  $\beta_{UC}$  are functions of the different influencing factors, such as time of wetness, relative humidity, temperature, sulphur dioxide (SO<sub>2</sub>) and chloride concentration in the environment.

It is noted that although values for the parameters in Equation (3-27) are published in the literature, they have only restricted value for prediction purposes. In Cole (2002) it is stated that “despite the extent of work into parametric models, no single model has been accepted by the scientific community and also the constants used in the model vary widely”. He concludes that this is caused by the fact that the factors influencing corrosion are not correctly considered in the models, due to the lack of understanding of the underlying processes. This statement is in accordance with Roberge et al. (2002), where it is furthermore observed that the corrosion rate can vary significantly between locations only meters apart, due to micro-environmental effects, e.g. the influence of local wind speed on the deposition rate of pollutant and thus on the corrosion rate. They conclude that phenomenological models may provide the framework for accounting for the influencing factors consistently, but to date no “single transferable and comprehensive environmental corrosivity prediction model” exists.

#### Marine immersion corrosion

For marine immersion corrosion a comprehensive model is presented in Melchers (2003a,b) for the entire corrosion process based on a phenomenological understanding, as illustrated in Figure 3.17. The model is limited to near-surface conditions in seawater, and due to the relatively homogenous conditions of this environment, Melchers (2003a,b) is able to show that it is sufficient to consider only temperature as an independent variable. The different phases in the model (kinetic controlled, diffusion controlled, anaerobic controlled) are calibrated to experimental data and thus allow for a long-term prediction of corrosion degradation. Additionally, in Melchers (2003b) an estimation of the uncertainty associated with the model is published.

### Carbonic acid corrosion in pipelines

CO<sub>2</sub> dissolved in water causes corrosion, its cathodic reaction is described by Equation (3-24). In pipelines transporting natural gas or oil, water is generally present to some extent and therefore corrosion takes place depending on CO<sub>2</sub> partial pressure and temperature. This relationship is described in deWaard and Milliams (1975) and later, in deWaard et al. (1991, 1995), refined to account for several additional influence parameters, especially the fluid flow velocity. It gives a conservative estimate of the steady state corrosion rate which is reached after an initial phase. Because the model is a “worst-case model” it does not consider the spatial aspects of the phenomenon, in spite of the localised nature of CO<sub>2</sub> corrosion. The deWaard-Milliams model is widely used and the relatively controlled environments in pipelines facilitate its application in reliability calculations and maintenance optimisation; examples are described in Sydberger et al. (1995), Hellevik et al. (1999) and CRIS (2004).

#### 3.5.3.3 Modelling Pitting Corrosion

Pitting corrosion in mild steels and low alloy steels is of primary interest when the critical failure mechanism is related to the containment of gas and liquids, e.g. in pipelines or pressure vessels. For overall structural strength considerations, it is noted in Melchers (1994) for marine corrosion, that general corrosion is more important, but that the differentiation between general corrosion and extensive spatially distributed pitting corrosion is not always clear. Furthermore, pitting and other forms of localised corrosion is of particular concern when considering stainless steels, see Ryan et al. (2002), but these are not treated hereafter.

#### Pit growth as a stochastic process

The pitting process can be split in two parts: pit initiation and pit propagation. Initiation is the formation of a damaged location of the passive layer on the metal surface. It is generally agreed that pit initiation takes place during a very short time period (micro-seconds), Melchers (1994). Modelling of this stage is difficult because it cannot be directly observed, and thus the precise location of the highly localised corrosion attack still appears to be unpredictable. In Ryan et al. (2002) it is noted that “the pitting process has been described as random, sporadic and stochastic, and the prediction of the time and location of events remains extremely difficult”. This has led to a long tradition of modelling pit initiation (and also propagation) as random processes, a review of which is given in Shibata (1996). Because these models are not of a phenomenological kind and must therefore be calibrated to data, extrapolation to other environments or materials (alloys) is crucial. The application of such models to maintenance optimisation is presented in Hong (1999).

#### Distribution of the size of the largest pit

Another widely applied approach to the modelling of pitting corrosion, when the deepest defect is of interest, is to describe the largest defect in a given area by extreme value statistics. This approach takes into account the spatial variation of the pitting corrosion phenomena. Such an approach was described in Finley (1967), modelling the deepest corrosion pit by a type I extreme value (Gumbel) distribution. This approach was latter refined by various researchers, see e.g. Laycock et al. (1990) or Scarf et al. (1992). Thereby, due account must be taken of the spatial variability of the pitting corrosion depths, i.e. the spatial correlation. The number of potential locations for pits within a certain area is usually very large, typically

there may be more than 1 pit per  $\text{mm}^2$  (Laycock et al. (1990)) and the pitting-depth correlation length will have a significant influence on the distribution of the deepest pits within a considered area.<sup>a</sup> The approach has the common shortcomings of all the empirical approaches, namely that extrapolation to other materials or environments is not possible.

### Modelling the temporal aspects

In Finley (1967), an example is given of how the maximum pits distribution can be combined with a propagation law. There a logarithmic formulation for the depth of the characteristic deepest pit depth at time  $t$  is applied because of its mathematical convenience rather than due to physical arguments. In Laycock et al. (1990) formulations are derived from the generalised extreme value distribution, including the description of area dependency and the time to first “through corrosion”. These are based on the assumption of the widely applied power law, see Equation (3-28), under the prerequisite that both the mean and the standard deviation of the pit-depth follow this law with the same exponent  $\beta_{LC}$ .

$$d_{LC,max}(t) = \alpha_{LC} t^{\beta_{LC}} \quad (3-28)$$

In Turnbull (1993) it is shown for pit growth that under simplifying assumptions the exponent  $\beta_{PC}$  can be deduced from electrochemical measurements (by measuring the electrical current in the specimen), but he concludes that direct measurement of the distribution of pit sizes together with statistical analysis is preferable.

Based on the above considerations, the application in RBI of a model that combines temporal and spatial aspects is illustrated in Faber et al. (2003a). It is stressed out that this model is not applicable for general predicting purposes, but is only valid in the (relatively homogenous) system for which its parameters are derived. It assumes that the distribution of the maximum corrosion pit can be described as a Type I extreme value distribution with parameters  $u_t = u_{max} \cdot t^{\beta_{LC}}$  and  $\alpha_t = \alpha_{max} \cdot t^{-\beta_{LC}}$ :

$$F_{D_{LC,max}}(d) = \exp(-\exp(-\alpha_t(d - u_t))) \quad (3-29)$$

Correspondingly, also the mean and the standard deviation of  $d_{LC,max}$  increase with  $t^{\beta_{LC}}$ , so that Equation (3-29) is consistent with Equation (3-28).

### Phenomenological modelling

Regarding phenomenological models it is stated in Turnbull (1993) in his review on pit propagation modelling that they “are too complex to set up and at the present stage of development are in most cases not user (engineer) friendly”. He furthermore notes that the complementary use of empirical modelling methods and more sophisticated physical models provide the most effective method for prediction.

---

<sup>a</sup> The models suggested in the literature, e.g. Shibata (1996) or Laycock (1990), implicitly assume independency between the individual pit dimensions when extrapolating to larger areas.

### 3.5.3.4 Spatial model

The here presented large-scale spatial model is based on Straub and Faber (2002). The considered structure is divided into finite elements, whose size can be chosen as is convenient, e.g. as the size of the inspected areas. Depending on the failure mode, either the average corrosion or the deepest corrosion defect is of interest. In case the average corrosion is of interest (for structures subject to uniform corrosion) each element is represented by the distribution of the average corrosion depth in the element,  $f_{d_{uc}}(d)$ . If the local corrosion is of interest, e.g. in pressure vessels, the element is characterised by the distribution of its largest corrosion defect,  $f_{d_{LC,max}}(d)$ <sup>a</sup>. As discussed in Section 3.5.3.3,  $f_{d_{LC,max}}(d)$  is dependent on the area of the element and is generally modelled as an extreme value distribution. The area dependency is modelled by assuming the size of the individual defects to be independent. Note that this assumption is conditional on the realisation of the random variables that represent common epistemic uncertainties. As an example, the parameters in Equation (3-29) can be modelled conditional on the temperature of the environment. *Given* a specific temperature, the assumption of independence between individual defect sizes is reasonable, if the area size is large compared to the correlation length of the spatial distribution of defect size.

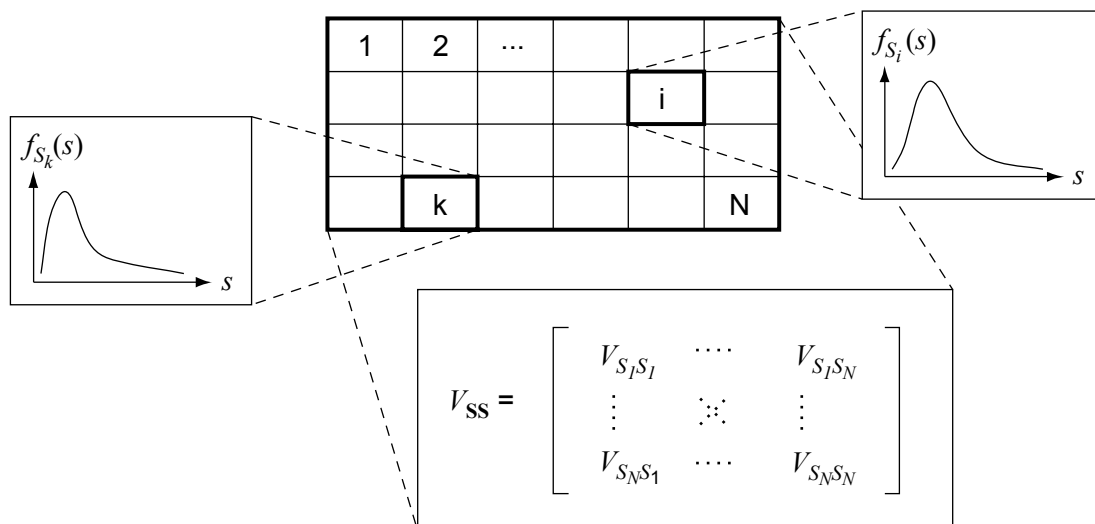


Figure 3.18 – Illustration of the system model, from Straub and Faber (2002a).

As the proposed model, illustrated in Figure 3.18, is a generic concept<sup>b</sup>, the size of the defect in the element (the largest or the average) is simply denoted by  $s$ . The individual element  $i$  is then represented by the random variable  $S_i$ . The  $S_i$ 's are described by the marginal distribution functions  $F_{S_i}(b)$ ,  $i = 1 \dots N$  and the covariance matrix,  $V_{SS}$ , that represents the

<sup>a</sup> This concept is, for most problems, advantageous in comparison to modelling every single defect separately. The latter often leads to mathematical problems due to the typically very large number of defects, as observed in Strutt (1998).

<sup>b</sup> An element can also be an individual hot spot in a steel structure subject to fatigue failures, with the defect being the largest crack at the hot spot.

stochastic dependency between the defects of the individual elements<sup>a</sup>. Clearly the individual  $S_i$ 's (and generally also the covariance matrix) are time dependent, but for the sake of clarity this is omitted in the notation. In principle the individual  $F_{S_i}(s)$  can be different for all elements. For many systems the model of the deterioration will, however, be identical for a large number of elements. For a pipeline with homogenous conditions along its axis, the prior model of corrosion depth will be the same for all elements along the bottom.

The stochastic dependencies, as expressed by the covariance matrix  $V_{SS}$ , are crucial in the modelling of the corrosion deterioration on a structural system. They are generally caused by common influencing factors, such as the temperature and other environmental conditions. To the author's knowledge no such models are published for corrosion processes in low alloy steels (considering large scale dependencies). In the absence of empirical models, the degree of dependency of the corrosion deterioration within the structure may be estimated by consideration of the involved uncertainties.

### 3.5.4 Uncertainties in corrosion modelling

The quantitative corrosion models applied by the profession are generally developed for design purposes and represent a sort of "worst case model" without clear definition of the underlying uncertainties. Apart from the models published in Melchers (2003b) and Sydberger et al. (1995), the author is not aware of any attempt to quantify the uncertainties involved in the corrosion predictions for real operational situations. Because such models are crucial for the development of a risk based approach to corrosion control, the reluctance of the corrosion engineers to quantify the uncertainties related to their models constitutes a significant drawback in corrosion modelling. Some of the problems involved in the quantification of model uncertainties are illustrated in the next paragraph, using the example of CO<sub>2</sub> corrosion on carbon and low alloy steels

Sydberger et al. (1995), based on a review of the original experiments and few additional in-service data, provide a rough estimate of the uncertainty related to the corrosion prediction by means of the DeWaards-Milliams equation in the form of a multiplicative factor. Because the original model does not distinguish between different possible forms of corrosion, they provide a different model uncertainty for pitting and longitudinal grooving corrosion. As, in addition, the original model does not give any information about the spatial variability, they presume that the calculated corrosion rate is the maximum time-averaged corrosion rate at any location of the pipeline, which neglects the fact that the maximum corrosion depth is increasing with increasing size. Furthermore, although the assumption of a constant time-averaged corrosion rate may be appropriate for design purposes, it can lead to misinterpretations of inspection results when changes or variations in the operational conditions are not accounted for. All these factors are ignored in the published corrosion reliability models.

---

<sup>a</sup> This second-order modelling of the inter-dependencies is, for most cases, considered appropriate for the level of knowledge on the correlation structure of the deterioration process. Alternatively the dependency can be included by explicitly modelling the common uncertain influencing factors.



### 3.5.5 Corrosion protection

Various corrosion protection systems are available for the different application areas; Roberge (1999) provides an extensive description of the different systems. They are based on different principles of the corrosion theory, and can be divided into the five groups:

- Cathodic protection systems
- Anodic protection systems
- Coatings
- Inhibitors
- Dehumidification systems

All systems prevent or decelerate corrosion as long as they function properly. This can be modelled by a probability of malfunction of the protection system, i.e. no corrosion occurs (or corrosion occurs with reduced velocity) given correct protection, but corrosion initiates given the protection system does not work. The problem is that there are in general different failure mechanisms for the protection systems and the velocity of corrosion will depend on the type of malfunction of the protection systems. Improper corrosion protection may in some cases lead to localised corrosion phenomena, which are hardly predictable. Another aspect, apart from the initial malfunction of a system, is the deterioration of the protection system. These aspects are illustrated on two common protection systems for steel structures:

#### Protective coating

It is noted in Roberge (1999) that protective coatings are probably the most widely used products for corrosion control. They isolate the steel from the environmental corrosives, and three different types can be distinguished: metallic, inorganic and organic coatings. Coatings are subjected to chemical and mechanical degradation and must be renewed periodically. However, only very few (empirical) models of such deterioration are published, e.g. Yamamoto and Ikegami (1996), and more research is needed in this field, see also Dickie (1992) who discusses strategies for the development of such models.

Published reliability calculations of corrosion subjected marine structures (Friis Hansen (1994), Guedes Soares and Garbatov (1999)) model the coating by introducing a corrosion initiation time which is equal to the lifetime of the coating. This model assumes that the coating will not be maintained or repaired. Furthermore it assumes that the coating is perfect in its initial state, i.e. no corrosion occurs at this stage, whereas in reality corrosion may also occur when the coating is intact, by diffusion of ions through the paint as described by Walter (1986).

The methods presented in this work aim at the inspection planning of structures that are well maintained, which includes renewal of the coating at appropriate time intervals, together with an appropriate quality control. The above model, assuming no replacement of the damaged coating, is therefore not relevant in the present context. Given a well maintained structure, the optimisation problem reduces to the determination of optimal maintenance actions on the coating itself. Inspection planning is thus only relevant for controlling the degradation of the coating, if at all. In many structures the coating is subject to corrective maintenance, because the consequences of failure of the coating are low if immediate detection of the failure is

assured. In other situations a planned maintenance schedule may be favourable, see also Goyet et al. (2002). If an application of RBI to the maintenance of the coating is considered, quantitative models of the coating degradation are required. Such models are, however, not generally available at present.

#### Sacrificial anodes (cathodic protection)

Cathodic protection systems are divided into impressed current systems and sacrificial anodes. The latter are based on the principles of the galvanic cell, where the cathodic reaction takes place at the steel and the less noble metal (the sacrificial anode) serves as the anode, which consequently is consumed by the process. The application of such a system on a fixed offshore structure is presented in Sharp et al. (2001).

The performance of such a system depends on the number of anodes, their size, their locations and their material. These factors determine the potential that provides the protection of the steel structure. Two possible failure modes of the system exist:

- When the negative (protection) potential is too small, the steel can corrode.
- Large negative potentials might lead to hydrogen embrittlement of the structure.

The electrical potential varies over the structure (more negative values occur in the vicinity of the sacrificial anodes), consequently also the probabilities of both failure modes vary with the location. As the anodes are consumed (and eventually replaced) during the lifetime of the structure, the potential and therefore the probabilities of failure also change with time. This has to be accounted for when modelling the protection system.

In a steel structure that is protected by sacrificial anodes, it is not corrosion that is the main concern, but the protection system itself. Corrosion is only an issue in case the system does not work correctly. Therefore it is the sacrificial anode and the resulting potential that must be modelled, with the two failure modes as listed above. Optimisation is then related to the design and maintenance of the sacrificial anodes.

#### 3.5.5.1 Accounting for protection systems in RBI

As illustrated in the two examples above, for corrosion protected structures (with the exception of those protected by inhibitors, see next paragraph) it is in general the protection system itself that becomes the main concern. For such structures, the malfunction of the protection system is considered as the failure event. This failure can lead to excessive corrosion defects, but in a decision analysis this will be considered in the expected cost of failure of the protection system. The state of nature  $\theta$  that is of interest is the performance of the protection system and no inspections are planned for the corrosion deterioration (except for the case where corrosion is the indicator of malfunction of the protection system). It is thus concluded that for corrosion protected structures RBI is not of relevance for the control of the corrosion; instead it may be for the optimisation of inspections on the protection systems.

Corrosion protection by inhibitors is fundamentally different from the other protection systems as it is recognised as a measure to decrease the corrosion rate, but not to fully prevent the corrosion. In addition, its performance can only be measured by inspection and monitoring of the corrosion on the structure. Consideration of inhibitors should thus be

included in the corrosion modelling. E.g. a multiplicative factor (modelled by a random variable) on the corrosion rate is used in Sydberger et al. (1995), but no such model based on data is readily available. In addition, operational factors are very important for the efficiency of the inhibitors and must be included in the model.

### 3.5.6 Failure modes

#### 3.5.6.1 Fracture in pressurised systems

This failure mode is evaluated using a semi-empirical model based on fracture mechanics to determine the pressure at which the pressure vessel fails as a function of the size and the geometry of the corrosion defect. This approach has its origins in the early seventies, Maxey et al. (1972) and Kiefener et al. (1973), and has since then become the most widely applied. It is furthermore used in several standards, including the B31G (1984). A review of the approach and different proposed modifications is given in Ahammed and Melchers (1996).

The model presented here is based on Ahammed and Melchers (1996), but modified to consider both local and uniform corrosion. The final failure can occur as either leakage or rupture, dependent on the size of the through-wall defect. The limit state function is written as

$$g_{C,p} = p_R - p_S \quad (3-30)$$

Here  $p_S$  is the applied pressure in the system,  $p_R$  is the structural resistance. Considering both uniform and localised corrosion, and approximating the local defect by a rectangular shape,  $p_R$  is given as<sup>a</sup>

$$p_R = 2S_f \frac{(d - d_{UC})}{D_p} \frac{1 - d_{LC}/(d - d_{UC})}{1 - d_{LC}/((d - d_{UC})M_p)} \quad (3-31)$$

The according geometrical model is shown in Figure 3.19.

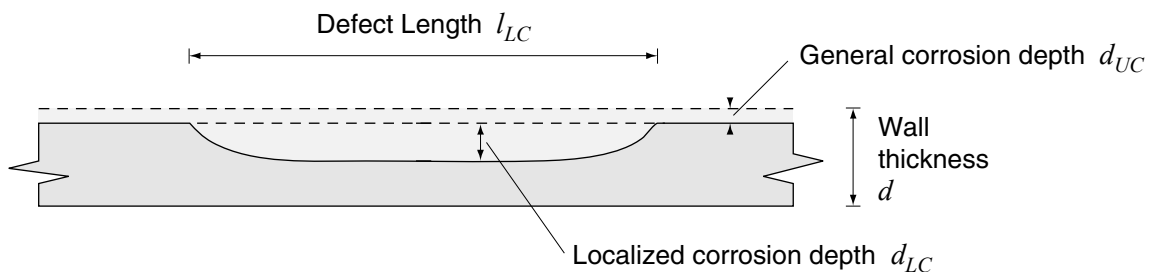


Figure 3.19 - Idealised corrosion defect.

<sup>a</sup> Equation (3-31) is based on the additional assumptions that  $d$  is relatively small compared to  $D_p$  and that the fluid density is small compared to the fluid pressure (neglecting gravity).

$D_p$  is the diameter of the pipe or vessel.  $S_f$  is the flow stress, related to the yield stress by a factor  $m_f$ , Equation (3-32). Ahammed and Melchers (1996) propose to model  $m_f$  by a Lognormal distribution with  $E[m_f] = 1.1$  and  $CoV_{m_f} = 0.05$ .

$$S_f = m_f S_y \quad (3-32)$$

$M_p$ , the Folias factor (also known as bulging factor) is a semi-empirical factor that covers the fracture mechanics aspects; it contains the additional parameter defect length  $l_{LC}$ . The Folias factor adopted from Ahammed and Melchers (1996) is

$$M_p = \sqrt{1 + 0.6275 \frac{l_{LC}^2}{D_p(d - d_{UC})} - 0.003375 \frac{l_{LC}^4}{D_p^2(d - d_{UC})^2}}, \quad \frac{l_{LC}^2}{D_p(d - d_{UC})} \leq 50 \quad (3-33)$$

$$M_p = 0.0032 \frac{l_{LC}^2}{D_p(d - d_{UC})} + 3.3, \quad \frac{l_{LC}^2}{D_p(d - d_{UC})} > 50$$

It is noted that in Stewart et al. (1994) a fully analytical model for predicting the burst capacity of pipelines with long smooth corrosion patches is presented. The model does not account for the influence of the defect length (thus assuming an infinite length), but provides a physical definition of the flow stress (instead of the empirical relationship given in Equation 3-32), and additionally accounts for the circumferential extent of the corrosion defect. Experimental verification, as also presented in Stewart et al. (1994), show very good agreement between the model and the test outcomes.

### 3.5.6.2 Leakage of non-pressurised systems

If failure occurs when the corrosion depth has reached the full thickness, the limit state function becomes simply

$$g_L = d - d_C \quad (3-34)$$

As with fracture in pressurised systems, this limit state is mainly associated with localised corrosion.

### 3.5.6.3 Structural failure due to loss of cross section

Corrosion leads to a reduction of structural resistance. Ultimately, this reduction can lead failure of the structure. Reliability calculations based on such a limit state have been presented e.g. by Guedes Soares and Garbatov (1996b) for ship structures. In its most simplest and generic form the limit state function looks as follows:

$$g_C = d - d_{crit} - d_{UC} \quad (3-35)$$

$d_{UC}$ , the depth of the general corrosion, is applied because localised corrosion normally has less influence on the structural resistance (apart from pressurised systems and crevice-like defects).  $d_{crit}$  is the critical member thickness at which failure occurs. This is a function of all other parameters (loading, geometry of the cross section, material properties), an explicit formulation for  $d_{crit}$  will not always exist.

### 3.6 Corrosion fatigue

Corrosion fatigue is of high relevance for (aluminium) aircraft structures, but occurs also commonly in steel structures. It is essentially a combination of localised (pitting) corrosion and fatigue: while the corrosion defect grows, the stress concentration at the tip of the defect increases. Once the stress intensity range  $\Delta K$ , caused by cyclic loading, exceeds the threshold  $\Delta K_{th}$ , fatigue crack growth can start and may finally cause failure. Because the modelling of corrosion fatigue follows to a large extent the fracture mechanics based crack growth models presented in Section 3.3, the phenomenon is only briefly outlined here. The modelling as presented is based on the work reported in Kondo (1989) and Harlow and Wei (1994). Three main stages are differentiated, namely pitting corrosion, the transition to a fatigue crack and the fatigue crack growth with final fracture.

#### a) Pitting corrosion

The corrosion pits are modelled as growing at a constant volumetric rate  $dV/dt$ . Because additionally a hemispherical shape of the pits is assumed, the calculated pit radius is proportional to  $t^{1/3}$ . In Kondo (1989) it is found from experiments on low alloy steels that the pits exhibit a constant aspect ratio of  $a/c \approx 0.7^a$ . The defect size before crack growth starts is thus described by

$$\begin{aligned} a(t) &= c_p t^{1/3} \\ 2c(t) &= 1.4c_p t^{1/3} \end{aligned} \quad (3-36)$$

The pit growth parameter  $c_p$  is depending on the material and the environment; based on a simplifying model it can be formulated as a function of electrochemical constants and parameters, Harlow and Wei (1994). Due to spatial variations of the electrochemical properties and consequently of  $c_p$ , the size of the individual pits vary. Because the size of the largest pit is of interest, an area dependency is introduced which must be accounted for: The parameters which exhibit spatial variations must be modelled as stochastic processes, or, simplifying,  $c_p$  is directly modelled by an extreme value distribution. This aspect has not been given any attention in the literature, but its consideration is essential when a consistent phenomenological modelling is required.

#### b) Transition criteria

Following Harlow and Wei (1999) the transition from the corrosion controlled phase to the fatigue controlled phase can be characterised by

$$\Delta K \geq \Delta K_{th} \quad \text{and} \quad \left( \frac{da}{dt} \right)_{FM} \geq \left( \frac{da}{dt} \right)_{Pit} \quad (3-37)$$

---

<sup>a</sup> The notation follows the fatigue crack growth modelling.

where the first condition is a prerequisite to the second. The process is thus assumed fatigue controlled if the calculated fatigue crack growth is faster than the corrosion growth. Note that the model is, simplifying, based on the assumption of no interaction between the chemical (corrosion) and the mechanical (stress ranges) deterioration processes.

### c) Fatigue crack growth and failure

This phase is modelled in accordance with the fatigue crack growth (FM) modelling: The corrosion and the transition model provide the initial crack size ( $a_0$ ,  $c_0$ ) and the number of cycles to initiation  $N_i$  in accordance with Figure 3.8. The fatigue crack growth then follows Section 3.3.3. Final failure (fracture) occurs when the critical stress intensity factor is exceeded or when the crack reaches the wall thickness, Section 3.3.4.

## 3.6.1 Reliability analysis

An example reliability analysis for aluminium structures subject to corrosion fatigue is presented in Harlow and Wei (1994) and later in Zhang and Mahadevan (2001); in Shi and Mahadevan (2003) the model is extended to include multiple site damage, a common phenomenon in aircraft structures. Whereas the parameters governing the fatigue dominated phase are generally well determined, the foundation of the parameters applied in the corrosion phase (the crack initiation phase) is less favourable, as discussed in Harlow and Wei (1994). Furthermore, the effects of area dependency as well as the interaction between individual pits are not included in the models. As a consequence, it may be required to model the corrosion phase by an empirically determined pit growth parameter  $c_p$ . Such an empirical model, however, possesses the same deficiencies as all empirical corrosion models, see Sections 3.5.3.1 and 3.5.3.2.

## 4 Inspection Modelling

### 4.1 Introduction

In the 1970's the need for quality assurance of non-destructive evaluation (NDE) methods was recognised and first attempts of assessing and modelling the inspection performance were made. In the same period it was first described how such models can be used to update probabilistic models of flaws, Tang (1973). Since then quantitative models for the representation of the quality of NDE were developed mainly within the aerospace, nuclear and offshore industries for techniques aimed at the detection of flaws and cracks, see Yang (1994) for an overview. Most of the developed models are empirical models based on round robin tests. Although attempts were made to derive inspection performance models based on physical models, Wall and Wedgwood (1994), these will not be discussed here. To date, there is still a limited availability of appropriate inspection performance models, which is mainly due to the large cost associated with the round robin tests. In addition, owing to the empirical nature of the models, the transferability of the models to environments, materials and operators different from those considered in the tests is not ensured.

This chapter is concerned with the quantitative modelling of inspection performance aimed at a consistent application in reliability updating. Many of the available models are derived for the semi-quantitative assessment and ranking of the different techniques. As a consequence, many published inspection performance models are not appropriate for the envisaged application in RBI. They are not considered in the following; instead the chapter concentrates on the models required for reliability updating in the framework of the Bayesian decision theory. It is essential that these models are formulated in a consistent and precise manner, which motivates the introduction of the Probability of Indication (*PoI*). This concept clarifies the relation between the event of detection and the event of indication of a defect. Furthermore, the application of the models in reliability updating necessitates the formulation of appropriate limit state functions, which are presented in Section 4.4. An important aspect, which has not been given sufficient attention in the past, are the uncertainties related to the modelling of inspection performance, as well as their effect on the dependencies between individual inspections. Sections 4.5 and 4.6 summarise concepts and models recently introduced by the author together with important conclusions from the related numerical investigations. Because the inspection performance models outlined in this chapter concentrate on inspections for flaws and cracks, the concluding Section 4.7 is dedicated to the differences in the modelling of inspections for corrosion control. It introduces the combined effect of defect measurements together with the uncertainty on whether the largest defect has actually been found. This new concept is essential when inspection planning for structures subjected to localised corrosion is considered.

The original contributions of the author to the subject as presented here are essentially published previously in Straub (2002), Straub and Faber (2003a) and CRIS (2004), with the exception of the models introduced in Section 4.7.2.

## 4.2 Inspection performance models

### 4.2.1 Probability of Detection (*PoD*)

The ability of inspections to detect a defect can be described by a Probability of Detection (*PoD*) curve as illustrated in Figure 4.1. The *PoD* is expressed as a function of the defect dimension  $s^a$  and generally increases with increasing size of the defect.

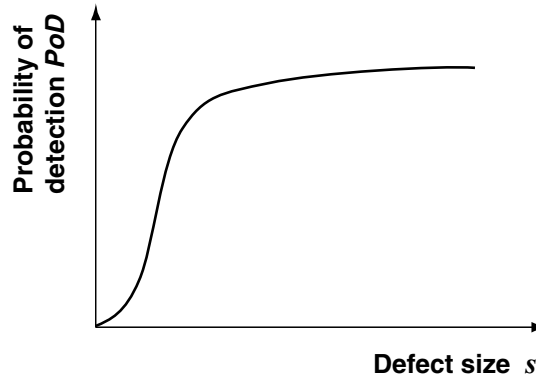


Figure 4.1 – The probability of detection (*PoD*).

The reason for expressing the ability to detect a defect by a probability measures is that the performance of inspections is dependent on many factors besides defect size, such as defect orientation, environmental conditions and inspector performance. In addition to these effects comes the inherent signal noise of the NDE equipment. The *PoD* is the mean rate of success when integrating the inspection performance over these uncertain factors. To express the *PoD* as a function of defect size, and not integrating over this parameter too, is justified by the following two observations: First, the defect size is the most important parameter for the integrity of the structure, and second, it allows for an analytical treatment of the inspection quality in the framework of fracture mechanics. Mathematically the *PoD* is a non-decreasing function of defect size  $s$  that is in the interval  $[0, 1]$  for any non-negative  $s$  and which fulfils  $PoD(0) = 0^b$ .

In the present work the following parametrical one-dimensional *PoD* models are used, where  $s$  is either defect depth or length:

- Log-logistics (log odds) model: 
$$PoD(s) = \frac{\exp(\alpha_D + \beta_D \ln(s))}{1 + \exp(\alpha_D + \beta_D \ln(s))} \quad (4-1)$$

---

<sup>a</sup> The variable  $s$  is used in this chapter to denote a one-dimensional defect size. In specific examples it is replaced by  $a$  for crack depth or  $l$  for crack length. In cases where a vector of defect dimensions is applied this is denoted by  $\underline{s}$ .

<sup>b</sup> Note that in many references this last condition is not fulfilled. In that case the *PoD* is not the Probability of Detection as defined here, but is identical with what is defined in Section 4.2.3 as the Probability of Indication.



$$- \text{ Exponential threshold model: } PoD(s) = P_0(1 - \exp(-s/\lambda_D)) \quad (4-2)$$

Additional formulations may be found in Berens and Hovey (1983). Two-dimensional  $PoD$  models are described by Rudlin and Wolfenstein (1992) and Straub (2002). Here only one model is applied for illustrational purpose, where  $a$  is the defect depth and  $l$  is the defect length:

$$- \text{ 2D log-logistics model: } PoD(a,l) = \frac{\exp(\alpha_{2D} + \beta_{D,a} \ln(a) + \beta_{D,l} \ln(l))}{1 + \exp(\alpha_{2D} + \beta_{D,a} \ln(a) + \beta_{D,l} \ln(l))} \quad (4-3)$$

Whether the  $PoD$  should be a function of defect depth or length depends on the inspection techniques. Many applied techniques are more sensitive to changes in the defect depth, their  $PoD$  models should thus be a function of the defect depth. This is illustrated by the numerical investigations in Section 4.3.3. Note that a two-dimensional  $PoD$  model is always more accurate than a one-dimensional model, although at the expense of increased complexity.

#### 4.2.2 Probability of false indication

The Probability of False Indication ( $PFI$ ) is the probability of obtaining an indication of a defect where none is actually present. The  $PFI$  must be defined relative to a reference area, but the definitions in the literature are often ambiguous and the resulting  $PFI$  values can only be used as a relative quantity. However, for the consideration in a risk-based framework a clear definition is essential. Thus, in the following the  $PFI$  for NDE on welded details subject to fatigue is expressed per 1mm of weld or per hot spot.

The  $PFI$  has no influence on the updated reliability after the inspection when it results in no-indication, but it changes the probability of (unnecessary) repair and consequently the total expected cost. Whereas the  $PFI$  is thus of importance in risk based inspection planning, it can be neglected for reliability based inspection planning.

#### 4.2.3 Probability of indication

It is suggested to combine the  $PoD$  and the  $PFI$  into a single variable, the Probability of Indication ( $PoI$ ). For in-service structures, neither the event of detection nor the event of false indication can be identified with certainty, in contrast to the event of indication: After an inspection resulting in an indication, it is actually not known, whether the indication is due to a detection of a defect or due to a false indication, but it is certain that there is an indication. Decisions on further maintenance actions will therefore be based on the event of indication and not on the actual (but unknown) defect. When evaluating the influence of inspections on the expected total life cycle costs, it is thus consistent to work with the event of indication, so that unnecessary repair is accounted for in the analysis.

The  $PoI$  is valid for a certain weld length only, as the  $PFI$  varies for different lengths. In general it is reasonable to formulate the  $PoI$  per inspected component or hot spot, dependent on the structural integrity model. The  $PoI$  can be derived from the  $PoD$  and the  $PFI$  by use of

the total probability theorem<sup>a</sup>: The event of indication (given a certain crack size  $s$ ) is either due to a false indication or a detection of that defect, its probability is thus written as

$$PoI(s) = P(I|s) = P(I|D \cap s)P(D|s) + P(I|FI \cap \bar{D} \cap s)P(FI \cap \bar{D}|s) \quad (4-4)$$

Because the probability of indication given detection or given false indication is 1, it is

$$PoI(s) = P(D|s) + P(FI \cap \bar{D}|s) \quad (4-5)$$

Assuming independence between the  $PoD$  and the  $PFI$ , and accounting for the fact that the  $PFI$  is independent of  $s$ , the  $PoI$  is finally derived as

$$PoI(s) = PoD(s) + (1 - PoD(s))PFI \quad (4-6)$$

The  $PoI$  as a function of the crack depth  $a$  is illustrated in Figure 4.2.

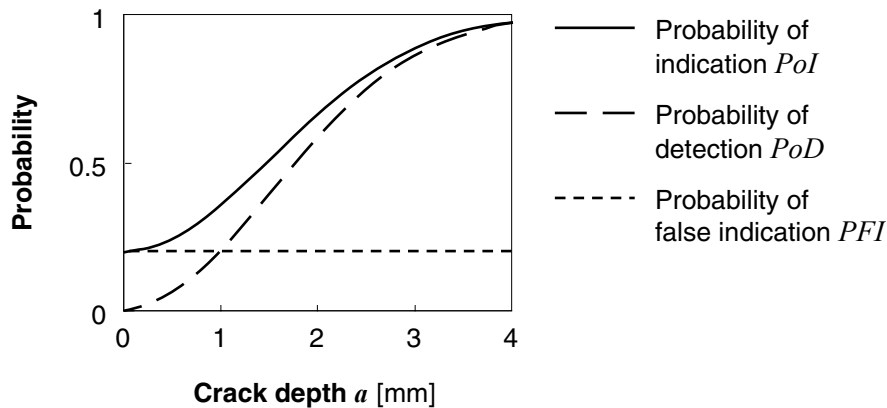


Figure 4.2 – Combining the  $PoD$  and the  $PFI$  to the Probability of Indication  $PoI$ .

#### 4.2.4 Accuracy of defect sizing

For NDE methods enabling a sizing of the defects, a regression model can be formulated which relates the measured size to the real size. The reader is referred to Zhang and Mahadevan (2001) for further details. Often a very simple model that assumes a constant additive measurement error  $\varepsilon_m$  is applied, where  $\varepsilon_m$  is a normal distributed random variable. The relationship between the measured size  $s_m$  and the actual size  $s$  is then described by Equation (4-7).

$$s = s_m - \varepsilon_m \quad (4-7)$$

An alternative is to model the measurement error by a multiplicative factor, see Sørensen et al. (1991).

<sup>a</sup> A different derivation of the  $PoI$  may be found in Straub (2002).

### 4.2.5 Inspection performance models as likelihood functions

The *PoD*, the *PFI* as well as the *PoI* model can be interpreted as likelihood functions, introduced in Section 2.2.4. They describe the probability of an inspection outcome given the state of nature, which is the variable of interest. The relation between the measured defect size  $s_m$  and the effective defect size  $s$ , which represents the measurement accuracy, can also be reformulated as a likelihood function, demonstrated by the illustration in Section 2.2.4. The inspection performance models are therefore directly applicable for probability updating. Alternatively, limit state functions can be described for the different outcomes based on the inspection performance models, as presented in Section 4.4. These are then applied for reliability updating by means of SRA.

## 4.3 Derivation of inspection performance models

### 4.3.1 The ICON project

The Intercalibration of Offshore NDT (ICON) project was a major EEC project aimed at assessing the quality of underwater inspection techniques on welded joints by round robin tests, see Rudlin and Dover (1996). Different inspection methods were evaluated in this project by comparing effective fatigue cracks in different types of specimens (the characterised defects) with results from inspection trials on these specimens. Data from this project is used in the following for the numerical investigations.

### 4.3.2 Statistical inference of the parameters

The parameters of the *PoD* curves,  $\mathbf{q} = (q_1 \dots q_n)^T$ , are obtained by a regression analysis, where the parameters are estimated by the maximum-likelihood method in accordance with Sørensen et al. (1995) based on the general text by Lindley (1965); an alternative description is provided by Berens (1989). The maximum-likelihood method not only gives a point estimation of the parameters  $\mathbf{q}$ , but also the joint distribution of  $\mathbf{q}$ , so that additionally the statistical uncertainty of the parameters can be determined.

### 4.3.3 Numerical examples and investigations

Based on the data from the ICON project inspection models are derived. Due to the full characterisation of the inspected welds, it is possible to distinguish between detections and false indications and the *PoD* and *PFI* are thus separately evaluated (instead of only evaluating the combined *PoI*). Figure 4.3 shows as an example the *PoD* curve derived for underwater Magnetic Particle Inspection (MPI) on tubular joints, together with the individual trial results. The parameter estimations are based on a total of 950 trial inspections on trial specimens containing 217 characterised defects.

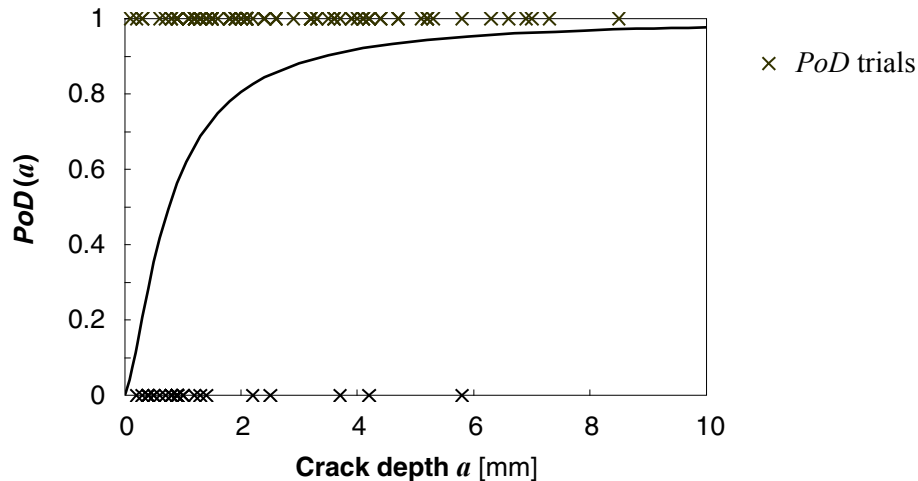


Figure 4.3 – PoD for underwater MPI on tubular joints using a log-logistics model.

In Figure 4.4 the resulting PoDs for underwater Alternating Current Field Measurement (ACFM) on tubular joints are illustrated, dependent on crack depth and crack length respectively, together with the confidence intervals. Note that both curves are derived from the same data set.

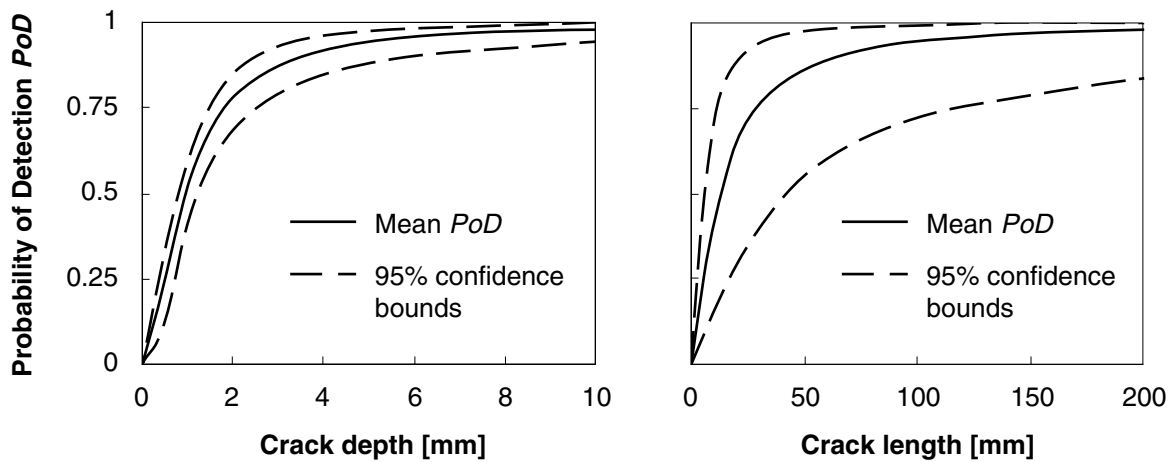


Figure 4.4 – Confidence bounds on the PoD for ACFM using a log-logistics model, Straub (2002).

From the confidence intervals in Figure 4.4 it is concluded that the crack depth is the more relevant criteria for this inspection technique, Straub (2002). This holds also for MPI. In Straub (2002) additionally a two-dimensional model is derived and the influence of the use of different models on the reliability updating of fatigue subjected details is investigated, one result is presented in Figure 4.5. Because two-dimensional models include more information than the one-dimensional models, they can be regarded as a reference, and it is seen that the use of a *PoD* model dependent on length underestimates the effect of the inspection on the reliability. Again, all *PoD* models are derived from the same trial data.

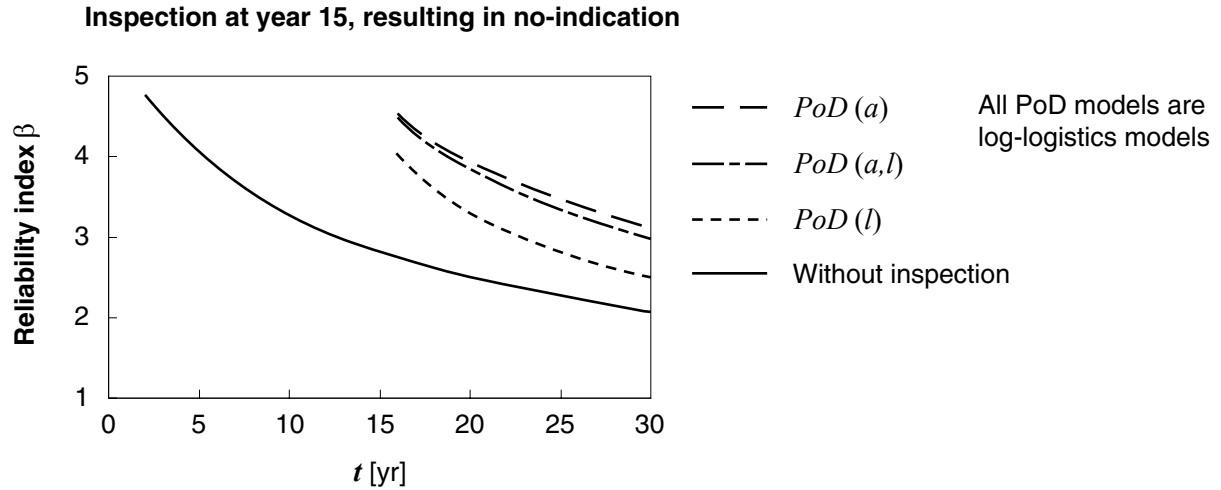


Figure 4.5 – Influence of the use of different *PoD* models on the reliability updating, from Straub (2002).

Here the log-logistics *PoD* model illustrated in Figure 4.3 is applied for the numerical investigations presented in Chapter 5. It is defined by Equation (4-1), its parameter values are multi-normal distributed with the values

$$\underline{\mathbf{q}} = \begin{bmatrix} \alpha_D \\ \beta_D \end{bmatrix}, \quad E[\underline{\mathbf{q}}] = \begin{bmatrix} 0.63 \\ 1.16 \end{bmatrix}, \quad V_{\underline{\mathbf{q}}\underline{\mathbf{q}}} = \begin{bmatrix} 0.0336 & 0.0079 \\ 0.0079 & 0.0524 \end{bmatrix}$$

The *PFI* is normal distributed with values

$$E[PFI] = 0.298 \cdot 10^{-3} \text{ mm}^{-1}, \quad V_{PFI} = 1.03 \cdot 10^{-9}$$

For the *PFI* model it is assumed that the inspected length at a hot spot is 0.5m; the resulting value for the *PFI* per hotspot is conservative due to the assumption of independence between individual false indications:

$$E[PFI] = 0.138 \text{ per hotspot}$$

The *PoI* is defined according to Equation (4-6).

#### 4.3.3.1 Inspection models from in-service observations

A different approach to the derivation of the *PoD* curve is pursued by Moan et al. (2000a). Based on a large amount of inspection data from in-service structures, the *PoD* is back-calculated together with the initial crack size. For this purpose, expert judgement is used to distinguish between propagating (fatigue) and non-propagating cracks. Assuming an exponential distribution for both initial crack size and *PoD*, their mean value can be derived from the mean size of the non-propagating cracks detected in the first inspection and of those detected in the second (but not in the first) inspection. From this procedure an exponential

*PoD* model with parameter  $\lambda_D = 1.95\text{mm}^a$  is found to be representative for the applied MPI inspections of tubular joints. As noted by Moan et al. (2000a) and as observed by comparison to the above presented model (see Figure 4.3), this model is more pessimistic than the commonly applied models, at least for small crack sizes.

## 4.4 Limit state functions for inspection modelling

### 4.4.1 Indication event

The event of indication of a defect, denoted by  $I$ , is used to update the probability of failure after the inspection according to Section 2.2.4. For the purpose of updating, the event is best described in terms of a limit state function (LSF). Note that the general literature only discusses LSF for the event of detection, but, as noted by Straub and Faber (2003a) and shown in the following, adaptation to the event of indication is straightforward if the *PoD* is replaced by the *PoI*.

The classical LSF for the description of the event of detection, see e.g. Madsen (1987), is given in Equation (4-8), where  $s_D$  is the detectable defect size.

$$g_D = s_D - s \quad (4-8)$$

Because the *PoD* is a monotonically increasing function, the probability of detecting a crack smaller than or equal to  $s$  is  $PoD(s)$ . If the *PoD* asymptotically becomes 1 for very large crack sizes, then  $s_D$  can be related to the *PoD* by

$$\begin{aligned} F_{s_D}(s) &= PoD(s) \\ f_{s_D}(s) &= \frac{d PoD(s)}{ds} \end{aligned} \quad (4-9)$$

This approach, in spite of its wide application, has some shortcomings. First, the *PoD* must be a distribution function, i.e. fulfil the above stated condition, which is not always the case: Many *PoD* models, such as the exponential threshold model (Equation 4-2), include a probability of non-detection even for the very large (infinite) defect. Additionally, as shown by Hong (1997), it is very difficult to include two-dimensional *PoD* formulations, and finally this LSF is not suitable for the extension to the event of indication, because the *PoI* is not a distribution function. Therefore another formulation is presented in the next section for the event of indication, based on an idea presented by Hong (1997) for the detection event.

For a given multidimensional crack size distribution  $f_{\underline{s}}(\underline{s})$ , the probability of an indication can be evaluated as

$$P(I) = \int_{\underline{s}} PoI(\underline{s}) f_{\underline{s}}(\underline{s}) \cdot d\underline{s} \quad (4-10)$$

---

<sup>a</sup> The exponential model is equivalent to that given in Equation (4-2) with parameter  $P_0 = 1$ .

The  $PoI$  can be replaced and the equation rewritten as

$$P(I) = \int_{\underline{s}} \left[ \int_0^{PoI(\underline{s})} f_u(u) du \right] f_{\underline{s}}(\underline{s}) d\underline{s} = \int_{g_I \leq 0} f_u(u) f_{\underline{s}}(\underline{s}) du d\underline{s} \quad (4-11)$$

where  $U$  is a uniformly distributed random variable with range from 0 to 1 and where the limit state function is

$$g_I = u - PoI(\underline{s}) \quad (4-12)$$

This is the classical structural reliability problem that can be evaluated by means of SRA. Similarly, as described by Hong (1997), the limit state function can be derived as

$$g_I = z - \Phi^{-1}(PoI(\underline{s})) \quad (4-13)$$

where  $Z$  is a standard normal distributed random variable and  $\Phi^{-1}(\cdot)$  is the inverse of the standard normal distribution function. Equation (4-13) is favourable for reliability evaluation by means of FORM or SORM and is applied for all examples presented in the further.

#### 4.4.2 Crack size measurement

Assuming the simple linear model for the sizing error described in Section 4.2.4, the LSF describing the event of a crack measurement that results in a measured size  $s_m$  is

$$g_M = s - (s_m - \varepsilon_m) \quad (4-14)$$

Note that this event is an equality event, which is of importance in the updating of the reliability after a detected crack has been measured.

### 4.5 Uncertainty in the inspection performance models

#### 4.5.1 Sources of uncertainty

Different factors contribute to the variability and the uncertainty in  $PoD$  and  $PoI$  models. In order to clarify the impact of these factors on the probabilistic inspection modelling it is suggested to classify them as follows (where (a) is an aleatory and (b) to (d) are epistemic uncertainties<sup>a</sup>):

- (a) Variability due to the scatter in the response signals (random noise)

---

<sup>a</sup> The concepts of aleatory uncertainty (random variability) and epistemic uncertainty, which is related to incomplete knowledge, are treated by e.g. Apostolakis (1990) and Faber (2003b). A short introduction is given by Straub and Faber (2003a).

- (b) Statistical uncertainty due to the limited set of trials in experimentally determined *PoD* / *PoI* models
- (c) Model uncertainty due to the empirical nature of the (parametric) model
- (d) Model uncertainty due to the effect of omitting all influencing factors other than defect dimensions in the *PoD* / *PoI* function<sup>a</sup>

If no uncertainty (aleatory and epistemic) were influencing the inspection performance then the *PoD* could only take values 0 or 1, as for each defect size it would be known whether the defect is detected or not. In reality this is not the case, and therefore the *PoD* function is defined as the mean rate of detection obtained by integration over the uncertain parameters. Random noise (a) is treated separately because aleatory uncertainty cannot be reduced (for a fixed inspection method and detection threshold). The statistical uncertainty (b) can be reduced by performing additional tests, the uncertainty due to the empirical formulation (c) can be reduced by considering and comparing different formulations, see e.g. Straub (2002). The uncertainty due to the disregarded factors (d) can be reduced when these are explicitly accounted for, i.e. the model of the inspection quality must be formulated as a function of these factors in order to facilitate reduction of this uncertainty. In the ICON project this is accounted for by establishing different models for the application of the inspection methods in underwater and in atmospheric conditions, therefore reducing the scatter in the *PoD* estimate.

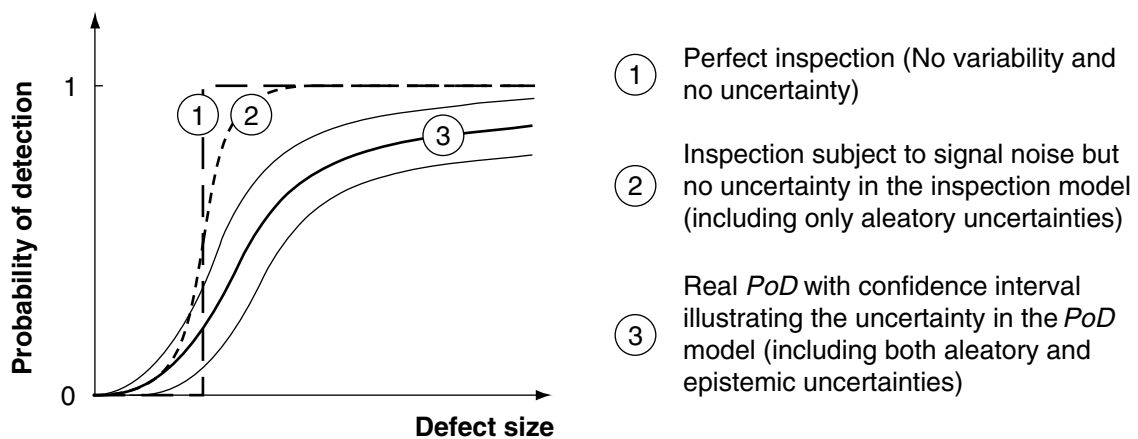


Figure 4.6 –The uncertainties in inspection modelling illustrated on the *PoD*.

#### 4.5.2 Probabilistic *PoD* formulation

Assume that there exists a “true” *PoD* curve for given inspection method, inspector, environment and defect type. This *PoD* curve is then the mean rate of detection obtained by

<sup>a</sup> Berens and Hovey (1983) state that “to model the *POD*, it can be assumed that there is a distribution of detection probabilities at each crack length where the scatter in this distribution is caused by the nonreproducibility of all factors other than crack length. Examples of such factors are differences in detectability due to operators, human factors, environments, and crack orientation, geometry or location.”



integration over the *aleatory* uncertainties associated with the inspection performance. As this is the “true” model, there would be no epistemic uncertainty on this model, *if it were known*. Because the true model is not known, it can only be estimated by performing *PoD* trials. This estimate is then subject to epistemic uncertainty, which can be described by a joint probability density function of the *PoD* parameters  $\underline{\mathbf{Q}}$ ,  $f_{\underline{\mathbf{Q}}}(\underline{\mathbf{q}})$ .

When performing *PoD* experiments, it is important to perform the trials for different selections of all the factors that might vary in field inspections. These include different inspectors, different environmental conditions, etc., to the extent that the application of the *PoD* curve is not restricted (e.g. to a specific environment). Data obtained from such trials can then be used for statistical analysis. However, as noted by Wall and Wedgwood (1994), round-robin tests are always subject to biases, which should be accounted for if possible.

### 4.5.3 Influence of the *PoD* uncertainty on the reliability updating

When considering the updating of the reliability of individual hot spots after an inspection, it is sufficient to use the mean *PoD* curve (or the mean *PoI* curve), which is given by Equation (4-15), see Hong (1997) for details.

$$E[PoD(s)] = \int_{\underline{\mathbf{Q}}} PoD(s|\underline{\mathbf{q}}) f_{\underline{\mathbf{Q}}}(\underline{\mathbf{q}}) d\underline{\mathbf{q}} \quad (4-15)$$

Note that this mean *PoD* is not equivalent to the *PoD* curve obtained by applying the mean values of the parameters,  $E[\underline{\mathbf{q}}]$ , to the *PoD* model. However, if the variance in the *PoD* estimates is sufficiently small, this may be utilised as a first approximation, i.e.

$$E[PoD(s)] \approx PoD(s|E[\underline{\mathbf{q}}]) \quad (4-16)$$

This approximation is valid for the MPI model introduced in Section 4.3.3.

## 4.6 Modelling the dependency between individual inspections

Considering an isolated inspection of one single potential defect location, the uncertainty in the *PoD* and *PoI* has no influence on the updating of the deterioration model, as reported above. However, inspections are normally not performed individually but on an entire system. Hitherto it has been assumed that the individual inspections are statistically independent, which generally is not the case due to common influencing factors such as environmental conditions and inspector characteristics. If the *PoD* and the *PoI* are regarded as stochastic models, these factors cause a dependency between the models for the individual inspections. The modelling of this dependency is first presented by Straub and Faber (2003a) together with a numerical investigation; a short summary is presented in the following.

Based on the above described considerations and uncertainty modelling it can be shown that the *PoD* / *PoI* functions of the inspections of different hot spots might be highly correlated, especially for similar and adjoining hot spots. This correlation can then be used to update the

*PoD / PoI* model by means of the inspection results, in analogy to the Bayesian updating of the crack size distribution. This in term will influence the reliability updating of structural systems after inspections, as presented in Chapter 6.

The numerical investigations performed by Straub and Faber (2003a) show that the influence of the inter-dependency between the performances of individual inspections on the updated system reliability is low. This is because a) the aleatory uncertainty in inspection performance is always independent, and b) the uncertainty in the inspection performance is small compared to the uncertainty on the deterioration state. The inclusion of the dependency is therefore advocated only for very critical systems or in systems with a very large number of similar hot spots. However, it should not be concluded that applying different inspectors or different NDE techniques (to ensure independency) is not advantageous. The presented model assumes that no gross errors occur during inspections. Independent inspections reveal such errors and therefore assure that the model assumptions are fulfilled. Additionally, for very critical details combination of different inspection methods can improve the *PoD*, see Yang and Donath (1983) or Horn and Mayo (2000).

## 4.7 Modelling inspections for corrosion control

The quantitative modelling of the performance of inspections for corrosion control has less tradition than that for inspections of fatigue subjected structures. Generally accepted formats, such as the *PoD* for crack detection, do not exist, although it is shown in the following that the models presented in Section 4.2 are also suitable for the description of corrosion related inspections.

Most inspections for corrosion (not those for very localised corrosion phenomena, such as SCC) are fundamentally different from the inspections for cracks, as they are measuring the (minimal) wall thickness<sup>a</sup>. The result of the inspection is not a discrete indication (respectively no-indication) event, but rather a measurement on a continuous scale. Therefore, for an ideal uniform corrosion mechanism, the inspection is sufficiently described by the measurement uncertainty. In a real structure, the corrosion depth will always shows some variation over the total area, but if general corrosion is identified as the critical failure mode and if the variations are limited, then the measurement uncertainty is still a sufficient description of the inspection performance. It can be described in analogy to the uncertainty in crack size measurements, Section 4.2.4.

For most problems, however, the maximum corrosion depth is of interest. The probability of missing the largest defect is consequently very important when modelling inspections on these structures. This has been neglected in previous publications. In the RACH project (1999) *PoD* trials were performed on pipes containing internal and / or external localised corrosion defects. Due to the localised nature of the defects, the trial results can be analysed as described in Section 4.3, resulting in *PoD* and *PFI* (and consequently in the *PoI*). Section 4.7.1 provides such a model.

---

<sup>a</sup> Most inspection techniques are based on ultrasonic or electromagnetic principles for the measurement of the wall thickness, see RACH (1999).

When updating the reliability based on the inspection performance models, the different situations must be accounted for separately: If general corrosion is the main concern, then the wall thickness measurements should be directly considered by means of a limit state function like Equation (4-14), taking into account the spatial variations of the general corrosion. If localised corrosion is of concern, the situation is slightly more complicated, and requires some additional considerations, which are presented in Section 4.7.2.

#### 4.7.1 Example inspection performance model for corrosion subjected structures

The applied inspection performance model is evaluated from trial data derived during a round robin test in analogy to Section 4.3; the model is first published in CRIS (2004). The inspection performance is described by the  $PoD$  and the measurement uncertainty  $\varepsilon_m$ ; the probability of false indications  $PFI$  is not available due to lack of data. For the numerical investigations to follow it is assumed that the  $PFI = 0$ , the  $PoI$  is therefore equal to the  $PoD$ . The  $PoD$  is described by a log-logistics model (Equation 4-1) with parameters  $\alpha_D$  and  $\beta_D$ . These are multi-normal distributed with

$$\underline{\mathbf{q}} = \begin{bmatrix} \alpha_D \\ \beta_D \end{bmatrix}, \quad E[\underline{\mathbf{q}}] = \begin{bmatrix} -1.07 \\ 2.571 \end{bmatrix}, \quad V_{\underline{\mathbf{q}}\underline{\mathbf{q}}} = \begin{bmatrix} 0.537 & -0.565 \\ -0.565 & 0.673 \end{bmatrix}$$

Due to the large uncertainties involved in these estimates, the full stochastic description of the parameters must be taken into account for the reliability updating; the approximation in Equation (4-16) is not valid for this model. The  $PoD$  model is illustrated in Figure 4.7.

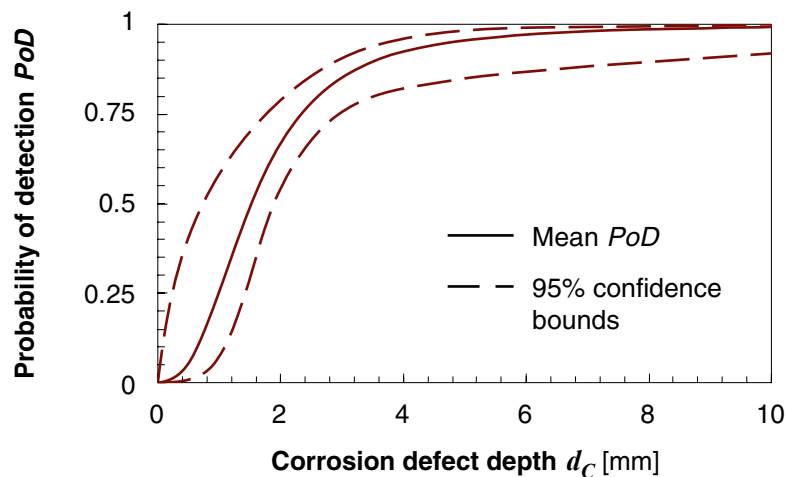


Figure 4.7 - Example  $PoD$  model for inspections on corrosion subjected pipelines.

The measurement uncertainty is modelled as Normal distributed,  $\varepsilon_m \sim N[0,0.8\text{mm}]$ .

Note that the inspection model is based on trials performed on pipeline elements approx. 2.5m long with wall thickness  $d$  in the range of 5 to 15mm and diameter 110 to 220 mm. When

applying the model to different dimensions, the uncertainty on the model is increased, but this is not considered in the presented examples.

#### 4.7.2 Reliability updating for structures subject to localised corrosion based on measurements

The inspection performance is described by means of the *PoI* and the measurement uncertainty. There are two different possible inspection outcomes, no-indication or indication and measurement of a defect resulting in a measured defect size  $s_o$ <sup>a</sup>. If no defect is indicated, the reliability is updated directly using the *PoI*, in analogy to the inspections for fatigue cracks. If a defect is found and measured, both *PoI* and measurement uncertainty must be taken into account, as it is unknown whether the indicated defect is the largest or not. This section introduces the updating of the defect distribution and the reliability for such situations.

The measurement error  $\varepsilon_m$  is neglected in the following for the sake of simplicity; the extension to the general case including  $\varepsilon_m$  is straightforward, as outlined later.

When a defect with size  $s_o$  is observed, although it is unknown if this is the largest defect, it is known that the largest defect, denoted by  $s$ , is equal to or larger than  $s_o$ . The observation of  $s_o$  can thus be used to update the probability density function (pdf) of the largest defect,  $f'_s(s)$ , by means of Bayes' rule, Equation (4-17).

$$f''_s(s|s_o) = \frac{L(s_o|s)f'_s(s)}{f_{s_o}(s_o)} \quad (4-17)$$

However, the corrosion model only describes the size  $s$  of the largest defect and gives no information about the number and the size of the other defects in the considered area<sup>b</sup>. It is therefore not possible to calculate the prior pdf of  $s_o$ ,  $f_{s_o}(s_o)$ , and the likelihood function  $L(s_o|s)$  cannot be determined for all  $s$ ; the available information on  $L(s_o|s)$  can be summarised as

$$\begin{aligned} L(s_o|s) &= f_o(s, s_o), & s_o \leq s \\ L(s_o|s) &= 0, & s_o > s \end{aligned} \quad (4-18)$$

with unknown function  $f_o(s, s_o)$ . It is tempting to assume  $L(s_o|s) = const$  for any  $s_o \leq s$ , but this neglects the fact that a defect of size  $s_o$  has been observed, which implies that

$$f''_s(s_o|s_o) \gg f''_s(s|s_o), \quad s > s_o \quad (4-19)$$

A different approach must thus be chosen. If it is assumed that the sizes of the individual defects in the area are independent, then it appears reasonable to assume that

---

<sup>a</sup> Denoting the measured crack size by  $s_o$  instead of  $s_m$  indicates that the observed defect is not necessarily the largest defect.

<sup>b</sup> This corrosion model is in accordance with Section 3.5.3. If the largest defect is decisive for the reliability, this model is by far the most practical one.

$$f_s''(s|s_o) = f_s'(s), \quad s > s_o \quad (4-20)$$

Based on this assumption and the likelihood function according to Equation (4-18), the full posterior pdf of  $s$  is given as

$$f_s''(s|s_o) = \begin{cases} 0, & s < s_o \\ P_1 \delta(s - s_o), & s = s_o \\ f_s'(s), & s \geq s_o \end{cases} \quad (4-21)$$

with  $\delta(\cdot)$  being Dirac's delta function. The constant  $P_1$  is determined from the condition that  $\int_s f_s''(s|s_o) ds = 1$  and results in

$$P_1 = F_s'(s_o) \quad (4-22)$$

The validity of the basic assumption in Equation (4-20) has been checked numerically by assuming knowledge on the distribution of the number of defects and the distributions of the individual defect sizes. The observed agreement between the full calculations and the assumption is good given independency of the individual defects and given that the expected number of defects is sufficiently large.

The observation of  $s_o$  is, however, not the only available information obtained from the inspection. Additionally, it is observed that no larger defect has been identified at the inspection. This event is denoted by  $\overline{I_L}$ , where  $I_L$  is defined as the intersection of the events  $I$  and  $L$ . It is

$$L = \{s > s_o\} \text{ and } I = \{z < \Phi^{-1}(PoI(s))\} \quad (4-23)$$

The definition of the event  $I$  follows the LSF describing indication, Equation (4-13). The event  $\overline{I_L}$  can be written as

$$\overline{I_L} = \overline{L} \cup \overline{I} \quad (4-24)$$

The updated pdf of the size of the largest defect is

$$f_s''(s|\overline{I_L} \cap s_o) = \frac{P(\overline{I_L}|s \cap s_o) f_s''(s|s_o)}{P(\overline{I_L}|s_o)} \quad (4-25)$$

Given  $s > s_o$ , the event  $\overline{I_L}$  is independent on  $s_o$ . The corresponding likelihood function is thus given by

$$P(\overline{I_L}|s \cap s_o) = \begin{cases} 1, & s \leq s_o \\ (1 - PoI(s)), & s > s_o \end{cases} \quad (4-26)$$

$P(\overline{I_L}|s_o)$  is determined by the condition  $\int_s f_s''(s|\overline{I_L} \cap s_o) ds = 1$  as

$$P(\bar{I}_L|s_o) = F'_s(s_o) + \int_{s_o}^{\infty} f'_s(s)(1 - PoI(s))ds \quad (4-27)$$

The resulting posterior pdf of the maximum defect size is a mixed distribution due to the Dirac delta function in Equation (4-21):

$$f_s''(s|\bar{I}_L \cap s_o) = \begin{cases} 0, & s < s_o \\ F'_s(s_o)\delta(s - s_o)P(\bar{I}_L|s_o)^{-1}, & s = s_o \\ (1 - PoI(s))f'_s(s)P(\bar{I}_L|s_o)^{-1}, & s > s_o \end{cases} \quad (4-28)$$

So far it has been assumed that the measurement is perfect, i.e.  $\varepsilon_m = 0$ . For the general case, when the measurement uncertainty is additive (Equation (4-7)),  $s_o$  must be replaced by  $s_o + \varepsilon_m$  and Equations (4-17 to 4-28) must be replaced by their expectations with respect to  $\varepsilon_m$ .

For the application in SRA it is helpful to evaluate the probability that the indicated defect is not the largest defect. This event is denoted by  $\bar{I}_s$  and is defined as  $\bar{I}_s = \{\bar{I} \cap L\}$ . It is

$$\begin{aligned} P(\bar{I}_s|\bar{I}_L \cap s_o) &= P(\bar{I} \cap L | (\bar{L} \cup \bar{I}) \cap s_o) \\ &= \frac{P((\bar{I} \cap L \cap \bar{L} \cap s_o) \cup (\bar{I} \cap L \cap s_o))}{P(\bar{I}_L|s_o)P(s_o)} = \frac{P(\bar{I} \cap L \cap s_o)}{P(\bar{I}_L|s_o)P(s_o)} \\ &= \frac{P(\bar{I} \cap L|s_o)}{P(\bar{I}_L|s_o)} = \frac{P(\bar{I} \cap L)}{P(\bar{I}_L|s_o)} = \frac{P(\bar{I}_s)}{P(\bar{I}_L|s_o)} \end{aligned} \quad (4-29)$$

From Equation (4-27) it is observed that

$$P(\bar{I}_L|s_o) = P(\bar{L}) + P(L \cap \bar{I}) = P(\bar{L}) + P(\bar{I}_s) \quad (4-30)$$

Therefore

$$P(\bar{I}_s|\bar{I}_L \cap s_o) = \frac{P(\bar{I}_s)}{P(\bar{L}) + P(\bar{I}_s)} \quad (4-31)$$

The updated probability of failure is calculated as

$$\begin{aligned} P(F|s_o \cap \bar{I}_L) &= P(F \cap \bar{I}_s|s_o \cap \bar{I}_L) + P(F \cap I_s|s_o \cap \bar{I}_L) \\ &= P(F|\bar{I}_L \cap s_o \cap \bar{I}_s)P(\bar{I}_s|\bar{I}_L \cap s_o) + P(F|\bar{I}_L \cap s_o \cap I_s)P(I_s|\bar{I}_L \cap s_o) \end{aligned} \quad (4-32)$$

From Equation (4-21) it follows that, given  $L$ , the pdf of  $s$  is independent on  $s_o$ ; the same applies therefore also to the probability of failure  $P(F)$ . Because additionally  $\bar{I}_s$  is a subset of  $\bar{I}_L$ , it is

$$P(F|\bar{I}_L \cap s_o \cap \bar{I}_S) = P(F|s_o \cap (\bar{I} \cap L)) = P(F|\bar{I}_S) \quad (4-33)$$

and

$$P(F|\bar{I}_L \cap s_o \cap I_S) = P(F|(\bar{I} \cup \bar{L}) \cap s_o \cap (I \cup \bar{L})) = P(F|s_o \cap \bar{L}) \quad (4-34)$$

The event  $\{s_o \cap \bar{L}\}$  is equal to  $\{s = s_o\}$ , which is the measurement event  $M$  in accordance with Section (4.2.4). The updated failure probability is thus written as

$$P(F|s_o \cap \bar{I}_L) = P(F|\bar{I}_S)P(\bar{I}_S) + P(F|M)P(I_S) \quad (4-35)$$

The first term in Equation (4-35) corresponds to the no-detection event, the second term to the measurement event when the largest defect is measured.

The corrosion model from CRIS (2004), which is introduced in Section 5.6, is utilised for a numerical investigation, together with the inspection model from Section 4.7.1: The updated reliability using Equation (4-35) is compared to the reliability updated using either only the no-indication event or the measurement event. Figure 4.8 shows the results for two different measurements (indicating a corrosion depth  $d_m$ ) as evaluated with SORM:

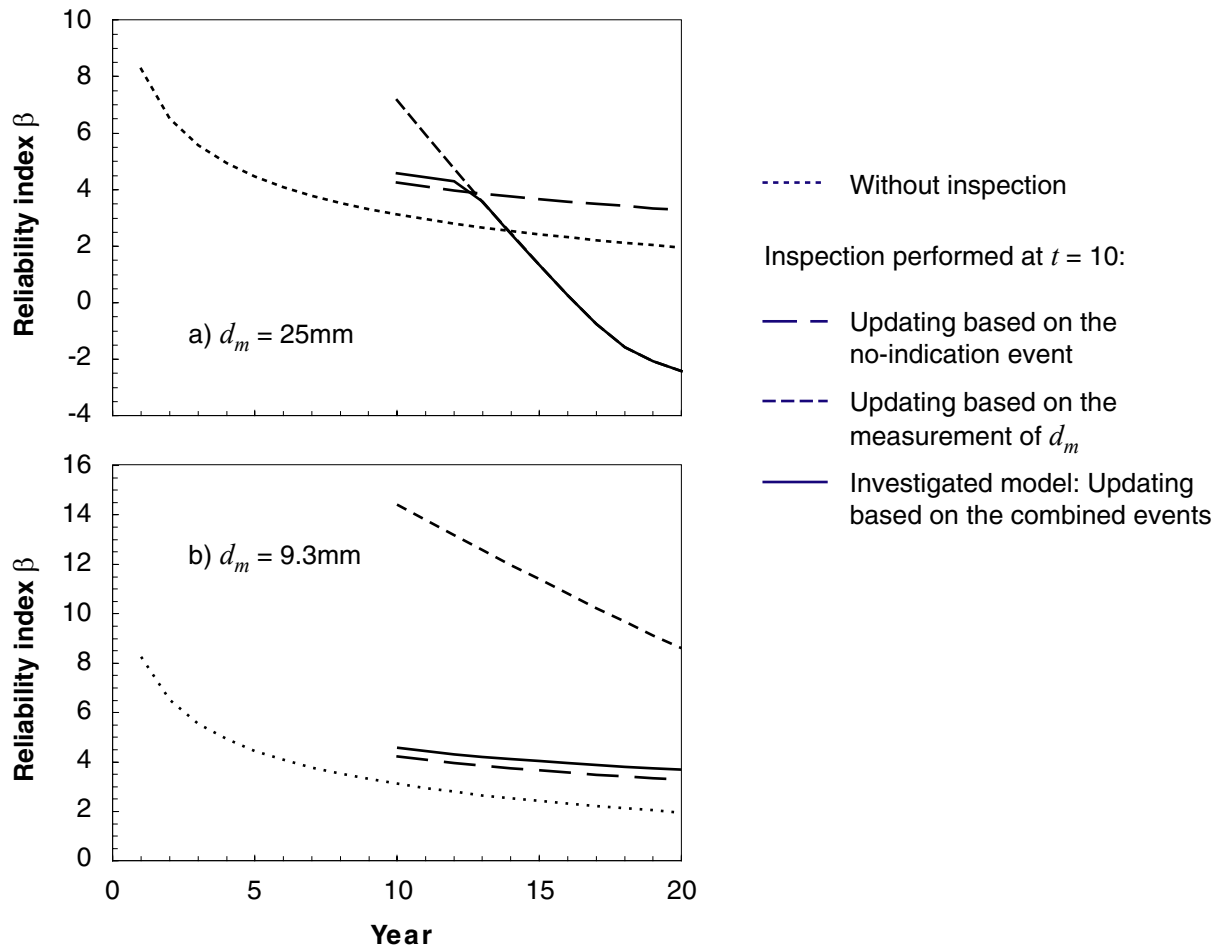


Figure 4.8 – Reliability updating after an inspection for localised corrosion.

The results in Figure 4.8 are interpreted as follows. The reliability updated with the combined events is always equal to or lower than the reliability updated by considering only the measurement event. This is because, if a defect has been found, accounting for the possibility that a bigger defect has been missed can only decrease the reliability. Where the probability of no-detection is decisive, the updated reliability is slightly higher if the measurement is considered. This can be explained by observing that the indication of a defect with depth  $d_m$  increases the probability of no-indication of a defect larger than  $d_m$ , Equation (4-27).

Based on these results, it is concluded that it is sufficient to apply the no-indication event and the measurement event separately. The event that yields the lower updated reliability is then considered alone, resulting in an approximation to the real reliability. As long as the measured corrosion defect is not very large, the no-indication event is decisive at any time during the service life. Such a situation is present in Figure 4.8b. For the case shown in Figure 4.8a this does not hold; here it is necessary to consider the no-indication event for the first time after the inspection and the measurement event for the later period. The distinction between these two situations is further discussed and applied in the generic approach to RBI for corrosion subjected structures, Section 5.6.



## 5 Generic modelling

### 5.1 Introduction

All engineering modelling is generic by nature. Its aim is the description of the considered physical (or other) process by means of its most influencing parameters and their interrelations. However, each occurrence in nature is unique due to the infinite number of influencing parameters, which cannot all be included in the model, and each model is thus generic (it includes a range of possible states<sup>a</sup>). Nonetheless is it not redundant to use the term generic for the approach presented in this thesis, as it emphasises the distinction between the traditional RBI procedures, which are performed for a particular hot spot, and the present procedure that performs the calculation for an entire group of hot spots by taking advantage of the generic properties of the modelling.

The traditional RBI procedures, which correspond to the methods as presented in Chapter 2, are computationally demanding due to the required probability evaluations. In addition, because automation of the calculations is not realistic at present, they can only be applied by an engineer with experience in probabilistic modelling and reliability analysis, as well as deterioration and inspection modelling. As traditional RBI procedures perform the inspection planning individually for specific hot spots, these disadvantages have restricted the application of the methods significantly: The apparent effort to compute risk based inspection plans is not balanced with the benefits for most potential application areas.

The basic idea of the generic approach is to perform the time-consuming RBI analysis not for single, individual hot spots, but for generic representations of these; i.e. (generic) inspection plans are evaluated for different values of the most influencing parameters (named generic parameters). Inspection plans for the specific hot spots in a structure are then derived by a simple interpolation between the generic inspection plans as a function of the specific values of the generic parameters. These parameters, which can also be conceived as indicators, are in general obtained from standard design procedures. Although the effort to compute the generic inspection plans is still large, the derivation of specific inspection plans by interpolation is very efficient, once a database containing the generic inspection plans has been established. Furthermore, if the interpolation procedure is presented in a suitable format, the application by engineers who are not necessarily familiar with all the technical aspects involved in RBI is highly facilitated. A software tool, named iPlan.xls, is developed for this purpose.

The traditional RBI analysis can be considered as an experiment with inputs (the parameters of the model) and outputs (the inspection plans). The presented generic approach simply establishes an empirical relationship between these inputs and outputs. This is illustrated in Figure 5.1. Due to its empirical nature, a detailed assessment of this relationship (model) is

---

<sup>a</sup> A structural model of a building is valid whether the house is painted yellow or grey. The yellow and the grey buildings are clearly two different ones, but the model is the same for both; it is thus generic with respect to the colour.

required. The influence of each parameter has to be evaluated numerically and the final model must be verified by comparison to direct calculations of inspection plans.

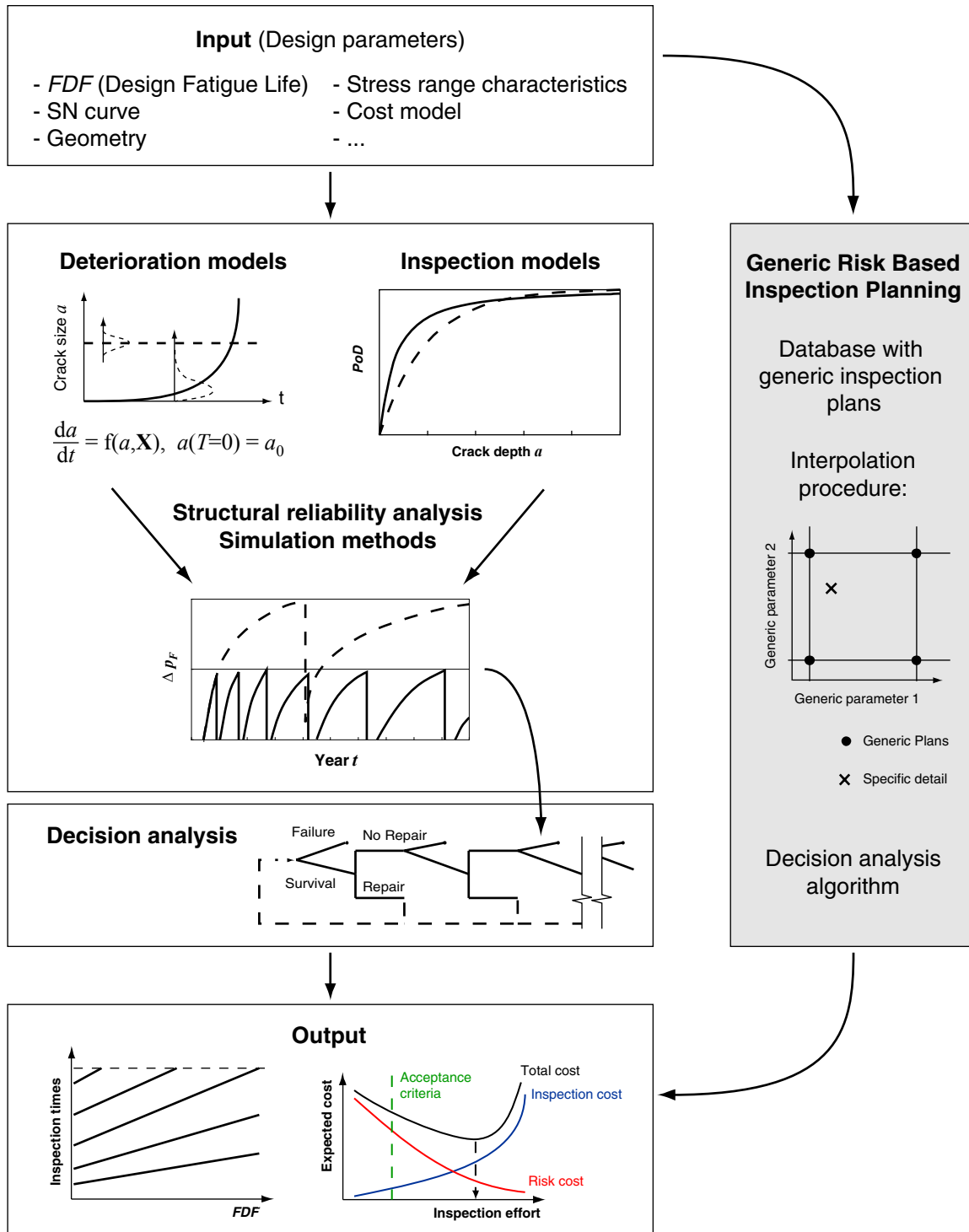


Figure 5.1 – Illustration of the generic approach to RBI.

The present chapter introduces the generic approach to RBI by a definition of its main components and a description of the computational procedure. Then its application to fatigue subjected structures is illustrated on a representative example, which comprises of a sensitivity analysis with a discussion of the influencing parameters and finally the design of an example database containing the generic plans. Practical aspects of the application are covered, including the actualisation of inspection plans after the inspections are performed and the updating of inspection plans when the fatigue loading is modified during the service life. The chapter concludes with Section 5.6, introducing the generic inspection planning for corrosion subjected structures. The methodology is for this purpose illustrated on the problem of CO<sub>2</sub> corrosion in pipelines and vessels.

## 5.2 Definitions

### Hot Spots

As described by Faber and Sorensen (1999) and in accordance with Section 3.2.2 it is assumed that the structural system for the purpose of inspection and maintenance planning may be represented by a number of critical locations or so-called hot spots, where either the a-priori probability of failure is orders of magnitude larger than at other points in the structure, or for which the consequences of failure are particularly high. Typical hot spots in fatigue subjected structures are situated in welded connections from where fatigue crack growth may initiate and propagate, Section 3.2.2 In this work the use of the term hot spot is extended to other deterioration mechanisms of a less discrete nature, such as corrosion, where a hot spot is typically an element as illustrated in Figure 3.18. Structural systems are generally composed of a group of hot spots, as identified in a risk analysis procedure and considered for RBI, and other structural members, whose required inspection and maintenance efforts are determined by means of a qualitative or semi-quantitative risk analysis, as outlined in Section 1.2.

### Generic parameters

Generic parameters are input parameters to the model that allow specifying the individual hot spots. A specific hot spot is characterised by a set of specific values of all generic parameters. If e.g. the thickness of the member at the hot spot is the only generic parameter, then all hot spots are fully characterised by their thickness<sup>a</sup>. All known influential parameters should be generic parameters. All influential parameters that can change from one hot spot to the other and which are not modelled as generic parameters will increase the model uncertainty and thus decrease the reliability. On the other hand, every additional generic parameter will increase the amount of computation effort in the calculation of the generic inspection plans. To define a parameter as generic parameter is furthermore only reasonable if its value can be determined for the individual hot spots.

---

<sup>a</sup> The name *generic parameters* is actually misleading, as these parameters are exactly NOT generic but are modelled with different values from one hot spot to another.

Generic representations

Inspection plans are evaluated for different values of the generic parameters. These values are named generic representations. If inspection plans are calculated for three different values of the thickness  $d_1$ ,  $d_2$  and  $d_3$ , then these three values are the generic representation of the generic parameter thickness. The generic representations are the supporting values of the interpolation used to determine the inspection plans for the specific hot spots.

Generic inspection plans

Generic inspection plans are the pre-fabricated inspection plans that are evaluated for all combinations of the generic representations and the considered values of the optimisation parameter according to Section 2.4.2. This optimisation parameter is either the threshold on the annual probability of failure  $\Delta p_F^T$  or the total number of inspections,  $n_{Insp}$ , if equidistant inspection times are sought. If there are  $n_{GP}$  generic parameters with  $n_{GR}(i)$  generic representations each and  $n_{OP}$  considered values of the optimisation parameter, then the total number of generic inspection plans is

$$n_{GIP} = n_{OP} \prod_{i=1}^{n_{GP}} n_{GR}(i) \tag{5-1}$$

The generic inspection plans consist of the calculated inspection times and the probabilities required for the evaluation of the decision tree as defined in Section 2.4.1. The generic inspection plans are stored in a database, which is named generic database and whose proposed design is presented in Section 5.3.2.

The definitions are illustrated in Figure 5.2, showing a situation with two generic parameters,  $GP_1$  and  $GP_2$ , each with two generic representations.

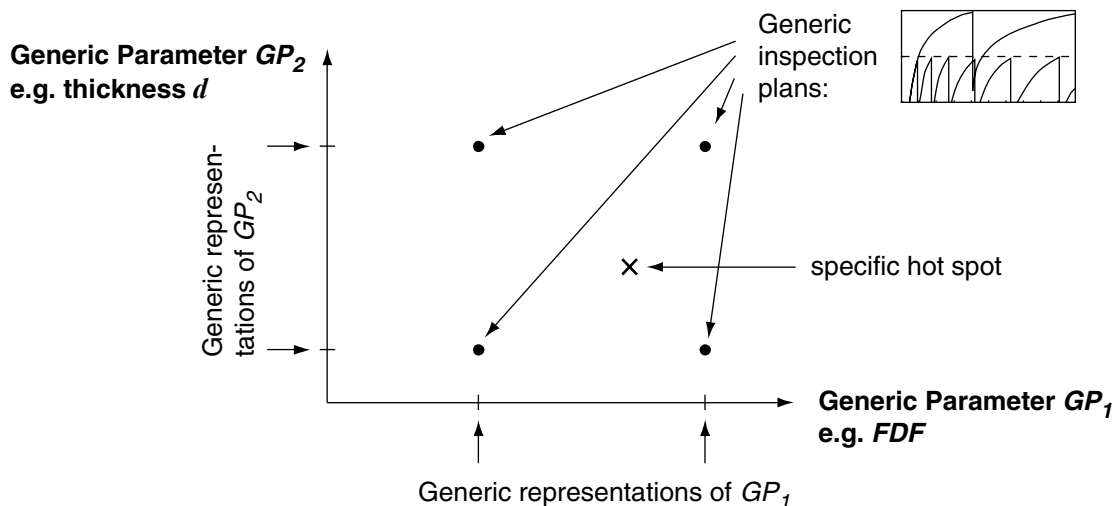


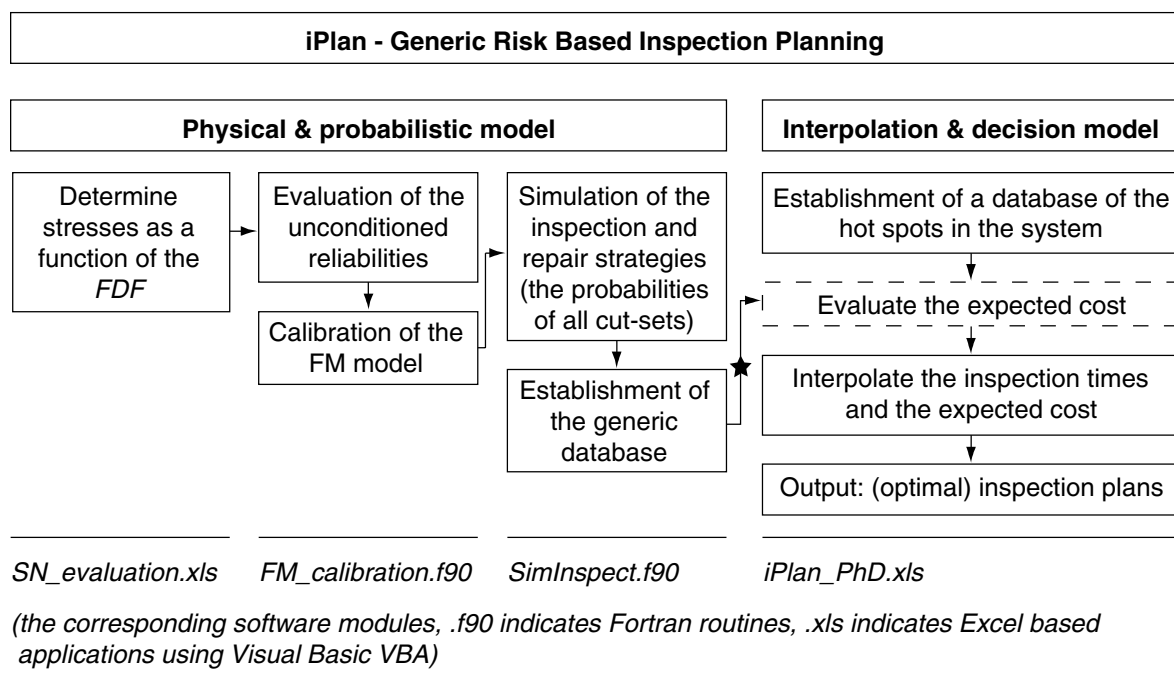
Figure 5.2 – Illustration of the definitions in the generic approach to RBI.

### 5.3 Computational aspects

For the practical implementation of the generic approach to RBI, a software tool named iPlan has been developed within the framework of this thesis. By means of describing the principles and the structure of iPlan, this section introduces the more practical aspects of the generic approach.

The iPlan software consists of two main parts. The purpose of the first part is the derivation of the generic inspection plans; the second part calculates the inspection plans for specific hot spots, based on a database of generic inspection plans. The first part includes all the physical and probabilistic modelling of the deterioration and failure modes, as well as the inspection performance. It computes all probabilities of the different intersections of events in the decision tree. This is the time-consuming part of the RBI calculations; as a consequence, a main priority for the software performing these tasks is its computational performance. For this reason, the software modules are provided as Fortran source codes, whose application requires experience in probabilistic deterioration and inspection modelling as well as reliability analysis. In contrast, the second part of iPlan is designed with a user-friendly interface, which facilitates the computation of the inspection plans by an engineer who is not necessarily an expert in all aspects of RBI. This concept ensures that after an initial effort by the specialist (namely the derivation of the generic inspection plans and the establishment of the second part of iPlan), the RBI can be performed in a highly efficient manner by the engineer who is responsible for the maintenance of the structure.

The general iPlan architecture, as it applies to fatigue subjected hot spots, is illustrated in Figure 5.3.



- Work & information flow
- ★ Generic inspection plans

Figure 5.3 – Architecture of iPlan for fatigue subjected hot spots.

### 5.3.1 Calculation of the generic inspection plans

The generic inspection plans are calculated according to the RBI methods presented in Chapter 2, for all different combinations of generic representations of the generic parameters. To illustrate the procedure, the derivation and application of a generic database for fatigue subjected hot spots, as outlined in Figure 5.3, is described in the following.

First the probabilistic SN deterioration model is established as a function of the generic parameters, i.e. the stress model has to be determined as a function of the  $FDF$ , in accordance with Straub (2001) and Section 5.5.1.2. Based on this model, a crack growth (FM) model is calibrated to the SN model according to Section 3.4, which requires the evaluation of the reliability with FORM or SORM for both models. This procedure is computationally demanding as it involves different levels of optimisation and it is of utmost importance that the applied algorithm is very stable.

With the established stochastic FM model, the probabilities of all branches in the decision tree (e.g. probabilities of failure given no failure and given no-repair at the previous inspections) are evaluated. These calculations are performed using crude Monte Carlo simulation (MCS). MCS is the only reliability evaluation technique where the accuracy of the outcome is not dependent on the starting values (which are required for every numerical solution) and so allows for a fully automated calculation procedure. Although it requires a large number of calls of the limit state functions (LSF)<sup>a</sup> and is consequently very time consuming, it is by far the most economical technique with regard to required man-days for the considered applications. Details on the required computational efforts needed for the presented examples are provided in Section 5.5.8.1. The parameter determining the accuracy as well as the computation time of the calculations is the number of simulations  $n_{MC}$ . The optimal choice of  $n_{MC}$  is ensured when a balance is achieved between the calculation accuracy and the computation time; Annex C provides a method for assessing the accuracy of the MCS in the calculation of inspection plans and discusses the optimal  $n_{MC}$ . Note that all results of MCS presented in this thesis are obtained with  $n_{MC} = 2 \cdot 10^6$ , if not otherwise stated.

Finally the generic inspection plans, consisting of inspection times and probabilities are stored in an appropriate format as described in the next section.

### 5.3.2 Format of the generic inspection plans

The information contained in the generic plans are

- a) the inspection times, which allow the description of the simplified decision tree according to Figure 2.8.
- b) the probabilities of occurrence of all different branches of this decision tree, Section 2.4.1.

Figure 5.4 illustrates the form in which these data is stored in iPlan, using the concepts of relational databases.

---

<sup>a</sup> Note that approx. 95% of the CPU time reported in Section 5.5.8.1 is spent for the computation of the LSF.

Generic parameters and threshold						
ID#	FM model	Insp. meth.	FDf	Thickness	Threshold	
GP_001	2D_NR	MPI ICON	2	7mm	$10^{-2}$	
GP_002	2D_NR	MPI ICON	2	7mm	$10^{-3}$	
⋮						
GP_059	2D_NR	MPI ICON	3	20mm	$10^{-4}$	
⋮						
GP_256	2D_NR	MPI ICON	10	150mm	$10^{-5}$	

Probability of failure $p_F$				
ID#	Year 0	Year 1	Year 2	Year $T_{SL,max}$
GP_001	0.0	2.4e-6	6.2e-6	6.2e-2
GP_002	0.0	2.4e-6	6.2e-6	2.4e-2
⋮				
GP_256	0.0	0.0	1.0e-6	2.1e-4

Annual probability of failure $\Delta p_F$				
ID#	Year 0	Year 1	Year 2	Year $T_{SL,max}$
GP_001	0.0	2.4e-6	3.8e-6	2.2e-3
GP_002	0.0	2.4e-6	3.8e-6	4.8e-4
⋮				
GP_256	0.0	0.0	1.0e-6	5.2e-6

Inspection years			
ID#	Inspection 1	Inspection 2	Insp. $T_{SL,max}$
GP_001	0	0	0
GP_002	21	0	0
⋮			
GP_256	8	17	0

Probability of indication $p_I$			
ID#	Inspection 1	Inspection 2	Insp. $T_{SL,max}$
GP_001	0	0	0
GP_002	0.070	0	0
⋮			
GP_256	0.012	0.025	0

Probability of repair $p_R$			
ID#	Inspection 1	Inspection 2	Insp. $T_{SL,max}$
GP_001	0	0	0
GP_002	0.023	0	0
⋮			
GP_256	0.0051	0.0098	0

Figure 5.4 – Proposed database model for the generic inspection plans.

The example database in Figure 5.4 contains  $n_{GIP} = 256$  generic inspection plans. Generic parameters are the FM model (here only one considered), the inspection technique (here only MPI considered), the  $FDf$ , the thickness and others which are not explicitly specified. The inspection plans are calculated for  $T_{SL,max}$  years.

The different relations used are all of the same principle form, its primary key being a ID which can be freely chosen (but must be unique). The plans are identified by the first relation “Generic parameters and thresholds”; it is used by iPlan to identify the plans relevant for the interpolation. All other relations contain the information needed to establish the decision trees corresponding to the inspection plans and in this way to calculate the corresponding expected costs.

The probabilities of failure are stored in the relations “Probability of failure” and “Annual probability of failure”. The data is thereby recorded for each year, the attributes being the years 0 to  $T_{SL,max}$ . The inspection times, as well as the probability of indication and the

probability of repair after the inspection are stored in respective relations, where the attributes are the individual inspections from the first inspection to the  $T_{SL,max}^{\text{th}}$  inspection. If the total number of inspections is exceeded, then a zero value is stored. Note that all relations must contain the same number of tuples (the term tuple denotes a record in relational databases), here 256.

### 5.3.3 Application of the generic inspection plans using iPlan.xls

The inspection plans for the specific hot spots are determined from the generic inspection plans by means of interpolation, as described in the next section. This requires a user-interface where the generic parameters of the specific hot spots can be entered and stored, and where the resulting inspection plans together with their expected cost are provided in a suitable format. iPlan uses a standard spreadsheet format for these tasks, because of its flexibility and because it allows to make the calculation procedures transparent. In addition, most engineers are familiar with these formats. Because computational performance is not crucial here, all functions are computed in Visual Basic. Annex D provides an overview on the developed tool named *iPlan.xls*.

### 5.3.4 Interpolation procedure

The proposed interpolation procedure is described in details in Annex E. It is a multi-dimensional linear interpolation, which is the simplest applicable algorithm. For the interpolation of the expected costs, an additional logarithmic transformation of the costs is advocated. More sophisticated interpolation methods are abandoned because of the empirical basis of the interpolation. It is believed that the most stable results are achieved by a simple scheme that is thoroughly tested to assure that enough interpolation points (generic inspection plans) are available. Higher order interpolations result in a less transparent procedure, which would make more it difficult to decide on the required generic representations.

## 5.4 Determination of the generic representations

The most important part in the design of the generic database is the determination of the generic parameters and their generic representations. The generic parameters to apply are generally obvious, following the argumentations from Section 5.2. The choice of the values for the generic representations is less evident and a sensitivity analysis is required. Based on the observed sensitivity and linearity of the inspection plans in regard to changes of the generic parameters, the generic representations are established. This procedure is purely empirical, but in some cases physical reasoning can be used to verify the conclusions and to support the final choice.

Figure 5.5 illustrates the determination of the generic representations for the generic parameter thickness from the fatigue example presented in Section 5.5. Due to practical reasons, the sensitivity analysis is performed by changing only one parameter and fixing all other parameters. The variations of the inspection times with respect to the member thickness



are clearly non-linear, an observation that is also supported by physical reasoning, see Section 5.5.7.2. As a consequence thereof, more than two generic representations are needed to represent the actual behaviour of the required inspection times in regard to changes of the generic parameter. Three values are chosen here, but additionally the extrapolation to larger thicknesses is allowed. This is justified by the fact that it can be shown that in all cases fewer inspections are required for thicker hot spots, Section 5.5.7.2.

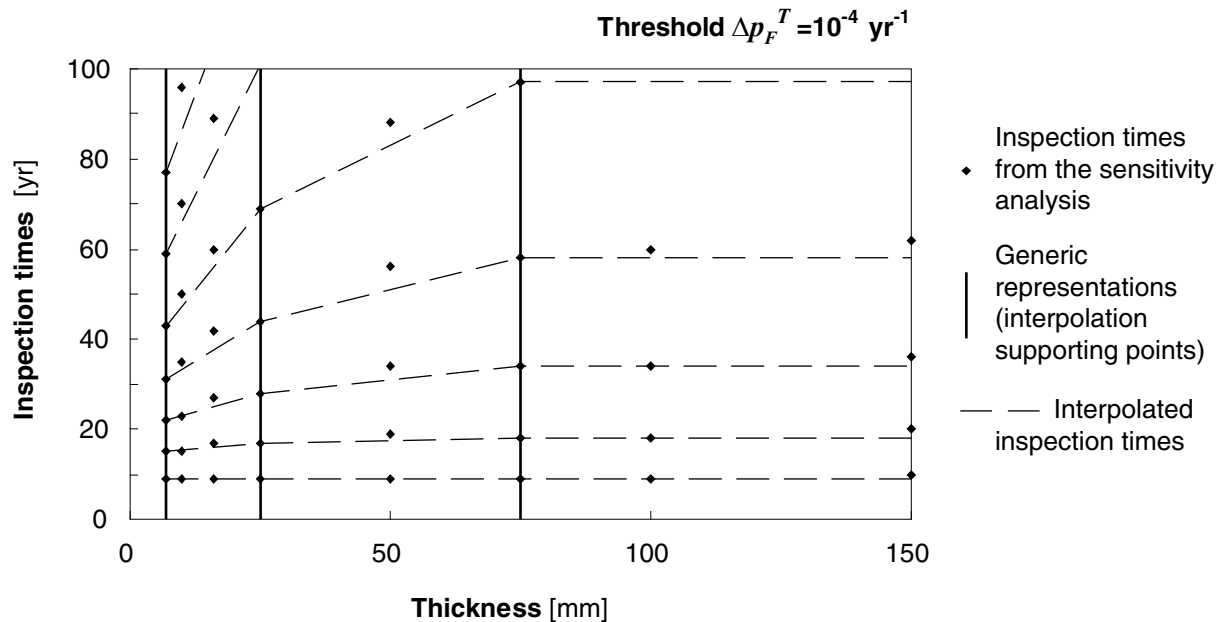


Figure 5.5 – Determination of the generic representations from a sensitivity analysis.

When determining the generic representations it is also necessary to take into account the expected costs as a function of the generic parameters; the costs corresponding to Figure 5.5 are illustrated in Figure 5.15. It is observed that the expected costs in general exhibit a behaviour similar to the inspection times.

Because the generic representations are determined by a one-dimensional sensitivity analysis, i.e. considering only changes of one parameter at a time, the final generic representations must be checked by verifying the resulting generic database. This is carried out by comparing directly calculated inspection plans with those obtained from the generic database. All these aspects are illustrated in details on an example for fatigue subjected structures, presented in the following section.

## 5.5 Generic modelling for fatigue

In this section a model for generic RBI of steel structures subject to fatigue is introduced and investigated. It is a fairly general model that is applicable not only to specific structures; it facilitates the numerical investigation of the influence of different generic parameters (sensitivity study). If generic inspection plans for specific application areas are developed, models different from the one here may be used.

The fatigue deterioration is described by calibrating the crack growth (FM) model from Section 3.3 and Annex B to the SN model from Section 3.2. This model is combined with the inspection model (Chapter 4) and then included in the RBI analysis as presented in Section 2.4. The result is a generic database containing the generic inspection plans, which allows for the calculation of specific inspection plans (prescribing the inspection times and methodology) as well as the expected costs associated with these.

## 5.5.1 Generic parameters in the SN fatigue analysis

### 5.5.1.1 Fatigue Design Factor or Fatigue Life

The most important fatigue characteristic, as obtained from a standard fatigue design calculation, is the design fatigue life  $T_{FL}$  (expressed in years) or equivalently the dimensionless Fatigue Design Factor  $FDF$ , a safety factor which is defined as the ratio between  $T_{FL}$  and the service life  $T_{SL}$ , Equation (5-2).

$$FDF = \frac{T_{FL}}{T_{SL}} \quad (5-2)$$

The  $FDF$  is used as a design criterion for fatigue in many codes (especially for offshore structures, see HSE (2001)) and it has a strong influence on the fatigue reliability of the hot spot under consideration; Figure 5.6 illustrates this influence.

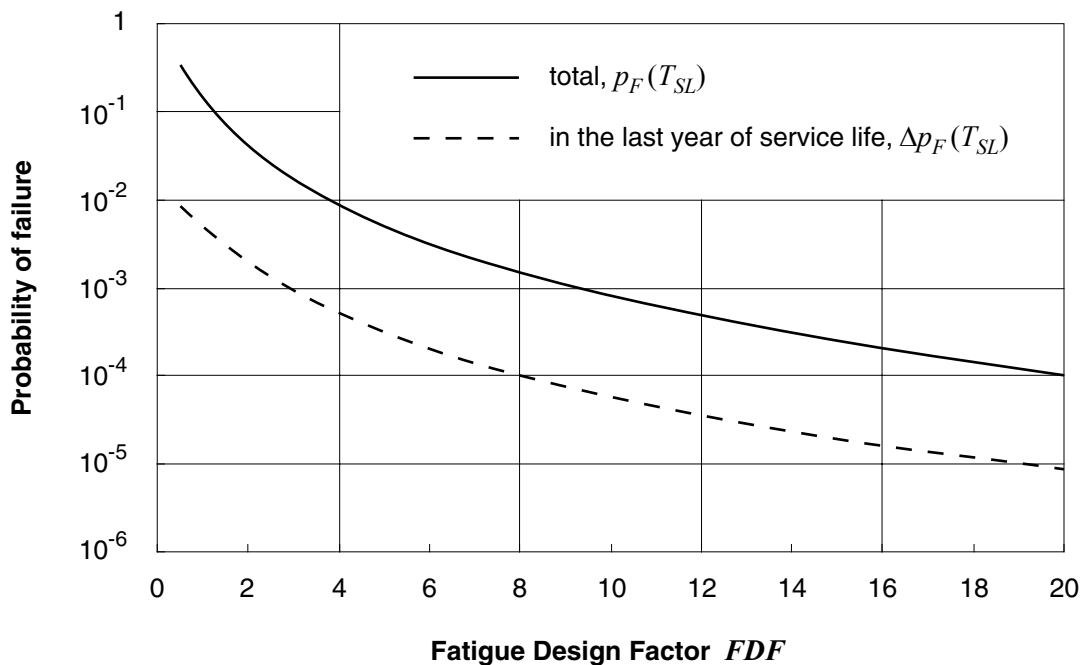


Figure 5.6 – Reliability of the reference case (Section 5.5.3) as a function of the  $FDF$  (without any inspections) for service life  $T_{SL} = 40\text{yr}$ .

The  $FDF$  is dependent on the service life, which can vary from structure to structure (variation in service life is discussed in section 5.5.1.4). It is thus proposed to not use the  $FDF$  as a generic parameter, but the design fatigue life  $T_{FL}$  which is related to the  $FDF$  by means of Equation (5-2). For a specific structure (where  $T_{SL}$  is given) it is equivalent to use the  $FDF$  or  $T_{FL}$  as a generic parameter, due to the linearity of Equation (5-2). The range of  $T_{FL}$  for which generic inspection plans are calculated should cover at least  $FDF = 1 \dots 10$ . As this depends on the  $T_{SL}$ , the minimum  $T_{FL}$  is given by  $FDF_{min} \cdot T_{SL,min}$ , the maximum  $T_{FL}$  by  $FDF_{max} \cdot T_{SL,max}$ . For the presented model the inspection plans are calculated for up to  $T_{SL,max} = 100$  years,  $T_{FL}$  is thus considered in the range  $20\text{yr} \leq T_{FL} \leq 1000\text{yr}$ .

Given the specific detail geometry and environment, and thus consequently the related SN curve, the  $FDF$  (or the  $T_{FL}$ ) is representative for the level of stress ranges in the member. The generic approach thus requires that the  $FDF$  ( $T_{FL}$ ) is related to a model of the stress ranges.

### 5.5.1.2 Stress range model

As noted in Section 3.2.5, the Weibull distribution is a commonly applied model for fatigue loads and covers different application areas. It is thus the logical choice for a general numerical investigation as presented hereafter.

The scale parameter in the Weibull distribution,  $k_{\Delta S}$ , is representative for the level of stress ranges at the hot spot. It is obtained from the design calculations. Because design calculations generally result in a design fatigue life ( $T_{FL}$ ), or equivalently a Fatigue Design Factor ( $FDF$ ), as discussed in Section 5.5.1.1,  $k_{\Delta S}$  is calculated by a deterministic function of these<sup>a</sup>. In a generic manner this can be written as

$$k_{\Delta S} = f_{FA}^{-1}(FDF) \quad (5-3)$$

where  $f_{FA}(\cdot)$  denotes the fatigue analysis resulting in the  $FDF$ , depending on the applied design SN curve and stress model. When the stress ranges are Weibull distributed, in the general case no analytical solution to Equation (5-3) exists, but for the simple case with a one-slope SN curve it can be written explicitly as

$$k_{\Delta S} = \left( \frac{1}{C_1^D} \Gamma \left( 1 + \frac{m_1}{\lambda_{\Delta S}} \right) FDF \cdot T_{SL} \nu \right)^{\frac{1}{m_1}} \quad (5-4)$$

Note the use of  $C_1^D$ , representing the characteristic value of the design SN curve. It follows from Equation (5-4) that  $k_{\Delta S}$  is a function of the Weibull shape parameter  $\lambda_{\Delta S}$ , the  $FDF$ , the service life  $T_{SL}$ , the annual cycle rate  $\nu$  and the parameters of the SN curve, here  $C_1^D$  and  $m_1$ .  $k_{\Delta S}$  must thus be evaluated separately for each combination of these.

The shape parameter of the Weibull distribution,  $\lambda_{\Delta S}$ , is often representative for a specific geometry and loading type. In Folsø et al. (2002)  $\lambda_{\Delta S}$  is a function of the of the total ship

---

<sup>a</sup> It is of course also possible to evaluate the scale factor directly from the design calculations, if the corresponding software allows this. However, the use of the  $FDF$  is more illustrative and allows for a direct comparison with the code requirements.

structure length; Wirsching and Chen (1988) give typical values of  $\lambda_{\Delta S}$  for offshore structures in the Gulf of Mexico and other regions. The following range of  $\lambda_{\Delta S}$  is assumed to cover a broad variety of applications:  $0.5 \leq \lambda_{\Delta S} \leq 1.5$ . Note that this includes as a special case the Exponential distribution (when  $\lambda_{\Delta S} = 1$ ).

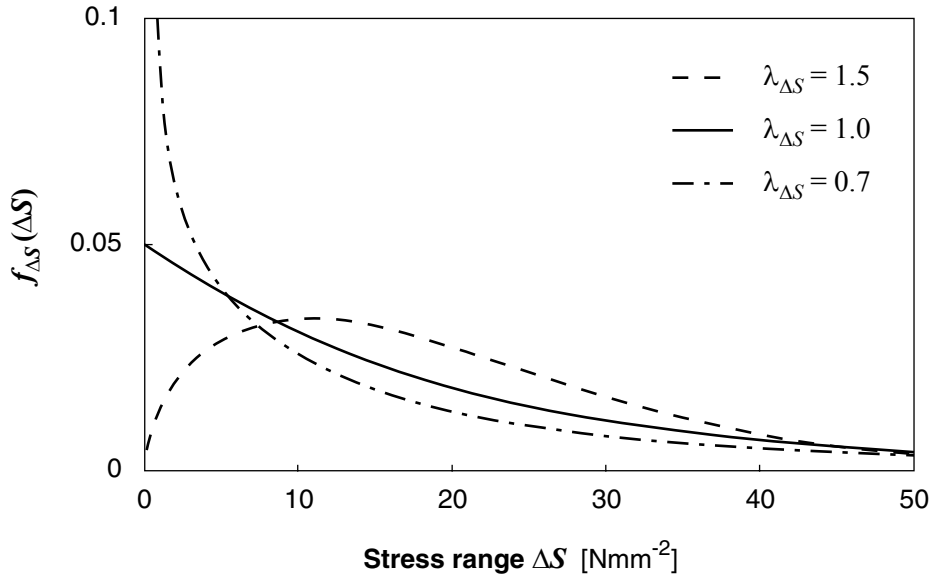


Figure 5.7 – Weibull probability density function with different shape parameter  $\lambda_{\Delta S}$ , all distributions with mean  $\mu_{\Delta S} = 20 \text{Nmm}^{-2}$ .

It is assumed that the uncertainty and the bias in the stress calculations can be expressed by the single random variable  $B_S$ , the error in the calculated stresses. This factor also includes inherent safety factors of the applied design format, which influence the  $FDF$  (respectively  $T_{FL}$ ). In the literature,  $B_S$  is commonly modelled by a lognormal distribution, mainly because of computational convenience. It is presumed that all the factors contributing to  $B_S$ , such as the uncertainty on the environmental load or the uncertainty on the SCF (stress concentration factor), can be modelled by the lognormal distribution, and that they are multiplicative, i.e.

$$B_S = \prod_i B_{S,i} \quad (5-5)$$

where  $B_{S,i}$  are the contributions from the individual uncertainties. The median and the  $CoV$  of the total  $B_S$  are then simply, Wirsching (1984),

$$\begin{aligned} \tilde{m}_{B_S} &= \prod_i \tilde{m}_{B_{S,i}} \\ CoV_{B_S} &= \sqrt{\prod_i \left(1 + (CoV_{B_{S,i}})^2\right)} - 1 \end{aligned} \quad (5-6)$$

Note that with the Weibull distributed stress ranges the factor  $B_S$  is actually multiplied with the scale factor  $k_{\Delta S}$ . Because  $k_{\Delta S}$  is a direct function of the  $FDF$ , a change in the mean value (and consequently also the median) of  $B_S$  is equivalent to a change in the  $FDF$ . There is thus

no need to calculate generic inspection plans separately for different  $\tilde{m}_{B_s}$ ; in the following this is done for illustrational purposes only.

The investigated range of the stress calculation error is  $0.05 \leq CoV_{B_s} \leq 0.6$ , respectively  $0.5 \leq \tilde{m}_{B_s} \leq 1.2$ .

### 5.5.1.3 Thickness

As stated in Section 3.2.3.2, in most design codes the fatigue life is explicitly modelled dependent on the wall thickness  $d$  at the considered hot spot. The standard SN curves are thereby valid for a reference thickness  $d_0$ . Because the fatigue life decreases with increasing thickness, see Maddox (1991), the stress ranges are adjusted if the thickness  $d$  exceeds  $d_0$ . The format of the thickness correction, as presented in Equation (5-7), is the same for the most common codes, but the values of its parameters  $d_0$  and  $q_d$  vary, where  $q_d$  is in the range of 0 to 0.3. The correction is introduced in the fatigue analysis by replacing  $\Delta S$  with  $\Delta S_d$ , the thickness adjusted stress range.

$$\Delta S_d = \Delta S \left( \frac{d}{d_0} \right)^{q_d}, \quad d \geq d_0 \quad (5-7)$$

Note that, for given  $FDF$ , this thickness correction is in most cases without influence on the final inspection plans. This is because the stress ranges are adjusted to the  $FDF$ , the correction from Equation (5-7) is thus compensated by lower stress ranges (lower values of  $k_{\Delta S}$ ).

However, the wall thickness is important in regard to the crack propagation and the inspection modelling, because it influences the ratio between the detectable crack size (as expressed by the  $PoD$ ) and the crack size at which failure occurs. Because the wall thickness is easily obtained from the design information, it is a logical choice for a generic parameter. This is first illustrated in Goyet et al. (2002b). Here, the following range is assumed to cover most practical applications:  $7\text{mm} \leq d \leq 150\text{mm}$ .

### 5.5.1.4 Service life time

The service life time  $T_{SL}$  is not a generic parameter according to the definition in Section 5.2, because inspection plans for a specific  $T_{SL}$  are not obtained by interpolation, but by cutting off the inspection plan at  $T = T_{SL}$ . This procedure is justified by the fact that the limit state functions (and thus the probabilities of the different events) are not influenced by  $T_{SL}$ , as long as  $T \leq T_{SL}$ . Consequently, only a maximum service life time  $T_{SL,max}$  must be chosen, which then includes all cases with lower service lives. The probabilities in the generic inspection plans are then calculated for  $T_{SL,max}$  number of years. The increase in the computation time is disproportionate to the increase of  $T_{SL,max}$  for fatigue problems, because of the non-linearity of the fatigue limit state functions; the choice of  $T_{SL,max}$  is thus of importance for the required computation time<sup>a</sup>. In this study, in order to include all possible situations,  $T_{SL,max} = 100\text{yr}$ .

---

<sup>a</sup> The computation time is especially large if a large service life is combined with a small design fatigue life  $T_{FL}$ .

### 5.5.1.5 Annual stress cycle rate

For a specific hot spot, the number of stress cycles per year,  $\nu$ , is known, and together with the design fatigue life,  $T_{FL}$ , the total number of cycles until fatigue failure (applying the design model) can be evaluated as

$$N_F = \nu T_{FL} \quad (5-8)$$

It is possible to not consider  $\nu$  and  $T_{FL}$  separately, but to calculate inspection plans for different  $N_F$  and to derive the specific inspection plans, with given  $\nu$  and  $T_{FL}$ , by means of Equation (5-8). This would have the advantage that the number of generic parameters would be reduced by one, resulting in a decrease in calculation time. However, if  $\nu$  is not explicitly stated, the probabilities cannot be calculated on a yearly basis, but only for an interval of cycles (e.g. after each  $(T_{FL,max} \nu_{max})/1000$  cycles). Unfortunately, because  $\nu$  can vary significantly, a large number of generic representations for  $N_F$  would be required, which increases the computational time significantly. It is thus concluded that the use of  $N_F$  as generic parameter is less effective than that of  $\nu$  and  $T_{FL}$  separately.

For this study,  $\nu$  is considered in the range of  $10^6$  to  $10^7$  per year.

### 5.5.1.6 SN curve

The applied SN curve reflects the structural detail type, the material, the environment and the applied quality control. Generic inspection plans must be evaluated separately for each SN curve, which is thus a generic parameter. In general the same SN curve as for the fatigue design verification is used for inspection planning purposes, but instead of the characteristic curve the full statistical description of the curve is applied. Some references on probabilistic models of SN curves are provided in Section 3.2.6.

For the numerical investigations the D curve from the DoE SN curves is applied, see e.g. SSC (1996). To evaluate the influence of using different SN curves, alternatively the EC 90 curve from the Eurocode 3 (1992) is used. Both curves are representative for stress ranges evaluated at the hot spot level in an atmospheric environment, which explains their similarity as illustrated in Figure 5.8. The main difference between the two is the cut off limit, which is only included in the Eurocode curve.

The  $CoV$  of the parameter  $C_1$  of the EC 90 SN curve is assumed to be the same as for the DoE D curve, which is supported by ECCS (1985). The parameters of the two SN curves are summarised in Table 5.1.

*Table 5.1 – Parameters of probabilistic SN curves.*

SN curve	$\check{m}_{C_1}^*$	$CoV_{C_1}$	$C_1^D$	$m_1$	$N_q$	$m_2$	$N_0$	$d_0$	$q_d$
DoE D	$3.99 \cdot 10^{12}$	0.51	$1.53 \cdot 10^{12}$	3	$10^7$	5	$\infty$	16mm	0.30
EC 90	$3.70 \cdot 10^{12}$	0.51	$1.42 \cdot 10^{12}$	3	$5 \cdot 10^6$	5	$10^8$	25mm	0.25

\*  $C_1$  is modelled as Lognormal distributed, Section 3.2.6.

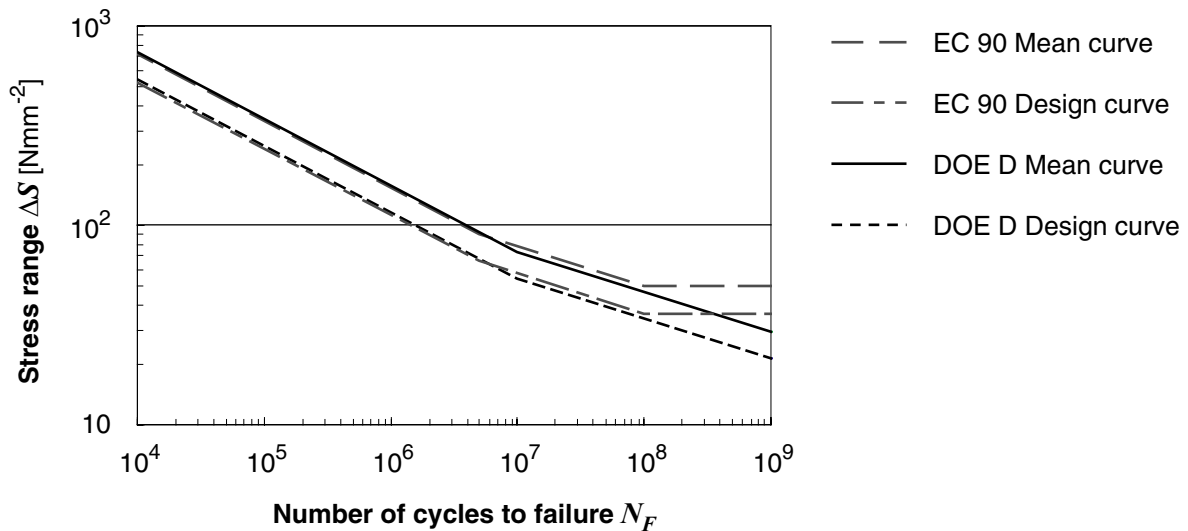


Figure 5.8 – Illustration of the two applied SN curves.

## 5.5.2 Generic parameters in the crack growth model

Which input parameters are required depends on the applied crack growth (FM) model; the following example is based on the 2D crack propagation model after Newman and Raju (1981) as presented in details in Annex B. Failure is thereby defined as the event that a crack exceeds the wall thickness at the hot spot. Many parameters entering the FM model are already specified in the SN model or are a direct function of those used in the SN model. They can be directly adopted and the subsequent sections are therefore limited to the parameters that are specific for the FM model.

### 5.5.2.1 Crack initiation model

Following the discussions in Section 3.3.2, the crack initiation model depends on the quality of the weld and therefore on the manufacturing process and the applied quality control. It is proposed to use two different models: the model based on Lassen (1997) representing high quality welds in modern steel structures and the model based on Moan et al. (2000a) for a lower weld quality. These are summarised as follows.

- Lassen's model predicts that the number of cycles to initiation is given through Equation (3-10), with parameter  $N_{I_0} \sim W[145 \cdot 10^3, 50 \cdot 10^3]$ , where  $N_{I_0}$  is correlated to the crack growth parameter  $C_P$  with correlation coefficient  $\rho_{N_{I_0}, C_P} = -0.5$ . The initial crack depth is modelled deterministically as  $a_0 = 0.1\text{mm}$ .
- Moan's model assumes that an initial crack is present at  $t = 0$ , i.e. the number of cycles to crack initiation,  $N_I$ , is zero. The initial crack depth thereby follows an exponential distribution with expected value  $E[a_0] = 0.38\text{mm}$ .

Additional information on the models is presented in Section 3.3.2.

### 5.5.2.2 Ratio of membrane to bending stresses

The Newman-Raju model accounts for the differences between bending and membrane stresses. The ratio of the bending to the membrane stresses,  $\eta_S$ , is a direct input to the model, in accordance with Annex B.  $\eta_S$  attain values between 0 and  $\infty$ . Instead of  $\eta_S$ , in the following the degree of bending,  $DoB$ , is used. It is related to  $\eta_S$  as

$$DoB = \frac{S_{b,0}}{S} = \frac{\eta_S}{1 + \eta_S} \quad (5-9)$$

The  $DoB$  must be modelled as a generic parameter because it can vary over the structure from one hot spot to the next. It can range from 0 to 1; however, due to the load shedding effect (see Annex B), for  $DoB = 1$  (pure bending) the crack growth model predicts an infinite fatigue life. The maximal value applied is thus  $DoB = 0.99$ .

### 5.5.3 Summary of the model

Table 5.2 and Table 5.3 summarise the parameter values of the SN and the FM model. Note that the parameters of the SN curves are provided in Table 5.1.

*Table 5.2 – Parameters of the SN model.*

Parameter	Dimension	Distribution	Mean	COV
$\Delta$	-	Lognormal	1	0.3
$\nu^*$	yr <sup>-1</sup>	Deterministic	10 <sup>6</sup> - 10 <sup>7</sup>	
$T_{SL,max}$	yr	Deterministic	100	
$T_{FL}^*$	yr	Deterministic	20 - 1000	
$k_{\Delta S}$	Nmm <sup>-2</sup>	Deterministic	corresponds to $T_{FL}$	
$B_S^*$	-	Lognormal	$\tilde{m} = 0.5 - 1.2$	0.05 - 0.60
$\lambda_{\Delta S}^*$	-	Deterministic	0.5 - 1.5	
$d^*$	mm	Deterministic	7 - 150	

\* Generic parameter, for which only the ranges of the parameter values are specified



Table 5.3 – Parameters of the FM model.

Parameter	Dimension	Distribution	Mean	COV
$\nu_e$	$\text{yr}^{-1}$	Deterministic	* <sup>1</sup>	
$\Delta S_e$	$\text{Nmm}^{-2}$	Deterministic	* <sup>1</sup>	
$DoB^*$	-	Deterministic	0 – 0.99	
$\ln C_p$		Normal	* <sup>2</sup>	0.77
$m_{FM}$	-	Deterministic	$m_{FM} = f(C_p)$ according to Equation (3-16)	
$Y_{NR}$	-	Lognormal	* <sup>2</sup>	0.1
$a_0^*$	mm	Depending on the applied initiation model		
$N_I^*$		Depending on the applied initiation model		
$a_0/c_0$	-	Deterministic	0.2	

\* Generic parameter.

\*<sup>1</sup> These values depend on the fatigue life and the applied SN curve according to Section 3.2.5.1.

\*<sup>2</sup> These values are calibrated to the SN model according to Section 3.4.

### 5.5.3.1 Reference case

In order to investigate the influence of different generic parameters on the final inspection plans, the reference case is introduced. The reference case is defined by the model parameters according to Table 5.2 and Table 5.3 and specific values of the generic parameters. These are, for the SN model,

- $\nu = 3 \cdot 10^6$ ;
- $T_{FL} = 120\text{yr}$  ( $k_{\Delta S} = 9.068$ );
- $T_{SL} = 40\text{yr}$ , which corresponds to an  $FDF = 3$ ;
- $\bar{m}_{B_S} = 1.0$ ,  $COV(B_S) = 0.25$ ;
- $\lambda_{\Delta S} = 0.9$ ;
- $d = 16\text{mm}$ ;
- SN curve: DoE D, according to Table 5.1.

The parameters of the FM model are

- $DoB = 0.6$ ;
- Crack initiation model according to Lassen (1997), see Section 5.5.2.1.

For the reference case, the parameters of the FM model that are dependent on the SN model are calculated as  $\nu_e = 3 \cdot 10^6$  and  $\Delta S_e = 26.12\text{Nmm}^{-2}$ . The calibration of the FM model to the SN model results in the parameter values  $\ln(C_p) = -29.61$  and  $Y_{NR} = 1.00$ . Detailed results for this reference case are presented in Section 5.5.6.

### 5.5.4 Inspection model for the numerical investigations

Two *PoD* models are chosen for the example; both models are introduced in Chapter 4. The first is a log-logistics model that is representative for Magnetic Particle Inspection (MPI) on tubular joints underwater; it is derived from experimental data as described in Section 4.3.3 and denoted by MPI ICON. The second is the exponential model for MPI on tubular offshore members established by Moan et al. (2000) from data gathered in-service, as summarised in Section 4.3.3.1.

Because Moan et al. (2000) do not specify the probability of false indication, the *PFI* from the first model is assumed valid for both models. The combined Probability of Indication, *PoI*, evaluated according to Equation (4-6), is illustrated for both models in Figure 5.9.

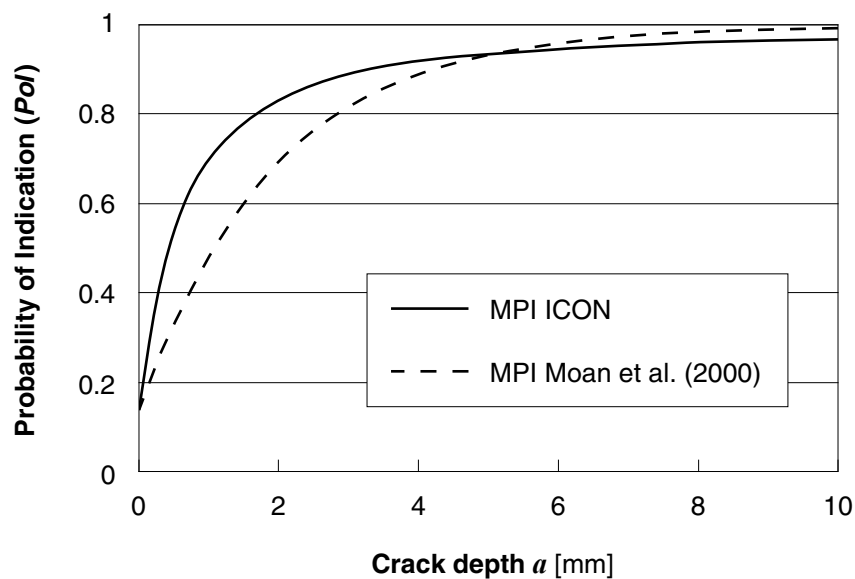


Figure 5.9 – Applied *PoI* models.

Note that the inclusion of false indication has little influence in the considered context, due to the fact that the applied decision rule (Section 2.4.1.1) assumes that indicated cracks are measured. False indications are thus, in most cases, identified by these measurements and consequently do not cause any further costs. The measurements are modelled by a measurement error  $\varepsilon_m$  in accordance with Section 4.2.4.

All parameters of the applied inspection models are summarised in Table 5.4. The reference model is the MPI ICON model; if not stated otherwise, this model is applied.

Table 5.4 – Parameters of the inspection models.

Parameter	Dimension	MPI ICON	MPI Moan
$PoD$ defined in		Equation (4-1)	Equation (4-2)
$\alpha_D$	} corresponding to a crack depth in [mm]	0.63	-
$\beta_D$		1.16	-
$P_0$	-	-	1
$\lambda_D$	mm	-	1.95
$PFI$	per hot spot	0.138	0.138
$\mu_{\varepsilon_m}^*$	mm	0	0
$\sigma_{\varepsilon_m}^*$	mm	0.5	0.5

\*)  $\varepsilon_m$  is modelled as normal distributed

### 5.5.5 Cost model for the numerical investigations

The cost model is not a generic parameter; the calculation of the generic inspection plans is independent of the costs. For the investigation and validation of the generic inspection plans, however, a cost model is required, which should be representative for the considered applications. The model applied for the numerical investigations is

$$C_F = 1, C_{Insp} = 10^{-3}, C_R = 10^{-2}, r = 0.05$$

where  $C_F$  is the cost of failure,  $C_{Insp}$  the cost of an inspection,  $C_R$  the cost of a repair, and  $r$  the real interest rate. The expected costs of the reference case are shown in Figure 2.11 for different strategies (i.e. different thresholds on the annual probability of failure).

Note that the evaluation of a different cost model (with the same interest rate) is straightforward because the individual costs enter the calculations in a multiplicative manner. As an example, the expected cost of failure can be written as  $C_F \cdot f(\mathbf{X})$  where  $\mathbf{X}$  is a vector of all parameters other than costs, including the interest rate. The same is valid for the expected cost of inspection and repair. This follows from Equations (2-24) to (2-29).

The influence of the interest rate is separately assessed and illustrated in Figure 5.10. Although the total expected cost varies significantly with the interest rate, the characteristic form of the diagram does not change drastically. Absolutely, by changing the interest rate from  $r = 2\%$  to  $r = 10\%$  the expected costs (net present values) decrease by a factor of 2.5 to 6. The optimal strategy changes from a threshold of  $\Delta p_F = 10^{-4}$  to  $\Delta p_F = 3 \cdot 10^{-4}$ . In general, the use of a higher interest rate will favour strategies with a higher threshold (i.e. with fewer inspections). This is because inspections represent an investment that reduces the risk in the future. They are consequently more effective (in economical terms) with a lower interest rate. For large interest rates it is more attractive for the operator to invest the money in alternative activities with a return on investment corresponding to this interest rate.

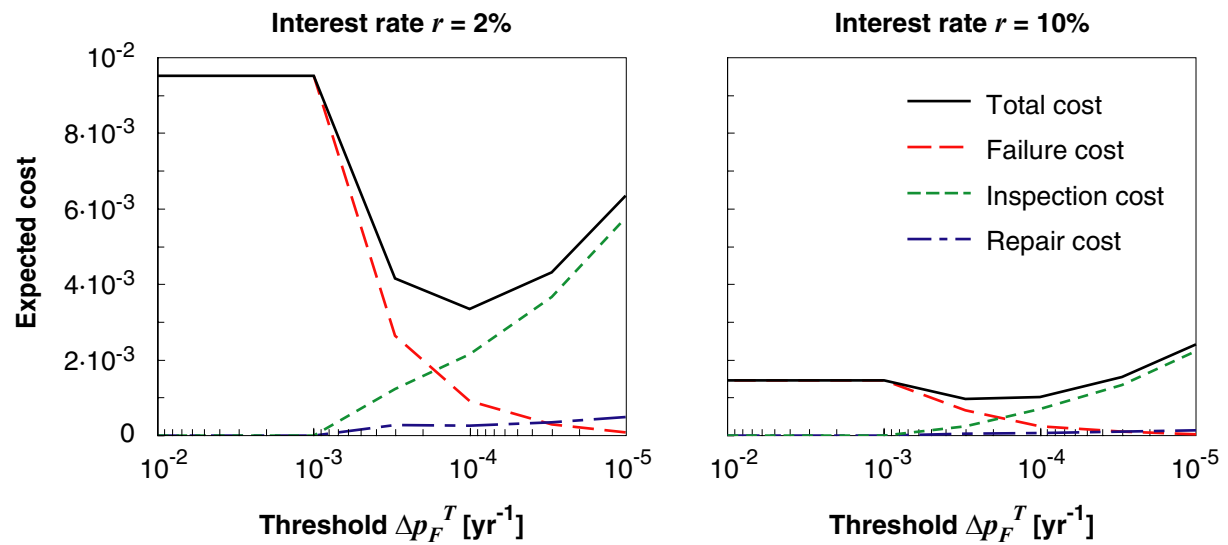


Figure 5.10 – The influence of the interest rate on the expected cost. Calculations are based on the reference case, Section 5.5.3.1.

Costs are case specific and may, depending on the location and the importance of the hot spot<sup>a</sup>, vary significantly. For practical applications, the cost model has to be specified by or in collaboration with the operator of the facility. It is advocated that societal costs are not included in the optimisation of the inspection efforts. This is justified by the fact that the decision maker in the inspection planning process is the operator of the structure<sup>b,c</sup>. Societal cost must be introduced in the derivation of the societal acceptance criteria, which are then introduced as a condition to the optimisation, in accordance with Equations (2-30) to (2-32). This is addressed in Chapter 7.

## 5.5.6 Results for the reference case

Some detailed results of the reference case are presented here to illustrate the full set of results obtained for each generic inspection plan. They additionally allow the verification of the models and the calculations. Some of the results have already been presented in earlier chapters and sections, in which case reference is made to the corresponding figure.

<sup>a</sup> Using the concept of the Residual Influence Factor *RIF* as presented in Chapter 7, the importance of a hot spot on the integrity of the overall structure can be evaluated. It is expressed as the probability of collapse given hot spot failure. This value can be used to calculate the (expected) cost of the reduction of system strength due to failure of a hot spot.

<sup>b</sup> Based on the same argument the applied interest rate must be that of the operator.

<sup>c</sup> For infrastructure facilities the operator is in many instances the state, which represents society. Societal costs then form a part of the operator's costs.

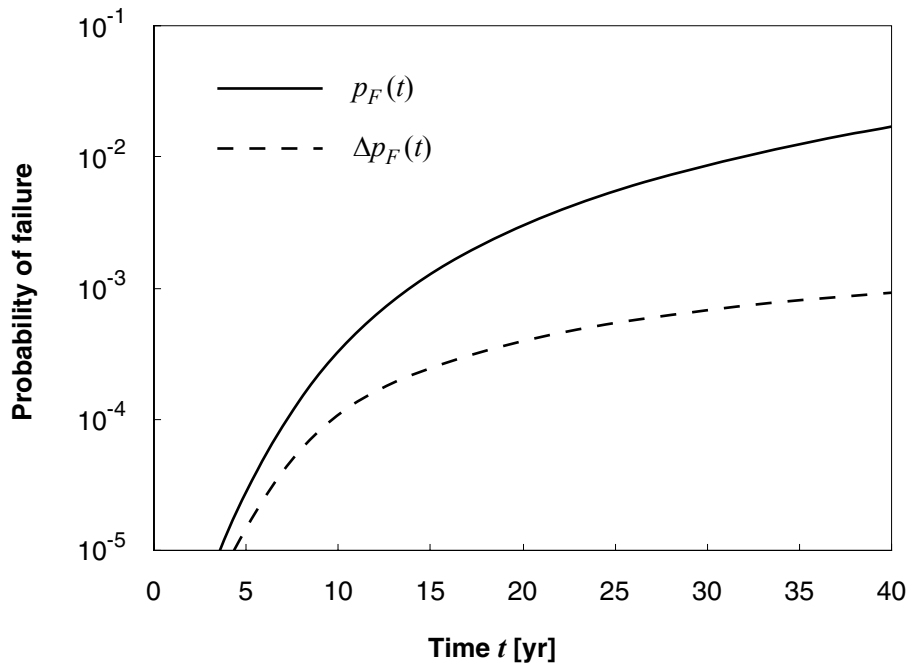


Figure 5.11 - Probability of failure for the reference case.

The probability of failure for the reference case is shown in Figure 5.11 for the case without inspections and in Figure 2.10 for the case with inspections resulting in no indication. Figure 5.12 illustrates the sensitivity factors  $\alpha$  of the reliability calculations<sup>a</sup>. Note the good correspondence of the two models with respect to the common variable  $B_S$ .

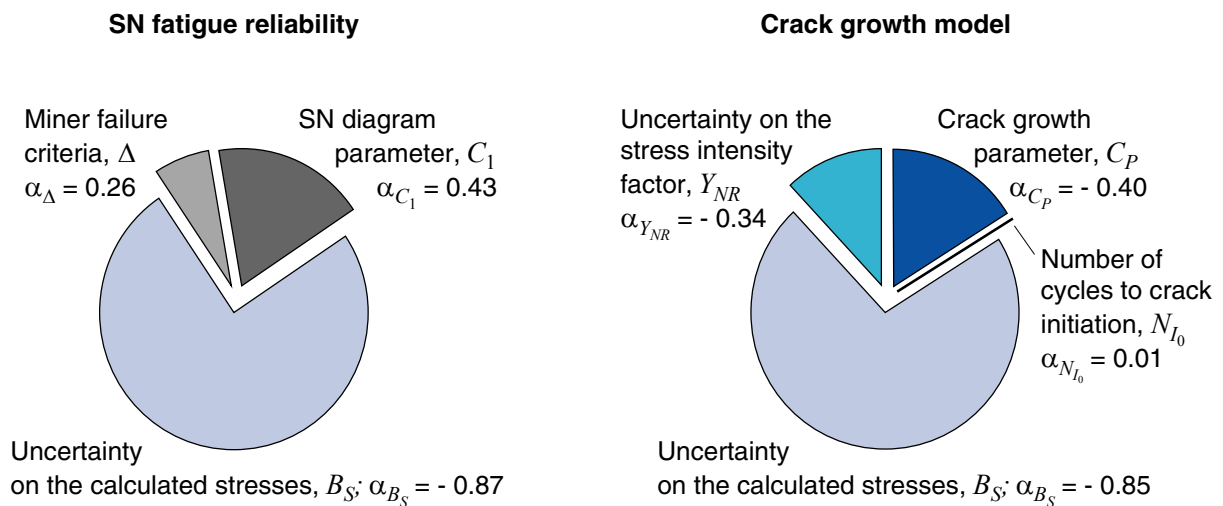


Figure 5.12 – Sensitivity factors of the random variables in the calculation of the reliability of the reference case ( $T=40\text{yr}$ ).

<sup>a</sup> The sensitivity factors, which are defined according to Madsen et al. (1986), are a measure for the relative importance of the uncertainty in the stochastic variable on the reliability index. However, for correlated random variables ( $C_P$  and  $N_{I_0}$ ) the interpretation of  $\alpha$  is not possible directly for the individual random variable.

For each of the considered thresholds  $\Delta p_F^T$ , ( $10^{-2}$ ,  $10^{-3}$ ,  $3 \cdot 10^{-4}$ ,  $10^{-4}$ ,  $3 \cdot 10^{-5}$ ,  $10^{-5}$  [ $\text{yr}^{-1}$ ]) the inspection times, as well as the corresponding annual probabilities of failure, are evaluated based on the assumption of no indication at the inspection. The resulting inspection times for all thresholds are provided in Table 5.5.

Table 5.5 – Full results for the reference case – inspection times.

Threshold [ $\text{yr}^{-1}$ ]	# inspections	Years of inspection							
$10^{-2}$	0	-							
$10^{-3}$	0	-							
$3 \cdot 10^{-4}$	2	17	33						
$10^{-4}$	3	9	17	27					
$3 \cdot 10^{-5}$	5	6	10	16	23	31			
$10^{-5}$	8	4	7	9	14	18	24	31	39

The total expected cost of the reference case, based on the threshold or the equidistant approach, are illustrated in Figure 2.11. Numerical values for the threshold approach are given in Table 5.6.

Table 5.6 - Full results for the reference case – expected cost [in  $10^3$ ].

Threshold [ $\text{yr}^{-1}$ ]	$E[C_T]$	$E[C_F]$	$E[C_{Insp}]$	$E[C_R]$
$10^{-2}$	4.4	4.4	0	0
$10^{-3}$	4.4	4.4	0	0
$3 \cdot 10^{-4}$	2.2	1.5	0.6	0.1
$10^{-4}$	2.1	0.5	1.4	0.1
$3 \cdot 10^{-5}$	2.9	0.2	2.6	0.2
$10^{-5}$	4.5	0.1	4.1	0.3

As noted in Section 5.5.5, the expected cost for an alternative cost model can be calculated by simply multiplying the expected cost of failure, inspection and repair in Table 5.6 by the respective ratio.

### 5.5.7 Results of the sensitivity analysis and determination of the generic representations

A one-dimensional sensitivity analysis is performed: The inspection plans are evaluated for the values of the generic parameters according to the reference case and one parameter is varied at a time. This section presents the outcomes of the sensitivity analysis in terms of the resulting inspection times and their corresponding expected cost, together with discussions of

the results. Based on these, the generic representations for the final example database are determined. The one-dimensional sensitivity analysis is sufficient if the influences of the different generic parameters on the inspection plans are fully independent of each other. This is generally not the case and an additional verification of the final database and interpolation scheme is thus required, which is provided in Section 5.5.9.

The results are presented for the three different thresholds  $\Delta p_F^T = 10^{-3}, 10^{-4}, 10^{-5} [\text{yr}^{-1}]$ . Three additional thresholds are included in the calculations, but the results for these are similar to those presented.

It is pointed out that the design fatigue life  $T_{FL}$  is kept constant. Although most parameters influence this parameter directly, this is compensated for by varying the level of stresses (the scale factor  $k_{\Delta S}$  varies accordingly). This is important for the interpretation of the results.

#### 5.5.7.1 Influence of the design fatigue life (Fatigue Design Factor $FDF$ )

Not surprisingly the necessary inspection effort varies significantly with the calculated design fatigue life  $T_{FL}$ , as observed in Figure 5.14. The required inspection effort varies non-linearly with  $T_{FL}$  over the total domain, which is in contradiction to earlier publications, e.g. Faber et al. (2003a), where a linear behaviour is observed. This difference is explained by the fact that the considered range of the fatigue life  $T_{FL}$ , as well as the service life  $T_{SL}$ , is much larger for the present study as compared to previous examples. If the domain of  $T_{FL}$  is split up into smaller intervals, inspection times can be determined with reasonable accuracy by linear interpolation. Consequently several generic representations are required for this parameter to appropriately represent the non-linear behaviour. The following values are proposed for the final generic database:

$$T_{FL} = 20\text{yr}, 50\text{yr}, 100\text{yr}, 250\text{yr}, 500\text{yr}, 1000\text{yr}$$

It is observed that the expected costs vary approximately linearly with the  $FDF$  in a logarithmic scale, so that a logarithmic interpolation procedure is sufficiently accurate with the proposed generic representations.

#### 5.5.7.2 Influence of the thickness

The results for the sensitivity analysis with respect to the wall thickness at the hot spot  $d$  are presented in Figure 5.15. The influence of the thickness is large for thin members. For these, the ratio of the detectable crack size to the critical crack size (which is equal to the thickness) is larger, which is unfavourable because the period during which a crack can be detected gets smaller. This phenomenon is illustrated in Figure 5.13. More inspections are consequently required for thinner members.

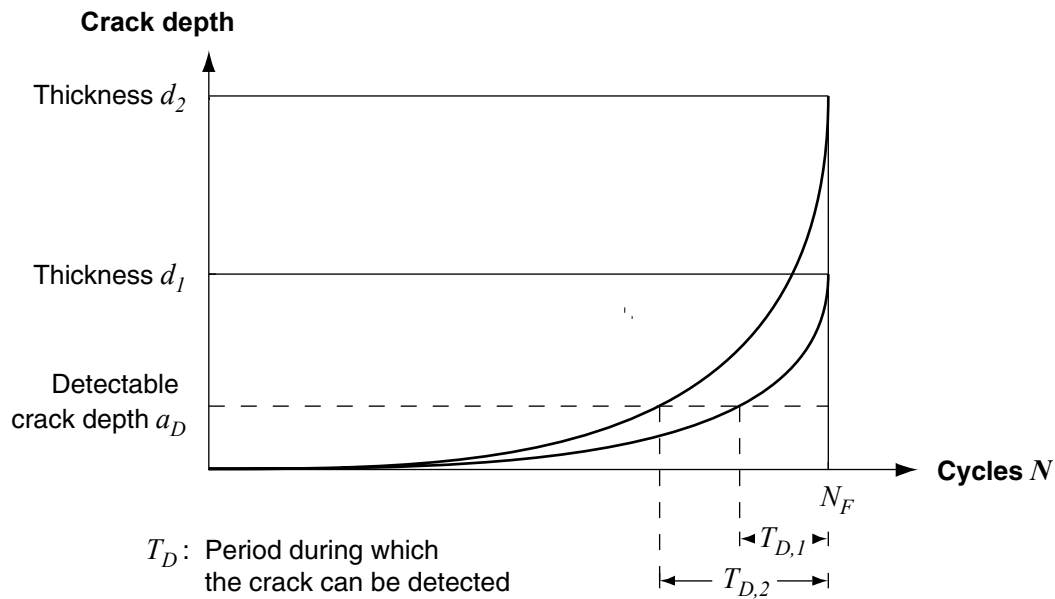


Figure 5.13 – Illustration of the wall thickness effect.<sup>a</sup>

With increasing wall thickness the required number of inspections asymptotically becomes constant, as well as the expected costs for the different strategies. Note that the time to the first inspection is not influenced by the thickness<sup>b</sup>, because this parameter has no influence on the SN fatigue reliability, in accordance with Section 5.5.1.3. It only influences the effect of inspections, i.e. the updated reliability after the inspections.

Based on the above discussion and the considerations already presented in Section 5.4, the generic representations are chosen as

$$d = 7\text{mm}, 25\text{mm}, 75\text{mm}$$

All members thicker than 75mm can (conservatively) be assumed represented by  $d = 75\text{mm}$ .

### 5.5.7.3 Influence of the annual cycle rate

If the SN curve is not linear but multi-linear then the reliability can vary, for a constant  $FDF$ , with the number of cycles per year,  $\nu$ . In addition, if the crack growth model includes a crack initiation phase, then  $\nu$  may influence the crack growth modelling. However, from the numerical results, as shown in Figure 5.16, it follows that these influences are small for the applied model. Consequently it appears reasonable to compute all inspection plans for the same value of  $\nu$  and to neglect the influence of a change in this parameter. If  $\nu$  is in the

<sup>a</sup> Based on the principle illustrated in Figure 5.13 it is proposed in some publications, e.g. Singh and Koenke (2000), to set the maximal inspection interval equal to the period during which a crack can be detected. However, this deterministic procedure ignores the uncertainties related to both the inspection performance and the crack growth model.

<sup>b</sup> The slight variations observed in Figure 5.15 are caused by the inaccuracies in the calculations.



range of  $10^6$  to  $10^7$  cycles per year, inspection plans with the following value are thus assumed representative:

$$\nu = 3 \cdot 10^6 \text{ yr}^{-1}$$

Note that this model is slightly non-conservative for larger values of  $\nu$ . For applications where  $\nu$  is outside the range of  $10^6$  to  $10^7 \text{ yr}^{-1}$ , the validity of this simplified approach must be checked.

#### 5.5.7.4 Influence of the shape parameter

Due to the bi-linear form of the SN curve, the fatigue reliability is influenced by the shape parameter  $\lambda_{\Delta S}$  of the Weibull distribution describing the stress ranges. For a SN curve with one slope only,  $\lambda_{\Delta S}$  has no influence on the inspection plans. The stress ranges are in that case fully described by means of  $E[\Delta S^{m_1}]$  which is a function of both  $\lambda_{\Delta S}$  and  $k_{\Delta S}$ ; because  $k_{\Delta S}$  is calibrated to the *FDF*, a change in  $\lambda_{\Delta S}$  has no influence as it is compensated by a change in the value of  $k_{\Delta S}$ .

For the present SN curve, both the inspection efforts as well as the expected costs increase approximately linearly with  $\lambda_{\Delta S}$  in the considered range. It is therefore sufficient to use as generic representations the borders of this range:

$$\lambda_{\Delta S} = 0.5, 1.5$$

#### 5.5.7.5 Influence of the uncertainty on the calculated fatigue stresses

As noted previously in Section 5.5.1.2, a change in  $\tilde{m}_{B_s}$ , the median of the lognormal distributed stress calculation error, is equivalent to a corresponding change of the *FDF* (respectively  $T_{FL}$ ). As an example, for the reference case the change in  $\tilde{m}_{B_s}$  from 1.0 to 0.7 is equivalent to a change in  $T_{FL}$  from 120yr to 530yr. This indicates that the influence of  $\tilde{m}_{B_s}$  on the inspection plans is significant, which is supported by the results of the sensitivity analysis represented in Figure 5.18. For practical applications, however, it is sufficient to calculate only generic inspection plans with  $\tilde{m}_{B_s} = 1$  and to derive the inspection planes for other values of  $\tilde{m}_{B_s}$  by changing the *FDF* accordingly.

The coefficient of variation of the uncertainty on the stress calculations,  $CoV_{B_s}$ , is a main contributor to the failure probability, as indicated by the sensitivity factors in Figure 5.12. It is therefore expected that a change of this parameter has a large influence on the resulting inspection plans, which is supported by the results as summarised in Figure 5.19. For the final generic database, due to the drastic changes in the inspection plan with  $CoV_{B_s}$ , several generic representation of this parameter are required. Based on Figure 5.19, the following are proposed here:

$$CoV_{B_s} = 0.1, 0.2, 0.3, 0.4, 0.5$$

From the results of the sensitivity study it is concluded that values of  $CoV_{B_s}$  above 0.5 are not economical. In such situations an enormous inspection effort is required to comply with the reliability thresholds, so that the use of more accurate fatigue stress calculations is preferable. Because the  $CoV_{B_s}$  is a direct function of the quality of the fatigue stress calculations, the

results presented in Figure 5.19 can be used to estimate the benefit of increasing the accuracy in the fatigue analysis.

In real applications, the determination of both  $\bar{m}_{B_s}$  and  $CoV_{B_s}$  is crucial. Although some indications on these values may be found in the literature, see Section 3.2.6, engineering judgement is to some extent required to establish these values for a specific fatigue analysis methodology. In addition, these values should periodically be reviewed, taking basis in the outcomes of performed inspections. When comparing the predicted probability of indication with the number of effectively observed indications, the estimates of  $\bar{m}_{B_s}$  and  $CoV_{B_s}$  can be continuously improved. Such a procedure is described in Moan et al. (2000b) and HSE (2002b). The therein reported results can only partially be applied to the here presented model because they are based on a one-dimensional crack growth model; they indicate a value of  $\bar{m}_{B_s}$  lower than 1, but combined with a large model uncertainty on the crack growth model (i.e. on the stress intensity factor).

#### 5.5.7.6 Influence of the degree of bending

In the considered tubular joints the load shedding reduces the local bending moment with increasing crack size, and so reduces the stresses at the later periods of the fatigue life. Because the later periods are those with the higher crack growth rate, this effect leads to a steadier crack growth behaviour. For tensile stresses, no such phenomenon occurs. Because a steady behaviour is favourable in view of the detectability of the crack, a hot spot with a higher *DoB* requires less inspections.

The same effect furthermore causes an increase in the probability of (unnecessary) repair for large values of the *DoB*, as reflected in the expected cost. Considering the calculated variations of the inspection times with the *DoB* as presented in Figure 5.20, the following values are suggested as generic representations:

$$DoB = 0, 0.6, 0.8$$

For all hot spots where the degree of bending is larger than 0.8, it is proposed to use the approximation  $DoB = 0.8$ . Although this may appear strongly conservative considering the results in Figure 5.20, the recommendation is justified by the fact that the uncertainties in the evaluation of the *DoB* are not explicitly taken into account.

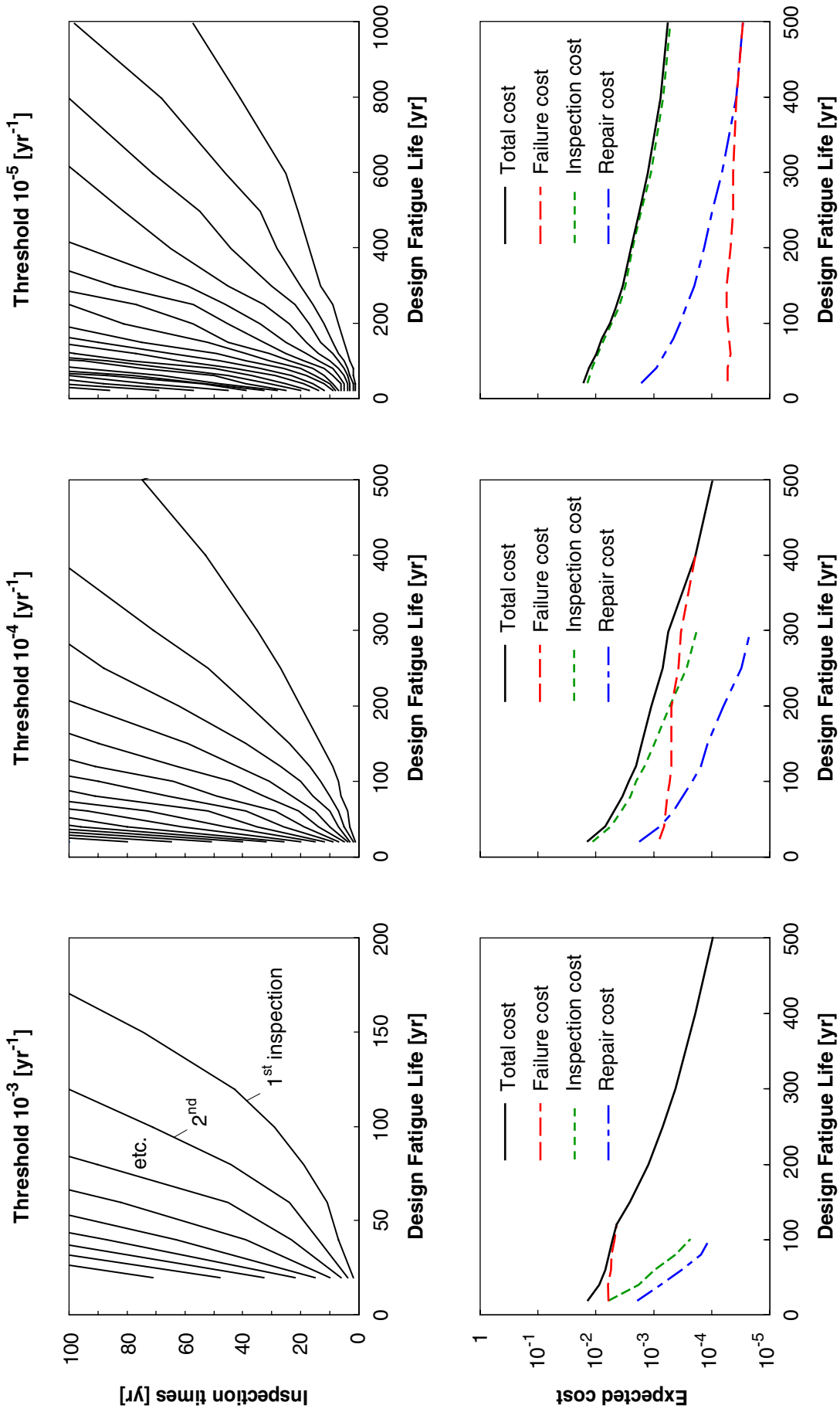


Figure 5.14 – Influence of the design fatigue life  $T_{FL}$  on the inspection plans (inspection scheduling and expected cost).

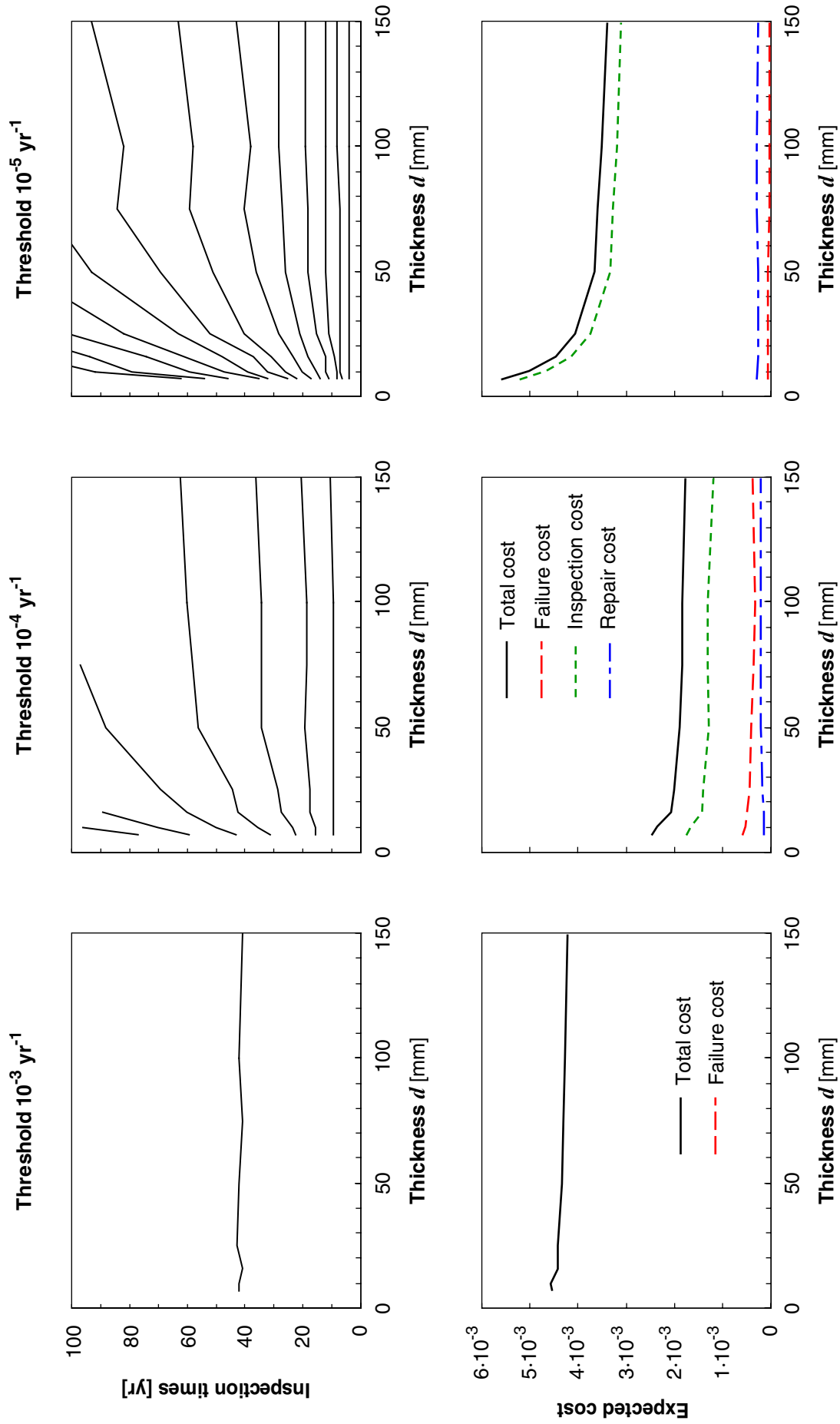


Figure 5.15 - Influence of the wall thickness at the hot spot,  $d$ , on the inspection plans.

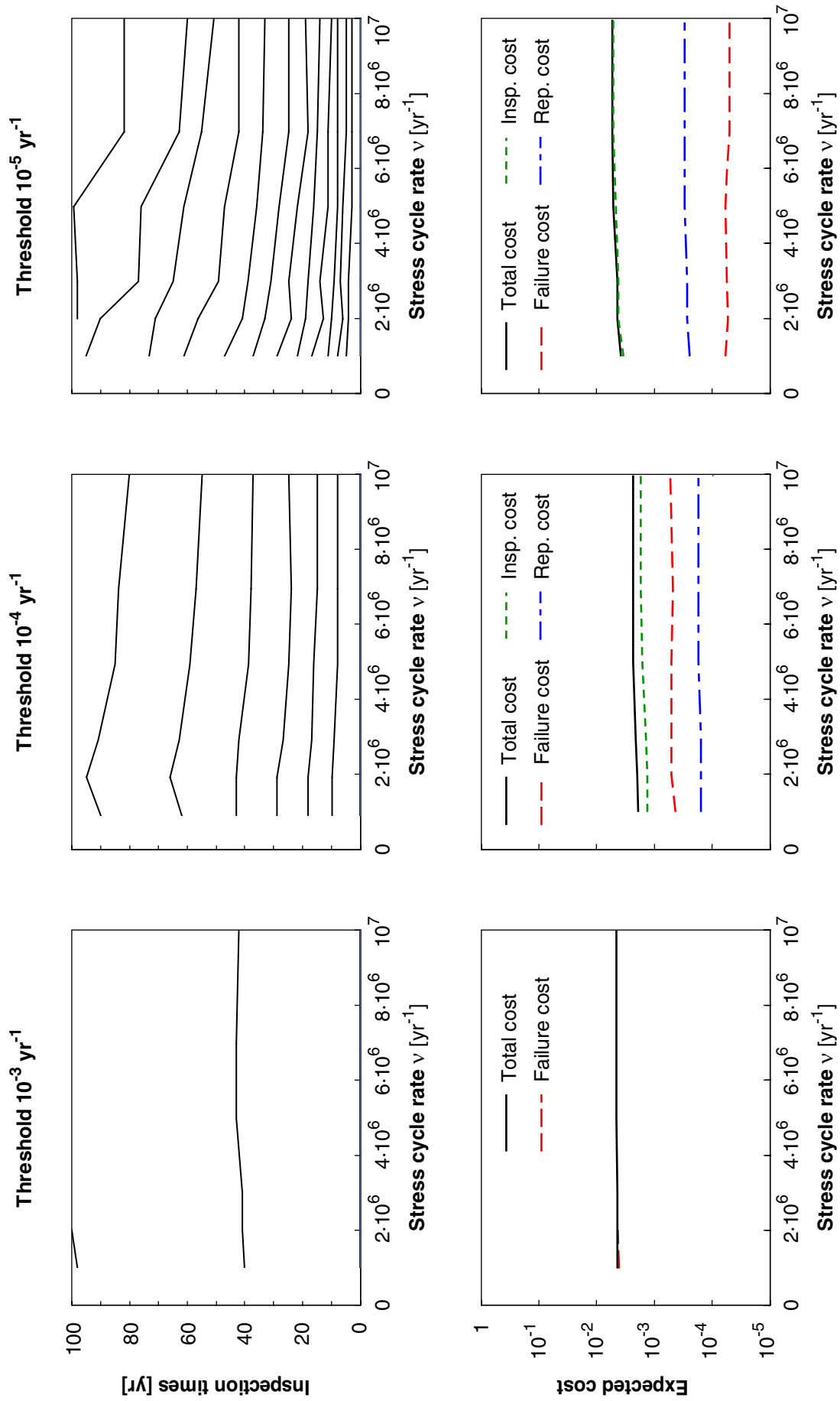


Figure 5.16 - Influence of the annual stress cycle rate on the inspection plans.

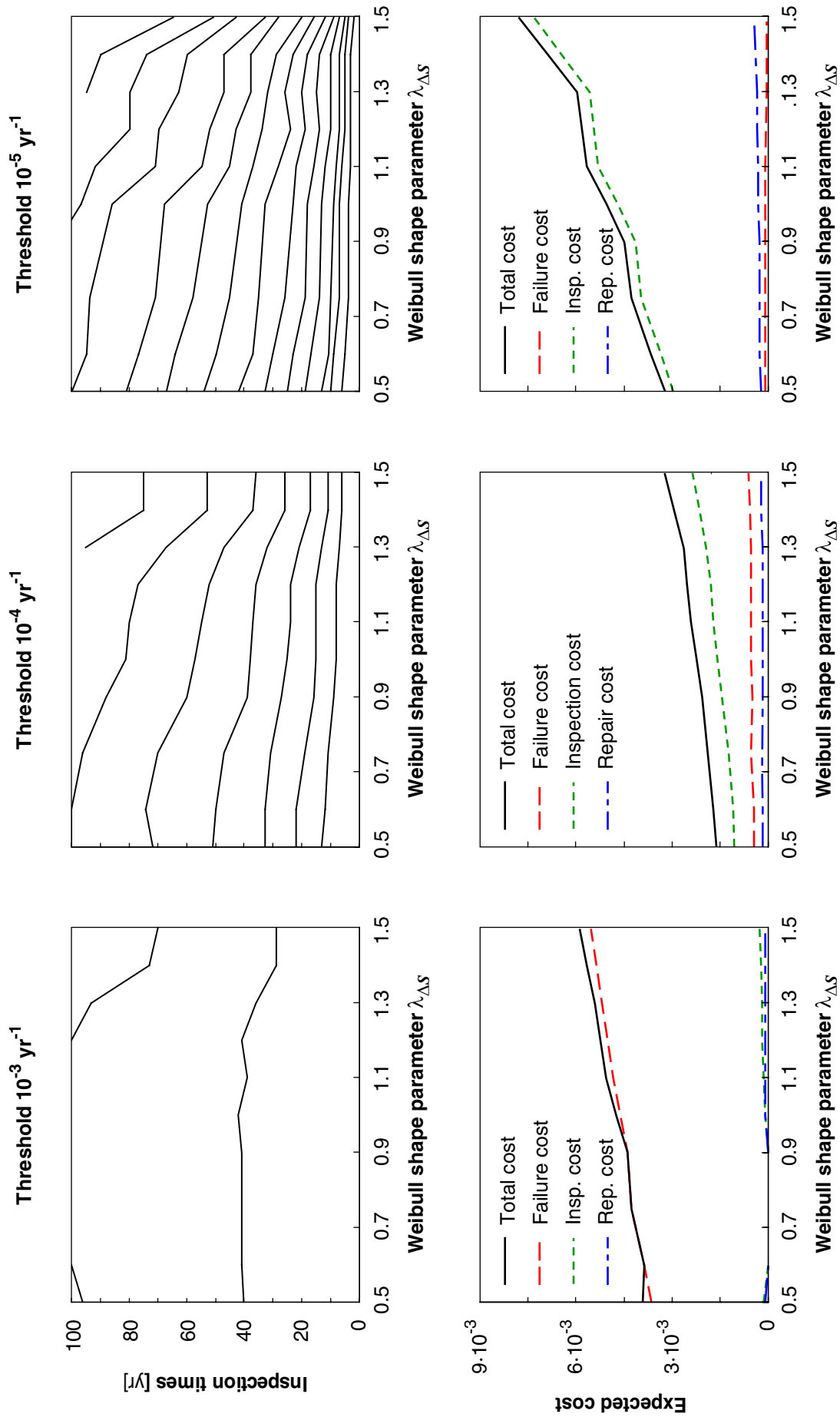


Figure 5.17 - Shape parameter of the Weibull distribution of stress ranges: Influence on the inspection plans.

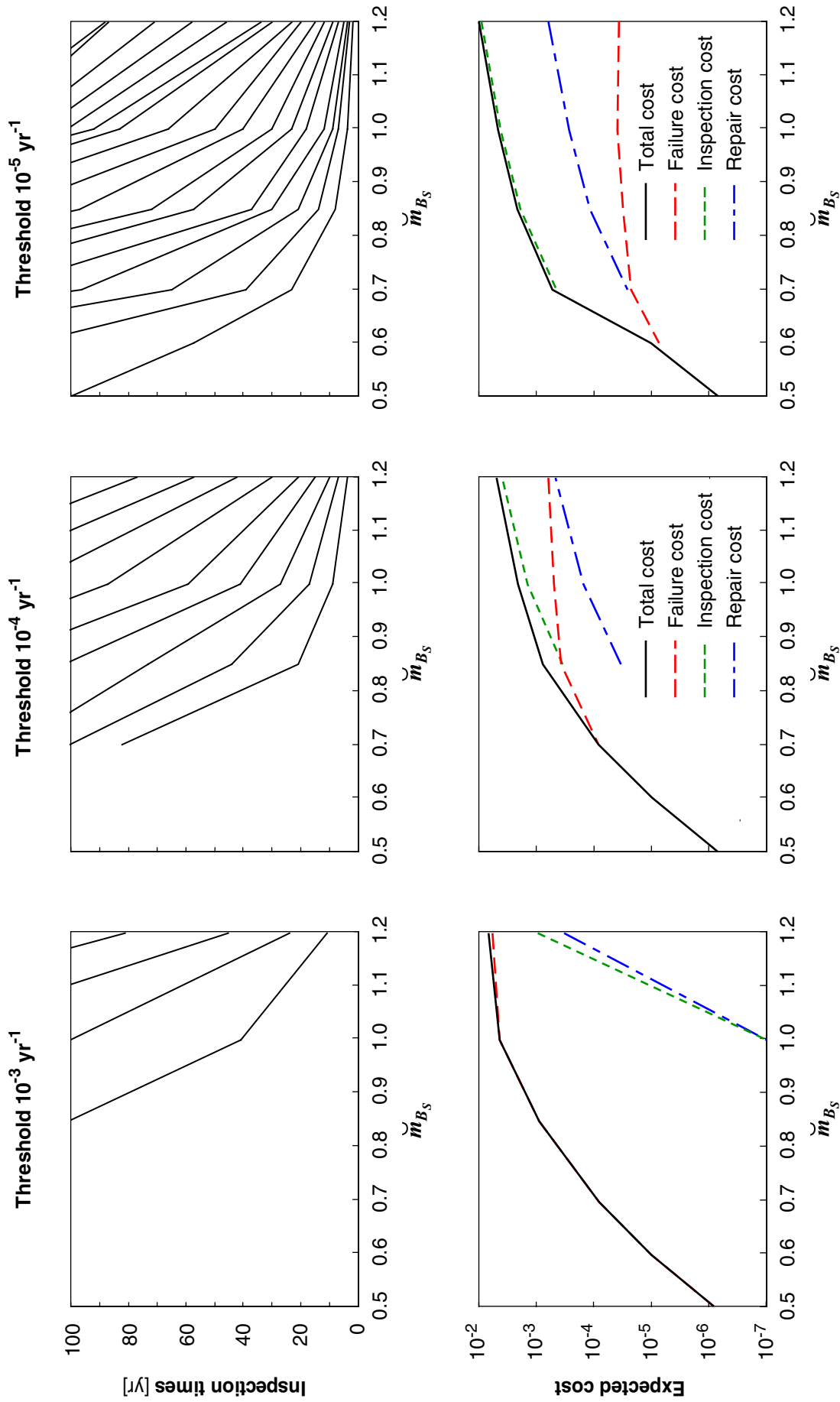


Figure 5.18 - Influence of the median of the uncertainty on the calculated fatigue stresses.

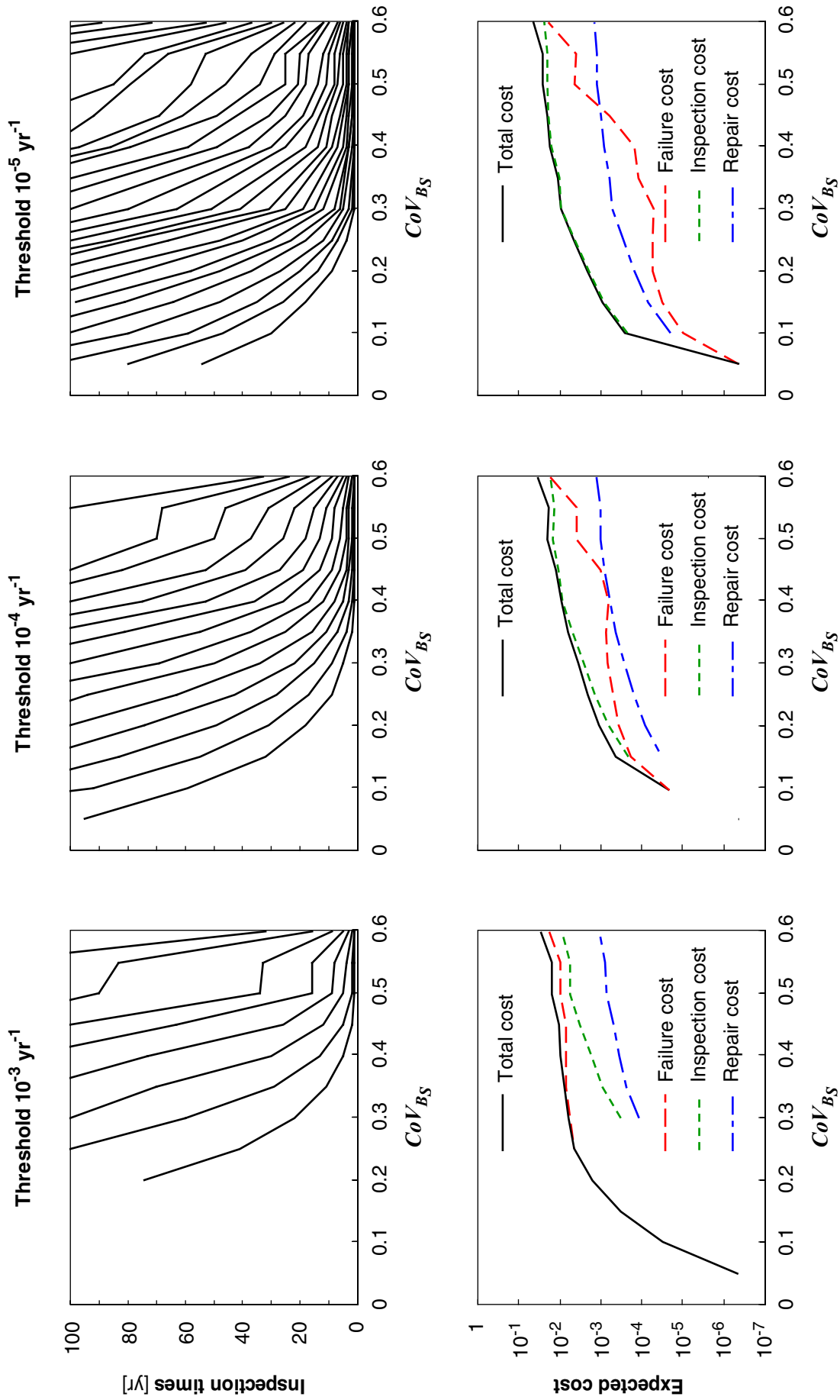


Figure 5.19 - Influence of the  $CoV$  of the uncertainty on the calculated fatigue stresses.



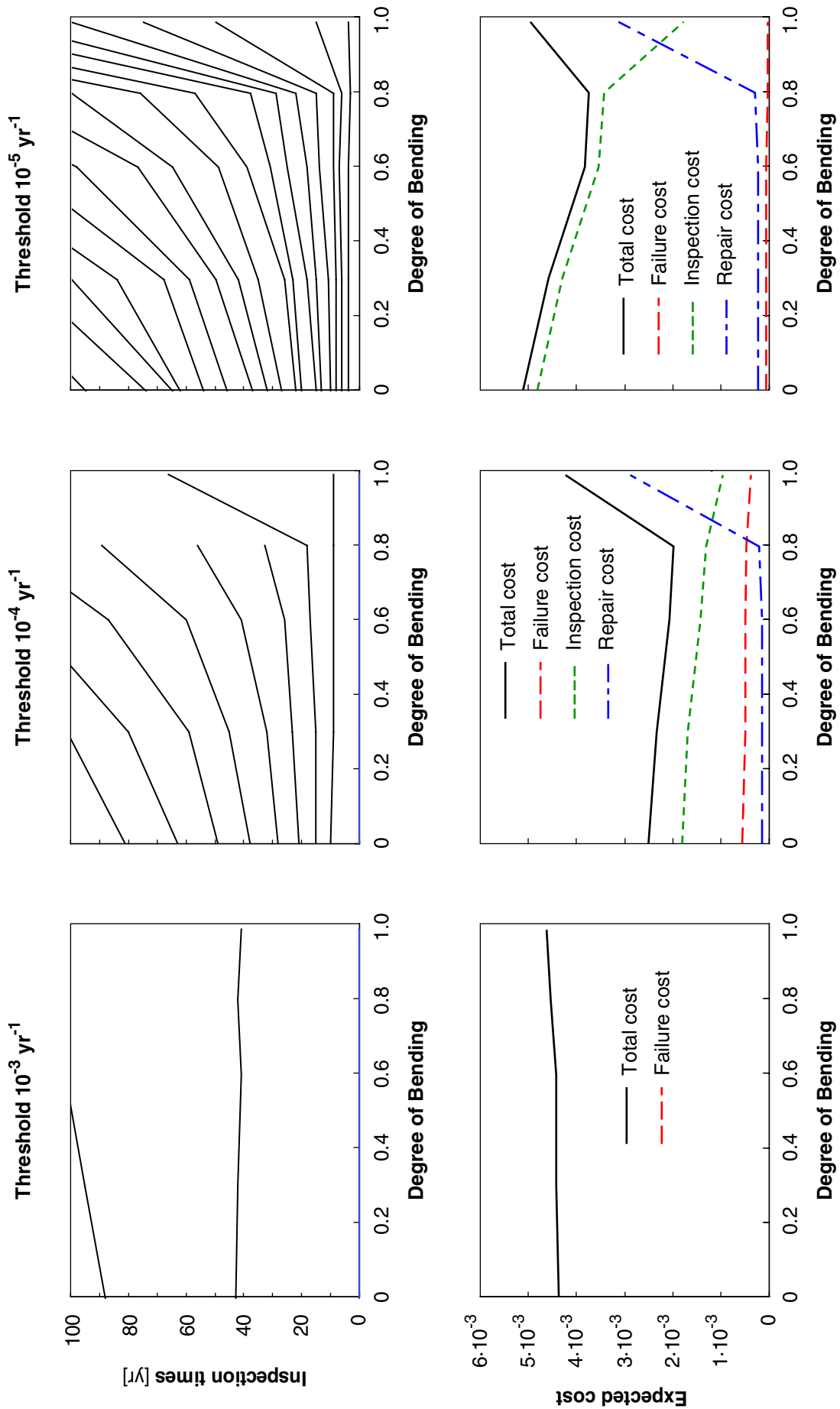


Figure 5.20 - Influence of the DoB on the inspection plans.

### 5.5.7.7 Influence of the SN curve

The SN curves describe a non-linear relation between the number of stress cycles and the stress ranges. Because the stress ranges are random variables, different SN curves give different fatigue reliabilities for equal design fatigue lives  $T_{FL}$ . This causes the change in the inspection plans when the EC 90 curve is applied instead of the DOE E curve. These two curves are very similar, see Figure 5.8, with the exception of the differences in the value of  $N_q$  and the endurance limit, which is included only in the EC 90 curve. From Figure 5.21 and Figure 5.22 it is observed that these differences cause substantial differences in the resulting inspection plans.

Because the influence that a change of the SN curve has depends on both the specific curves as well as the stress range model, a prediction of this influence is difficult. However, based on the presented results it is concluded that the inspection plans must be evaluated separately for different SN curves.

### 5.5.7.8 Influence of the initial crack size

It is reminded that the crack growth model is calibrated to the SN model. As a consequence, in accordance with the thickness effect illustrated in Figure 5.13, it is conservative to apply a model with a small initial crack size; the same holds for models with a large crack initiation period. For these models, more time of the total fatigue life (which is equal for all models) is spent in the crack imitation phase; the period during which the crack is detectable is thus smaller and the inspection intervals must be shortened. This does not signify that a poorer welding quality is advantageous: A poorer weld quality should be accounted for by corresponding SN curves, which will lead to smaller  $FDF$  and so increase the required inspection efforts.<sup>a</sup>

These phenomena are observed for the investigated models: Figure 5.21 and Figure 5.22 illustrate the difference when assuming Moan's model instead of the reference model. With the poorer weld quality (Moan's model) fewer inspections are required to comply with the threshold criterion  $\Delta p_F^T$ .

### 5.5.7.9 Influence of the inspection method

When applying an inspection with a lower quality, more inspections are required to comply with  $\Delta p_F^T$  compared to using a technique with higher quality. If both considered inspections have the same cost, then also the total expected costs will be higher. However, it is not always obvious which the best inspection technique is. Between the two investigated models, the reference model (MPI ICON) is more optimistic in the lower crack size range, Moan's model predicts a higher inspection quality for larger crack sizes. From the results presented in Figure 5.21 and Figure 5.22 it is observed that Moan's model is more pessimistic for the considered application. This is explained by the fact that most of the fatigue life is spent in the lower crack size range.

---

<sup>a</sup> However, these effects point out that a more robust design (increasing the FDF by decreasing the stresses) leads to fewer inspections than a design where the fabrication quality is improved. This should be taken into account when optimising fatigue design.

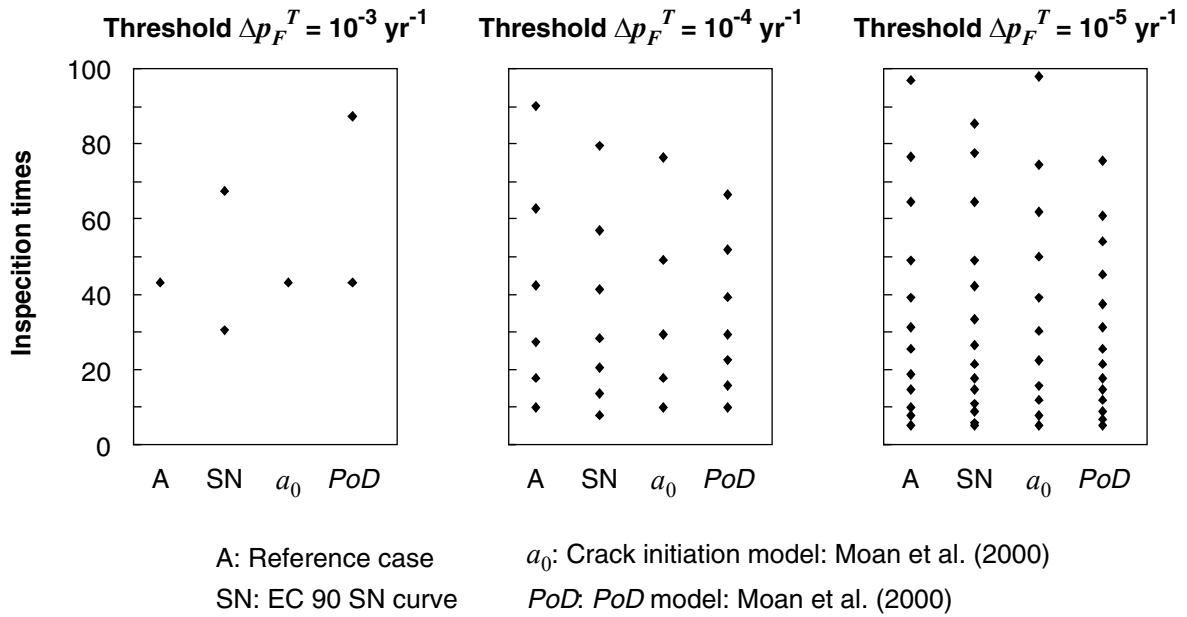


Figure 5.21 – Inspection times for the different discrete generic parameters.

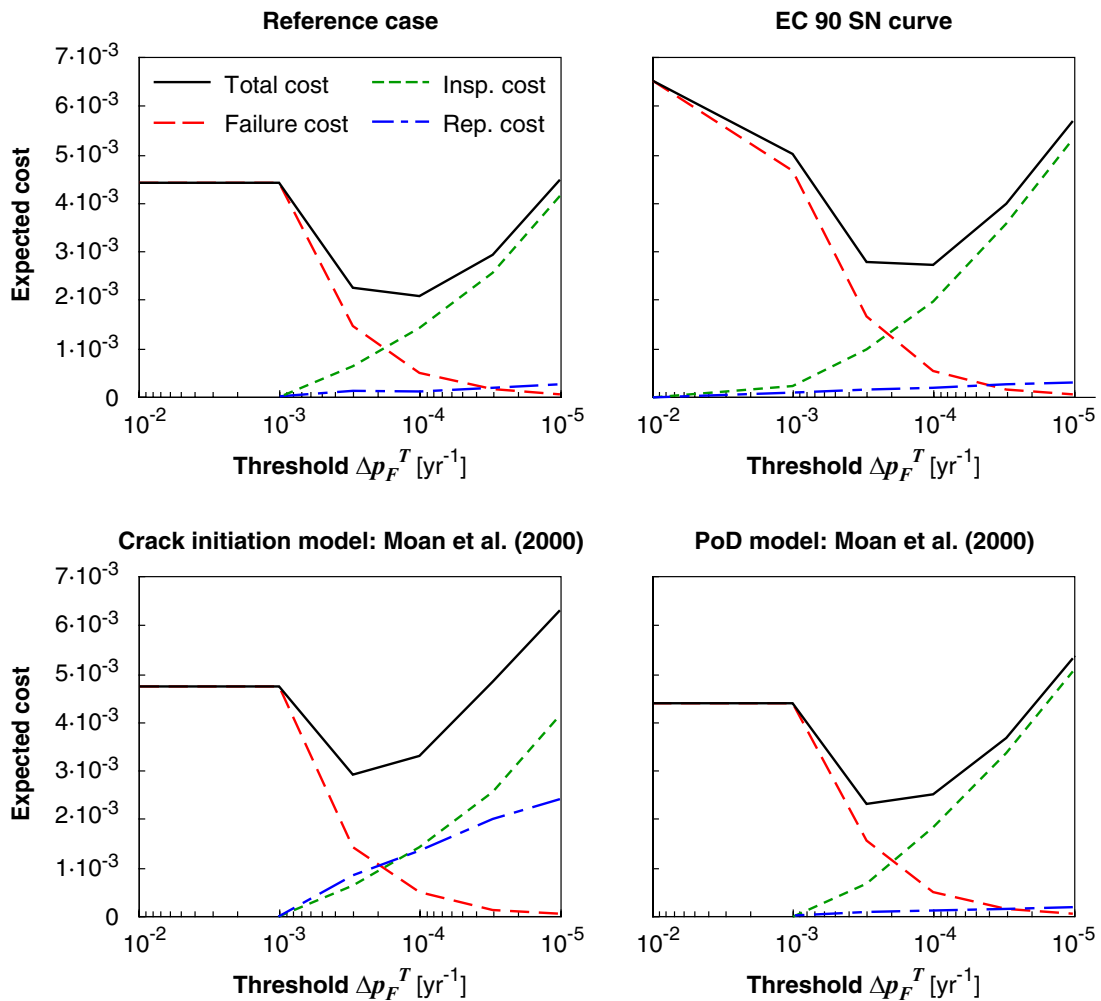


Figure 5.22 – Expected cost for the different discrete generic parameters.

### 5.5.8 Derivation of the generic database

In Section 5.5.7 the determination of the generic representations is documented for all generic parameters. Based on these, an example database is established to demonstrate the generic approach and to verify the proposed database design. The resulting database is implemented in *iPlan.xls* as outlined in Annex D.

To reduce the computational effort for the establishment of the database, only two generic representations for  $CoV_{Bs}$  are included in the database, namely 0.3 and 0.4. Furthermore only one SN curve and one crack initiation model is considered. The total number of generic inspection plans is thus

$$n_{GIP} = \frac{6 \cdot 6 \cdot 3 \cdot 1 \cdot 2 \cdot 2 \cdot 3 \cdot 1 \cdot 1 \cdot 2}{\begin{matrix} n_{OP} & T_{FL} & d & \nu & \lambda_{\Delta S} & CoV_{Bs} & DoB & SN \\ (\Delta p_F^T) & & & & & & \text{diag.} & \text{initiation} \\ & & & & & & & \text{Crack} \\ & & & & & & & \text{PoD} \end{matrix}} = \underline{\underline{2592}}$$

#### 5.5.8.1 Computational efforts

The calibration of the FM model to the SN model is computationally efficient due to the use of FORM algorithms for the reliability calculations. Because the calibration is independent of the *PoD* and the applied threshold  $\Delta p_F^T$ , it is performed for 216 different cases only; thereby one calibration takes on average 650 CPU seconds on a standard PC (Pentium III).

In the calculation of the inspection plans most of the computational time is spent for simulating crack growth histories, as this requires a large numbers of calls to the LSF which are solved numerically in accordance with Annex B. Again, these simulations are not dependent on the *PoD* and the applied threshold  $\Delta p_F^T$ . The inclusion of an additional threshold does not change the computation time significantly, because the same simulations of the crack growth history can be used. The computation time is thus analysed for the 216 cases with different crack growth models, each representing 12 generic inspection plans: The total computation time is 78 CPU days and the average for one case is 8.7 CPU hours. However, this performance is subject to large scatter: The standard deviation for the calculation of one case is evaluated as 7.8 CPU hours. In addition, the minimum observed effort for one case is 850 CPU seconds, whereas the maximum is 34 CPU hours. This indicates the importance of the evaluation of the LSF, as these cases only differ in this calculation step. It is noted that the computation time is a function of the reliability; it increases with decreasing reliability. The largest computation times thus occur for small  $T_{FL}$ <sup>a</sup>. This also indicates that the observed computation times can be significantly reduced if the inspection plans are calculated for a maximum service life time  $T_{SL,max}$  of only 50yr instead of 100yr.

---

<sup>a</sup> This is caused by the fact that the numerical solution to the coupled differential equation in the LSF (see Annex B) is much more demanding for large crack sizes. These occur more frequently when simulating cases with low reliability.

### 5.5.9 Verification of the generic database

For the purpose of verification of the generic database derived according to the previous sections, 10 hot spots with arbitrary chosen parameters are selected. The specific parameters of these hot spots are provided in Table 5.7. The other parameters are identical for all hot spots: Service life  $T_{SL} = 40\text{yr}$ ,  $\bar{m}_{B_S} = 1.0$ , SN curve DoE D, the crack initiation model according to Lassen (1997) and the ICON inspection model.

For all hot spots, inspection plans are derived by

- a) direct calculation, i.e. both the calibration of the FM model, as well as the simulation of the final inspection plans are performed with the specific parameters of these hot spots;
- b) the generic approach, i.e. through interpolation between the generic inspection plans in the database.

The results from the two methodologies are then compared in terms of the resulting inspection times and total expected cost, in order to verify the suitability of the generic database and the interpolation procedure.

*Table 5.7 – Different hot spots for the verification of the generic database.*

Hot spot	$T_{FL}$ [yr]	$\nu$ [ $10^6 \text{ yr}^{-1}$ ]	$CoV_{B_S}$	$\lambda_{\Delta S}$	$d$ [mm]	$DoB$
1	200	2	0.30	0.70	10	0.2
2	135	4	0.35	0.90	40	0.3
3	83	6	0.33	1.10	20	0.4
4	64	8	0.30	1.30	13	0.5
5	175	5	0.40	1.50	50	0.6
6	302	1	0.35	1.00	30	0.7
7	79	3	0.35	1.00	8	0.8
8	160	1	0.30	0.60	12	0
9	400	2	0.30	0.80	45	0.4
10	300	7	0.35	1.20	10	0.5

#### 5.5.9.1 Inspection times

A first measure for the quality of the generic approach is the agreement in the total number of inspections during  $T_{SL}$ . These are summarised for all hot spots in Figure 5.23. The results for the threshold  $\Delta p_F^T = 10^{-2} \text{ yr}^{-1}$  are thereby excluded; during the considered service life,  $T_{SL} = 40\text{yr}$ , no inspections are required for all inspection plans with this threshold.

The resulting inspection times are compared for the different thresholds individually. Figure 5.24 presents this comparison for  $\Delta p_F^T = 10^{-4} \text{ yr}^{-1}$ . The results for the other thresholds, which are not presented here, are similar to those presented: When the required inspection times in Figure 5.24 are at earlier times according to the direct calculations for a specific hot spot, then the same is observed for other thresholds too.

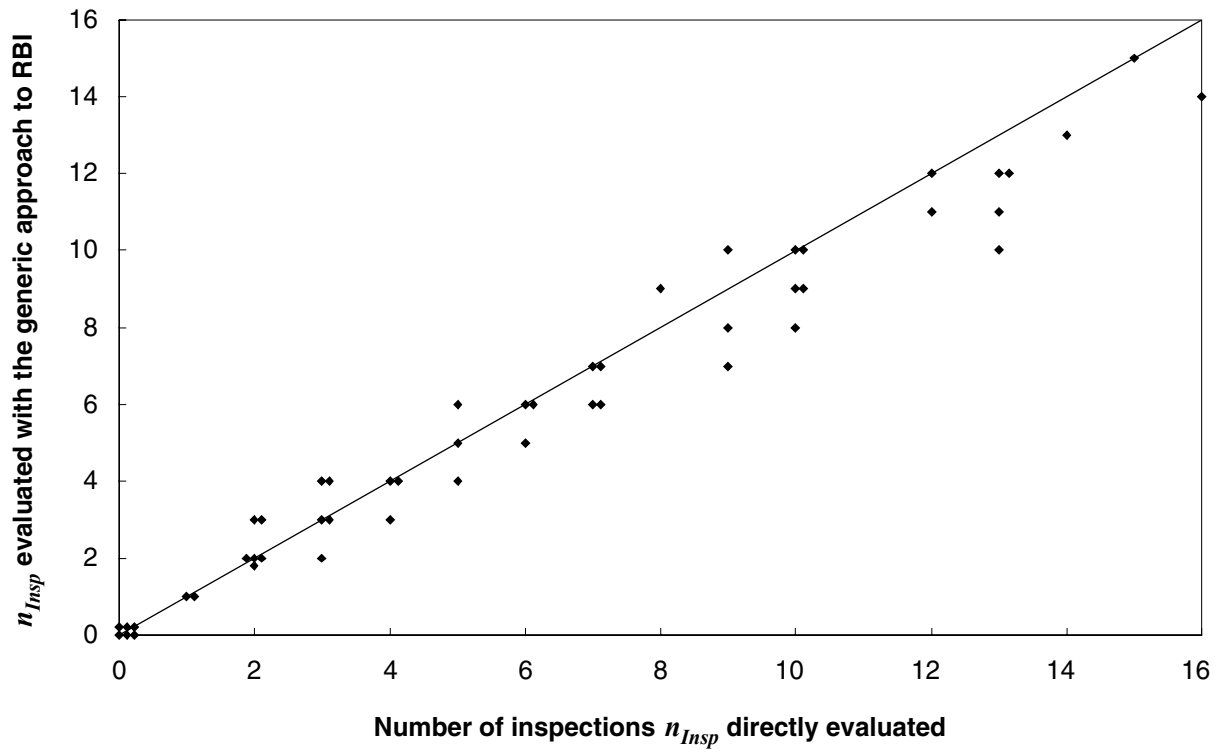


Figure 5.23 – Comparison of the total numbers of inspections between the direct calculations and the generic approach (for all different hot spots and thresholds).

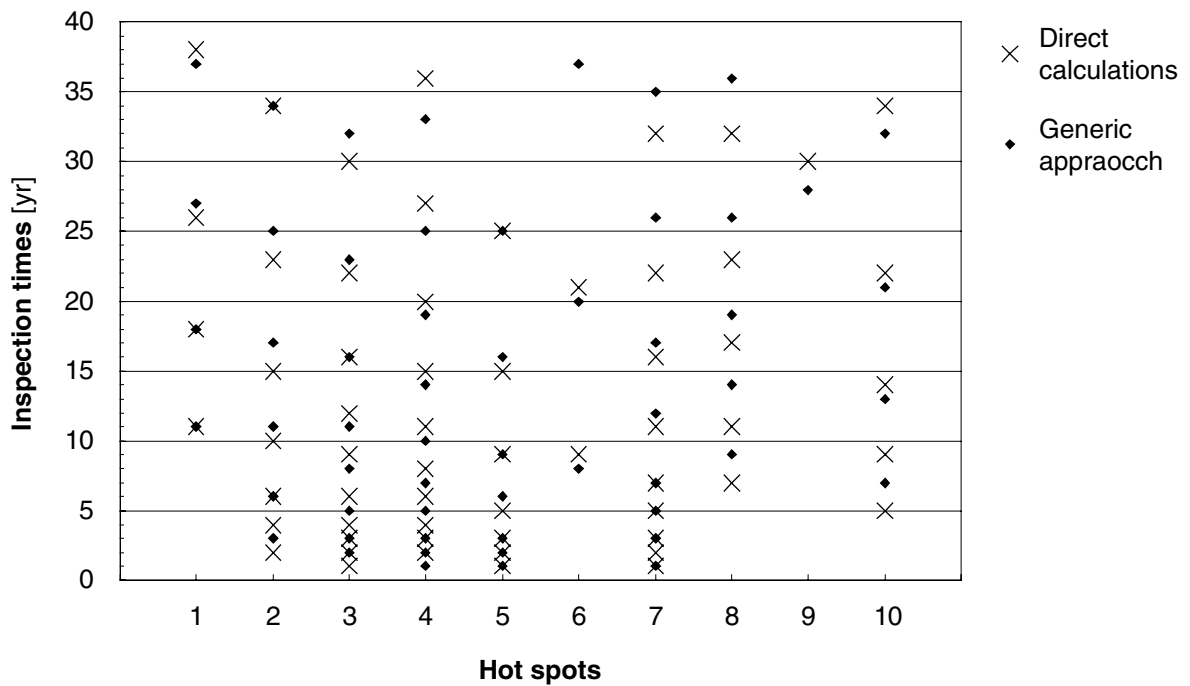


Figure 5.24 – Comparison of the inspection times between the direct calculations and the generic approach for  $\Delta p_F^T = 10^{-4} \text{ yr}^{-1}$ .

### 5.5.9.2 Expected cost

Figure 5.25 presents the total expected costs for the different hot spots as obtained by the direct calculations and as obtained from the generic approach. Thereby both the linear and the logarithmic interpolation schemes are applied, in accordance with Annex E. When comparing the individual cost components (expected failure, repair and inspection cost) separately, no general trend is observable: Whereas the observed difference in the total expected cost for some hot spot is due to differences in the expected failure costs, for others it is caused by differences in the expected inspection and repair costs.

The assumed cost model follows the one defined in Section 5.5.5 and applied in the sensitivity analysis. The agreement between the expected costs has also been checked for other cost models (including different interest rates) and the results are not significantly different from those presented in Figure 5.25.

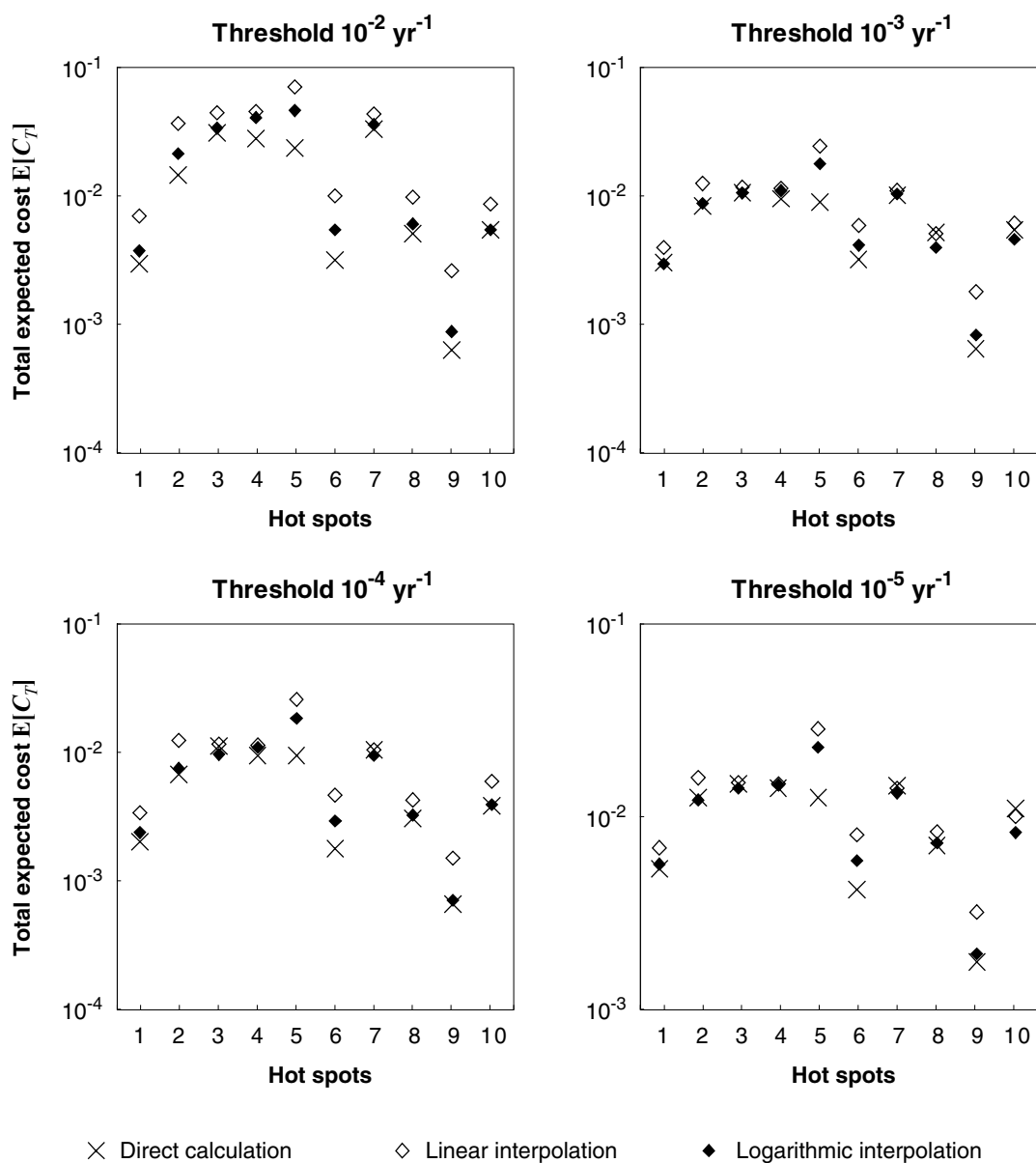


Figure 5.25 – Comparison of total expected cost.

### 5.5.9.3 Conclusion

The verification of the generic database and the interpolation procedure is an important task in the generic approach to RBI. Because the relation between the generic inspection plans and the inspection plans for the specific hot spots is purely empirical, such a verification can only be performed by comparing the results of the generic approach to inspection plans directly calculated. Such a comparison is provided in Figure 5.23 to Figure 5.25.

When comparing with the inspection plans resulting from direct calculations, it must be borne in mind that these plans also are not exact solutions, but that they are subject to the scatter arising from the inaccuracy of the simulation procedure, Annex C. On the other hand, this scatter is reduced for the inspection plans from the generic approach. These plans are based on a set of inspection plans, each determined with  $n_{MC}$  simulations, and the total number of simulations is thus much larger for the interpolated inspection plans. For small deviations between the results from the directly calculated inspection plans and those derived through the generic approach, it is therefore not possible to interpret whether these are due to the calculation accuracy or the imprecision of the generic interpolation scheme.

With regard to the inspection times, it is observed that the deviations between the results from the two calculation methods vary among the different hot spots, yet it is not possible to identify one single factor that is responsible for these deviations. The inspection plans derived by means of the generic approach seem to underestimate the number of inspections  $n_{insp}$  for inspection plans with large numbers of inspections, Figure 5.23. However, the few investigated hot spots do not allow any conclusion on a general trend.

With regard to the expected cost, the logarithmic interpolation scheme is superior to the linear one for a large majority of the investigated hot spots and cost models (the latter are not included in the presented results). This is not surprising considering that the logarithm of the expected cost varies for many parameters approximately linearly with the parameter values, as observed in the sensitivity study, Section 5.5.7. In analogy to the resulting inspection times, it is not possible to identify single factors that cause the deviations in the total expected costs as evaluated by the two methods.

The largest deviations in the total expected costs between the two methods do not occur for the same hot spots as the largest deviations in the resulting inspection times. This is explained by the fact that the interpolation of the total expected costs is independent of the interpolation of inspection times. It indicates that the generic database contains no systematic errors.

The main conclusions drawn from the presented comparison is that the agreement of the interpolated inspection times as well as of the expected cost is reasonably good. Additionally, it is not possible to identify single factors which are responsible for the observed deviations in the comparison. This signifies that it is difficult to predict how the generic database is improved most efficiently. It is therefore concluded that the presented generic database and interpolation scheme are sufficiently accurate for the envisaged applications (the determination of inspection plans to comply with given acceptance criteria and the optimisation of inspection, maintenance and design). It is furthermore recommended that the logarithmic interpolation scheme be used for the evaluation of the expected costs from the generic database.



### 5.5.10 Actualisation of inspection plans

All inspection times are derived based on the assumption of no-indication at all previous inspections. This enables the efficient computation of the total expected cost of an inspection strategy with reasonable accuracy, Section 2.4.1. However, when inspections result in indications, these inspection times are no longer accurate, and the inspection plan must be actualised. A procedure to plan the inspections after an indication of a defect is thus required. Such a procedure is highly facilitated by the generic approach, as the evaluation of a new inspection plan with different parameters is straightforward.

Not all possible inspection outcomes other than no-indication can be anticipated at the inspection planning stage<sup>a</sup>. Thus, once a crack is indicated and possibly measured, an engineering assessment must be performed to determine the optimal mitigation action in this specific situation. As part of this assessment, the generic parameters representing the repaired hot spot must be determined. Typically the *FDF* will change after an indication and again after a repair, but, depending on the mitigation action, other parameters, such as the uncertainty on the stress calculations, may also vary. Based on the new values of the generic parameters, the corresponding inspection plan can be obtained directly from the generic inspection plans. This procedure is illustrated in Figure 5.26.

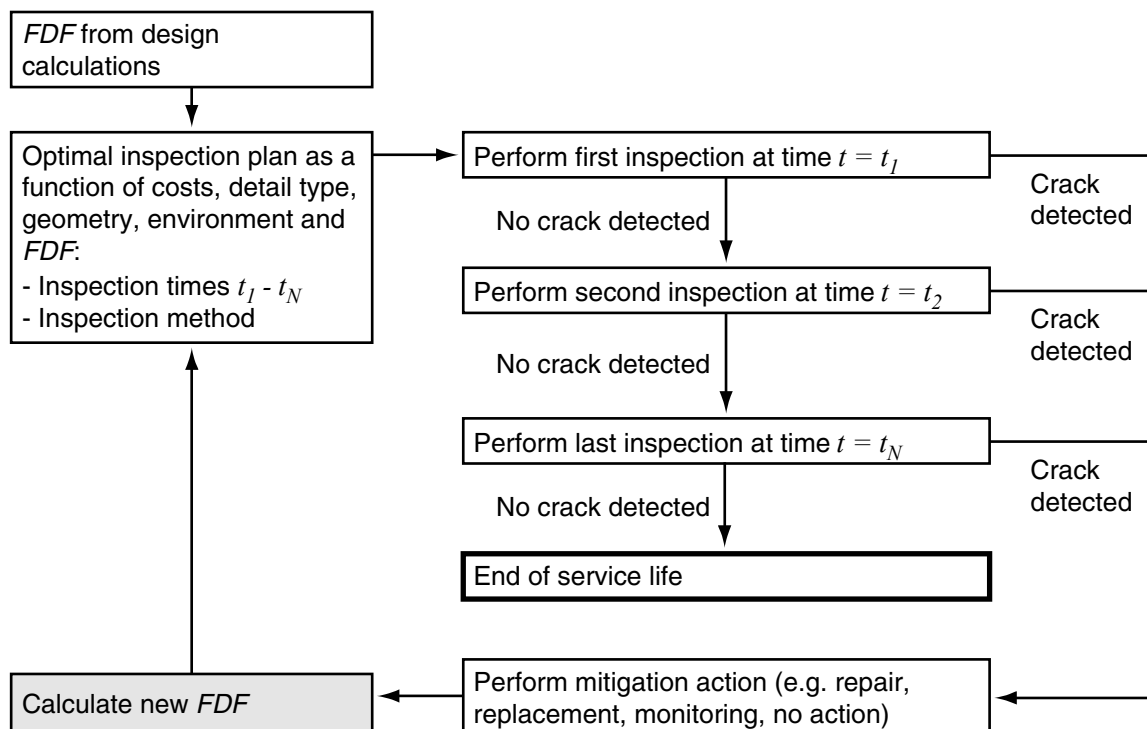


Figure 5.26 – Application and actualisation of the inspection plans.

<sup>a</sup> The possible inspection outcomes after an indication are many. Generally a measurement is performed, resulting in a measured defect size  $s_m$ . As this is a continuous variable, the determination of optimal actions after the indication would require the definition of different intervals for  $s_m$ , and for each of these intervals the optimal action must be assessed. This is not a practical approach due to the required computational efforts.

### 5.5.11 Accounting for modifications in the fatigue loading

In many cases the stochastic characteristics of the fatigue loading at a hot spot change during the service life of the structure, due to a change in the loading conditions or a modification of the structure. These load modifications are easily accounted for in the standard SN calculations, due to the cumulative nature of the Palmgren-Miner model: the damage accumulated before the modification is simply added to the damage occurring after the modification. Unfortunately, this does not hold for the FM model, which is highly non-linear, and consequently some additional considerations are required when accounting for load modifications in RBI.

An empirical approach to account for load modifications, fully based on the generic approach, is introduced in this section. The problem is first presented in view of the SN approach, where some new parameters are established allowing for dealing with the load modifications based on the already evaluated generic database. Figure 5.27 illustrates these new parameters:

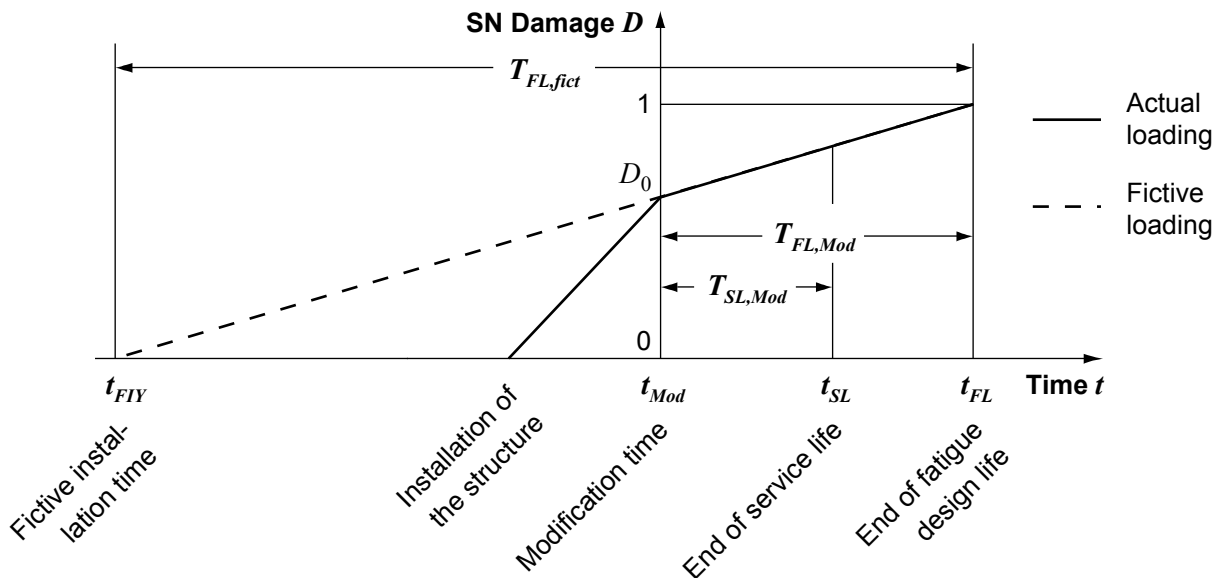


Figure 5.27 – The load modification problem interpreted deterministically in the context of the SN model.

$D_0$  denotes the SN damage at the time of modification,  $t_{Mod}$ . At  $t_{Mod}$  the already accumulated damage is entirely described by  $D_0$  in consistency with the philosophy of the SN model. This can include various modifications of fatigue loading before  $t_{Mod}$ . In a first step, the concept of the fictive installation year, denoted by  $t_{FIY}$ , is introduced: A hot spot that were installed at  $t_{FIY}$ , with fatigue loading as illustrated by the fictive loading in Figure 5.27, would have an SN damage equal to  $D_0$  at the time of modification  $t_{Mod}$ . This fictive loading is equal to the actual loading after the modification and is characterised by  $T_{FL, fict}$  in accordance with Figure 5.27. The actual fatigue life after the modification is  $T_{FL, Mod}$  and can be calculated as

$$T_{FL,Mod} = (1 - D_0)T_{FL,fict} \quad (5-10)$$

Generally the problem is considered at the time of modification  $t_{Mod}$ <sup>a</sup> and the design service life at that time is

$$T_{SL,Mod} = t_{SL} - t_{Mod} \quad (5-11)$$

A new Fatigue Design Factor can now be evaluated as

$$FDF_{Mod} = \frac{T_{FL,Mod}}{T_{SL,Mod}} \quad (5-12)$$

In the framework of the SN approach the  $FDF_{Mod}$  contains all relevant information on the reliability of the hot spot subject to load modifications. However, due to the non-linear crack growth behaviour, it is not consistent to calculate an inspection plan from the generic inspection plans with parameter  $FDF_{Mod}$ . This is illustrated in Figure 5.28, where the actual behaviour of the crack is compared to the behaviour implied by calculating the new inspection plan based on  $FDF_{Mod}$ .

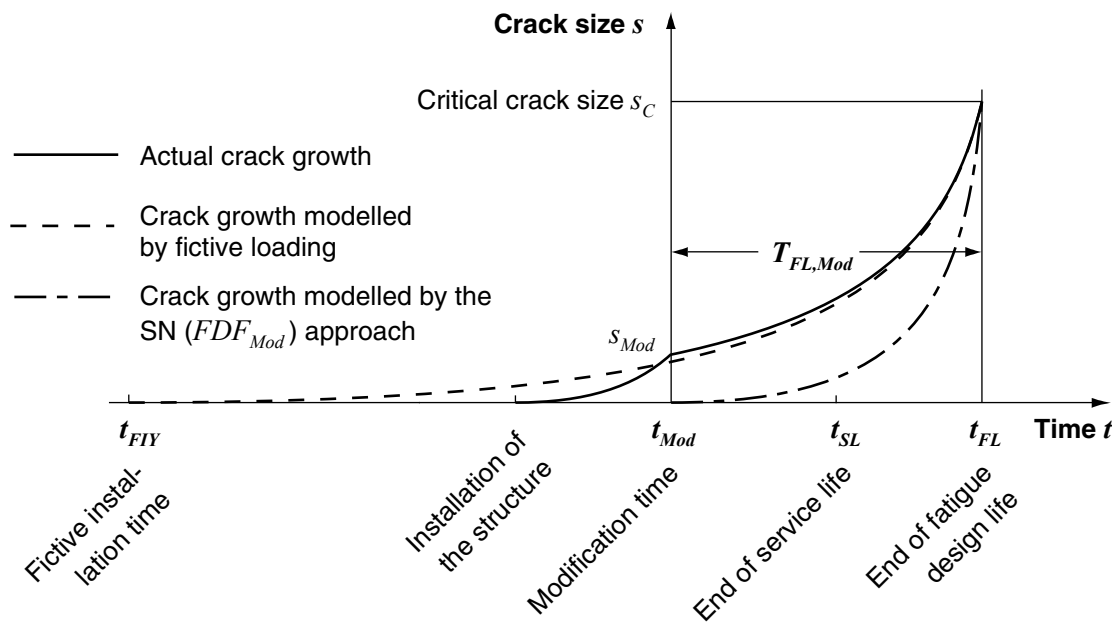


Figure 5.28 – The load modification problem interpreted deterministically in the context of the crack growth model.

<sup>a</sup> The inspection planning is often performed at the time of a reassessment, which in turn may be initiated by a modification of the use (and consequently the loading conditions) of the installation.

As a consequence of the situation depicted in Figure 5.28, a procedure is proposed which is based on  $t_{FIY}$  and  $T_{FL, fict}$ : The inspection plan is evaluated from the generic database as for a hot spot with installation year  $t_{FIY}$  and design fatigue life  $T_{FL, fict}$  and is then truncated before  $t_{Mod}$ . This procedure approximates the loading before the modification with that after the modification, but the service life before  $t_{Mod}$  is adjusted to account for the real fatigue damage in the first period, namely  $D_0$ .

Additionally, when the inspection planning is performed during the service life of the structure, it is of interest to include already performed inspections, which are not necessarily in compliance with the new inspection plans. Because inspection intervals as obtained using the threshold approach are, with the exception of the first, generally increasing with time, it is conservative to shift the inspection times in the positive direction (towards future dates). This can be utilised to account for previously performed inspections.

Figure 5.29 summarises the proposed approach for the derivation of the inspection times for hot spots that are subject to load modifications and /or previously performed inspections:

1. An inspection plan is evaluated from the fictive installation year  $t_{FIY}$ , with design fatigue life  $T_{FL, fict}$ .
2. Inspection plans are shifted to account for the last inspection performed.
3. If inspections are necessary before  $t_{Mod}$ , but not performed, then they are required at  $t_{Mod}$ . The subsequent inspections are then shifted accordingly. The inspection plan is finally truncated at  $t_{Mod}$ .

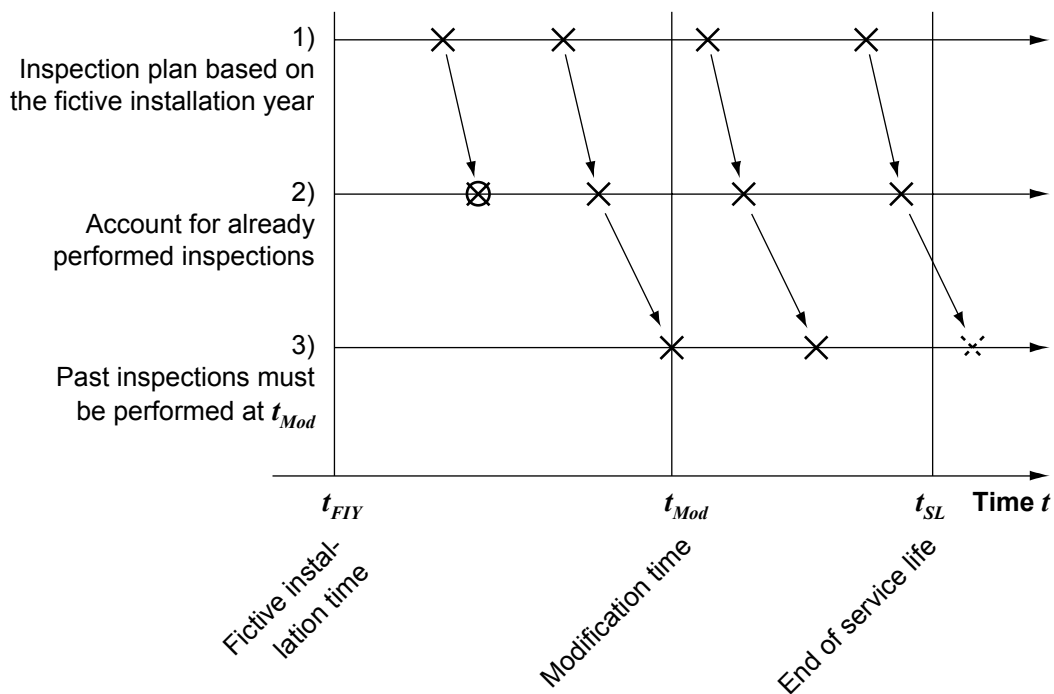


Figure 5.29 – Illustration of the proposed approach to the identification of inspection times for hot spots subject to a modification of the loading.

The presented methodology results in an approximation of the “exact” inspection plan. The latter is obtained by the explicit consideration of the specific stress range models in the different periods. Therefore, in the framework of the RBI application as described in Faber et al. (2003), the proposed method is tested against an “exact” calculation, where both the first and the second load period are directly modelled, and is found to provide good approximations. An example of such a comparison is shown in Figure 5.30.

The direct simulation is based on the assumption of full correlation between the random variables before and after the modification. Calculations have additionally been performed assuming partial independency of the random variables. However, this latter assumption generally results in non-conservative inspection plans, containing fewer inspections; in particular are no inspections required at year  $t = 0$ .

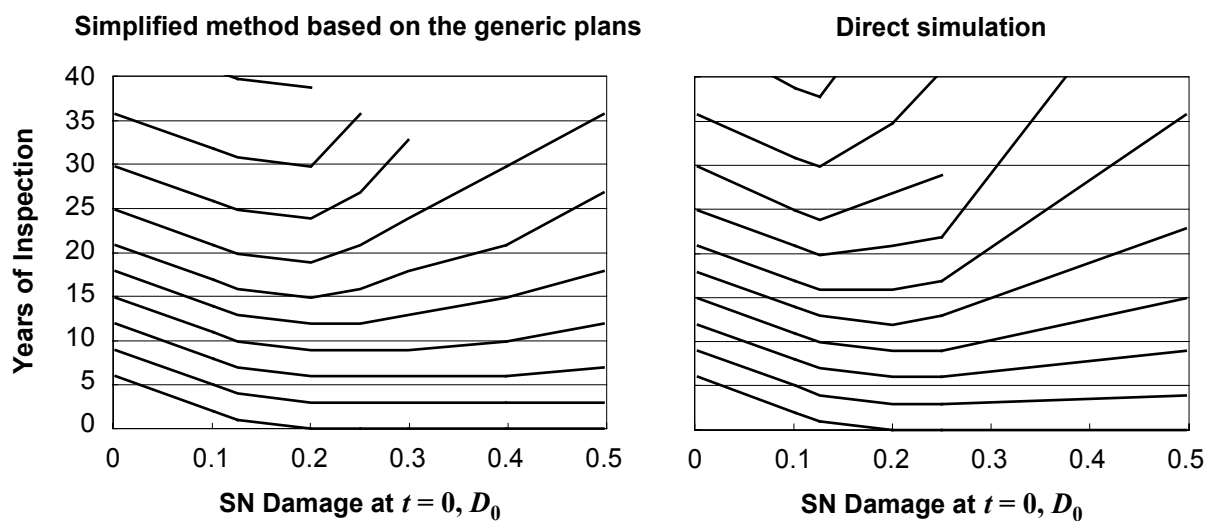


Figure 5.30 - Comparison of the simplified approach for load modifications (left) to a full analysis of the total load history: inspection times for threshold  $10^{-5}$  as a function of the damage at the time of modification.

The difference between the two results is caused by the fact that for the simplified method the stochastic model of the crack size at  $t_{Mod}$  is generally not the same as for the model with the full load history. The simplified method only provides an approximation, as indicated in Figure 5.28. Although the simplification is conservative for most cases, including those presented in Figure 5.30, it is not necessarily conservative in all situations. Still, it is concluded that in the absence of a more accurate model the method provides a useful decision support.

## 5.6 Generic modelling for corrosion

The generic approach to RBI for corrosion subjected structures is first proposed in Straub and Faber (2000); Faber et al. (2003b) emphasises the importance of such an approach for a consistent evaluation of the risks for all types of equipment and systems in an installation. To the operator, who is responsible for the safe operation of an entire facility, this is of importance for the management of the risks and the documentation to the relevant authorities. Although the necessity of such approaches is recognised, the non-availability of suitable predictive corrosion models (at least in the open literature) presents a main drawback to the application of RBI. This is the reason why, in contrast to the applications on fatigue subjected structures, this section does not present a readily applicable procedure. Instead it is limited to the demonstration of the possibilities of the approach for the planning of corrosion control.

A generic approach to RBI for corrosion problems is based on the principles as presented in the former sections and as illustrated on fatigue subjected hot spots. However, the differences in the decision problems for the two deterioration modes, already shortly discussed in Section 2.6, prevent a direct adaptation of the approach to corrosion subjected structures. The specifics of RBI for corrosion control are separately discussed for three different situations:

- (a) Structures which are corrosion protected represent fundamentally different decision problems, as noted in Section 3.5.3. For most protection systems it is not the corrosion deterioration that is inspected but the protection system itself. It is the latter that has to be considered for RBI. Generic approaches to RBI for protection systems will depend highly on the principles of the protection system and are not further discussed here.
- (b) Structures and systems where inspections for corrosion most likely result in no-indication: Examples of such applications are structures that are subject to highly localised defects. For these, inspection plans can be established similar to those for fatigue subjected structures, with inspection plans assuming no-indication at the inspections. In contrast to the application for fatigue, the spatial characteristics of the deterioration are more difficult to account for and system considerations are necessary. These aspects are treated in Chapter 6.
- (c) The application on structures that are designed with corrosion allowances: Because the assumption of no-indication at the inspections will in general be violated, all published approaches for such problems propose to base the inspection plan on the assumption that the detected corrosion defect is not larger than a given size  $d_R$ , see also Section 2.6. Otherwise the inspected hot spot is repaired. Unfortunately this approach neglects that the assumed event (the event of a measured corrosion depth less than a specified limit  $d_R$ ) contains less information than the actual observed event, namely the measurement of a specific corrosion depth  $d_m$ . As an illustration consider an inspection plan for  $d_R = 12\text{mm}$ : if at the first inspection a corrosion depth of 1mm is measured, the following inspections will be the same than if 10mm were measured. Both inspection plans are incorrect, because

$$P(F|d_m \leq d_R) \neq P(F|d_m) \quad (5-13)$$

For the case where  $d_m=10\text{mm}$ , the actual probability of failure after the inspection may be much higher than the one contained in the inspection plan which is  $P(F|d_m \leq d_R)$ , the inspection plan is thus non-conservative in such cases. This problem has not been accounted for previously, but it is crucial for a generic approach; a generic approach cannot anticipate every possible inspection outcome  $d_m$  and requires some assumption on (respectively grouping of) these outcomes.

To demonstrate that a generic approach to RBI for corrosion subjected structures, despite the difficulties involved, is not only feasible but also highly practical, a generic approach to RBI for pipelines exposed to  $\text{CO}_2$  corrosion is introduced in the following section.

## 5.6.1 Generic approach to RBI of pipelines subject to $\text{CO}_2$ corrosion

### 5.6.1.1 Generic modelling

Pipelines which are susceptible to corrosion are often designed with corrosion allowance; the general decision problem is thus described by situation (c) above. The problem that arises is that a specific measurement contains more information than the assumption on which the inspection plan is based. A complete inspection plan would take into account the full (infinite) number of possible outcomes at the inspections, but, clearly, such an approach is not practical. Any pre-established inspection plan must be based on some simplifications. Because  $\text{CO}_2$  corrosion damages are typically of a localised nature, the probability of missing the largest defect, introduced in Section 4.7, must be taken into account. This aspect, which has not been considered previously, allows formulating consistent simplification rules as shown in the following.

It is demonstrated in Section 4.7 that as long as the measured corrosion depth  $d_m$  is small, the probability of missing the largest defect is dominant for the updated reliability. An inspection plan that is calculated based on no-indication (or indication of only a small defect) is thus valid as long as no large defect has been measured. The measured size at which the inspection plan is no longer valid, denoted by  $d_{lim}$ , is case and time dependent: the inspection plan which is still valid after a corrosion depth measurement  $d_m$  at year 10 may not be valid if the same defect size is measured at year 2.  $d_{lim}$  is determined by the following criterion:

If an inspection is planned at  $t_1$ ,  $d_{lim}$  is evaluated as

$$d_{lim}(t_1) = \max d_R(t_1), \quad \text{s.t.} \quad P(F(t_2) \cap \bar{I}_S) \gg P(F(t_2) \cap I_S) \quad (5-14)$$

where  $t_2$  is the time of the next inspection or the end of service life.  $I_S$  is the event of indication of the largest corrosion defect. The inequality constraint in Equation (5-14) demands that  $p_F$  at time  $t_2$  due to a measured defect is much smaller than  $p_F$  due to a defect that has not been indicated at  $t_1$ <sup>a</sup>.  $d_{lim}$  is thus dependent on  $t_2$  and consequently also on the inspection plan (defined by the threshold  $\Delta p_F^T$ ) and the service life time  $T_{SL}$ . Because the repair decision is made based on the measured (and not on the actual) corrosion depth,  $d_{lim}$  is additionally dependent on the accuracy of the measurement.

---

<sup>a</sup> The two sides of the inequality correspond to the two additive terms in Equation (4-35).

Generic inspection plans can be calculated based on  $d_{lim}$ . The inspection plans are valid as long as  $d_m(t) < d_{lim}(t)$ . Although inspection plans with  $d_R = d_{lim}$  are not inevitably cost optimal, it is believed that the optimal  $d_R$  is in most cases close to  $d_{lim}$ . This follows from the fact that for  $d_R < d_{lim}$  the required repair effort increases without changing the required inspection efforts significantly. For  $d_R > d_{lim}$  repairs are not performed in situations where the probability of failure is high; additional inspections are then needed. This hypothesis is also supported by the results of the numerical investigations, presented later in Section 5.6.2.2.

Although the total expected cost of an inspection strategy can be evaluated by assuming that the hot spot is repaired given that  $d_m \leq d_R$ , this may not always be the optimal solution. Instead of repairing, an alternative is to adopt the inspection plan to the actual measurement. This is discussed in Section 5.6.3.

### 5.6.1.2 Corrosion model

It is noted that the example presented in the following is of an illustrative character. The applied model, which was originally developed for design purposes, must be reviewed before a real application can be advocated. Especially the aspects of temporal and spatial variability are treated in a highly simplified manner, yet the model reflects the current state of the art in corrosion reliability modelling.

The deWaards-Milliams model is the most common model for carbonic acid corrosion (CO<sub>2</sub> corrosion) in pipelines. A short overview is presented in Section 3.5.3.2; it is originally published in deWaard and Milliams (1975) with modifications in deWaard et al. (1991, 1995). A simplified version of this model is applied here, in accordance with CRIS (2004). It predicts a constant corrosion rate based on the main influencing parameters operating temperature  $T_o$  and pressure  $P_o$ , as well as the partial pressure of CO<sub>2</sub>,  $P_{CO_2}$ . Other influencing parameters, such as the flow rate or the pH are not explicitly accounted for. The corrosion rate  $r_{CO_2}$  is

$$r_{CO_2} = 10^{(5.8-1710/T_o+0.67 \cdot \log_{10} f_{CO_2})} \quad (5-15)$$

Where the temperature  $T_o$  is expressed in [K] and the CO<sub>2</sub> fugacity  $f_{CO_2}$  is calculated from

$$f_{CO_2} = P_{CO_2} \cdot 10^{P_o(0.0031-1.4/T_o)} \quad (5-16)$$

The partial pressure of CO<sub>2</sub> is a function of the operating pressure and the fraction of CO<sub>2</sub> in the gas phase,  $n_{CO_2}$ :

$$P_{CO_2} = n_{CO_2} P_o \quad (5-17)$$

The calculation of the corrosion depth at time  $t$  includes a model uncertainty, which is, following Sydberger et al. (1995), described by a multiplicative factor  $X_M$ :

$$d_c(t) = X_M r_{CO_2} t \quad (5-18)$$

CO<sub>2</sub> corrosion is typically of a localised nature. The spatial characteristics of the deterioration are thus of importance, however, the model only predicts the maximum defect in a pipe



element (hot spot), yet the size of these hot spots is not stated in the references. Simplifying, it is assumed that the reference size for the model is the same as for the inspection models, i.e. the individual hot spots are pipe elements with length 2-3m and diameters 110-220mm.

The considered failure mode is leakage, i.e. the failure event occurs when the corrosion depth  $d_c(t)$  exceeds the wall thickness of the pipe,  $d$ . The extension of the model to the bursting failure mode is straightforward, in accordance with Section 3.5.6. Note that for most applications the uncertainty related to the failure mechanism is smaller than the uncertainty on the corrosion process.

### 5.6.1.3 Generic parameters

The following generic parameters with respective ranges are proposed for the example:

- Wall thickness:  $d = 15 - 50\text{mm}$
- Temperature:  $E[T_o] = 20 - 80^\circ\text{C}$ ,  $CoV_{T_o} = 0.05 - 0.30$
- Operating pressure:  $E[P_o] = 50 - 200\text{ bar}$

$d$  enters the limit state function, Equation (3-13),  $T_o$  and  $P_o$  are parameters of the corrosion model.

### 5.6.1.4 Inspection modelling

The inspection model (with parameters  $\alpha_D$ ,  $\beta_D$  and  $\varepsilon_m$ ) is provided in Section 4.7.1. As stated there, it is valid for pipelines with a wall thickness  $d$  of maximal 15mm; its validity for thicker pipelines is not ensured. The application of this model to situations with  $d > 15\text{mm}$  is thus purely illustrative.

### 5.6.1.5 Model parameters

The full set of parameters is summarised in Table 5.8.

*Table 5.8 – Parameters of the CO<sub>2</sub> corrosion model and the corresponding inspection model.*

Parameter	Dimension	Mean	Standard dev.	Distribution type
$T_{SL}$	yr	30	-	Deterministic
$d$	mm	5 – 50	0.05 $d$	Normal
$T_o^*$	°C	20 – 80	1.5 - 9	Normal
$P_o$	bar	50 – 200	0.1 $\mu_{P_o}$	Normal
$n_{CO_2}$	-	0.01	-	Deterministic
$X_M$	-	0.4	0.32	Weibull
$\varepsilon_m$	mm	0	0.8	Normal
$\alpha_D$	-	-1.07	0.73	Normal
$\beta_D$	-	2.571	0.82	Normal
$\alpha_D$ and $\beta_D$ are correlated with factor $\rho_{\alpha_D\beta_D} = -0.94$				

\* Although the temperature is here provided in [°C] it enters the corrosion model in [K].

A reference case (in analogy to the investigation for fatigue subjected structures) is introduced with the following values of the generic parameters:

- Wall thickness:  $d = 30\text{mm}$
- Temperature:  $\mu_{T_o} = 30^\circ\text{C}$ ,  $CoV_{T_o} = 0.1$
- Operating pressure:  $E[P_o] = 100\text{ bar}$

### 5.6.1.6 Cost model

The observations made for the cost model of fatigue subjected structures (Section 5.5.5) are valid also here. For the numerical investigations the following model is applied:

$$C_F = 1, C_{Insp} = 0.02, C_R = 0.1, r = 0.05$$

Note that the ratio of repair to failure cost as well as the ratio of inspection to failure cost is smaller than in the cost model for the fatigue case.

## 5.6.2 Example results

### 5.6.2.1 Reference case

$d_{lim}$  calculated for the reference case according to Equation (5-14) is shown in Figure 5.31. As noted previously, it is a function of the inspection time, but also of the inspection strategy (here defined by the threshold  $\Delta p_F^T$ ). The resulting  $d_{lim}$ 's reflect the linear corrosion model with time-invariant parameters.

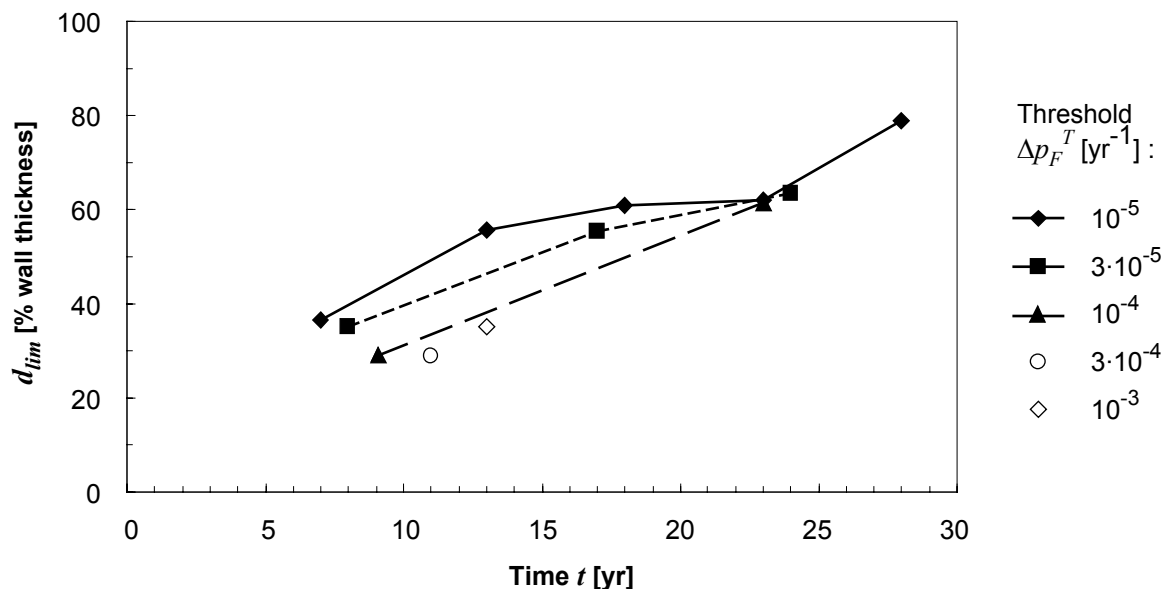


Figure 5.31 -  $d_{lim}$  as a function of time for the reference case.

All results for the reference case are summarised in Table 5.9 and Figure 5.32.

Table 5.9 – Results for the corrosion reference case – inspection times.

Threshold [yr <sup>-1</sup> ]	# inspections	Years of inspection					
10 <sup>-2</sup>	0	-					
10 <sup>-3</sup>	1	13					
3·10 <sup>-4</sup>	1	11					
10 <sup>-4</sup>	2	9	23				
3·10 <sup>-5</sup>	3	8	17	24			
10 <sup>-5</sup>	5	7	13	18	23	28	

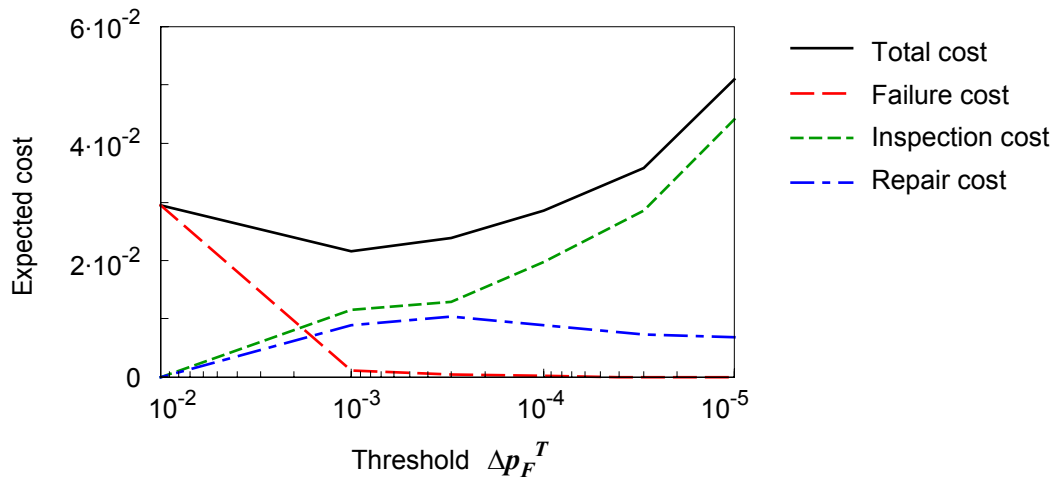
Figure 5.32 – Expected cost for the CO<sub>2</sub> corrosion reference case.

Figure 5.32 shows that the expected cost of repair decreases with increasing inspection effort and decreasing threshold  $\Delta p_F^T$ . The explanation for this phenomenon is the variable value of the repair criterion  $d_R = d_{lim}$  depending on the threshold, in accordance with Figure 5.31. The fewer inspections required for higher thresholds must be compensated with more stringent repair criteria. These lead to additional (unnecessary) repairs or to earlier repair actions (repairs that could be performed at a later time are already performed at an earlier time because no inspection is foreseen later).

### 5.6.2.2 Comparing different repair criteria

The proposed approach, namely using  $d_{lim}$  as the (variable) repair criterion, is compared with the use of a constant repair criterion  $d_R$ , as suggested in previous publications (see Section 2.6 for references). It is pointed out that for the application in a generic approach to RBI the use of a constant  $d_R$  is not consistent as previously discussed, yet the calculation of total expected cost using  $d_R$  is still possible before any inspection results are available. Table 5.10 presents the resulting inspection times as a function of  $d_R$  for  $\Delta p_F^T = 10^{-5}$ .

Table 5.10 – Inspection times for the corrosion reference case for different  $d_R$  threshold  
 $\Delta p_F^T = 10^{-4} \text{ yr}^{-1}$ .

Repair criteria $d_R$	Years of inspection					
$d_R = d_{lim}$	9	23				
10%	9	22				
20%	9	23				
30%	9	23				
40%	9	19				
50%	9	16	26			
70%	9	12	15	19	23	28

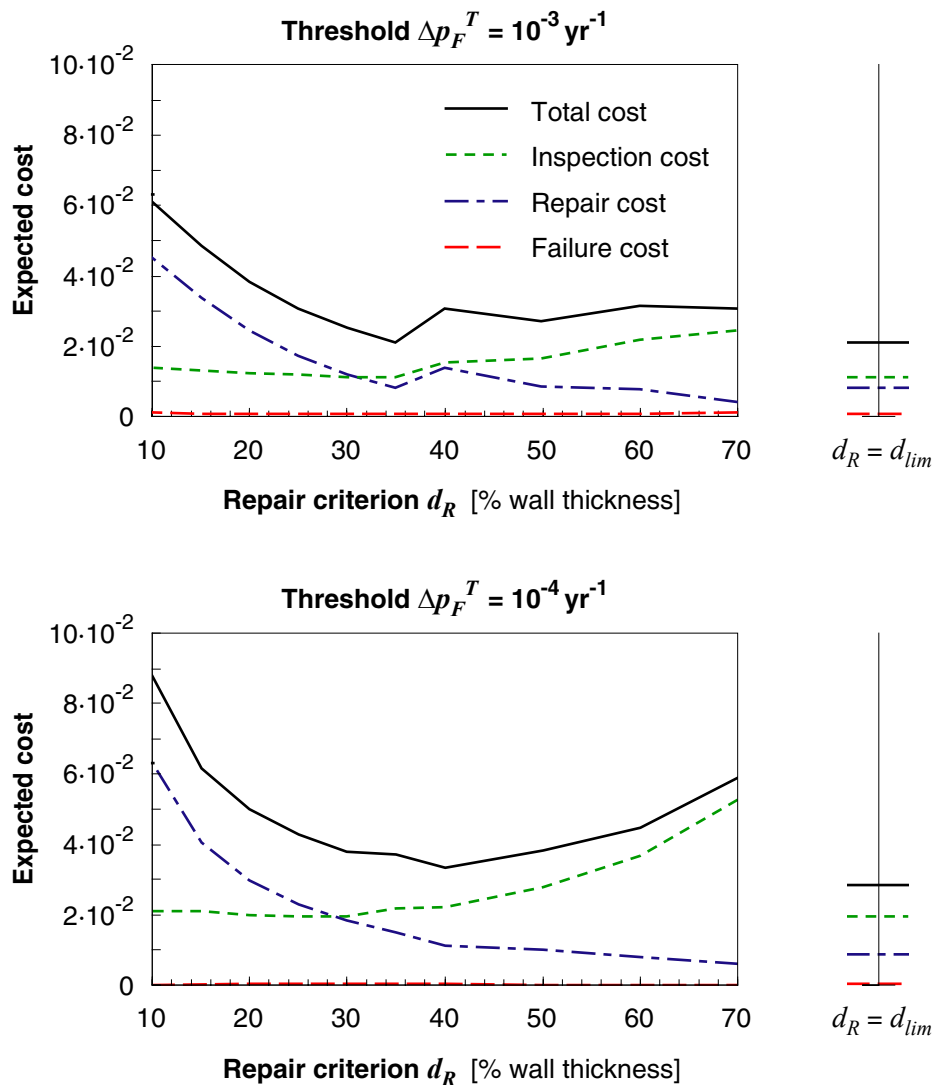


Figure 5.33 – Expected cost for different repair criteria (reference case).

Figure 5.33 shows the expected cost as a function of the repair criterion. For both illustrated thresholds the proposed approach, using  $d_R = d_{lim}$ , is cost optimal. Because for  $\Delta p_F^T = 10^{-3}$  only one inspection is required, the  $d_{lim}$  criterion is equivalent to a constant  $d_R = 0.35d$ . For  $\Delta p_F^T = 10^{-4}$  several inspections are required and the  $d_{lim}$  strategy is advantageous because it allows for a larger  $d_R$  at the second inspection as compared to  $d_R$  at the first inspection.

### 5.6.2.3 Results of the sensitivity analysis

The inspection plans resulting as a function of the generic parameters are analysed in analogy to the parameters in the generic approach for fatigue subjected structures. When comparing results to those from the fatigue example it should be borne in mind that in the model presented here no equivalent to the *FDF* exists. In the fatigue example the *FDF* was kept fixed; when changing other parameters such as the thickness of the hot spot, this was compensated by a change of the stress range model (the parameter  $k_{\Delta S}$ ). No such factor exists for the corrosion model, which entails that some of the combinations presented here may well be unrealistic: If the mean operating temperature in the system is increased from 30°C to 80°C then also the design (the wall thickness) would most probably be altered.

Because the applied example for corrosion has only illustrative character, the presentation of the results is limited to the most important aspects, with the aim of demonstrating the capabilities of the generic approach to RBI for corrosion subjected structures.

Figure 5.34 illustrates that for the considered model the required inspection times are approximately a linear function of the wall thickness:

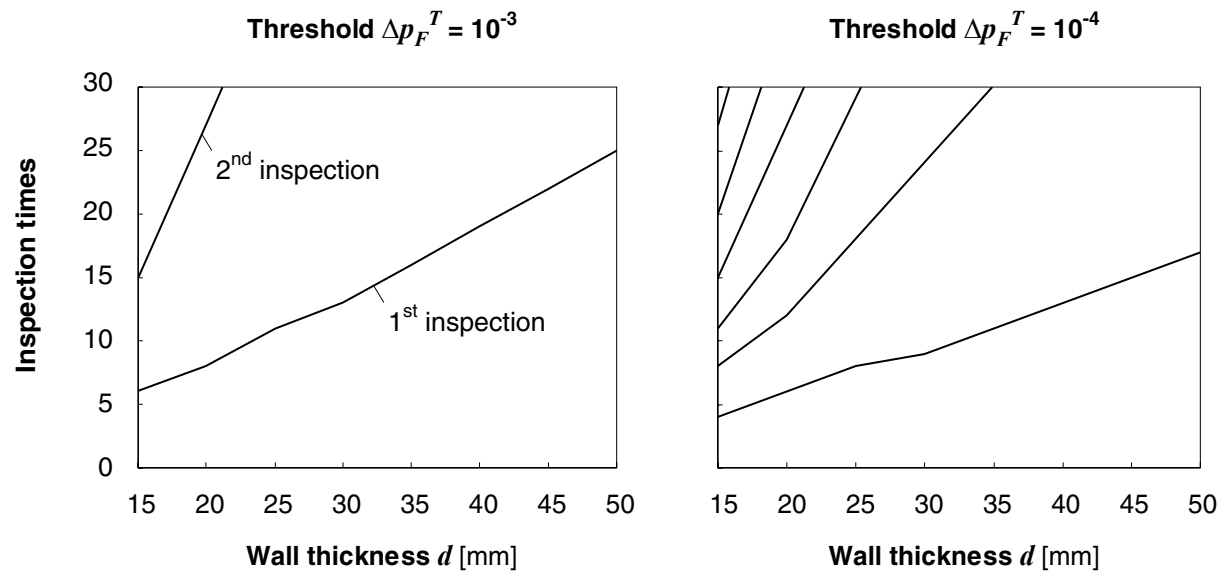


Figure 5.34 – Inspection times as a function of the wall thickness  $d$ .

Figure 5.35 presents the inspection times as a function of the mean operating temperature. The results reflect the large influence of the temperature on the corrosion progress.

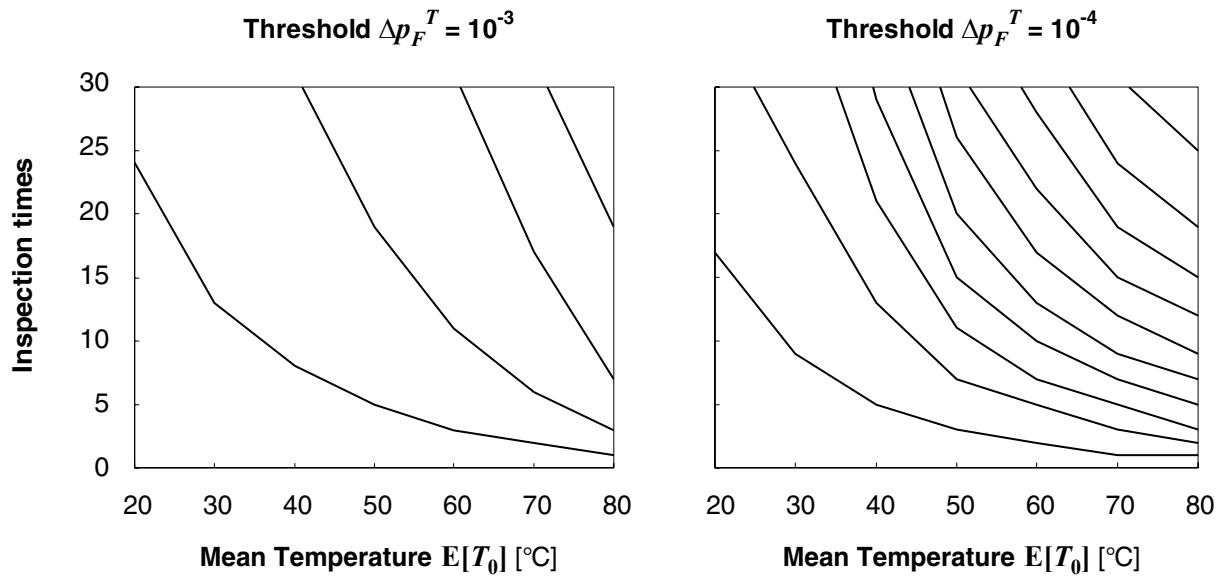


Figure 5.35 – Inspection times as a function of the mean gas temperature in the pipeline.

The scatter in the operating temperature, as expressed by  $\sigma_{T_0}$ , has only a small influence on the reliability and consequently also on the required inspection effort, which is shown in Figure 5.36.

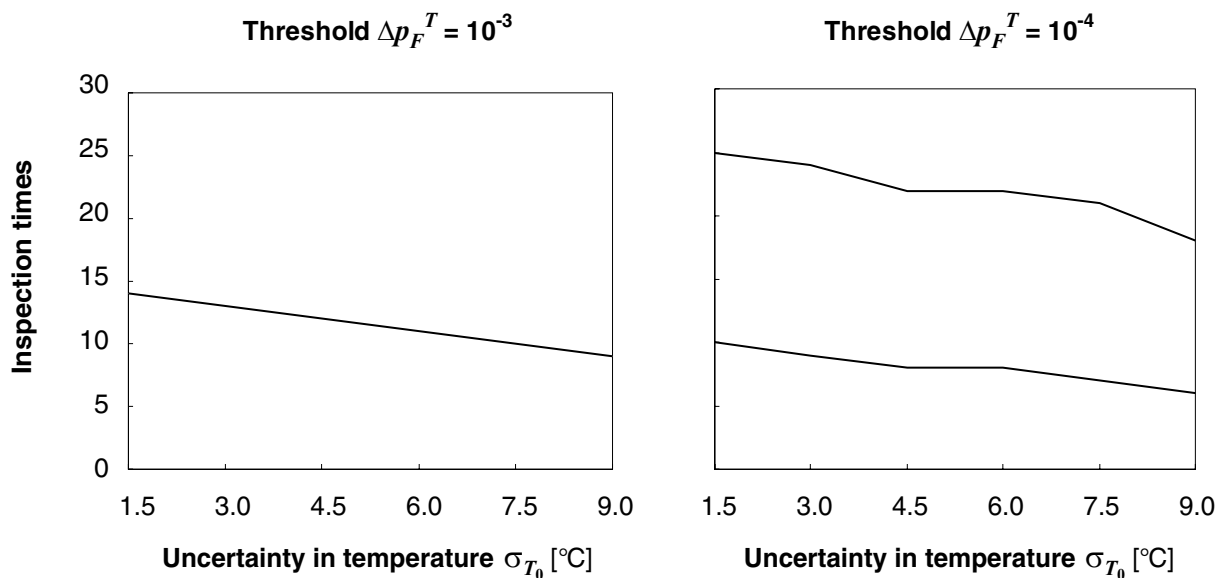


Figure 5.36 – Inspection times as a function of the standard deviation of the gas temperature.

The operating pressure has a substantial influence on the corrosion rate, which is reflected in Figure 5.37. Furthermore, the influence of this variable would increase if bursting failure were taken into account, especially for high values of  $P_o$ .

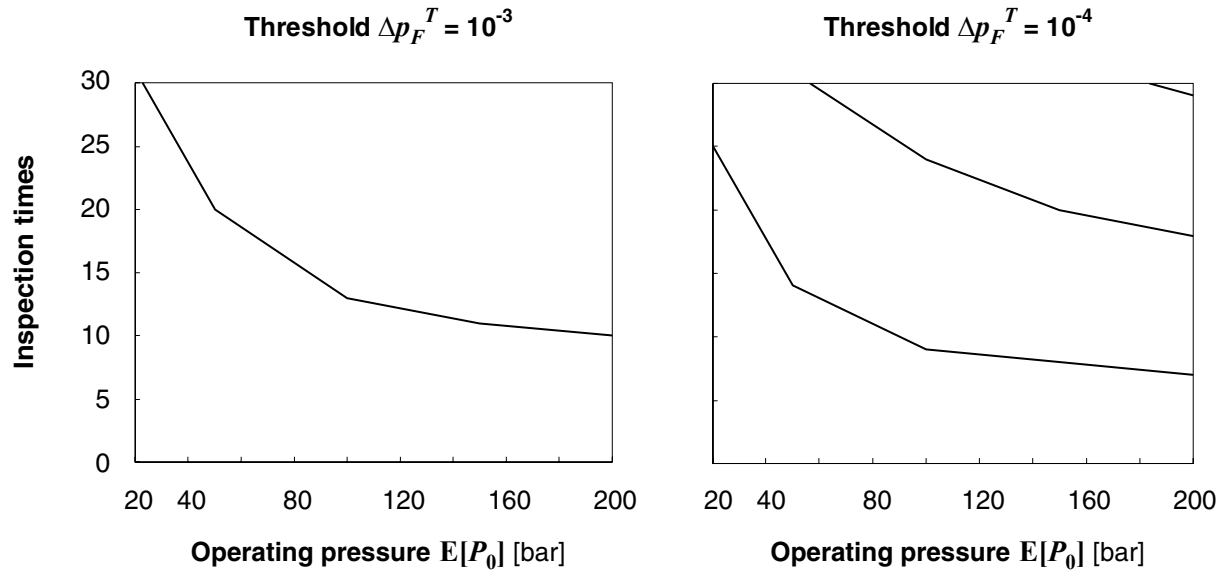


Figure 5.37 – Inspection times as a function of the mean operating pressure.

Figure 5.38 presents the influence of the different parameter values on the expected costs for the reference case. Only the results for the threshold  $\Delta p_F^T = 10^{-3} \text{ yr}^{-1}$  are included as this is for most cases the optimal strategy with the given cost model.

For the considered model the mean temperature is the most influencing parameter with respect to the expected costs, followed by the wall thickness and the operating pressure  $P_o$ . For low  $P_o$ , the predicted corrosion rate, and consequently the expected cost, are close to zero. In the present model the influence of the operating pressure depends strongly on the fraction of  $\text{CO}_2$  in the gas phase. In practice this parameter may also be subject to fluctuations and uncertainties which should be taken into account.

For any existing pressure vessel or pipeline, the design and the operating conditions are fixed<sup>a</sup>. At the design stage, however, the wall thickness can be chosen and sensitivity analysis as shown in Figure 5.38 may be used for the optimisation of the wall thickness with respect to the expected total life cycle cost.

<sup>a</sup> The operating parameters are in general not altered to influence the corrosion behaviour.

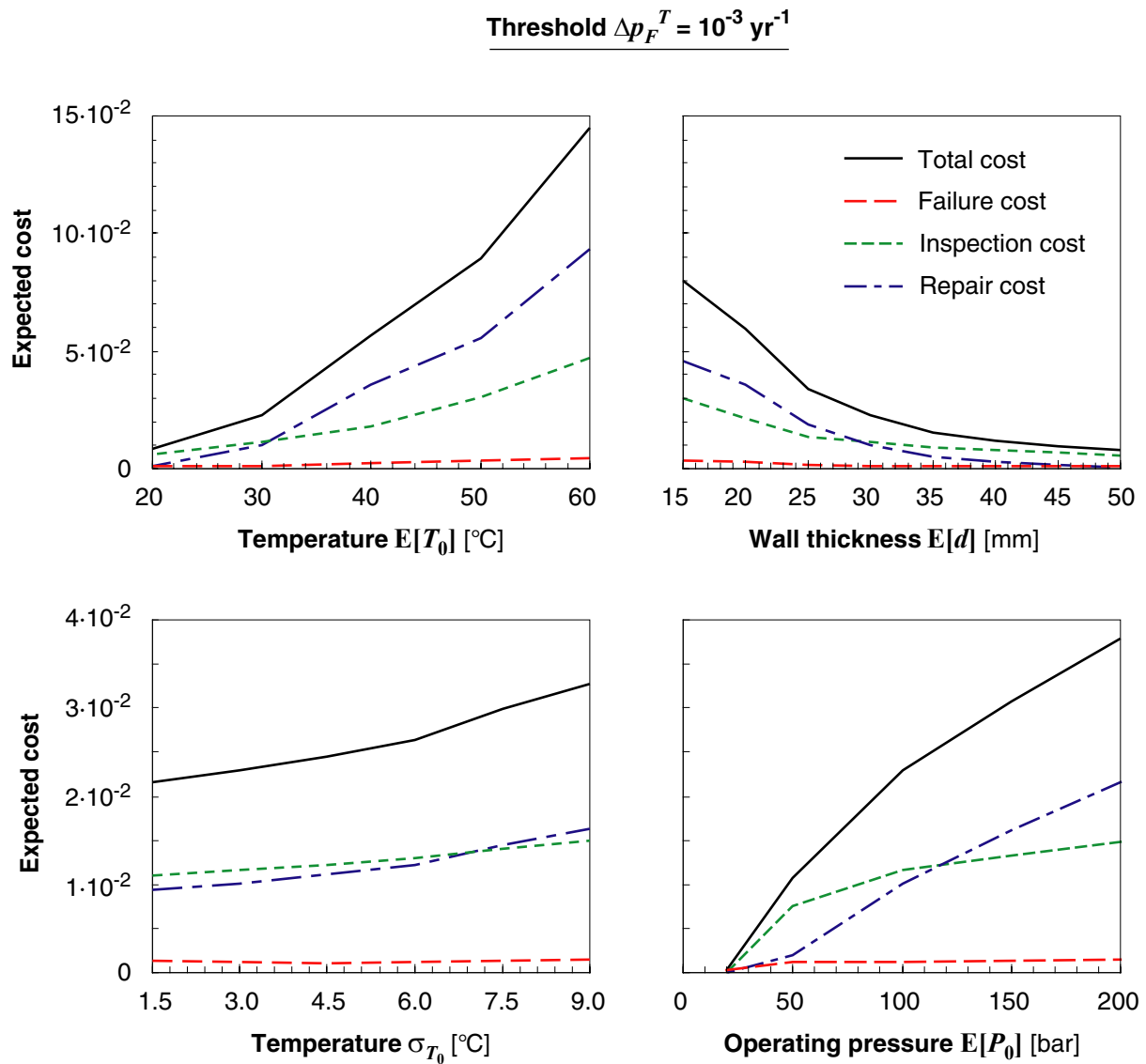


Figure 5.38 – Expected cost for the threshold  $\Delta p_F^T = 10^{-3}$  as a function of the different design and operating parameters.

### 5.6.3 Actualisation of inspection plans

The resulting inspection plans are based on the assumption that all defects measured at inspections are smaller than  $d_R = d_{im}$ . As long as this assumption is fulfilled, the inspection plans are valid without any further actions; otherwise the validity of the inspection plans necessitates a repair. However, for small  $d_R$  repairing may not always be the optimal action to take; instead it could be more economical to leave the hot spot in service and to account for the observed  $d_m$  with increased inspection effort. This inspection effort must be determined by a tailor-made inspection plan. Consequently, if a defect larger than  $d_R$  is measured, a reassessment is required to decide on the optimal action, which may also include additional measures such as monitoring certain model parameters like the temperature  $T_o$ .



Given that the parameters of the model (e.g. temperature) are constant or stationary with renewal frequencies much larger than the inspection frequency, and given that no additional information on these variables is available during the service life, the procedure follows the one described for fatigue subjected hot spots. It is illustrated in Figure 5.39.

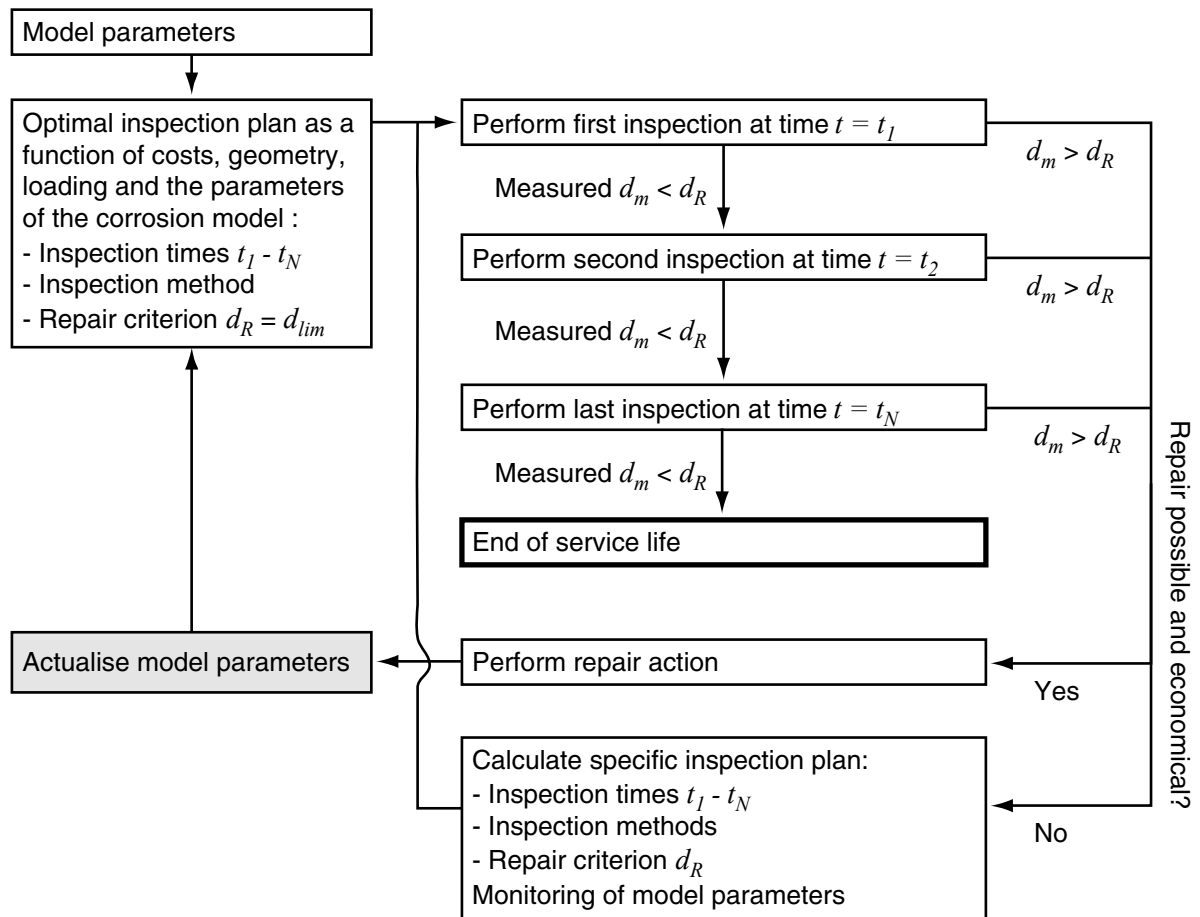


Figure 5.39 – Actualisation of inspection plans for corrosion if no additional information on the influencing parameters is available.

In situations where it is possible to monitor parameters of the corrosion model, this additional information must be included in the inspection planning procedure. For this purpose, the service life is divided into periods (yearly or shorter intervals). At the beginning of each period, the model parameters are updated by consideration of the past measurements of these parameters. Because the inspection plans are based on the assumption of time-invariant parameters, equivalent values must be computed from the observed time-series. These are the parameter values that lead to the same deterioration as the process describing the real behaviour of the parameters, in accordance with the equivalent stress range  $\Delta S_e$  for the description of fatigue stress range process<sup>a</sup>. The derivation of such an equivalent value is

<sup>a</sup> Such equivalent values must also be used for the situations where no monitoring is possible and where the parameters are described by a stationary process, see Figure 5.39.

illustrated in Figure 5.40 for the operating temperature  $T_o$ . Note that the equivalent temperature is not the mean value, but corresponds to the non-linear influence of  $T_o$  described by Equation (5-15) and (5-16).

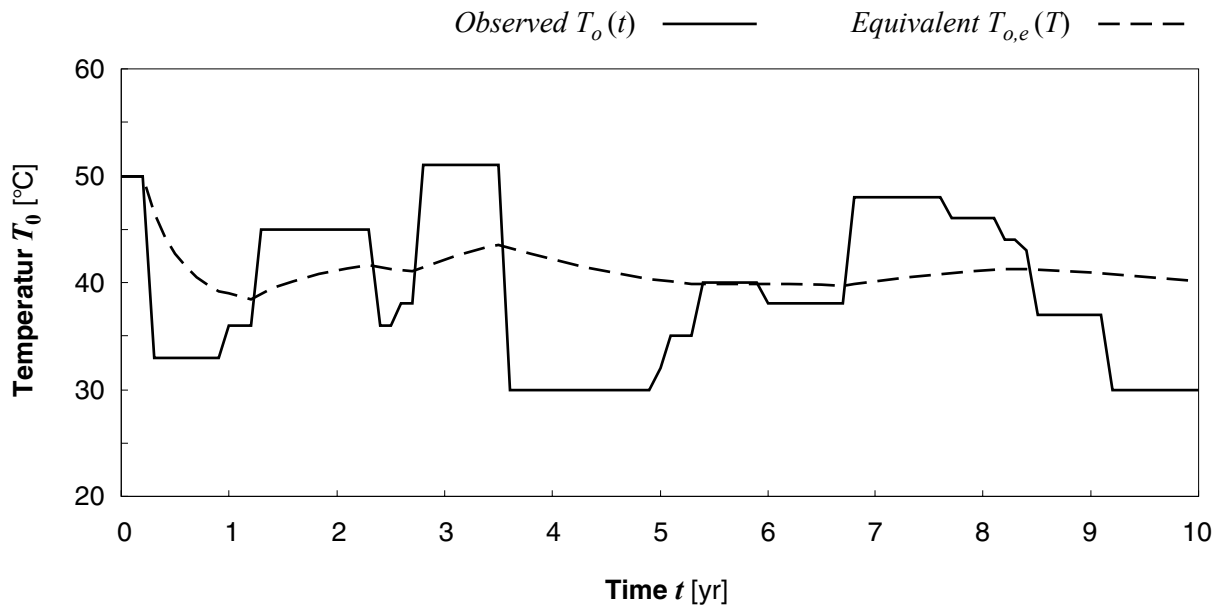


Figure 5.40 – Illustration of the equivalent temperature as a function of time.

Based on the updated equivalent values of the parameters of the corrosion model, the inspection plan is obtained from the generic database. This inspection plan is adjusted to take into account the previously performed inspections. The inspection plan then allows determining whether an inspection is to be performed in the present period. If not, the procedure is repeated for the next period. If an inspection is performed, no action is taken as long as the measured corrosion defect size  $d_m$  does not exceed the repair criterion  $d_R = d_{lim}$ . If  $d_m$  is larger than  $d_R$ , it must be decided whether the hot spot should be repaired or not. If a repair is performed, the parameters of the model must be changed accordingly; the procedure then continues with inspection plans based on the actualised parameters. If no repair is performed, alternative mitigation actions must be taken, such as the establishment of a tailor-made inspection plan. The procedure is illustrated in Figure 5.41.

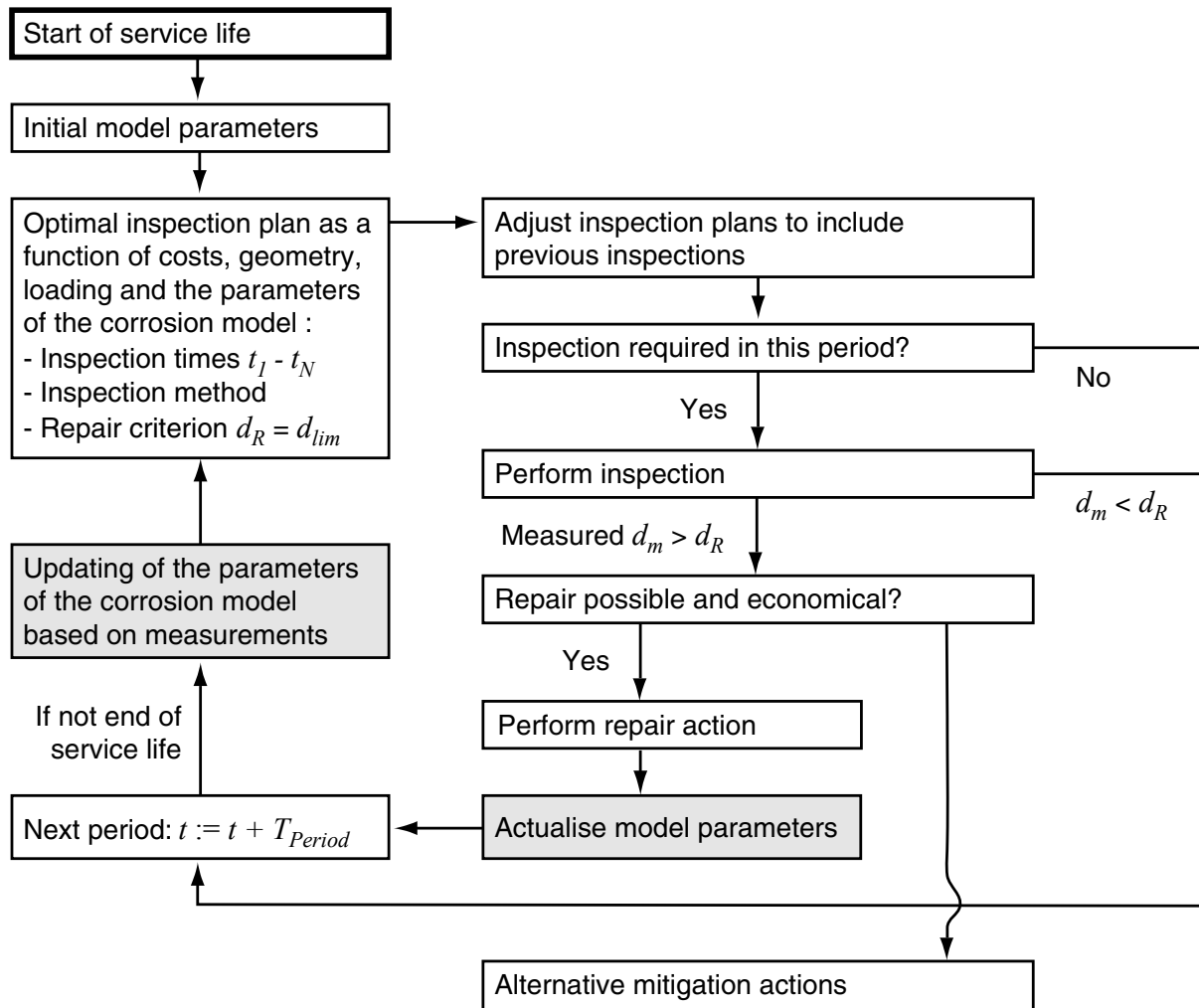


Figure 5.41 – Actualisation procedure for the inspection planning of corrosion subjected structures when influence parameters are monitored.

#### 5.6.4 Conclusions on the generic approach to RBI for corrosion subjected structures

The presented example demonstrates the suitability of a generic approach to RBI for corrosion subjected structures in analogy to the approach for fatigue subjected structures. An additional advantage of the generic approach for corrosion risk management is that the inspection plans can be continuously actualised when new information on the influencing parameters is available. Examples of such information are e.g. the continuous measurements of the operating temperature and pressure.

In the example, the temporal characteristics are treated in a highly simplified manner, by considering all variables as time-invariant. As a consequence, the corrosion rate is modelled as being constant with time. This approach is appropriate when the influencing variables are either constant or stationary with large renewal frequencies (as compared to the inspection frequency). For the latter case, the input parameters to the model can be determined as

equivalent values. However, because the model involves several parameters that are processes of time, the computation of such equivalent values requires knowledge on the joint characteristics of these processes. The problem is thus more complicated than indicated by Figure 5.40 and requires further elaboration before practical applications can be envisaged. When the processes are not stationary the generic approach can still be useful, because many of the influencing processes can be measured, such as the operating temperature and pressure. The actual equivalent values representative for the past can then be evaluated directly from the measurements. These values, which are continuously actualised, may then be applied as input parameters to the inspection planning. This is discussed in Section 5.6.3.

The spatial characteristics of the problem were excluded in the presented example, where only one hot spot is considered which is fully inspected and described by the distribution of the largest defect. A real structural system generally consists of a number of such single hot spots, whose corrosion characteristics are inter-dependent. Such a structural system can be represented by the model introduced in Section 3.5.3.4. The determination of how many and which hot spots to inspect must be performed by considering system effects as introduced in Chapter 6.

## **6 Risk based inspection planning for structural systems**

### **6.1 Introduction**

In the previous chapters, risk based inspection planning (RBI) is presented for individual hot spots. Hot spots are defined in Section 5.2 and correspond to the critical locations in the structure with respect to the risk related to the considered deterioration mechanism. In line with this model, a structural system is for the purpose of inspection and maintenance planning represented by a system consisting of hot spots and their interrelations. The different types of interrelations between the individual hot spots in the system are outlined in Section 6.2. In Straub and Faber (2002a) it is shown that an optimal inspection strategy for the system can only be identified by consideration of the interrelations between the hot spots. Section 6.3 identifies the relevant decision problems for the inspection planning for structural systems. The following two sections overview new approaches as introduced in Straub and Faber (2002a and b) to an optimisation of the inspection efforts based on consideration of both the interrelations in the systems and the involved decision problems. The concluding section aims at providing guidelines to the integration of the theoretically sound procedures in practical approaches which are applicable to industrial purposes.

The effect of stochastic dependencies in the deterioration model from one hot spot to another is investigated in some studies, including Moan and Song (1998), Cramer and Friis-Hansen (1994), Faber and Sørensen (1999) and Lotsberg et al. (1999). These studies, however, do not attempt to include these effects in the decision modelling, possibly due to the practical difficulties involved in such procedures. Although its importance is pointed out by many authors, a procedure aiming at the integral consideration of the entire system in RBI is attempted in only few studies, e.g. Faber et al. (1992a). These approaches are based on an informal decision analysis where the number of considered hot spots is systematically reduced. Unfortunately, as noted in Faber and Sørensen (1999), they have not been demonstrated to be practical, mainly due to numerical effort and stability. As demonstrated in this chapter, the generic approach to RBI offers new possibilities to overcome these difficulties.

### **6.2 System effects in RBI**

#### **6.2.1 Types of dependencies between hot spots**

The system is defined by the individual hot spots and their interrelations (the stochastic and functional inter-dependencies). In the previous chapters the considerations are limited to the individual hot spots, which are related to the system by means of the cost model; the cost of failure of the hot spot is commonly expressed as a function of the importance of the hot spot for the system. In Chapter 7 this hot spot importance is furthermore used to derive the

acceptance criteria for the individual hot spots. However, this does neglect the functional and stochastic dependencies between the hot spots themselves, as illustrated in Figure 6.1.

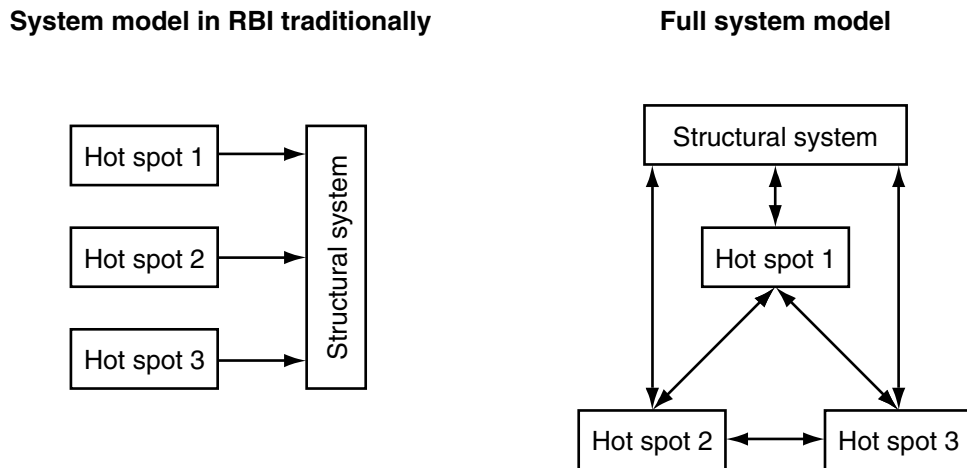


Figure 6.1 – System model traditionally assumed vs. full system model.

As discussed later, some of the interrelations depicted on the right-hand side of Figure 6.1 can be neglected for specific applications. Note that the traditional RBI model presented in the earlier chapters is a special case of the full model and is thus (implicitly) based on neglecting most of the interrelations in the system. In the following the different types of interrelations are introduced; these definitions facilitate an overview on the system effects in RBI.

### 6.2.1.1 Dependencies in deterioration performances between hot spots

The deterioration performance at the individual hot spots in a system is often inter-dependent. If the deterioration at the hot spot  $i$  is described by the marginal distribution of the size of the largest defect  $S_i$ , then the dependency between the deterioration can be expressed by a joint distribution of all  $S_i$ . Such a model is presented in Section 3.5.3.4, where it is assumed that the dependency is described with sufficient accuracy by the covariance matrix  $V_{SS}$ .

The stochastic dependency is caused by common influencing factors within the system. For fatigue, entire groups of hot spots are generally subject to the same realisation of the load process. The fatigue loading at these hot spots is therefore highly dependent given that no observations of this process are available<sup>a</sup>. Additionally, the weld quality may be similar within one production lot, introducing a correlation between the individual initial defect sizes and between the individual SN fatigue resistances. For corrosion subjected steel structures, the environmental conditions, like temperature, are often the same or highly dependent between different hot spots in the system.

<sup>a</sup> When observations are available, then the common influencing variable becomes deterministic or its uncertainty is reduced to the extent where it is only of minor importance. This variable can thus be explicitly addressed and then only represents a functional dependency but no stochastic dependency.

For steel structures, only few published studies are concerned with the modelling of such dependencies; e.g. in Vrouwenvelder (2004) the dependency in the weld quality from one hot spot to the next is estimated by comparing the scatter in fatigue performance within one production series to the scatter in a general group of hot spots represented by the same SN curve. Mathisen and Larsen (2002) estimates the stochastic dependency between the fatigue performances in individual segments in a mooring chain based on engineering judgement. For corrosion of steel structures, the author is not aware of any publications dealing with large-scale spatial dependencies of the corrosion process (i.e. dependencies between individual hot spots and not within one hot spot). For most applications it is therefore required to estimate the degree of dependency between the influencing factors at the different hot spots. Based on these estimates, the dependency between the deterioration performances at the hot spots is calculated.

### 6.2.1.2 Dependency of failure consequences on the state of the system

In the RBI procedures presented in the previous chapters it is assumed that the consequence of hot spot failure can be modelled by a fixed cost  $C_F$ . This cost accounts for the conditional probability of collapse of the structure given hot spot failure,  $P(COL|F)^a$ . However, this probability depends also on the state of the remaining hot spots. In other words, the probability of structural collapse given failure of  $i$  hot spots does generally not increase linearly with  $i$ ; to not account for this relationship explicitly is thus non-conservative. These dependencies are discussed in Section 7.3.2; it is found that these effects in general cannot be considered explicitly, because accounting for all possible combinations of hot spot failures is not feasible. It is thus suggested that crude inspections, which allow the identification (and subsequent repair) of failed hot spots, are performed in regular intervals for all hot spots. In this case the assumption of independent occurrences of failure events is valid and the probability of two failures coinciding is thus relatively small for hot spots with a high reliability; see Section 7.3.2 for further discussion.

### 6.2.1.3 Dependency of inspection costs on the number of inspected hot spots

The marginal cost of inspection of the  $i^{\text{th}}$  hot spot is generally not independent on the total number of inspected hot spots. For many structures, the inspection costs consist to a large extent of fixed components, such as the cost of accessing the hot spots or the cost of temporary disuse of the structure, and only a minor part of the costs is variable. The cost of inspection of the individual hot spot,  $C_{Insp}$ , must thus be evaluated by considering the total number of inspections, which will favour the grouping of inspections into inspection campaigns. When performing RBI for individual hot spots this aspect is generally taken into account in a second phase: Once the individually optimal inspection plans are evaluated, inspections times are adjusted in order to profit from reduced marginal inspection costs.

---

<sup>a</sup> This indicator for the redundancy of the structure is derived later in Chapter 7.

#### 6.2.1.4 Dependency between the inspection performance at different hot spots

The inspection performance is generally not independent from one hot spot to the next, due to common influencing factors, such as the inspector characteristics or environmental conditions. This is treated in Section 4.6 and it is concluded that for most structures these effects can be neglected.

### 6.2.2 Inference from inspection results at other hot spots

An important effect of the dependencies between the inspection performances at different hot spots is that the outcome of an inspection at one hot spot contains information about the state of the other hot spots. For systems with large numbers of hot spots, this is of utmost importance, because this allows basing the maintenance decisions on a set of “sample inspections”. Considering offshore structures, it is noted in Banon et al. (1994) that full inspection coverage of the deterioration sensitive parts is not a realistic assumption. The same holds for most large engineering structures, especially for those where in principle all spots are hot, such as pipelines or most large concrete structures. In practice, for these kinds of structures, NDE is applied to only a few hot spots because full inspection coverage would not be economical. However, it is only by consideration of the degree of dependency between the deterioration at different hot spots that this optimal coverage can be assessed. This is the subject of the following section.

## 6.3 RBI for systems

This section introduces the general decision-theoretic problems when inspection planning of structural systems is envisaged. As discussed in Straub (2003), there are two fundamentally different types of structural systems in regard to the underlying decision model: The first type are structural systems where mitigation actions, such as repair or replacement, are performed only for the entire system, the second type are those where the mitigation actions are carried out only for a selection of hot spots, based on knowledge of the condition of the individual hot spots. These two situations are considered separately in the following.

### 6.3.1.1 Common mitigation actions

In structural systems consisting of hot spots subject to identical conditions and for which preventive and corrective maintenance actions are the same for all hot spots, the decision on repairing all hot spots is taken when a certain percentage of the hot spots have reached an unacceptable state<sup>a</sup>. For such systems, the inspection and maintenance planning problem is equivalent to a quality control problem. For time invariant problems the optimisation of the inspect effort is straightforward and can be performed according to the classical references, e.g. Ang and Tang (1975). The relevant question is how many hot spots to inspect (the

---

<sup>a</sup> Concrete structures subject to corrosion of the reinforcement often fall into this category.



optimal inspection coverage). Wall and Wedgwood (1998) apply this approach in a simplified manner to the determination of the cost optimal inspection coverage.

Considering deteriorating systems, Faber and Sørensen (2002) extend the classical solution and introduce so-called condition indicators. The indicators (inspection results) give information about the condition of the overall structure at different points in time. By evaluating this information at different times and for different inspection coverage, the optimal number and time of inspections can be assessed. It is in principle possible to represent this problem by a decision tree similar to those presented in Figures 2.7 and 2.8. The two mitigation actions considered in these trees, namely “no action” and “repair of the hot spot”, can be directly adopted when the second is changed to “repair of all hot spots in the system”. The optimisation is, however, more complex, because the number of hot spots to inspect is an additional parameter which must be considered together with the inspection times.

The solution of such problems requires that the general optimisation problem is constrained, in analogy to the threshold approach for single hot spots, in order to be computationally feasible. A possible solution is to fix the percentage of hot spots which are inspected and then to determine the inspection times using the threshold approach. By doing this for different percentages of hot spots inspected, the optimal inspection coverage can be identified. This is only an approximation to the optimal solution, because the number of hot spots inspected can in principle vary from one inspection to the next. For practical applications it should be envisaged to solve the problem through a generic approach.

RBI for systems with common mitigation actions is not considered further because it is less relevant for steel structures. Most steel structures have large reliabilities against deterioration failures; the replacement of entire systems or sub-systems because of the risk related to deterioration is thus seldom economical.

### 6.3.1.2 Individual mitigation actions: Adaptive strategies

In many structural systems, hot spots are only repaired after a previous indication of a defect, i.e. the decision on repair is not made for a group but only for individual hot spots; fatigue subjected joints generally fall into this category. The inspection outcome of a hot spot has thus no direct bearing on the repair decisions for other hot spots. For illustrational purposes consider a simple system with two dependent hot spots A and B, where A is inspected. Even when a large defect is indicated at A will B not be repaired unless a defect is indicated at B itself. A reasonable strategy is thus to inspect A and to decide on an inspection of B based on the outcome of the first inspection. In Straub and Faber (2002a) such approaches to inspection planning are denoted adaptive strategies, because the inspection plan for a specific hot spot is adapted to the inspection outcomes at other locations. As demonstrated in Straub and Faber (2002a), system effects can only be accounted for by applying such adaptive inspection planning procedures.

Figure 6.2 shows a simple adaptive decision model, where the classical decision tree from Bayesian preposterior decision analysis, Figure 2.5, is extended by including a second decision rule  $d_2$ . This decision rule determines the additional inspections  $e_2$  to be performed, based on the outcome of the first inspections,  $z$ . The repair decision is given by the decision rule  $d$ , based on the outcome of all inspections.

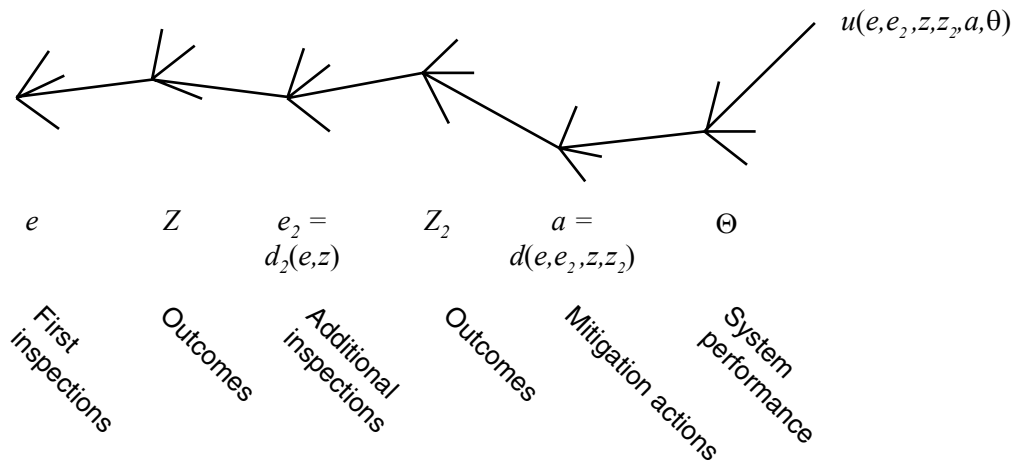


Figure 6.2 – Decision tree illustrating the adaptive strategy to inspection planning for systems, from Straub and Faber (2002a).

The decision tree in Figure 6.2 includes only one additional decision parameter, namely  $d_2(e, z)$ . However, the determination of optimal adaptive inspection plans is far more complicated than the RBI for individual hot spots. This has several causes which are listed in the following:

- The number of possible outcomes of  $z$  is much larger than for single hot spots. For the latter it is sufficient to consider only no-indication or indication (with an additional measurement) of the defect. For the system, the number of indications can vary between zero and  $n_{insp}$ , together with corresponding defect measurements.
- The assumption of no-indication at the inspections is not justified. Unless the number of inspected hot spots,  $n_{insp}$ , is very small, the probability of no-indication at all inspected hot spots is low.<sup>a</sup>
- The decision rule  $d_2$  is not obvious: In contrast to the decision rule on the repair action, where only the state of the individual hot spot is of concern,  $d_2$  is a function of the outcome of  $z$ , which includes a large number of different possible values, as discussed above. In addition, whereas  $d$  is either no-action, repair or replacement,  $d_2$  can result in different numbers of additional inspections.
- The decision tree as depicted in Figure 6.2 is not the only possible strategy. In principle it is also possible that after the performance of a second set of inspections  $e_2$  with respective outcomes  $z_2$  it is decided to perform additional inspections.

The following two sections give an overview on two different approaches aimed at providing an insight and a solution to the problems outlined above.

<sup>a</sup> Most publications that consider inspections on systems make the assumption of no-indication. If no-indication is assumed, the solution of the optimisation problem is greatly facilitated, because simplifications can be made similar to those in RBI for single hot spots.

## 6.4 RBI for systems based on the generic approach

This section summarises the methodology introduced in Straub and Faber (2002b), developed for deterioration subjected structural systems for which the decisions on mitigation actions are taken for all hot spots individually, following the above discussion. The methodology is based fully on the generic approach to RBI: its basic idea is to replace the optimisation of the inspection efforts for the entire system by the optimisation of the inspection efforts for all hot spots individually, which is facilitated by the generic approach to RBI. The system is introduced in the analysis by considering the effect of the different dependencies, as depicted in Figure 6.1, on the parameters of the hot spots. If the parameters of the individual hot spots are constantly updated with all available information in the system, then it is ensured that the optimal inspection plan for the individual hot spot is also optimal in view of the entire system.

The updating of the hot spot parameters through information from other hot spots is performed in a simplified manner, based on the  $FDF^a$ : When inspection outcomes from dependent hot spots are available, this information is used to update the reliability of the considered hot spot<sup>b</sup>. For computational efficiency, the updated reliability is then assumed fully represented by an updated value of the  $FDF$ , whereas all other parameters do not change. This is illustrated in Figure 6.3 which shows the updated reliability of a hot spot after the inspection of dependent hot spots, together with the corresponding updated  $FDF$ . The details and the implications of this procedure are documented in Straub and Faber (2002b).

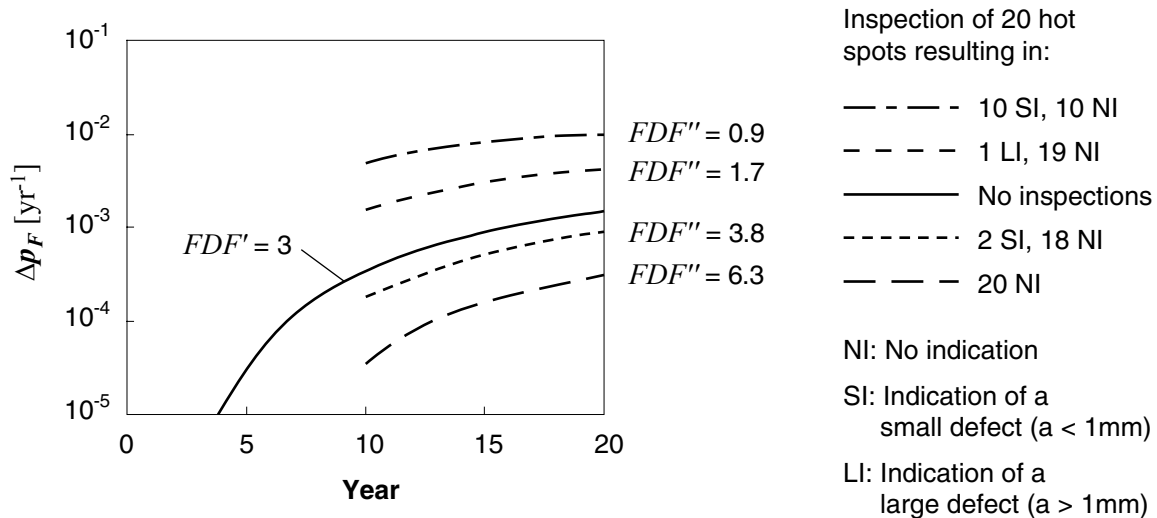


Figure 6.3 – The updated reliability by considering inspections of dependent hot spots in the system, from Straub and Faber (2002b).

<sup>a</sup> Note that the concept is developed for fatigue subjected hot spots. The extension to other deterioration modes is in principle straightforward, but requires that an indicator corresponding to the  $FDF$  is formulated. Such an indicator is proposed in Straub (2000) for corrosion.

<sup>b</sup> This strategy is implicitly adaptive: the inspection efforts at the non-inspected hot spots are determined as a function of the  $FDF$ . By updating the  $FDF$  based on the inspection outcomes at the other hot spots, the inspection efforts at the non-inspected hot spots are automatically adapted.

It is noted that the effect of dependency, as illustrated in Figure 6.3 depends on the applied probabilistic model and especially on the assumed dependency between the hot spots.

The above described procedure is a very efficient tool for the inspection planning of systems, because for each value of the *FDF* the corresponding optimal inspection plan is obtained using the generic approach presented in Chapter 5. It facilitates the management of all available information in the system and the calculation of the actual reliability of all hot spots and thus the entire system at any time. The optimisation of the inspection efforts, however, requires that all (functional and stochastic) dependencies between the hot spots are explicitly addressed and quantified. *After* an inspection is performed such a task is straightforward according to the methodology outlined in the above, but in inspection planning (pre-posterior analysis), it is required that the effect of a planned inspection on the dependent hot spots is quantified also. A direct effect of such a planned inspection is that the marginal cost of inspection for the other hot spots is decreased, which is easily included in the analysis. More difficult to include is the aspect that each planned inspection will potentially supply information about the condition of all dependent hot spots; this is addressed in the following.

An inspection at hot spot A has a value because it facilitates the targeted application of mitigation actions on A. When performing RBI for single hot spots, this value is balanced with the cost of the inspections in order to identify the optimal inspection efforts. For the system, an inspection of hot spot A has an additional value, because it also provides information about the hot spot B (when this is dependent on A). Inspecting A has a value for hot spot B because the additional information enhances the chance that the planned inspection efforts on B are optimal. Based on the Value of Information (VOI) concept from the Bayesian decision analysis, as outlined in Section 2.3.5.1, the value of this information can be calculated. This is demonstrated in Straub and Faber (2002b), from which an example is presented in Figure 6.4. It shows the expected value of sample information *EVS* obtained for a hot spot from the inspection of dependent hot spot.

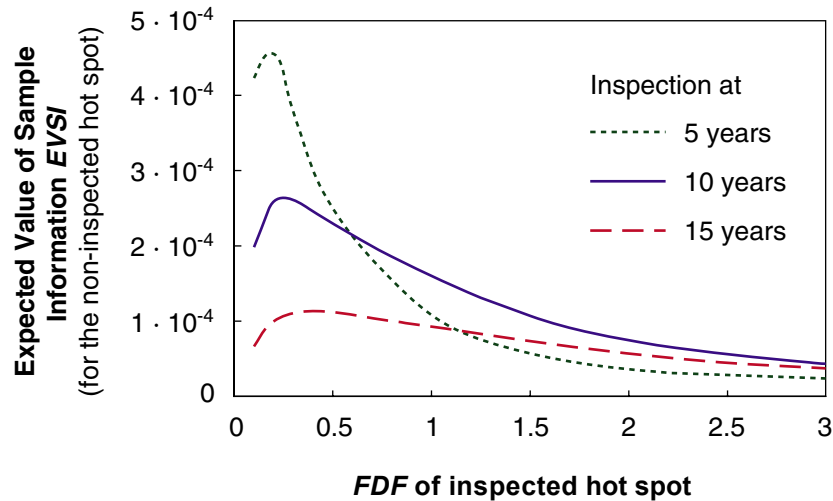


Figure 6.4 – The expected value of information for a hot spot ( $FDF = 2$ ), by inspection of a dependent hot spot; from Straub and Faber (2002b).<sup>a</sup>

When several hot spots are inspected, the  $EVSI$  is evaluated accordingly, although with increased computation efforts. Figure 6.5 illustrates the  $EVSI$  from inspections of  $n_{Insp}$  hot spots with equal  $FDF$ . For increasing  $n_{Insp}$  the  $EVSI$  approaches asymptotically the expected value of perfect information ( $EVPI$ ), which is equal to the value of knowing the true value of the  $FDF$  of the non-inspected hot spot.

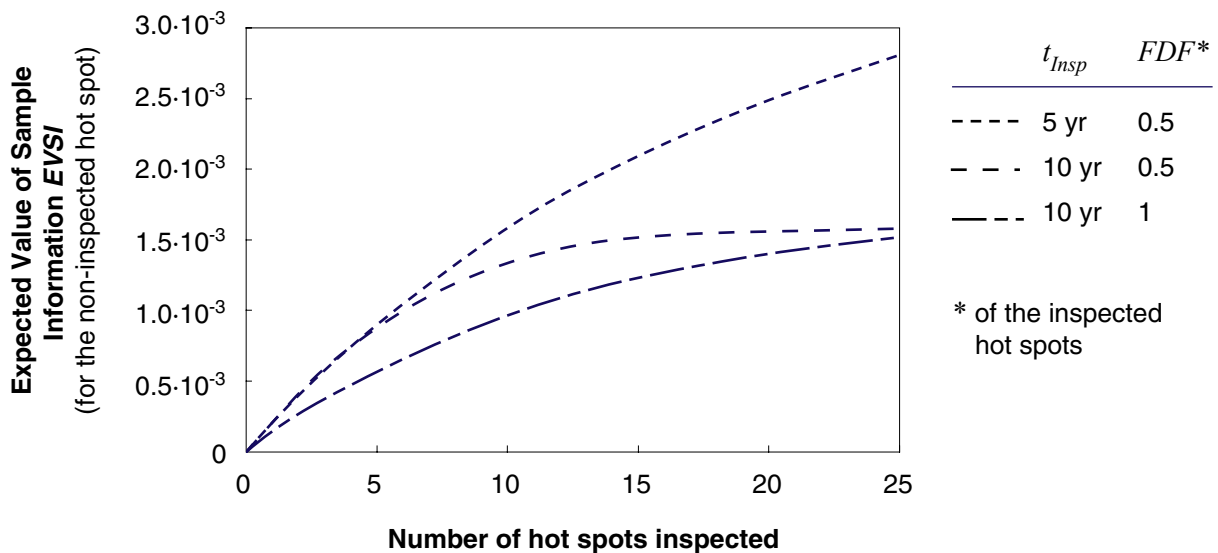


Figure 6.5 – The expected value of information for a hot spot ( $FDF=2$ ) from inspecting  $n_{Insp}$  dependent hot spots in the system at time  $t_{Insp}$ .

<sup>a</sup> In Straub and Faber (2002b) it is proposed to use results like those presented in Figure 6.4 to plan the installation and inspection of “indicator hot spots” in the system. Such indicators, which must be easy to inspect and must have little influence on the system capacity, should be designed to give the maximum information on the other hot spots in the system. From Figure 6.4 it is observed that these indicators optimally should have a very low  $FDF$ .

The final optimisation in the system is performed on a hot spot level by including in the analysis the *EVSI* as an additional benefit of the inspections. Computationally the problem is solved through an iterative procedure; the solution is greatly simplified by the fact that the hot spots with the lowest reliability should always be inspected first, given that the inspection cost are the same for all hot spots. Unfortunately, although all probability evaluations are performed previously, the full optimisation is still time consuming. Further developments in regard to the optimisation procedure are thus necessary before the full optimisation described in this section is applicable for industrial purposes. A concept is thus introduced in the following section for time-invariant problems, which is believed to give helpful insights and which can be combined with the above approach to a practical solution for RBI of entire systems as presented in Section 6.6.

## 6.5 Considering system effects through the system PoD

This section summarises the findings from Straub and Faber (2002a). It introduces a simple format for the consideration of the effect of dependencies between the deterioration at the individual hot spots. A system Probability of Detection,  $PoD_S$ , is formulated, which is an extension of the  $PoD$  for single inspections as introduced in Chapter 4. Based on a simplified adaptive inspection planning procedure, the expected number of defects indicated is evaluated. The  $PoD_S$  provides an indication of the effect of the dependency and can be applied as part of a simplified approach to the planning of inspections of a system.

In Straub and Faber (2002a) different formulations for the  $PoD_S$  are considered, resulting in the proposal of the following definition:

$$PoD_S = E \left[ \frac{\text{Number of identified critical defects}}{\text{Total number of critical defects in the system}} \right] \quad (6-1)$$

For deteriorating structures a critical defect is defined as a defect that leads to failure of a hot spot before the next inspection. From the definition in Equation (6-1) it follows that the  $PoD_S$  is dependent not only on the inspection technique, but also on the deterioration model and the decision model.

The anticipated decision rule for the calculation of the  $PoD_S$  is the one previously illustrated in Figure 6.2: A first set of inspections is performed on  $n_{Insp}$  hot spots.  $n_{Insp}$  can be expressed as

$$n_{Insp} = \gamma n_{HS} \quad (6-2)$$

where  $\gamma$  is the inspection coverage and  $n_{HS}$  the number of hot spots in the system. The decision rule  $d_2$  (see Figure 6.2) is as follows: If the  $n_{Insp}$  inspections result in the indication of more than  $q \cdot n_{Insp}$  critical defects, then all hot spots are inspected, otherwise no additional inspections are performed. Figure 6.6 shows the calculated  $PoD_S$  for different values of the correlation coefficient  $\rho_S$  (between the defect sizes at the individual hot spots), which is a measure for the degree of dependency between the individual hot spots.

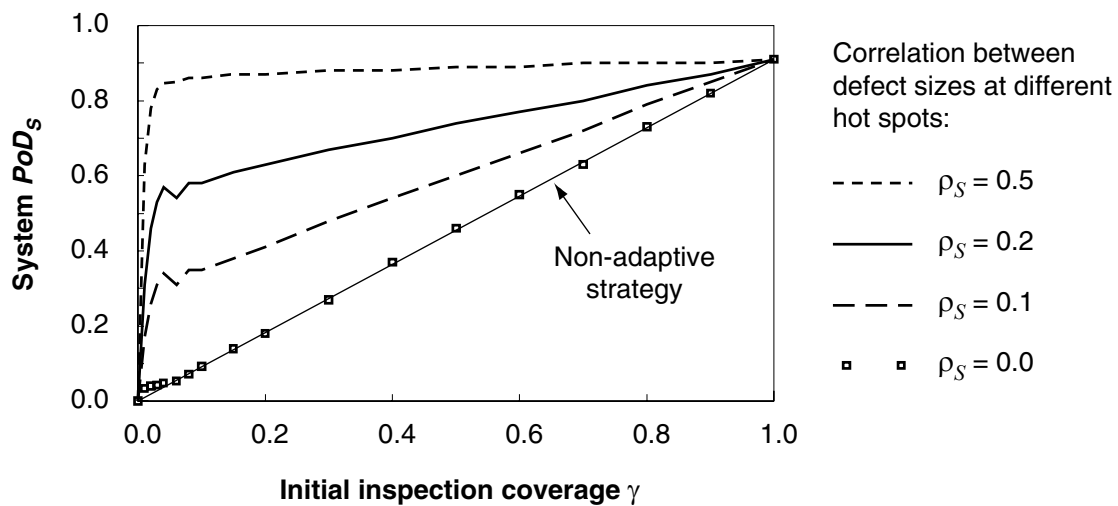


Figure 6.6 – System  $PoD_s$  for different values of the correlation between the defect sizes at the individual hot spots; the decision parameter is  $q=0.3$ , the assumed total number of hot spots is  $n_{HS}=400$ . From Straub and Faber (2002a).<sup>a,b</sup>

From Figure 6.6 it is observed that already for low correlation between the defect sizes at the individual hot spots the inspection performance is substantially improved by applying an adaptive strategy. However, for systems with no dependency between the individual hot spots, the adaptive strategy does not improve the  $PoD_s$ . For such systems no information can be obtained on the other hot spots in the system. The parameter  $q$  has also a substantial influence on the  $PoD_s$ , but, as shown in Straub and Faber (2002a), does not significantly change the form of the curve. The important parameter for the optimisation of the inspection efforts is the derivation of the  $PoD_s$  with respect to  $\gamma$ . Neglecting the fluctuations in Figure 6.6 as caused by the calculation procedure, the  $dPoD_s(\gamma)/d\gamma$  has the general form as shown in Figure 6.7 for a specific case.

<sup>a</sup> The maximum value of the  $PoD_s$  is the probability of detecting a critical defect at the individual hot spot, here 0.91.

<sup>b</sup> The fluctuations of the  $PoD_s$  for low inspection coverage  $\gamma$ , as observed in Figure 6.6, are caused by the discrete nature of the analysis: For  $q=0.3$ , when 10 hot spots are inspected, it is required that three critical defects are indicated, whereas when 11 hot spots are inspected, four critical defects must be indicated to trigger further inspections. The “effective”  $q$  is thus  $3/10 = 0.3$  as opposed to  $4/11 = 0.36$ .

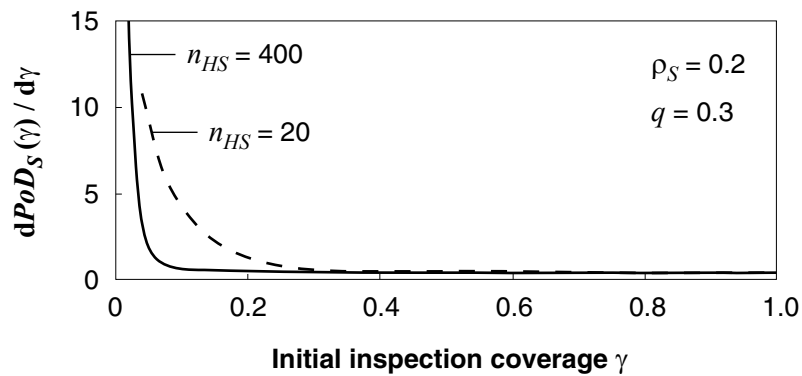


Figure 6.7 – The (smoothed) derivation of the  $PoD_S$  with respect to the initial inspection coverage for two systems with different numbers of hot spots.

$dPoD_S(\gamma)/d\gamma$  represents the additional information gained on the system by increasing the inspection coverage. When  $dPoD_S(\gamma)/d\gamma$  reaches a constant value, then the only information gained by increasing the inspection coverage is on the condition of the inspected hot spot, but no further information about the system can be obtained. This is in accordance with the observation from Section 6.4: With increasing numbers of inspections, the expected value of information obtained asymptotically approaches the *EVPI*. This signifies that additional inspections are not economical; exceptions are hot spots which are so critical that they should be inspected in any case. This is demonstrated in Straub and Faber (2002a), where the optimal  $\gamma$  and  $q$  are evaluated by accounting for the expected cost of inspection, repair and failure; the optimal  $\gamma$  is reached when  $dPoD_S(\gamma)/d\gamma$  approaches the constant value.

The  $PoD_S$  is a function of  $n_{HS}$ , as observed in Figure 6.7; the information obtained on the system is dependent on the absolute number of inspected hot spots rather than on the relative inspection coverage. This must be taken into account by calculating the  $PoD_S$  for the approximate number of hot spots in the considered system or sub-system.

The  $PoD_S$  is a simple concept which allows quantifying the information obtained on the system as a function of the inspection coverage and the stochastic dependency between the deterioration at different hot spots. However, it does not account for temporal aspects; for the application on deteriorating structures it must therefore be combined with the generic approach to RBI, as presented in the next section.

## 6.6 Implementation of RBI for systems in practical applications

The generic approach allows for a very efficient consideration of the dependencies between the deterioration at the individual hot spots after the inspections are performed, as outlined in Section 6.4. This procedure is based on the updating of the *FDF* and a consequent updating of the inspection plans, which are evaluated as a function of the *FDF*. The method also enables an optimisation of the total inspection efforts, as demonstrated in Straub and Faber (2002b). However, due to the required numerical efforts, further research is required to simplify the methodology before an industrial application of the full optimisation can be envisaged.



On the other hand, the  $PoD_S$  concept as summarised in Section 6.5 only facilitates the identification of the optimal inspection coverage at a specific point in time and gives no information about the optimal inspection times. For application on deteriorating structures it is thus required to combine the  $PoD_S$  with an RBI procedure. Such a procedure is proposed in the following; it provides a practical approach to the inspection planning for systems with a stochastic dependency between the deterioration at different hot spots.

The procedure is illustrated in Figure 6.8: As for all RBI procedures, after the identification of the hot spots, the influencing parameters (the values of the generic parameters) must be determined for all individual hot spots (A)<sup>a</sup>. In addition, the dependencies between the deterioration at the different hot spots must be estimated (B); the hot spots are then arranged in groups with hot spots that have large dependencies and each group is considered separately in the subsequent operations (C). The procedure requires that a generic database with inspection plans, in accordance with Chapter 5, is evaluated. Furthermore, a routine that performs the updating of the  $FDFs$  based on the inspection outcomes at dependent hot spots must be established for the considered deterioration model, as described in Straub and Faber (2002b).

Based on the generic approach, the inspection plans are evaluated for the individual hot spots (D). When the first hot spots are due for inspections according to their individual inspection plans, then all inspections that should be performed in this period<sup>b</sup> are considered jointly (E). Based on a simplified analysis using the  $PoD_S$ , the number of hot spots to inspect is then reduced to correspond with the optimal coverage (F). This semi-quantitative procedure should also take into account the relation between inspection costs and the number of jointly inspected hot spots, Section 6.2.1.3. Note that the optimal coverage, as discussed in Section 6.5, depends on the total number of hot spots, which entails that the total number of hot spots inspected should not be reduced below a value of approximately 10 hot spots<sup>c</sup>. After the inspections are performed (G), the inspection plans of all hot spots are then updated with the inspection outcomes, in accordance with the procedure introduced in outlined in Section 6.4 (H). It must then be checked if the updated inspection plans of the non-inspected hot spots justify the postponement of the inspections to the next inspection campaign, otherwise additional inspection must be performed. The procedure is then repeated for the next period when inspections are required (E).

---

<sup>a</sup> The characters in braces correspond to the labels in Figure 6.8.

<sup>b</sup> Period is understood here as the +/- one year.

<sup>c</sup> This also follows from the observation that a minimum number of inspections at other hot spots is required to reduce the  $FDF$  substantially, Figure 6.5. The minimum number depends on the degree of dependency, e.g. for the ideal case of full dependency between all hot spots, it is sufficient to inspect one hot spot. However, it is estimated from the investigated models that for most applications to real structures 10 hot spots is a minimum value.

(B) Estimate the stochastic dependency between individual hot spots. (A) Determine parameters of all hot spots in the system.

(C) Organise hot spots in groups with large dependencies.

(D) Determine individual inspection plans for all hot spots in a group, based on the generic approach:

(E) Identify all hot spots to be considered in the next inspection campaign:

(F) Reduce number of inspections by consideration of the system  $PoD_S$  (this requires an additional routine in *iPlan.xls*):

(G) Perform inspections.

(H) Update the inspection plans with the inspection results, by means of updating the  $FDF$ . Check if additional inspections are required in the current period. If not, repeat the procedure for the next inspection campaign:

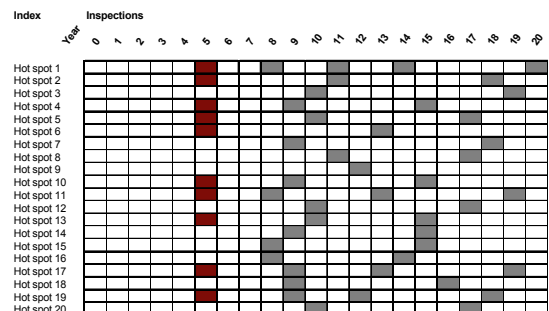
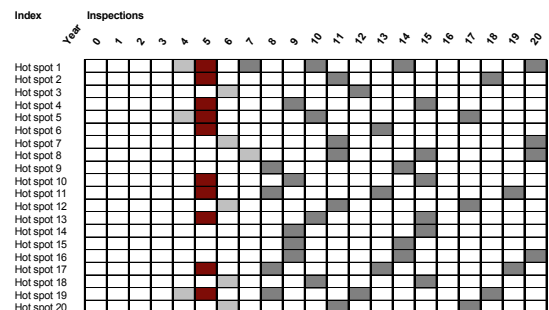
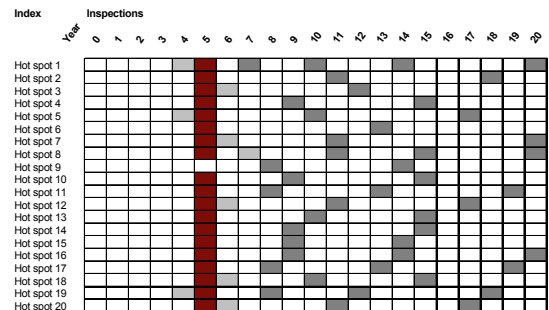
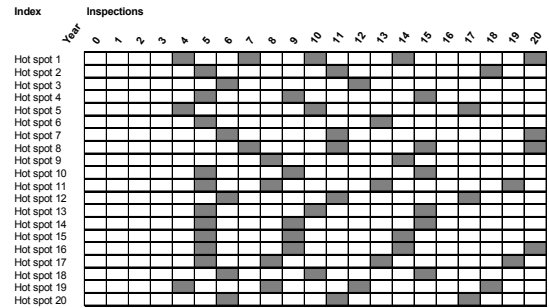


Figure 6.8 – Illustration of the proposed procedure for the inspection planning of large systems.

### 6.6.1 Comments on the proposed approach

The presented approach requires that the degree of dependency between the deterioration performances at the different hot spots can be estimated quantitatively. As noted, only few studies on this subject have been published to date. The estimation for a specific structure must thus rely on a tailor made assessment and to some degree on engineering judgement.

Reducing the number of inspected hot spots through consideration of the stochastic dependencies between the deterioration at the individual hot spots should only be envisaged for systems consisting of less than 15 to 20 hot spots. As noted in the previous section, the number of inspected hot spots should not be reduced below a minimum number, which entails that for small systems always all hot spots should be inspected.

The presented approach does not account for large structures where the inspection plans for all individual hot spots do not require any inspection. Because an inspection provides information on the entire system, as expressed by the expected value of sample information, in some instances it can be advantageous to perform some sample inspections, even though these are not required for the individual hot spots. This situation is discussed in Straub and Faber (2002b).

The dependency of inspection costs on the total number of inspections must be taken into account, Section 6.2.1.3. The proposed approach addresses this relationship in a semi-quantitative manner, but no explicit rules are prescribed. If the marginal costs of inspections are very low as compared to the total inspection cost, then more, if not all, hot spots should be inspected. If the total inspection cost increases linearly with the number of inspections, then this aspect can be neglected.

The approach does not directly address the aspects of combined hot spot failures as already discussed in Section 6.2.1.2. It is reminded that this is valid if, and only if, regular crude inspections are performed on all hot spots, aimed at identifying (and repairing) failed hot spots.

## 6.7 Discussion

RBI procedures have been developed in the past for individual hot spots; the structural system was not explicitly addressed in the analysis. However, inspection planning is always performed on a system. It is therefore of importance that the implications of applying a model for single hot spots are understood. In addition, for most large structural systems an optimal inspection strategy can only be evaluated through the use of an explicit system model. This is outlined in the present chapter based on work described in Straub and Faber (2002a and b) together with the introduction of a practical procedure for the explicit consideration of the system in RBI in Section 6.6.

The context in which the presented generic approach to RBI must be positioned is pointed out in Chapter 1: The purposeful application of the approach requires a general asset integrity management strategy that considers the entire structure and all possible failure modes (besides deterioration phenomena this includes e.g. damages due to accidental loads on the structure). In this phase the relevant system for inspection planning is identified; in accordance with

Sections 6.1 and 6.2 this system is defined as consisting of the hot spots and their interrelations with each other and the entire structure, Figure 6.1. For each specific application such a model must be defined prior to the inspection planning. Based on this system model, the considerations in this chapter should provide the means for a consistent optimisation of the inspection efforts in this system. However, it is important that this system model corresponds to the model of the entire structure which underlies all decisions in regard to the asset integrity management in general.

## 7 Risk acceptance criteria

### 7.1 Introduction

Risk based inspection planning (RBI) facilitates the determination of optimal inspection efforts. Each inspection plan is associated with a specific risk to the public, to personnel, to business and to the environment. Therefore, when there is only one decision maker and when all possible consequences of failure can be consistently integrated into one single variable, then there is no need for separate risk acceptance criteria (RAC). The optimal risk is the risk implied by the optimal inspection plan and a rational decision maker would simply follow this inspection plan. Unfortunately, such ideal situations are rare and several reasons exist why risk acceptance criteria are required in practice. These are discussed in the following.

For most risks arising from deteriorating structures, several decision makers are involved. Although the optimisation of the inspection efforts is performed by the operator of the structure (the first decision maker), many of the risks affect society as a whole (the second decision maker). For practical reasons it is in general society that, through its authorities, codes and regulations, imposes RAC, which then form a constraint on the optimisation performed by the operator, in accordance with Figure 1.1.

In many instances the operator of a structure itself has different objectives which he does not want to integrate in one single objective function. The objectives concerning the safety of personnel, the public and the environment are then accounted for by means of RAC, whereas the business objectives are addressed by the RBI procedure directly. The operator of the structure may also decide to perform the optimisation not on a hot spot level but for the entire structure: The optimal reliability of deteriorating hot spots is evaluated in general; this is then used as a basis for reliability based inspection planning where the necessary inspections to comply with a specific criterion are determined. No additional optimisation for the individual hot spots is performed.

As noted in Straub and Faber (2003b), for many applications RAC are not established through an optimisation approach but from revealed preferences. This concept is based on the fact that the preferences of the decision makers are revealed in current practice, rules and regulations. By inferring the RAC underlying these and then applying them to the inspection planning process, it is ensured that the RBI is consistent with the general policy of the decision maker. However, these RAC are in many cases suboptimal. Not only is it not ensured that the current practice is optimal<sup>a</sup>, but furthermore does the revealed preferences approach in general not take into account the different risk reduction cost (*RRC*)<sup>b</sup> related to different activities, which entail that the optimal RAC is not the same for all activities.

---

<sup>a</sup> A major shortcoming of the approach is that progress in society (e.g. the increase in life expectancy) is not accounted for, see also Slovic (2000).

<sup>b</sup> Also referred to as *marginal cost of reliability* or *cost of a safety measure*.

Based on Straub and Faber (2003b), this chapter elaborates approaches for the derivation of the RAC, primarily following the revealed preferences concept. Section 7.2 introduces the derivation of RAC directly for the individual hot spots. The subsequent Section 7.3 introduces the RAC for the individual hot spots as a function of the RAC for the entire system; this also includes a model for describing the importance of the hot spot for the system (the redundancy of the system with respect to hot spot failure). In Section 7.4 it is then shown how these approaches can be integrated into a single one. The chapter concludes with some considerations on the appropriateness of the presented RAC.

Although named *risk* acceptance criteria, the acceptance criteria are actually expressed in terms of maximum allowable annual probabilities of failure,  $\Delta p_F^{max}$ , in accordance with Rackwitz (2000). Nonetheless, the term RAC is used here because it is required that  $\Delta p_F^{max}$  is a function of the consequence of the hot spot failure. It would, however, be more precise to denote the presented criteria by the term *risk based acceptance criteria* as in Straub and Faber (2003b).

## 7.2 Acceptance criteria derived directly for individual hot spots

### 7.2.1 Risk acceptance criteria explicitly specified

#### 7.2.1.1 Target reliabilities

The Probabilistic Model Code, JCSS (2002), defines target reliability indexes as a function of the consequence of failure and the *RRC*, see also Vrouwenvelder (2002). These criteria are obtained from an optimisation approach in regard to societal costs, and are claimed to be compatible with current practice and observed failure rates (revealed preferences). For (existing) structures where in-service inspections represent the most economical risk reduction measure, the relative cost for increasing the safety is generally large. This implies that the acceptance criteria are lowered, and the target annual failure probabilities suggested in JCSS (2002) are then  $\Delta p_F^{max} = 10^{-3} \text{ yr}^{-1}$  for minor consequences,  $\Delta p_F^{max} = 5 \cdot 10^{-4} \text{ yr}^{-1}$  for moderate consequences and  $\Delta p_F^{max} = 10^{-4} \text{ yr}^{-1}$  for large consequences of failure. Definitions of the different consequence categories are given in terms of the ratio of failure cost (including reconstruction) to construction cost. The provided  $\Delta p_F^{max}$  are intended for individual failure modes and it is noted in Rackwitz (2000) that they must be adjusted if there are many equally likely failure modes with comparable failure consequences. This is in accordance with the system model presented in Section 7.3.

#### 7.2.1.2 Fatal Accident Rate

Some authorities and codes explicitly specify a maximum allowable failure rate or a maximum allowable risk to different groups of people exposed (personnel, public). Different examples of such criteria are summarised in Paté-Cornell (1994). These criteria are to a large extent based on revealed preferences (i.e. on observed failure rates) and combined with some optimisation considerations.

A common format for such explicit RAC is the Fatal Accident Rate (*FAR*), Aven (1992) and Vinnem (1998). The *FAR* is defined as the number of fatalities per 100 million hours of exposure; it is a measure for the acceptable risk to the individual and provides no direct information on the acceptable expected loss of lives per structure. The *FAR* is often used in quantitative risk analysis (QRA) as it allows dealing efficiently with risks that vary within the considered facility or operation.

For many structural elements (hot spots), risk is mainly related to a possible collapse of the entire structure; the application of *FAR* criteria in such a context is discussed in Straub and Faber (2003b). For those hot spots for which failure is leading to a local (in a limited area) endangering of personnel or public, the *FAR* can be applied to specify a maximum failure probability. Typical examples of such hot spots are found in e.g. pressurised systems.

The acceptable probability of failure per year for a hot spot  $\Delta p_F^{max}$  is then

$$\Delta p_F^{max} = \frac{(FAR^{max} - FAR_{OS})}{P(FA|F)} \cdot \frac{24 \cdot 365}{10^8} \quad (7-1)$$

where  $FAR^{max}$  is the acceptable *FAR* value as prescribed from regulations,  $FAR_{OS}$  is the *FAR* value due to all other accident scenarios and  $P(FA|F)$  is the probability of a fatality given hot spot failure for any person in the endangered area. An overview on available models for the estimation of  $P(FA|F)$  is provided in Vinnem (1998).

## 7.2.2 Risk acceptance criteria derived directly from codes

For new-built structures, structural codes prescribe a minimum safety against fatigue failures<sup>a</sup>. These design criteria implicitly correspond to an accepted risk of fatigue failure for individual hot spots. When  $\Delta p_F^{max}$  is set equal to the implied probabilities of failure, the compliance of the inspection plans with the structural code can be demonstrated.

The approach is outlined in the following for the fatigue reference case introduced in Section 5.5, based on Faber et al. (2000) and Moan and Vardal (2001). The design criteria as specified in the NORSOK standard (1998) for welded joints are considered. Therein it is required that a hot spot which cannot be inspected<sup>b</sup> has a Fatigue Design Factor (*FDF*) larger than 10 when the consequences of fatigue failure are substantial and  $FDF \geq 3$  for minor consequences. Substantial consequences are, qualitatively, defined as those entailing either possible loss of live, significant pollution or major financial consequences.

---

<sup>a</sup> For corrosion in principle the same holds, yet the design criteria provided by codes are often of a qualitative nature. In order to implement the approach presented in this section, these must be “translated” into quantitative criteria which are comparable with the applied corrosion models.

<sup>b</sup> The criteria for the hot spots which are not inspected are relevant as these reflect the unconditional maximal allowable probabilities of failure. For hot spots that are inspected, NORSOK (1998) provides no details on the required inspections (inspection intervals, technique) which would allow inferring the implicit  $\Delta p_F^{max}$  consistently.

Based on the reliability of the reference case as illustrated in Figure 5.11, the  $\Delta p_F^{max}$  is for the two consequence categories depicted in Figure 7.1.

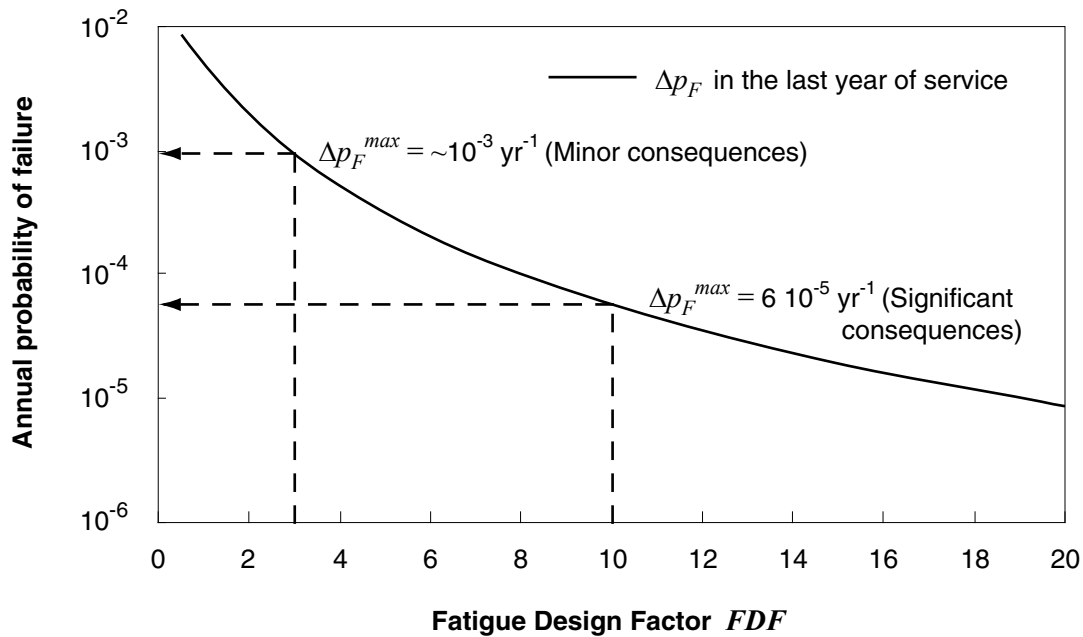


Figure 7.1 – Acceptance criteria for the fatigue reference case in accordance with the NORSOK standard.

From Figure 7.1 the acceptance criteria according to NORSOK (1998) are for the reference case obtained as  $\Delta p_F^{max} = 10^{-3} \text{ yr}^{-1}$  for hot spots with minor consequences of failure and as  $\Delta p_F^{max} = 6 \cdot 10^{-5} \text{ yr}^{-1}$  for those with significant consequences of failure. It is emphasised that these criteria are only valid for the applied probabilistic model. If e.g. the uncertainty on the calculated stress ranges is increased, then also  $\Delta p_F^{max}$  increases.

The approach represents a useful tool for the simple and consistent determination of  $\Delta p_F^{max}$ . In accordance with Faber (2000), it provides a reference for comparison of the reliabilities calculated in the inspection planning procedure: The notional reliabilities are calibrated to the code requirements which are considered to represent “best practice”. For this reason, it is recommended to use this approach for all applications, if only as a means of verifying other, possibly more refined approaches.

### 7.3 System approach to acceptance criteria for individual hot spots

This section presents the derivation of RAC based on consideration of the entire system<sup>a</sup>. Such approaches are believed to be of high relevance for hot spots whose consequence of failure is primarily related to the possible collapse of the structure. Most hot spots in fatigue subjected structures fall into this category. Although the presented methodology is applicable

<sup>a</sup> The system is modelled according to Section 6.1.



to any structure with these characteristics, the explanations concentrate on the application to fixed offshore structures subject to fatigue.

The approach is a top-down approach, i.e. in a first step it is required to specify an annual acceptable probability of collapse of the structure, denoted by  $\Delta p_{COL}^{max}$ . The acceptance criteria for the individual hot spots are then obtained as a function of this value.

### 7.3.1 Risk acceptance criteria for collapse of the structure

Stahl et al. (1998) compare acceptance criteria for the ultimate collapse of offshore platforms as obtained by different approaches including the derivation from an optimisation approach, from observed failure rates, from *FAR* values specified during a QRA and from consideration of code requirements in regard to the overall collapse capacity. Stahl et al. (1998) find that the  $\Delta p_{COL}^{max}$  obtained from these different approaches correspond reasonably.

For fixed offshore structures, code requirements to the global capacity of the structure are generally expressed in terms of the Reserve Strength Ratio (*RSR*), defined as the ratio of the mean system capacity to the nominal design load. The discussion is in the following focused on the inference of  $\Delta p_{COL}$  from the *RSR*, as this not only provides the means for the evaluation of  $\Delta p_{COL}^{max}$ , Section 7.3.1.1, but additionally allows to define a simple indicator for the redundancy of the structure, as demonstrated in Section 7.3.2.

#### 7.3.1.1 Relation between *RSR* and overall collapse probability

The *RSR* values are generally evaluated by a push-over analysis. A general relation between *RSR* and the probability of collapse can be obtained by consideration of the following limit state function (references are given by Stahl et al. (1998), see also HSE (2002a)):

$$g_{COL} = R - H^\delta B \quad (7-2)$$

where *R* is the effective capacity of the platform, *H* is a stochastic variable modelling the maximum annual wave height, and *B* and  $\delta$  are factors relating the wave height to the structural load. *B* is a stochastic variable that accounts for the model uncertainty. For the example,  $\delta = 2.2$  is assumed in accordance with Stahl et al. (1998).

The *RSR* value as evaluated by a push-over analysis can be related to characteristic values of *R*, *b* and *H* in the following way (where the index *C* identifies the characteristic values):

$$RSR = \frac{R_C}{B_C H_C^\delta} \quad (7-3)$$

It is assumed that *R* and *B* can be modelled probabilistically as Lognormal distributed random variables and *H* as a Gumbel distributed random variable. The characteristic values for *R*, *b* and *H* are defined as 5%, 50% and 98% quantile values of their probability distributions. The coefficients of variation are chosen as

$$COV_R = 0.15 \quad COV_B = 0.10 \quad COV_H = 0.16$$

This stochastic model corresponds to the one given in Stahl et al. (1998) with the exception of the choice of the Gumbel distribution for  $H$ .

The reliability corresponding to a  $RSR$  value is then determined by structural reliability analysis (SRA) using the above given limit state function, Equation (7-2). The mean values of  $R$ ,  $B$  and  $H$  are determined by choosing two and evaluating the third according to Equation (7-3). The results are given in Figure 7.2.

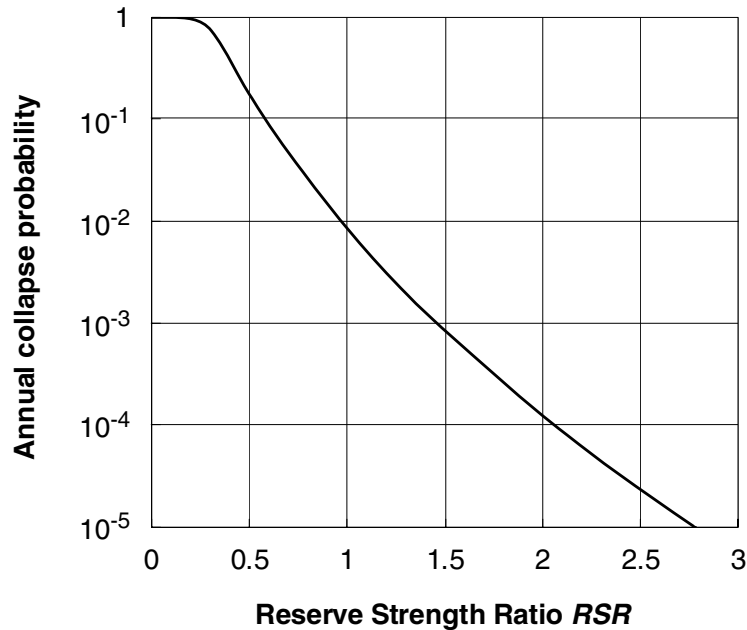


Figure 7.2 - Relation between the  $RSR$  and the annual probability of collapse, Straub and Faber (2003b).

### 7.3.1.2 Acceptable probability of collapse caused by (fatigue) deterioration

If deterioration<sup>a</sup> in a structure is considered separately from the other failure modes, and if collapse caused by a fatigue failure is not considered as the main collapse mode, then acceptance criteria for fatigue failure can be expressed as a function of the acceptable risk of collapse due to the predominant structural collapse mechanism. For the considered fixed jacket structures this is generally an extreme weather event. The annual probability of collapse due to wave loads can be inferred from the  $RSR$  in accordance with Figure 7.2. If e.g. an  $RSR = 2$  is accepted, it is concluded that  $\Delta p_{COL}^{max} = 1.2 \cdot 10^{-4} \text{ yr}^{-1}$ .

The total accepted risk related to structural collapse includes the entire set of possible collapse mechanisms. Collapse due to fatigue failure at one or several hot spots represents only a fraction of all possible mechanisms. Risk acceptance criteria for collapse due to fatigue

<sup>a</sup> The presented approach allows for considering different deterioration mechanisms such as fatigue and corrosion together. The individual event is failure of a hot spot, which can be caused by any possible deterioration mechanism and it is not necessary to distinguish between different types of deterioration. However, the presentation in this section concentrates on fatigue failures.

failure, denoted by  $\Delta p_{COL,F}^{max}$ , should therefore be stricter than the overall criteria. These criteria may be determined as

$$\Delta p_{COL,F}^{max} = \psi \cdot \Delta p_{COL}^{max} \quad (7-4)$$

In accordance with Faber et al. (2003a) the determination of the factor  $\psi$  may be approached by taking basis in the risk analysis as part of the concept studies and design verification as well as in experiences from similar facilities. There is, however, little data on severe structural fatigue failures available; establishing a representative statistic is thus not possible. Lacking specific information, a value of  $\psi = 0.1$  is assumed in the following. In Section 7.4 it is demonstrated how  $\psi$  can be determined by calibration to code requirements.

### 7.3.2 Risk acceptance criteria for individual hot spots based on a system model

Following Straub and Faber (2003b), in this section the acceptance criteria for the individual hot spots are derived as a function of the overall criterion  $\Delta p_{COL,F}^{max}$ . The allocation of the risk to the different hot spots is thereby based on indicators for the following system characteristics:

- *Redundancy* (of the structural system)
- *Complexity* (the number of critical hot spots)
- *Dependency* (between the different failure and collapse modes)

The indicators for these characteristics follow from the system model as introduced in the following.

#### 7.3.2.1 Modelling the structural system

System strength is represented by the annual probability of collapse,  $\Delta p_{COL}$ , which is a function of the state of the individual hot spots. For the purpose of simplification the hot spots are modelled as either intact or failed, i.e. no continuous decrease of the hot spot's performance is considered.  $F_i$  denotes the event of failure of the  $i^{\text{th}}$  hot spot and  $\bar{F}_i$  the event of survival of the  $i^{\text{th}}$  hot spot. The principal form of the degradation of the system strength towards collapse is illustrated in Figure 7.3, where one possible realisation of  $\Delta p_{COL}$  is shown.

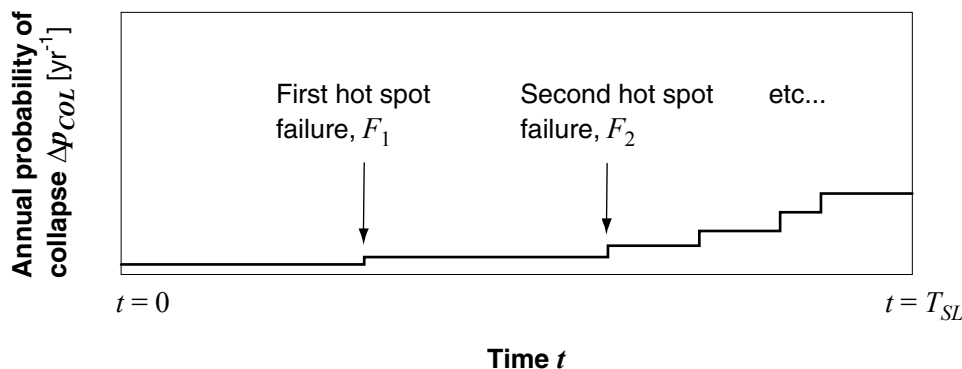


Figure 7.3 –Illustration of system deterioration model: One possible realisation.

The simplification allows for modelling the system as a series system, illustrated in Figure 7.4 for a structure with two hot spots. For a structure with  $n_{HS}$  hot spots the system accordingly consists of  $2^{n_{HS}}$  elements.

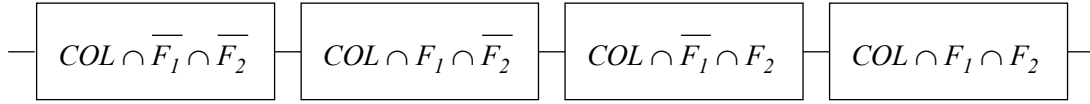


Figure 7.4 – System reliability model (with two hot spots).

With the introduction of conditional events of collapse the model presented in Figure 7.4 is modified to the one shown in Figure 7.5. Therein the event of any (i.e. one or more) hot spot failure is denoted by  $F$ .

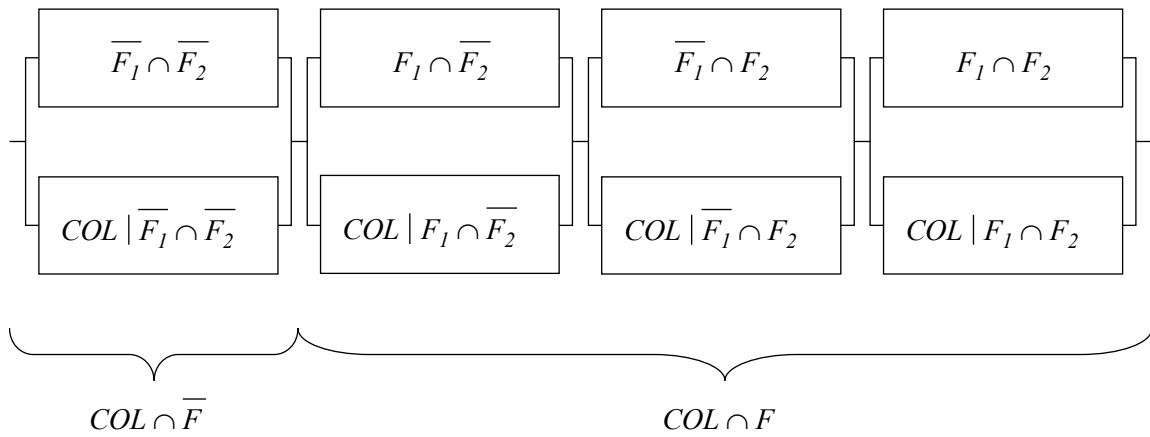


Figure 7.5 – System reliability model (with two hot spots) using conditional collapse events.

The total annual probability of collapse  $\Delta p_{COL}$  is evaluated from the probabilities of the individual events as shown in Figure 7.5. For this system with two hot spots  $\Delta p_{COL}$  is calculated from Equation (7-5); it is the probability of failure of a series system with mutually exclusive events. Equation (7-5) is based on a reference time period of one year.

$$\Delta p_{COL} = P(COL|\bar{F}_1 \cap \bar{F}_2)P(\bar{F}_1 \cap \bar{F}_2) + P(COL|F_1 \cap \bar{F}_2)P(F_1 \cap \bar{F}_2) + P(COL|\bar{F}_1 \cap F_2)P(\bar{F}_1 \cap F_2) + P(COL|F_1 \cap F_2)P(F_1 \cap F_2) \quad (7-5)$$

Equation (7-5) is simplified further by the following approximations, which are justified by the generally large fatigue reliability of welded joints in offshore structures:

$$\begin{aligned} P(F_1 \cap \bar{F}_2) &\approx \Delta p_{F_1} & P(COL|F_1 \cap \bar{F}_2) &\approx \Delta p_{COL|F_1} \\ P(\bar{F}_1 \cap F_2) &\approx \Delta p_{F_2} & P(COL|\bar{F}_1 \cap F_2) &\approx \Delta p_{COL|F_2} \end{aligned} \quad (7-6)$$

$\Delta p_{COL|F_i}$ , the annual probability of collapse given failure of hot spot  $i$ , describes the redundancy of the structure with respect to hot spot failure.

Because collapse not related to hot spot failures is treated separately, only the probability of collapse combined with hot spot failure,  $\Delta p_{COL \cap F}$ , is considered here. It is

$$\Delta p_{COL \cap F} = \Delta p_{COL} - \Delta p_{COL|\bar{F}} \approx \Delta p_{COL} - \Delta p_{COL|\bar{F}} \quad (7-7)$$

Approximating  $\Delta p_{COL|\bar{F}}$  by  $\Delta p_{COL|\bar{F}}$  is again justified by the generally large fatigue reliability.

If the occurrences of the individual hot spot failures are fully dependent, then the middle terms in Equation (7-5) become zero. If the hot spot failures are independent<sup>a</sup>, then the last term in Equation (7-5) (which accounts for the combined hot spot failure events) can be neglected as a consequence of

$$P(F_1 \cap F_2) \ll \max[P(\bar{F}_1 \cap F_2), P(F_1 \cap \bar{F}_2)] \quad (7-8)$$

In that case the probability of collapse due to a fatigue failure is rewritten as

$$\Delta p_{COL \cap F} = \left( \Delta p_{COL|F_1} - \Delta p_{COL|\bar{F}} \right) \Delta p_{F_1} + \left( \Delta p_{COL|F_2} - \Delta p_{COL|\bar{F}} \right) \Delta p_{F_2} \quad (7-9)$$

In order to relate the overall fatigue acceptance criteria  $\Delta p_{COL,F}^{max}$  with criteria for the individual hot spots,  $\Delta p_{COL \cap F}$  is replaced by  $\Delta p_{COL,F}^{max}$  and  $\Delta p_{F_i}$  is replaced by  $\Delta p_{F_i}^{max}$ , the fatigue acceptance criteria for the individual hot spots. When  $\Delta p_{COL,F}^{max}$  is given, a second condition is needed to the derivation of the  $\Delta p_{F_i}^{max}$ . Lacking specific information a practical approach is to require that the contribution to the risk is equal for all hot spots<sup>b</sup>, therefore

$$\left( \Delta p_{COL|F_1} - \Delta p_{COL|\bar{F}} \right) \Delta p_{F_1}^{max} = \left( \Delta p_{COL|F_2} - \Delta p_{COL|\bar{F}} \right) \Delta p_{F_2}^{max} = \frac{\Delta p_{COL,F}^{max}}{2} \quad (7-10)$$

For hot spot  $i = 1$  the acceptance criteria is therefore

$$\Delta p_{F_1}^{max} = \frac{1}{2} \frac{\Delta p_{COL,F}^{max}}{\left( \Delta p_{COL|F_1} - \Delta p_{COL|\bar{F}} \right)} \quad (7-11)$$

For  $n_{HS}$  critical hot spots the acceptance criteria are derived accordingly, for hot spot  $i$  being

<sup>a</sup> Dependency between fatigue performances at different hot spots is considered separately in the next section.

<sup>b</sup> Ideally this simple requirement is replaced by an optimisation. This would entail that the allocation of the risk to the different hot spots is a function of the *RRC* associated with the individual hot spots.

$$\Delta p_{F_i}^{max} = \frac{1}{n_{HS}} \frac{\Delta p_{COL,F}^{max}}{\left( \Delta p_{COL|F_i} - \Delta p_{COL|\bar{F}} \right)} \quad (7-12)$$

In Equation (7-12), which is valid for independent hot spot failures,  $n_{HS}$  is the indicator for the complexity of the structure and  $\Delta p_{COL|F_i}$  is the indicator for the redundancy of the structure. The latter can be determined as a function of the Residual Influence Factor ( $RIF$ ). The  $RIF$ , which in some references is also named Damaged Strength Ratio ( $DSR$ ), has a long tradition in RBI for offshore structures, see e.g. Kirkemo (1990). It is, for each hot spot  $i$ , defined as the ratio of the capacity of the damaged structure to the capacity of the intact structure, Equation (7-13).

$$RIF_i = \frac{RSR_{F_i}}{RSR_{intact}} \quad (7-13)$$

The  $RIF$  can vary between 0 (no redundancy) and 1 (failure of the hot spot has no influence on the structural capacity). In accordance with Straub and Faber (2003b),  $\Delta p_{COL|F_i}$  is related to the  $RIF_i$  by means of the following considerations: The probability of collapse of the damaged structure is determined from  $RSR_{F_i}$  and the relation depicted in Figure 7.2. Because  $RSR_{intact}$  is fixed for a given structure, each  $RIF_i$  thus corresponds to one value of  $RSR_{F_i}$  and consequently also to a specific value of the probability of collapse  $\Delta p_{COL|F_i}$ .

Based on these relations, the acceptance criteria for the individual hot spots are determined as a function of the  $RIF_i$ , the  $RSR_{intact}$  and the number of hot spots  $n_{HS}$ . They are illustrated in Figure 7.6 for a particular  $RSR_{intact}$ ;  $\Delta p_{COL,F}^{max}$  is thereby inferred from the  $RSR$  according to Section 7.3.1 as  $10^{-5} \text{ yr}^{-1}$ .

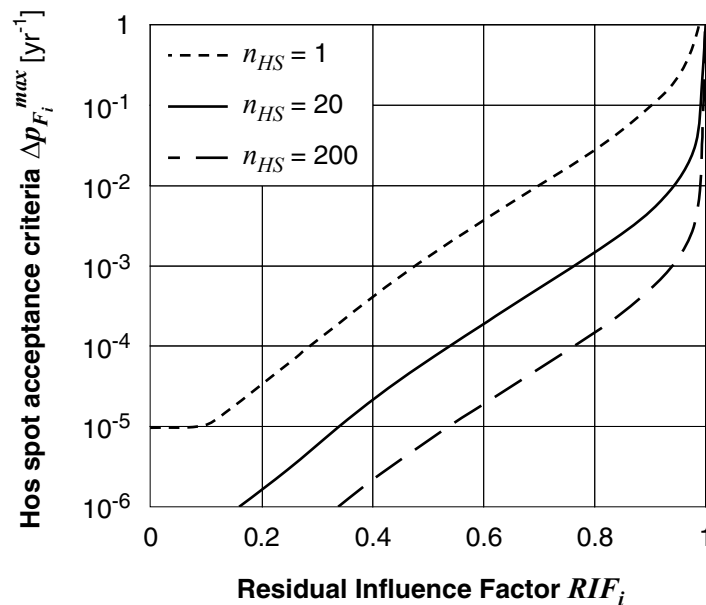


Figure 7.6 – Acceptance criteria for independent hot spots in a structure containing  $n_{HS}$  hot spots ( $RSR_{intact} = 2.05$ ,  $\psi = 0.1$ ).

From Equation (7-12) and from Figure 7.6 it follows that the  $\Delta p_F^{max}$  for the individual hot spots decreases with increasing number of hot spots. This appears paradoxical on first sight, but is explained by the fact that the increased redundancy is considered separately through the *RIF*. It is observed that the effect of the increased redundancy (*RIF*) is generally larger than that of the correspondingly increased number of potential failure modes (hot spots).

### 7.3.2.2 Accounting for the dependency between individual hot spots failure modes

In the previous section it was assumed that the failure events at the individual hot spots occur independently. This condition is generally not fulfilled, due to common influencing factors, as discussed in Chapter 6. Whereas these dependencies are beneficial in regard to the information obtained from inspections, they may have an adverse effect on the system probability of collapse. This is because the terms of higher order in Equation (7-5), which describe the probability of joint occurrence of hot spot failures, can no longer be neglected. In fact, for some structures (like ship hulls) the probability of collapse due to the failure of several hot spots may be dominant. Unfortunately, it appears impractical to include the dependencies in the model presented above, because the number of additional terms in Equation (7-5) is prohibitive. In Straub and Faber (2003b) it is thus proposed to base the acceptance criteria on the assumption of independent hot spot failure events. The dependencies must then be accounted for by ensuring a fast detection of failed hot spots. It is shown in Straub and Faber (2003b), on a simplified model, that when all failed hot spots are identified and repaired during adequate periods, then the assumption of independent hot spot failure events is valid.<sup>a</sup>

This has implications on the inspection strategy: Whereas for critical hot spots NDE is of importance for the identification of defects prior to the inspection<sup>b</sup>, periodical inspections that aim at detecting failed hot spots should be performed for all hot spots. These inspection periods must be determined by consideration of the relevant deterioration modes, with due attention on the assumptions regarding temporal variability of the deterioration processes; see also Straub and Faber (2003b) for further considerations.

## 7.4 Integration of the different approaches

When applying a system approach in accordance with Section 7.3, a main difficulty is the identification of  $\Delta p_{COL,F}^{max}$ , the acceptable probability of collapse as caused by deterioration failures. An optimisation approach is, in principle, preferred for the determination of this factor, Faber (2000), yet such an approach is outside the scope of this work. Determining the criterion as a function of the *RSR* and  $\psi$  by means of Figure 7.2 and Equation (7-4) is sound, but should not be applied without some additional verification. Note that a) the annual

---

<sup>a</sup> This is not in contradiction to assuming dependency between the defect sizes at the individual hot spots, as accounted for in Chapter 6. Even when the defect sizes are dependent is the probability of coincidence of two failure events very small when the considered time period is sufficiently small.

<sup>b</sup> Critical hot spots are those where the RAC determined as a function of the *RIF* require that NDE is performed. Such inspections are then planned using RBI.

probabilities of collapse in Figure 7.2 represent notional reliabilities and that b) the determination of the factor  $\psi$  in the presented example is somewhat arbitrarily. It is therefore proposed to calibrate the factor  $\psi$  to the acceptance criteria specified in codes; as an example the NORSOK (1998) criteria introduced in Section 7.2.2 are considered. This calibration allows taking advantage of the benefits of the system approach while at the same time ensuring compatibility with code requirements.

#### 7.4.1 Calibration of the systems approach to the code

In a first step the reliability implied by the code criteria is determined as described in Section 7.2.2. Because this reliability is dependent on the probabilistic model, slight variations for the individual hot spots may occur. A typical set of hot spot parameters should thus be selected. Assume that the fatigue reference case (Section 5.5) is representative. The implied  $\Delta p_F^{max}$  is then  $10^{-3} \text{ yr}^{-1}$  and  $6 \cdot 10^{-5} \text{ yr}^{-1}$  for minor and significant consequences of failure respectively, according to Section 7.2.2.

In a second step, the curve describing  $\Delta p_F^{max}$  as a function of the *RIF* (Figure 7.6) is fitted to the code requirements. For this purpose, the code requirements must be interpreted with respect to the underlying assumptions in regard to the relation between the terms “minor” and “significant” consequences and the *RIF*. Note that the code criteria are independent of the number of hot spots  $n_{HS}$ . Because  $n_{HS}$ , together with acceptance criteria for collapse  $\Delta p_{COL}^{max}$  and the share of the accepted risk allocated to fatigue failures  $\psi$ , can be included into one single variable, denoted by  $\psi_1$ , there is no need to specify  $n_{HS}$  explicitly. For this purpose Equation (7-12) is rewritten as

$$\Delta p_{F_1}^{max} = \frac{1}{n_{HS}} \frac{\Delta p_{COL}^{max} \psi}{\left( \Delta p_{COL|F_i} - \Delta p_{COL|\bar{F}} \right)} = \frac{\psi_1}{\left( \Delta p_{COL|F_i} - \Delta p_{COL|\bar{F}} \right)} \quad (7-14)$$

$\psi_1$  can be interpreted as the acceptable annual probability of collapse due to failure of a single hot spot. This implies that the factor  $\psi$  is a function of  $n_{HS}$ : If more hot spots are present in the system, then the part of the accepted risk that is allocated to deterioration failures is increased.

As a numerical example a structure with  $RSR_{intact} = 2.05$  is considered, corresponding to Figure 7.6. In accordance with Kirkemo (1990) “significant” consequences for a hot spot are interpreted as a value of *RIF* = 0.7. This allows determining the final  $\Delta p_{F_1}^{max}$  values as a function of the *RIF*, illustrated in Figure 7.7.



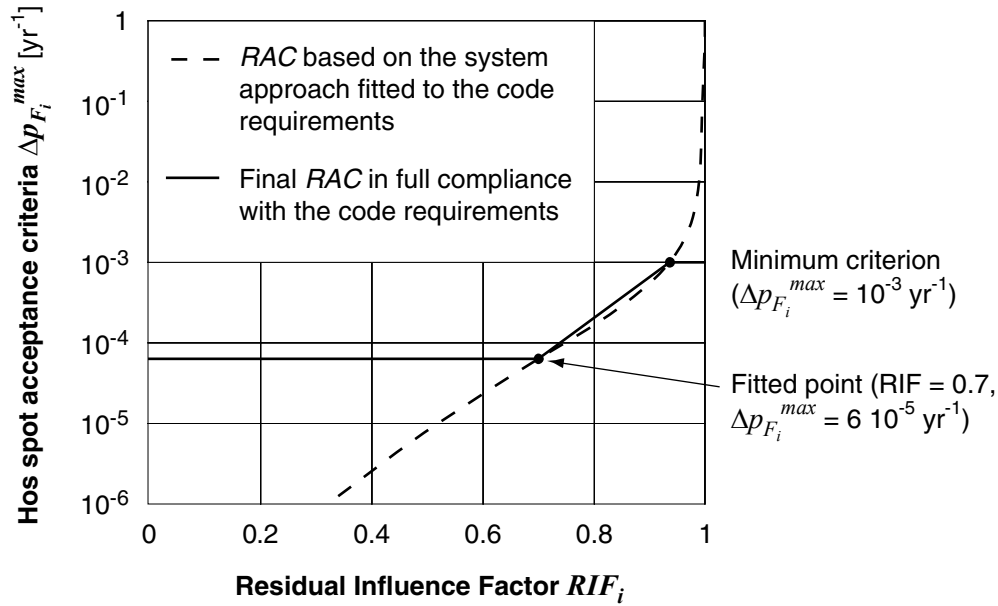


Figure 7.7 – Integrated approach to RAC considering the system ( $RSR_{intact} = 2.05$ ).

Note that the curve is fitted to pass through the point defined by  $RIF = 0.7$  and  $\Delta p_F^{max} = 6 \cdot 10^{-5} \text{ yr}^{-1}$ . The fitted variable is  $\psi_1$  in Equation (7-14), or equivalently  $\psi$  for given  $n_{HS}$  and  $\Delta p_{COL}^{max}$ . Calculated values of  $\psi$  for different cases are given in Table 7.1.

Table 7.1 – Share of fatigue risks on the total acceptable collapse risks, as implied by the NORSOK (1998) criteria.

$RSR_{intact}$	$\Delta p_{COL}^{max} [\text{yr}^{-1}]$	$n_{HS}$	$\psi$	$\psi_1$
2.05	$10^{-4}$	200	<b>0.12</b>	<b><math>6 \cdot 10^{-8}</math></b>
2.05	$10^{-4}$	20	<b>0.01</b>	<b><math>6 \cdot 10^{-8}</math></b>
1.6	$5.5 \cdot 10^{-4}$	200	<b>0.09</b>	<b><math>2.5 \cdot 10^{-7}</math></b>
1.6	$5.5 \cdot 10^{-4}$	20	<b>0.01</b>	<b><math>2.5 \cdot 10^{-7}</math></b>

From the results in Figure 7.7 it is found that, based on the presented model, the “minor” consequences in NORSOK (1998) correspond to a  $RIF \geq 0.94$ .

The curve as depicted in Figure 7.7 changes only slightly for different values of the  $RSR_{intact}$  and the final RAC is thus valid for all hot spots similar to the reference case<sup>a</sup>. However, often the  $RSR_{intact}$  is dependent on the importance of the structure and this should also be reflected in the final  $\Delta p_F^{max}$ . Because a change of  $\Delta p_{COL}^{max}$  is compensated by an according change of  $\psi$ , this must be considered differently; the  $RIF$  representative for “significant” consequences

<sup>a</sup> As pointed out previously, they are *not* valid for hot spots with different values of  $B_S$  (the uncertainty on the calculated fatigue stresses) or of any other parameter influencing the SN fatigue reliability, with the exception of the  $FDF$ .

should vary with the importance of the structure. This is consistent with the code specifications, because the expected consequences of hot spot failures are given by the product of the probability of collapse given hot spot failure with the expected consequences of collapse (which are a direct function of the importance of the structure).

## 7.5 Conclusions

The approaches for the derivation of RAC presented in this chapter are to a large extent based on the principles of revealed preferences, with the exception of the target reliability indexes given in JCSS (2002). To base the RAC on the preferences revealed in existing codes and practice is preferred by most decision makers, because it circumvents the problem that the probabilities evaluated by means of SRA are considered “notional” probabilities, which are not directly comparable to the “real” probabilities. In addition, legal concerns prevent the decision makers from adopting an optimisation approach without demonstrating compliance with given code requirements. On the other hand, it has been pointed out, e.g. Faber (2000), that acceptance criteria should ideally be based on optimisation. Such optimisation approaches date back to Rosenblueth and Mendoza (1971) for structures subject to infrequent (accidental) loads; their application to time-variant failure modes is presented in Rackwitz (2000). These approaches are outside the scope of this work, but some of the aspects are outlined in Straub and Faber (2003b) in view of their application to fatigue subjected hot spots.

Generally, consistent (and optimal) RAC require that the  $\Delta p_F^{max}$  for the individual hot spots are formulated as a function of

- the redundancy of the structure with respect to failure of the hot spot;
- the importance of the structure, respectively the expected consequences of structural collapse;
- the risk reduction cost (*RRC*) for the possible safety measures;
- the number of hot spots in the structure.

The system approach presented in Section 7.3 in principle allows addressing these factors explicitly. However, it is pointed out that it is difficult to determine the optimal total acceptable risk of collapse as caused by deterioration. This is not attempted in the present work. Instead it is proposed, Section 7.4, to calibrate the approach to the RAC provided in codes. This combined approach represents a highly practical procedure for the determination of RAC. It is consistent with current regulations (and therefore current practice) and shows, at least for the presented example, good agreement with the criteria presented in the Probabilistic Model Code, JCSS (2002). It is thus concluded that the derived criteria are not far from optimal. A disadvantage of the approach is that the inconsistencies of the code (in regard to optimality of the criteria) are adopted. This includes the fact that the RAC do not account for the cost of risk reduction associated with the hot spots<sup>a</sup> and that they are

---

<sup>a</sup> The RAC in the code are specified for fatigue design. Risk reduction through inspections is, however, often more expensive than risk reduction through improved design.

independent of the total number of hot spots (failure modes). If a deviation from the acceptance criteria given in the code is allowed, then the system model can provide the means for addressing these parameters consistently.

The importance of ensuring that failed components are detected (and repaired) within an appropriate period is pointed out. As discussed in Section 7.3.2.2, such regular “crude” inspections are required to verify that the approximation by a system with independent hot spot failures is valid. This must be taken into account in the general maintenance procedure.



## 8 Conclusions and outlook

### 8.1 Conclusions

The basic principles of risk based inspection planning (RBI), originating from the Bayesian decision analysis and structural reliability analysis, were formulated for fatigue subjected steel structures in the early 1990s. Since then, the application of the methodology has been limited to relatively few industrial projects. While theoretically sound and accepted by the scientific community, the methodology has failed to gain acceptance in practice; the integration of the methodology in the general asset integrity management procedures has been hindered by the complexity and the required computational efforts of the approach, which made it very difficult to implement the methodology, especially the reliability updating, in an efficient software tool. As a consequence, most operators and owners of structures base their maintenance decisions on empirical procedures, which are either of a semi-quantitative or a fully qualitative nature. These procedures make it difficult to learn from past experience, due to the lack of a full quantification of all influencing factors, which vary among structures and within one structure. In addition, inconsistencies in the applied maintenance strategies can arise because the risks from the different deterioration phenomena and locations in a structure cannot be directly compared. These disadvantages of alternative procedures have motivated the development of a computationally efficient procedure fully based on the Bayesian decision analysis.

The presented generic approach to RBI overcomes the drawbacks of the methodology regarding the required computational efforts and facilitates the integration in a highly reliable and efficient software tool, as illustrated by the development of iPlan, Annex D. The basic idea of the approach is to perform the demanding probability calculations beforehand for generic representations of the structural details subject to deterioration (the *hot spots*); the results of these calculations are then stored in a database. For the application of RBI, the identified hot spots of the considered structure<sup>a</sup> are represented in terms of so-called generic parameters; these include all relevant information for the modelling of the deterioration mechanism. Based on a simple interpolation algorithm, the inspection plans are then obtained for all hot spots from the pre-established database, as a function of their respective generic parameters.

Apart from computational efficiency, the approach is beneficial because it provides a clear definition and quantification of the influencing parameters (the generic parameters) and thus enables a comparison between results from different structures. Such a standardisation promotes the quality of the procedure, because past experiences can be used to improve the underlying models, see also HSE (2002b). This is of particular interest in view of the model uncertainties (such as the uncertainty on the fatigue stress calculation or the uncertainties

---

<sup>a</sup> The approach is applicable to all types of deteriorating engineering steel structures, including e.g. building structures, ship hulls, pressure vessels or pipelines.

related to the predicted corrosion rate). The difficulties involved in the estimation of these variables have been emphasised in Chapters 3 and 5. An inspection strategy based on the generic approach ensures that the inspection results can be related to values of the generic parameters and therefore to the underlying models. In doing so, the approach facilitates the learning from in-service experience: the model uncertainties can be periodically updated by comparing the model predictions to the outcomes of the inspections. For many deterioration models such an approach is highly relevant for improving the estimates of the related model uncertainties.

The presented approach has already demonstrated its applicability in several industrial projects on fatigue subjected structures; some of these are reported in Faber et al. (2003b) and Rouhan et al. (2004) for fixed offshore structures, as well as in Goyet et al. (2004) for FPSO's (floating production, storage and offloading units).

### **8.1.1 Originality of work**

The present work has two main objectives: The first is the provision of a reference for the development and the application of the generic approach to RBI as discussed above. The second objective is the advancement of RBI in general through new developments towards the extension of the methodology to deterioration mechanisms other than fatigue and towards the integral treatment of large structural systems. In the context of RBI, a structural system is characterised by the individual hot spots and the functional and stochastic dependencies between these.

The first objective of this work is met by a review of the state-of-the-art in decision theory, deterioration modelling and inspection modelling in view of an application in RBI. On this basis, the generic approach is elaborated through the following new developments:

- A general framework for a generic approach to RBI is established. This includes a clear definition of the different elements of the approach, such as e.g. the generic inspection plans or the generic parameters.
- A procedure for the calculation of the generic inspection plans is described together with an investigation of its accuracy.
- A method for the interpolation of the generic inspection plans is introduced.
- A software design for the application of the generic approach is developed.
- Methods and rules for designing the generic plans are developed and exemplified by an application to fatigue subjected structures.
- For corrosion subjected structures, consistent decision rules for the planning of repairs based on the inspection outcomes are identified. It is demonstrated that these rules enable the application of generic RBI for structures subject to localised corrosion.
- Practical procedures for the actualisation of the inspection plans based on the inspection outcomes are described. These are combined with the development of a methodology for the inspection planning of structures that are subject to modifications in the loading conditions.

The second objective of this work has been addressed through various original contributions, most of which are related to the integral RBI of structural systems. Such an approach is opposed to the traditional RBI procedures which consider all hot spots in a structure individually. These new developments include:

- The nature of maintenance decisions in structural systems is explored. Differentiating between different repair strategies, it is shown how the maintenance optimisation problem should be formulated for different types of systems.
- A system model that allows the consideration of dependencies between the deterioration at the individual hot spots is formulated. Taking basis in the generic approach, this model is applied to the optimisation of inspection efforts in systems. Besides a complete calculation of the optimal strategy, also a practical approach to the consideration of the system effects is proposed.
- A conceptual framework for the modelling of uncertainties in the inspection performance models is introduced. This framework allows for modelling the dependencies between the inspection performances at different locations; the effects of these dependencies are investigated in Straub and Faber (2003a).
- The reliability updating based on the combined effect of indication and measurement of a corrosion defect is introduced. Such a model is essential for the description of the quality of inspections on structures subject to localised corrosion defects and thus for the application of RBI for such deterioration mechanisms.
- Based on the concept of the residual influence factor (*RIF*) it is demonstrated how risk acceptance criteria are to be formulated for the system as a function of the redundancy and the complexity of the structure. Following Straub and Faber (2003b) it is outlined how the dependencies between deterioration failures at the individual hot spots can be addressed in this context.

### 8.1.2 Limitations

The limitations of the approach are outlined in Chapter 1 and 6, namely the restriction to identified deterioration modes and locations, as well as the need for a deterioration model that provides a physical description of the damage in terms of defect sizes. It has been pointed out that the presented approach must be embedded in a general asset integrity management strategy, which requires a clear definition of the interfaces between the RBI and the general strategy. By doing so, the purposeful application of the presented approach is ensured.

For many deterioration modes, the calculated (notional) probabilities of failure are dominated by the model uncertainties. It has been noted that in many instances these uncertainties are difficult to assess. These difficulties must not prevent from an application of the presented methodology, because conceptually these difficulties are just an additional model uncertainty; it is exactly the presented methodology that provides the means of taking all uncertainties into account. However, when the methodology is used to demonstrate compliance with acceptance criteria, a calibration of the probabilistic models to present codes and standards, as presented in Chapter 7, is required, to ensure that the models are consistent with present practice.

## 8.2 Outlook

### 8.2.1 On the probabilistic models

Any application of the methodology presented in the present work requires probabilistic models of both the deterioration as well as the inspection performances. In some areas, these models are highly developed and are readily applicable, as demonstrated in Faber et al. (2003) for fixed offshore structures subject to fatigue. In other areas, and especially for other deterioration mechanisms, such models are still lacking or are incomplete. A major challenge is to bridge the gap between the specialised material scientists interested in the physical understanding of the deterioration processes and the structural engineers requiring quantitative models that describe the stochastic characteristics of the process; in particular the inclusion of epistemic uncertainties in the models is a common source of misunderstandings. It is believed that research in probabilistic deterioration models can be advanced by improved cooperation and communication between the specialists in the various fields.

In regard to the temporal characteristics of the deterioration processes, the above outlined necessity for research on improving the probabilistic models is widely acknowledged. On the other hand, the necessity for models describing the large scale spatial dependencies in the deterioration behaviour has only recently been fully recognized. In the present work, the importance of such models is demonstrated in Chapter 6: They are essential for a realistic description of the system reliability for large structures with high stochastic dependencies between the deterioration at the various locations (hot spots) in the structure; typical examples of such structures are corrosion subjected pipelines or ship structures subject to fatigue deterioration. Additionally it is demonstrated that models of the spatial variability are also required for a full optimisation of the inspection efforts in systems, because they determine the amount of information obtained from one inspection on the state of the entire structure. As a consequence, for many large engineering structures, RBI cannot be applied without some knowledge on the spatial characteristics of the deterioration processes. In line with Vrouwenvelder (2004) it is thus concluded that research towards the improved understanding and modelling of the spatial aspects of deterioration mechanisms is highly relevant. It is suggested to depart from the general concept of modelling the system by means of the largest defects at the hot spots, as introduced in Section 3.5.3.4. Based on such a general concept, models for the individual applications can be derived by analysing the functional and stochastic dependencies in the system<sup>a</sup>, supported by new experimental research and re-evaluation of old tests.

### 8.2.2 On the RBI procedures

In the context of RBI, a structural system is characterised by the individual hot spots and the functional and stochastic dependencies between these. A procedure for the full optimisation

---

<sup>a</sup> In Straub and Faber (2003a) such an analysis is performed for establishing a model that describes the dependencies among the inspection performances in a series of inspections.



of inspection efforts for structural systems based on the generic approach is summarised in Section 6.4. As opposed to the traditional RBI procedure, this approach takes into account the system as a whole and is not restricted to the consideration of all hot spots individually. However, at present, such an approach does not appear applicable in practice because of the required computational efforts<sup>a</sup>. A pragmatic procedure is proposed in Section 6.6; it replaces the time consuming optimisation by an approximate estimation of the optimal inspection coverage. Once the inspections are performed, the generic approach facilitates accounting for the effect of the inspection results on the entire structural system. Although a procedure for the approximate estimation of the optimal inspection coverage is outlined in this work, additional investigations and sensitivity studies are required in order to provide explicit rules for this optimisation. Due to the relevance of such an approach for engineering structures with a large number of hot spots, further developments in this direction are of high relevance.

For many corrosion subjected structures the probabilities of failure are dominated by the uncertainties of slowly varying processes that describe parameters which influence the corrosion rate. Many of these parameters are direct functions of the use of the structure; an example is the temperature in process systems, which is typically a non-ergodic process. Such processes are difficult to describe and predict, but in many instances they can directly be monitored and recorded with little efforts. In Section 5.6 it is proposed to use such data to periodically update the input parameters of the inspection planning procedure. In the author's opinion, this approach is of high practical relevance for corrosion subjected structures (and to a lesser degree also for fatigue subjected structures), but further developments are still required. The identified research needs are:

- The elaboration of the procedure for cases where several slowly varying processes (which describe parameters influencing the deterioration model) interfere.
- The development of rules and methods for updating the uncertainties of the processes in the future based on past measurements.
- The establishment of a procedure for dealing with parameters of the deterioration model for which only partial measurements are available.

When these problems are addressed, and when corresponding deterioration and inspection models are available, the generic approach is believed to have a particular potential for widespread application on pipelines and pressure vessels.

The significance of inspections aimed at the detection of failed hot spots is outlined in Section 7.3. In Straub and Faber (2003b) it is demonstrated on a simplified deterioration model how the effect of such inspections can be assessed; the concept is based on the calculation of the probability of joint occurrence of several hot spots failures. For fatigue subjected structures with high degrees of redundancy, such as ship hulls, the concept provides a means to evaluate a minimum inspection interval. In contrast to the presently applied qualitative determination of such intervals, this concept allows for explicitly formulating the required efforts as a function of the characteristics of the loading. The application of such an approach, however,

---

<sup>a</sup> The availability of faster computers, together with the development of enhanced algorithms, may promote the use of the approach in the future.

requires future investigations based on more detailed deterioration models, especially in regard to the combined spatial and temporal variability of the loading process.

### **8.2.3 On the application and validation**

The presented generic approach facilitates further research into the optimal fatigue design taking into account the full life-cycle costs. The effect of changing one or several design parameters on the total expected maintenance cost can be directly assessed and compared with the design cost. Such investigations can serve as a basis for the derivation of optimal risk acceptance criteria, which take into account the risk reduction costs.

It is important that the application of the presented generic approach to RBI in practice is accompanied by a regular reassessment of the input parameters. When inspection results are available, they provide information about the real probabilities of indication and failure. The comparison of the predicted probabilities of indication to these inspection results allows for validating the method and improving the estimates of the model uncertainties. For this purpose it is proposed to extend the proposed format of the generic database, Annex D, to also include the storage of inspection results, which will highly facilitate the risk management and decision support. When such database systems are already in use for the general maintenance of the structure, the generic database should be integrated into these systems.

## Annexes

### A Analytical solutions for the expected SN damage when the stress ranges are Weibull distributed

For the special but fairly typical case when the stress ranges can be modelled by a two parameter Weibull distribution with scale parameter  $k_{\Delta S}$  and shape parameter  $\lambda_{\Delta S}$ , analytical solutions for the accumulated damage are given in the following:

For the case of a simple one-slope SN diagram with parameters  $C_1$  and  $m_1$ , as represented by Equation (3-1), the expected damage per cycle is

$$E[\Delta D_i] = \frac{1}{C_1} k_{\Delta S}^{m_1} \Gamma\left(1 + \frac{m_1}{\lambda_{\Delta S}}\right) \quad (\text{A-1})$$

For the case of a one slope SN diagram with cut off (Equation (3-2) with  $\Delta S_q = \Delta S_0$ ), the expected damage per cycle is

$$E[\Delta D_i] = \frac{1}{C_1} k_{\Delta S}^{m_1} \Gamma\left(1 + \frac{m_1}{\lambda_{\Delta S}}, \left(\frac{\Delta S_0}{k_{\Delta S}}\right)^{\lambda_{\Delta S}}\right) \quad (\text{A-2})$$

For the general case described by Equation (3-2), the expected damage per cycle is given by Equation A-3. This includes the two slope SN diagram without cut off which is a special case of Equation (3-2) with  $\Delta S_0 = 0$ .

$$E[\Delta D_i] = \frac{k_{\Delta S}^{m_1}}{C_1} \Gamma\left(1 + \frac{m_1}{\lambda_{\Delta S}}, \left(\frac{\Delta S_q}{k_{\Delta S}}\right)^{\lambda_{\Delta S}}\right) + \frac{k_{\Delta S}^{m_2}}{C_1} \Delta S_q^{m_1 - m_2} \left[ \Gamma\left(1 + \frac{m_2}{\lambda_{\Delta S}}, \left(\frac{\Delta S_0}{k_{\Delta S}}\right)^{\lambda_{\Delta S}}\right) - \Gamma\left(1 + \frac{m_2}{\lambda_{\Delta S}}, \left(\frac{\Delta S_q}{k_{\Delta S}}\right)^{\lambda_{\Delta S}}\right) \right] \quad (\text{A-3})$$

If  $N_q$  instead of  $\Delta S_q$ , or  $N_0$  instead of  $\Delta S_0$ , is defined, then the following relationships are useful:

$$\begin{aligned} \Delta S_q &= (C_1/N_q)^{1/m_1} \\ \Delta S_0 &= (C_1/N_0)^{1/m_1}, & \text{1 slope with cut off} \\ \Delta S_0 &= (C_1 \Delta S_q^{(m_2 - m_1)}/N_0)^{1/m_2}, & \text{2 slope with cut off} \end{aligned} \quad (\text{A-4})$$



## B Comparing different crack propagation models

Three different crack growth laws are presented and compared in view of their possible application in RBI. It is thereby of interest to evaluate the differences in  $f_s(\mathbf{s}|t)$ , the distribution of the crack size at different times  $t$  for the individual models. To enable a comparison between the various approaches, the crack growth laws are all calibrated to the same SN model.

### B.1 SN model

The SN model is in accordance with Section 3.2. The limit state function is

$$g_{SN} = \Delta - \nu \cdot T \cdot E[\Delta D_i] \quad (\text{B-1})$$

As the stress ranges are assumed represented by the Weibull distribution,  $E[\Delta D_i]$  is determined according to Annex A. The parameters of the SN model are presented in Table B.1. The applied SN diagram is the DoE D curve (which is equal to the HSE 1.00P curve), in accordance with SSC (1996) and HSE (2001). The scale parameter  $k_{\Delta S}$  is fitted so that it represents a Fatigue Design Factor  $FDF = 2$ .

Table B.1 – Parameters of the SN model (DoE D curve).

Parameter	Dimension	Distribution	Mean	COV
$\Delta$	-	Lognormal	1	0.3
$\nu$	yr <sup>-1</sup>	Deterministic	10 <sup>7</sup>	
$T_{SL}$	yr	Deterministic	40	
$k_{\Delta S}$ (FDF=2)	Nmm <sup>-2</sup>	Deterministic	7.448	
$B_S$	-	Lognormal	1	0.25
$\lambda_{\Delta S}$	-	Deterministic	0.9	
$C_1$	(Nmm <sup>-2</sup> ) <sup><math>m_1</math></sup>	Lognormal	4.48e12	0.51
$m_1$	-	Deterministic	3	
$m_2$	-	Deterministic	5	
$N_q$	-	Deterministic	10 <sup>7</sup>	
$N_0$	-	Deterministic	$\infty$	
$d$	mm	Deterministic	16	

The reliability of the SN model, as evaluated with FORM, is shown in Figure B.1.

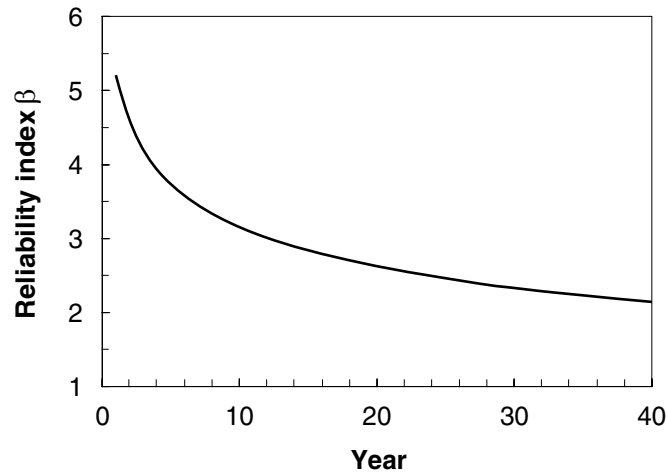


Figure B.1 – Reliability of the considered SN fatigue model.

## B.2 Different crack growth laws

Three different crack growth models are in the following calibrated to the same probabilistic SN model. The inspection plans evaluated with these are then compared in order to determine the influence of different levels of sophistication in the FM modelling. The first two models are commonly applied in the published RBI approaches, the third is a variation of the second model including a threshold on the stress intensity factor range.

First the three models are presented, then the parameters subject to calibration are discussed. Because crack initiation models are treated separately, an initiation time  $N_I = 0$  is assumed. Also the initial crack geometry is chosen the same for the three models; its influence is investigated and discussed separately in Section 5.5 (as a generic parameter).

### B.2.1 Standard two-dimensional crack growth law

This model is applied in the RBI study described in Faber et al. (2003b). It is based on the Newman-Raju (1981) empirical stress intensity factor equation and it has, with slight modifications, a long tradition in RBI, see e.g. Pedersen et al. (1992).

The extended Paris law for the crack growth in the depth and the length direction (in the two extreme points along the crack front) is

$$\begin{aligned} \frac{da}{dN} &= C_{P,a} (\Delta K_a)^{m_{fm}} \\ \frac{dc}{dN} &= C_{P,c} (\Delta K_c)^{m_{fm}} \end{aligned} \quad (\text{B-2})$$

The necessary boundary conditions are given by the number of cycles to initiation,  $N_I$ , and the corresponding initial crack size  $a_0$  and  $c_0$ :

$$a(N = N_I) = a_0, \quad c(N = N_I) = c_0 \quad (\text{B-3})$$

### B.2.1.1 The adapted Newman-Raju solution

The Newman-Raju (1981) empirical stress intensity factor equation assumes a semi-elliptical geometry of the crack at any time, which is thus fully described by the crack depth  $a$  and the crack length  $2c$ . The geometrical model is sketched in Figure B.2.

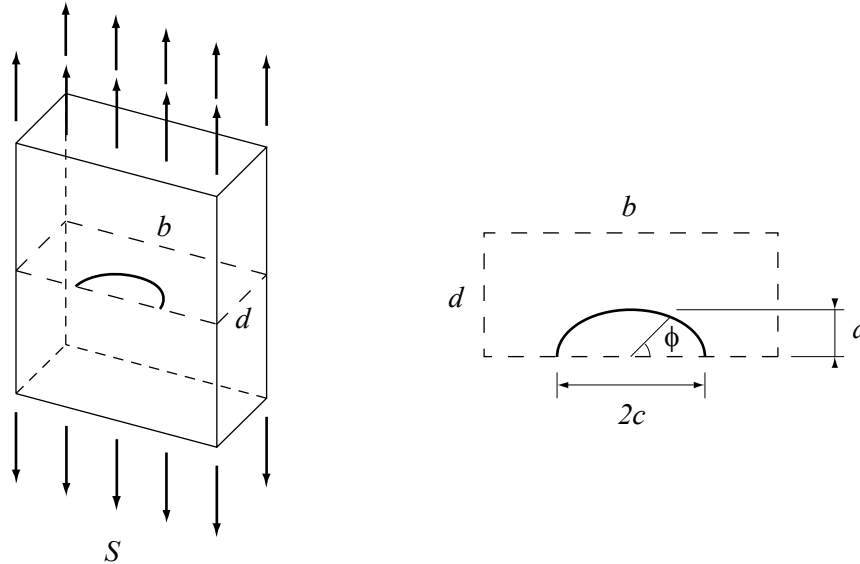


Figure B.2 – The crack geometry for the Newman-Raju model.

The empirical solution by Newman-Raju (1981) for the stress intensity factor in any angle  $\phi$  along the crack front in a finite plate is of the form

$$K_{I, NR}(\phi) = (S_t + H_{NR}(\phi) \cdot S_b) \sqrt{\pi \frac{a}{Q_{NR}}} F_{NR}(\phi) \quad (\text{B-4})$$

The Newman-Raju solution for  $K_{I, NR}$  is valid in the following parameter ranges only:

$$0 < a/c \leq 1, \quad 0 \leq a/d < 1, \quad 0 \leq \phi \leq \pi \quad (\text{B-5})$$

To obtain the stress intensity factors in Paris' equation (B-2), the Newman-Raju solution (B-4) is multiplied by the correction factor  $Y_{NR}$  accounting for the model uncertainties in the expression.

Both  $F_{NR}(\phi)$  and  $H_{NR}(\phi)$  in Equation (B-4) are factors that account for the boundary conditions and are given in the following. They are dependent on crack depth and length, as well as plate thickness  $d$  and width  $b$ . The finite-width correction is, however, neglected here and an infinite plate is assumed, in accordance with Pedersen et al. (1992).  $Q_{NR}$  is a factor defined by the elliptical form of the crack and approximated by Equation B-10.  $S_t$  are the stresses arising from uniform tensional loading and  $S_b$  are the outer fiber stress from bending loads. They are given in terms of the total stress  $S$  and the bending-to-membrane stress ratio  $\eta_S$  as

$$S_t = \frac{S}{1 + \eta_S}, \quad S_{b,0} = \frac{S}{1/\eta_S + 1} \quad (\text{B-6})$$

$S_{b,0}$  are the bending stresses before a crack occurs. Here corrected bending stresses are applied, that account for the load shedding that takes place during crack growth in tubular structures. The model is due to Aaghaakouchak et al. (1989) and assumes a decrease from the initial bending stresses  $S_{b,0}$  that is linear with increasing crack depth:

$$S_b = S_{b,0} \left( 1 - \frac{a}{d} \right) \quad (\text{B-7})$$

Equation B-4 is valid for a plane plate. To account for the presence of the weld, the  $K_{I, NR}$  must be multiplied by a magnification factor  $M_k$ , which is originally given by Smith and Hurworth (1984) and is here taken from Pedersen et al. (1992):

$$M_k = 1 + 1.24e^{-22.2\frac{a}{d}} + 3.17e^{-357\frac{a}{d}} \quad (\text{B-8})$$

As for the solution of Equation B-2 only the extreme angles are of interest, the stress intensity factors can be written as

$$K_a = K_{I, NR} \left( \phi = \frac{\pi}{2} \right) M_k Y_{NR}, \quad K_c = K_{I, NR} (\phi = \pi) M_k Y_{NR} \quad (\text{B-9})$$

### B.2.1.2 Empirical parameters in the Newman-Raju solution

The factor  $Q_{NR}$  is approximated with

$$Q_{NR} = 1 + 1.464 \left( \frac{a}{c} \right)^{1.65}, \quad \frac{a}{c} \leq 1 \quad (\text{B-10})$$

The function  $F_{NR}(\phi)$  is

$$F_{NR}(\phi) = \left( M_1 + M_2 \left( \frac{a}{d} \right)^2 + M_3 \left( \frac{a}{d} \right)^4 \right) f_\phi(\phi) g_\phi(\phi) \quad (\text{B-11})$$

where

$$M_1 = 1.13 - 0.09 \left( \frac{a}{c} \right) \quad (\text{B-12})$$

$$M_2 = \frac{0.89}{0.2 + \left( \frac{a}{c} \right)} - 0.54 \quad (\text{B-13})$$



$$M_3 = 0.5 - \frac{1}{0.65 + \left(\frac{a}{c}\right)} + 14 \left(1 - \frac{a}{c}\right)^{24} \quad (\text{B-14})$$

and

$$f_\phi(\phi) = \left[ \left(\frac{a}{c}\right)^2 \cos^2 \phi + \sin^2 \phi \right]^{\frac{1}{4}} \quad (\text{B-15})$$

$$g_\phi(\phi) = 1 + \left( 0.1 + 0.35 \left(\frac{a}{d}\right)^2 \right) (1 - \sin \phi)^2 \quad (\text{B-16})$$

For the considered special cases, they become

$$f_{\phi,a}\left(\phi = \frac{\pi}{2}\right) = 1, \quad g_{\phi,a}\left(\phi = \frac{\pi}{2}\right) = 1 \quad (\text{B-17})$$

$$f_{\phi,c}(\phi = \pi) = \sqrt{\frac{a}{c}}, \quad g_{\phi,c}(\phi = \pi) = 1.1 + 0.35 \left(\frac{a}{d}\right)^2 \quad (\text{B-18})$$

Equivalently the function  $H_{NR}(\phi)$  is

$$H_{NR,a}\left(\phi = \frac{\pi}{2}\right) = H_2, \quad H_{NR,c}(\phi = \pi) = H_1 \quad (\text{B-19})$$

with

$$H_1 = 1 - 0.34 \cdot \left(\frac{a}{d}\right) - 0.11 \left(\frac{a}{c}\right) \left(\frac{a}{d}\right) \quad (\text{B-20})$$

and

$$H_2 = 1 + G_1 \left(\frac{a}{d}\right) + G_2 \left(\frac{a}{d}\right)^2 \quad (\text{B-21})$$

with

$$G_1 = -1.22 - 0.12 \left(\frac{a}{c}\right) \quad (\text{B-22})$$

and

$$G_2 = 0.55 - 1.05 \left(\frac{a}{c}\right)^{\frac{3}{4}} + 0.47 \left(\frac{a}{c}\right)^{\frac{3}{2}} \quad (\text{B-23})$$

### B.2.1.3 Solution strategy

The coupled differential Equation (B-2) has to be solved numerically. Because the equation has no physical meaning for  $a > d$ , its evaluation may lead to numerical difficulties. The problem can be circumvented by rewriting the equation as

$$\begin{aligned} \frac{dc}{da} &= \frac{C_{P,c}}{C_{P,a}} \left( \frac{\Delta K_c}{\Delta K_a} \right)^{m_{FM}} & c(a_0) &= c_0 \\ \frac{dN}{da} &= \frac{1}{C_{P,a} (\Delta K_a)^{m_{FM}}} & N(a_0) &= 0 \end{aligned} \quad (\text{B-24})$$

Equation B-24 is solved<sup>a</sup> to give the number of cycles to reach a certain crack depth,  $N(a)$ , and the associated crack length,  $c(a)$ . If the crack depth after  $N$  cycles is of interest<sup>b</sup> then Equation B-24 is solved for different  $a$ 's and  $a(N)$  is obtained by interpolation between the different  $a$ . If, despite of the numerical difficulties, alternatively Equation B-2 is applied, then  $a(N)$  is the direct result.

### B.2.1.4 Parameter values

The Paris parameter  $C_{P,a}$  is calibrated to the SN model. The Paris parameter in the width direction is, in accordance with Newman and Raju (1981), modelled by

$$C_{P,c} = 0.9^{m_{FM}} C_{P,a} \quad (\text{B-25})$$

The parameter  $m_{FM}$  is a function of  $C_{P,a}$  as described by Equation (3-16).

The initial crack depth  $c_0$  is modelled in terms of the ratio  $r_{aspect} = a_0 / c_0$  following Section 3.3.2.3.

## B.2.2 Simple one-dimensional Paris law

The one-dimensional Paris law is given by Equation B-26.

$$\frac{da}{dN} = C_P \Delta K^{m_{FM}}, \quad a \geq a_0 \text{ and } K < K_{IC} \quad (\text{B-26})$$

The crack depth  $a$  is obtained by integrating Equation B-26 over all applied stress cycles. The necessary boundary conditions are given by the number of cycles to initiation,  $N_I$ , and the corresponding initial crack size  $a_0$ :

---

<sup>a</sup> The Bulirsch-Stoer method or alternatively the fourth order Runge-Kutta method is applied, see Press et al. (1989).

<sup>b</sup> This is the case in the Monte Carlo simulation as applied for inspection planning.

$$a(N_I) = a_0 \quad (\text{B-27})$$

The stress intensity factor  $K$  is obtained by LEFM analysis (parametric approximations or FE analysis, analytical solutions are generally not available).  $K$  is in general a function of  $a$  and  $a/d$ . A common model is given as (see e.g Madsen et al. 1986)

$$K = Y_G(a) S \sqrt{\pi a} \quad (\text{B-28})$$

where  $Y_G(a)$  is a geometry factor accounting for the crack size and the considered geometrical boundary conditions and can be obtained from experiments. It is possible to derive a one-dimensional  $Y_G$  from a two-dimensional  $Y_G$  such as the empirical Newman-Raju solution (Section B.2.1) with assumed depth-to-length ratio  $a/c$ . Figure B.3 and Figure B.4 show the Newman-Raju geometry function for constant  $a/c$  and a bending-to-membrane stress ratio  $\eta_s = 1$ , where also the magnification factor  $M_k$ , Equation B-8, is included.

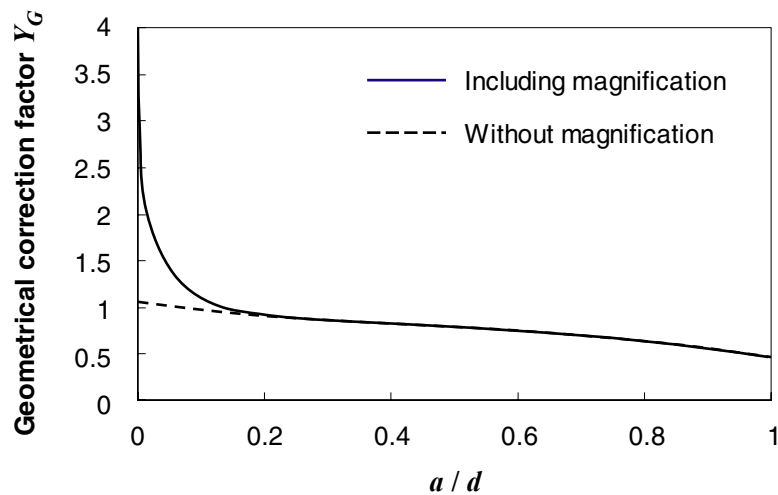


Figure B.3 – Geometry factor  $Y_G(a)$  for constant  $a/c = 0.2$ .

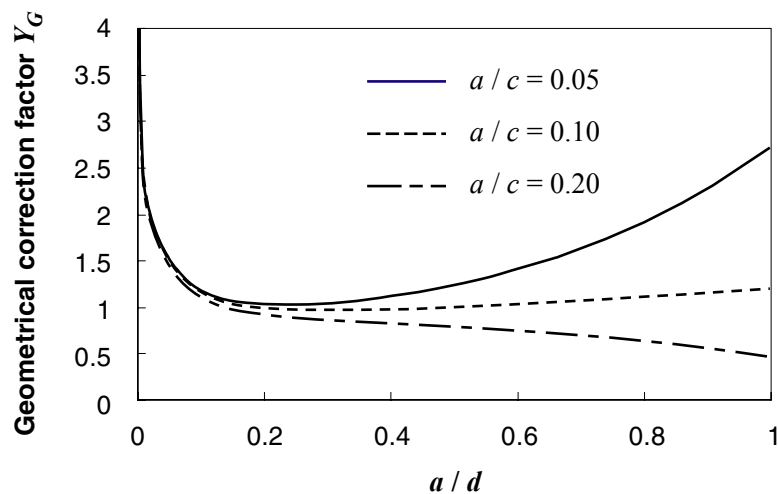


Figure B.4 – Geometry factor  $Y_G(a)$  for different constant  $a/c$ .

The one-dimensional crack growth model is evaluated by separation and integration of the variables in Equation B-26<sup>a</sup>, see e.g. Madsen et al. (1986):

$$C_P \cdot \Delta S^{m_{FM}} \cdot (N - N_I) = \int_{a_0}^a \frac{dz}{Y_G(z)^{m_{FM}} (z \cdot \pi)^{m_{FM}}} \quad (\text{B-29})$$

In general the crack depth after  $N$  cycles is of interest which is obtained by solving Equation B-29 with respect to  $a$ . If the geometry function is approximated by a constant value, i.e. if its dependency on  $a$  is neglected, then an explicit solution for  $a$  exists:

$$a(N) = \left( a_0^{(2-m_{FM})/2} + \frac{2-m_{FM}}{2} C_P (Y_G \pi^{1/2} \Delta S)^{m_{FM}} (N - N_I) \right)^{2/(2-m_{FM})}, m_{FM} \neq 2 \quad (\text{B-30})$$

This is the model applied. The constant  $Y_G$  is obtained from the calibration of the model to the SN model. Its distribution type and COV are in accordance with Faber et al (2000).

### B.2.3 Model including the crack-closure effect

The one-dimensional crack growth model based on the formulation by Elbers (1971) is

$$\frac{da}{dN} = C_P \Delta K_{eff}^{m_{FM}} \quad (\text{B-31})$$

$K_{eff}$  is evaluated according to Equation (3-15) as a function of  $K$ , the stress ratio  $R_S$  and the stress intensity at which the crack opens, denoted by  $K_{op}$ .  $K$  is derived as described in the previous section for the classical Paris law. In analogy to that model,  $Y_G$  is assumed constant with respect to  $a$ .  $R_S$  must be determined by the stress calculations or estimated from experience.  $K_{op}$  is determined by the calibration to the SN model, as this is the parameter for which least information is available.

The crack size after  $N$  cycles can, in principal, be evaluated as for the classical one-dimensional Paris law. In analogy to Equation B-29 it is

$$C_P \cdot (N - N_I) = \int_{a_0}^a \frac{dz}{\Delta K_{eff}(z)^{m_{FM}}} \quad (\text{B-32})$$

The integration in Equation B-32 has to be solved numerically. Note that if  $\Delta K_{eff}$  is equal to zero for any value between  $a_0$  and  $a$ , then the integral has no solution. In that case the crack stops to propagate; due to the assumed constant amplitude loading no further crack propagation is possible and the crack depth  $a$  cannot be reached.

Following the discussion in Section 3.3.3.3, the stress ranges are approximated by the equivalent stress range  $\Delta S_e$ , assuming a constant amplitude loading. This assumption is

---

<sup>a</sup> Given constant amplitude loading, as discussed in Section 3.3.3.3.

crucial for this crack growth model, because in case  $\Delta S_e$  is below the threshold at which crack growth occurs, the crack will not propagate.

#### B.2.4 Parameters of the models

The parameters of the models are calibrated to the SN model according to the procedure described in Section 3.4. Figure B.5 shows the goodness-of-fit of the three calibrations.

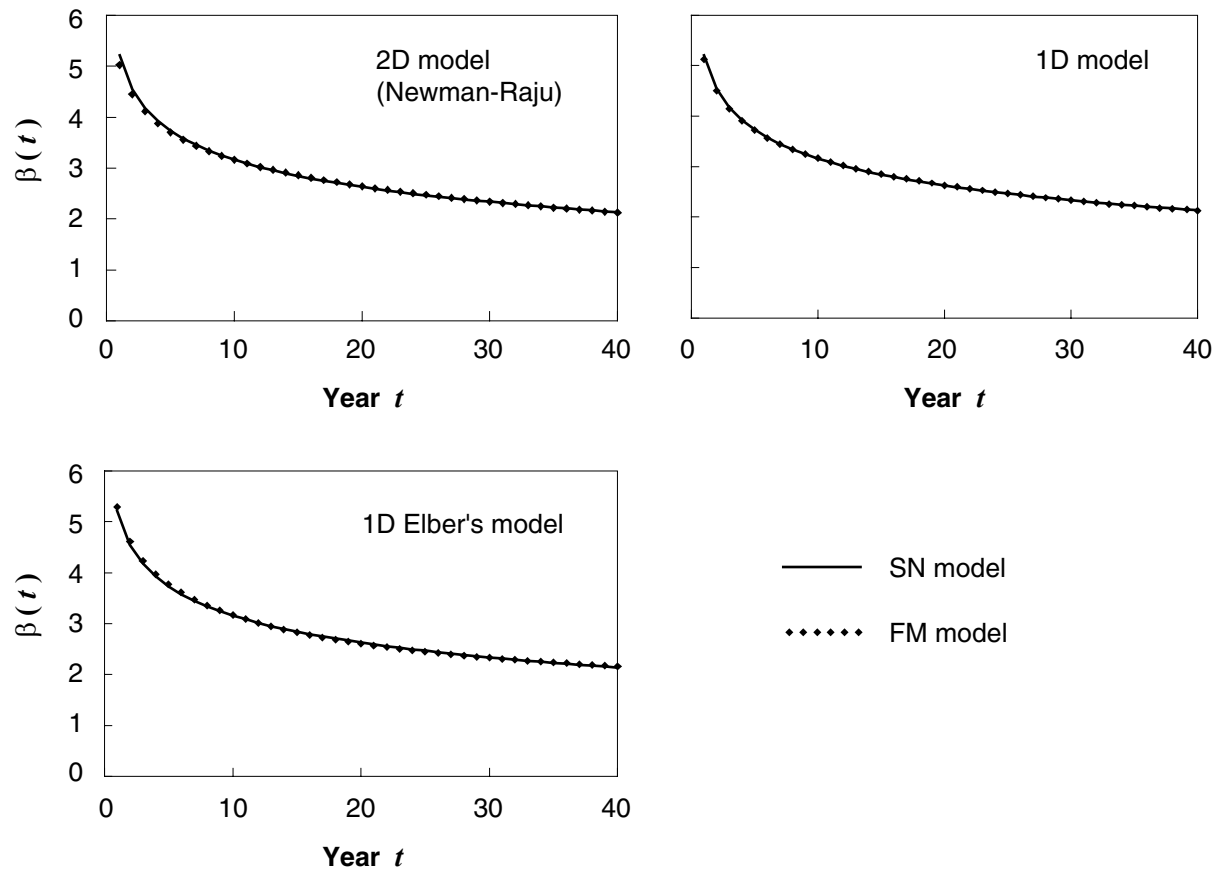


Figure B.5 – Calibration of the FM models to the SN model.

In Table B.2 the resulting parameters are collected for all cases. The calibrated parameters are all in the physically admissible domain. From the differences in  $\ln C_p$  it is apparent that the predicted crack growth behaviour is different for the three models.  $Y_G$  in the 1D model is very low, which can be interpreted as an indication that the simple model is not well suited for the considered problem.  $K_{op}$  is low compared to the values published for  $\Delta K_{th}$ . This can be explained by the applied constant amplitude loading. If  $\Delta S_e$  is below the threshold, the model predicts zero crack growth. This underestimation of the real situation with variable amplitude loading is compensated by a lower  $K_{op}$ .

Table B.2 – Parameters of the calibrated FM models.

Parameter	Used in model #	Dimension	Distribution	Mean	COV
$v_e$	1-3	yr <sup>-1</sup>	Deterministic	10 <sup>7</sup>	
$T_{SL}$	1-3	yr	Deterministic	40	
$\Delta S_e$	1-3	Nmm <sup>-2</sup>	Deterministic	22.26	
$B_S$	1-3	-	Lognormal	1	0.25
$\eta_S$	1	-	Deterministic	1.5	
$K_{op}$	3	Nmm <sup>-3/2</sup>	Deterministic	34.3*	
$R_S$	3	-	Deterministic	0.5	
$\ln C_P$	1	Corresponding to N & mm	Normal	-30.91*	0.77
	2		Normal	-25.08*	0.77
	3		Normal	-28.02*	0.77
$m_{FM}$	1-3	-	Deterministic	$m_{FM} = f(C_P)$ according to Equation (3-16)	
$Y_{NR}$	1	-	Lognormal	1.20*	0.1
$Y_G$	2	-	Lognormal	0.285 *	0.1
	3	-	Lognormal	1	0.1
$a_0$	1-3	mm	Exponential	0.11	0.11
$a_0/c_0$	1	-	Deterministic	0.2	
$d$	1-3	mm	Deterministic	16	

\* these parameters are calibrated to the SN model

### B.3 Results

The crack propagation models resulting from the calibration were analysed using Monte Carlo Simulation (MCS). Figure B.6 shows the resulting probability density functions for the crack size after 40 years as evaluated for the three different models. The probability of failure  $p_F$  (which is equal to the probability of the crack having reached the material thickness) is therein presented in a separate diagram.  $p_F$  should in principle be the same for all approaches, and the deviations are due to the approximate nature of the FORM algorithm used in the calibration. Comparing the results shown in Figure B.5 to the those presented in Figure B.6 it becomes apparent that for the 1D model the  $p_F$  is overestimated by FORM by about 50% ( $\beta_{FORM} = 2.13$  compared to  $\beta_{MCS} = 2.3$ , where the MCS was performed with 2 Mio. realisations). In this case the inaccuracies can be improved by applying SORM instead of FORM in the calibration algorithm.

Figure B.6 illustrates that although the models have similar reliability indexes with regard to through-cracks, their crack size distributions vary considerably. This is also reflected in Figure B.7 where the three crack growth models are shown with the parameters taken as their mean values. The model following Elber thereby shows no crack growth due to the threshold, which, for the mean values of the parameters, is not exceeded.

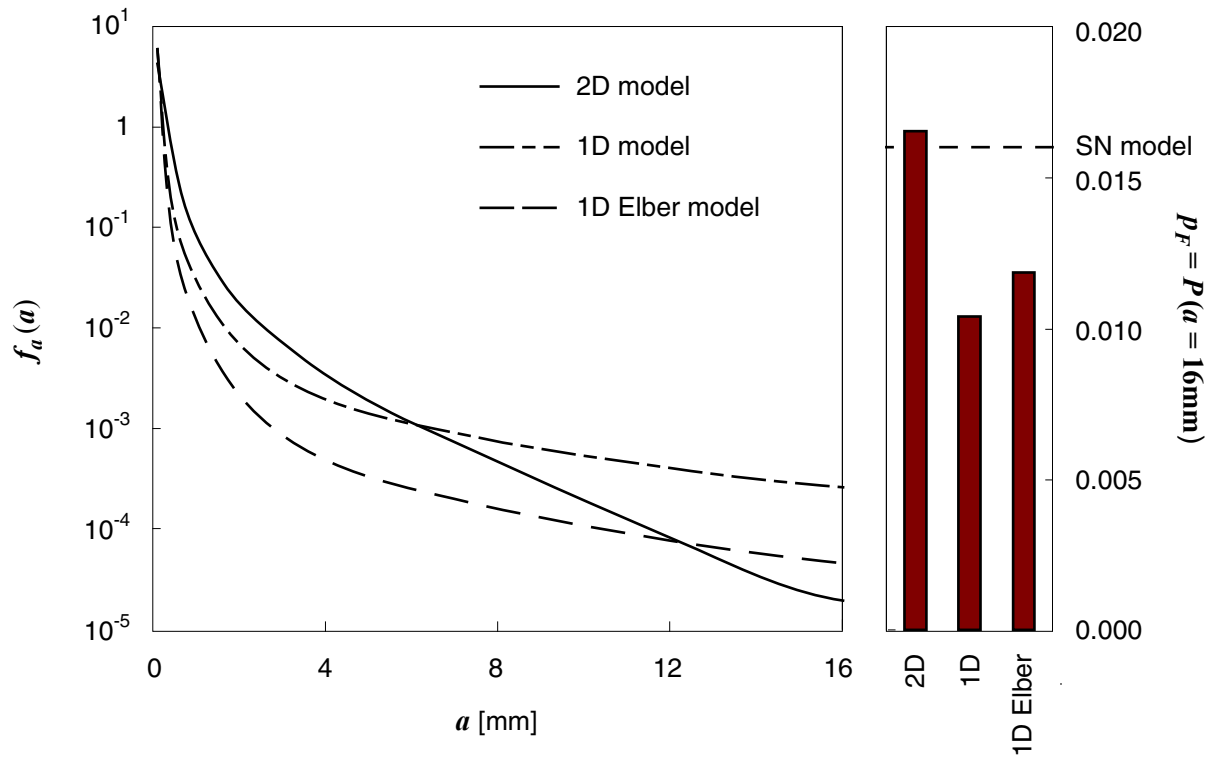


Figure B.6 – Probability density function of the crack depth after 40 years for the three different models.

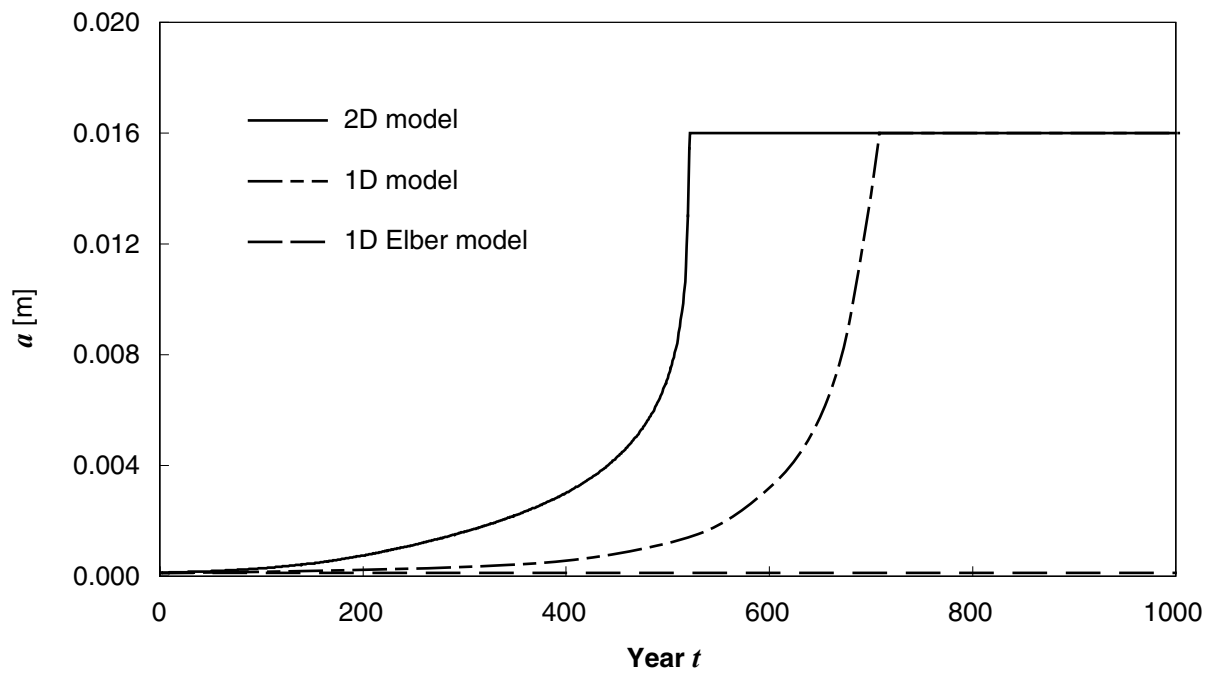


Figure B.7 – Crack growth prediction for the three models when applying the mean values of all random variables.

## B.4 Conclusions

The results demonstrate that the choice of the crack growth model is of crucial importance. Unfortunately, the comparison does not allow judging which model is best; however, some important conclusions can be drawn based on the results. An important check for any model is to verify if the calibration leads to realistic values of the calibrated parameters. In the presented example, this criterion is best fulfilled by the 2D crack growth model. Additionally, when comparing the resulting models, it can be checked which model is most conservative in regard to the inspection planning. Although the inspection times have not been calculated for the presented examples, based on Figure B.6 and Figure B.7 it is realised that the 2D crack growth model exhibits the fastest crack growth. This model will consequently demand for more inspections to comply with a given acceptance criterion  $\Delta p_F^{max}$ . The 1D model on the other hand will lead to the lowest number of inspections required.



## C Accuracy of the Monte Carlo simulation

When evaluating the reliability by means of Monte Carlo simulation (MCS), the number of simulations  $n_{MC}$  determines the accuracy of the calculation results. The optimal  $n_{MC}$  must thus be identified in order to achieve a balance between the computational efforts and the accuracy of the resulting inspection plans. This annex first introduces the concepts for evaluating the accuracy of MCS in general, following Melchers (1999b); it then introduces a specific methodology for the application in RBI. A discussion on the final choice of  $n_{MC}$  concludes this annex.

### C.1 Accuracy of MCS in general

In MCS, each outcome of the simulation is a sample of the population of  $g(\mathbf{X})$ , the limit state function (LSF) with probabilistic parameters  $\mathbf{X}$ . These allow to estimate the probability  $p$  that  $g(\mathbf{X}) \leq 0$ : the Monte Carlo estimate of a probability,  $p_{MC}$ , is an unbiased estimator of the true probability  $p$ .

If the indicator function  $I_F$  is introduced as

$$\begin{aligned} I_F[g(\cdot)] &= 1, & g(\cdot) &\leq 0 \\ I_F[g(\cdot)] &= 0, & g(\cdot) &> 0 \end{aligned} \quad (C-1)$$

then the sample statistics of  $p_{MC}$  are given by Equations (C-2) and (C-3), with  $\hat{\mathbf{x}}_i$  being the  $i^{\text{th}}$  vector of random simulation outcomes.

$$E[p_{MC}] = \frac{1}{n_{MC}} \cdot \sum_1^{n_{MC}} I_F[g(\hat{\mathbf{x}}_i)] \quad (C-2)$$

$$S^2[p_{MC}] = \frac{1}{n_{MC}} \cdot \frac{1}{n_{MC} - 1} \cdot \left( \sum_1^{n_{MC}} I_F^2[g(\hat{\mathbf{x}}_i)] - n_{MC} \cdot E^2[p_{MC}] \right) \quad (C-3)$$

As  $I_F^2[x] = I_F[x]$ , Equation (C-3) can be rewritten as

$$S^2[p_{MC}] = \frac{E[p_{MC}] - E^2[p_{MC}]}{n_{MC} - 1} \quad (C-4)$$

and the sample variation is thus a direct function of the sample mean. This is in accordance with the formulation by Shooman (1968). Because  $p_{MC}$  is determined as the sum of independent sample functions, its distribution approaches a Normal distribution for  $n_{MC} \rightarrow \infty$  according to the central limit theorem.

## C.2 Accuracy of MCS for inspection planning

A main objective of the MCS in inspection planning is the determination of the time of inspections (given by the time until a certain annual probability of failure, the threshold  $\Delta p_F^T$ , is exceeded). The accuracy of the MCS can thus be expressed by the probability of an error in the determination of the inspection year,  $P(\varepsilon_{t_{insp}})$ . This error includes errors of only one year, but also errors of several years. As discussed in Section C.3, based on the presented methodology it is possible to also evaluate the probability of an error of two years or generally an error of  $x$  years.

If a specific accuracy is desired, the required number of simulations  $n_{MC}$  clearly depends on the outcome of the simulations, and would thus have to be determined during the simulation. This is not a practical procedure for the evaluation of the inspection plans and a different approach is proposed. It takes basis in the fact that the sample statistics of the MCS estimate is a function of only  $p_{MC}$  and  $n_{MC}$ . Additionally an assumption regarding the increase in the annual failure probability with time must be made, which may be taken from the calibration calculations performed with FORM. The approach is introduced in the following together with an illustration on the calculations for the RBI project reported in Faber and Straub (2003).

First the decrease in reliability with time is evaluated from the calibration calculations. This is expressed by the change in the annual probability of failure, denoted by  $\Delta^2 p_F$  and defined in Equation (C-5) in accordance with Figure C.1.

$$\Delta^2 p_F(t_1) = \frac{\Delta p_F(t_1 + \Delta t/2) - \Delta p_F(t_1 - \Delta t/2)}{\Delta t} \quad (C-5)$$

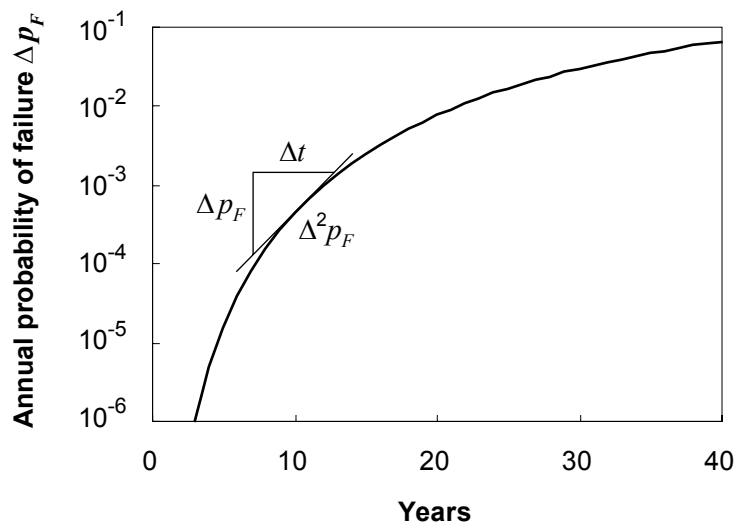


Figure C.1 – Annual increase of  $\Delta p_F$  for a generic inspection plan with  $FDF = 1$ .

For the illustration, three different generic inspection plans are considered. They are defined by the deterioration models from Faber and Straub (2003) together with the generic parameters presented in Table C.1. The reliability of case A is illustrated in Figure C.1. Table

C.1 additionally gives the values of  $\Delta^2 p_F$  as obtained by the FORM calculations performed during the calibration of the crack growth model to the SN model.

Table C.1 – Values of the generic parameters and yearly increase of the annual probability of failure for three generic cases.

Case	Generic parameters				$\Delta^2 p_F$ [yr <sup>-2</sup> ] around $\Delta p_F^T$ [yr <sup>-1</sup> ]		
	$FDF$	$CoV_{B_s}$	$d$ [m]	$DoB$	$\Delta p_F^T = 10^{-5}$	$\Delta p_F^T = 10^{-4}$	$\Delta p_F^T = 10^{-3}$
A	1.0	0.16	0.010	0.0	9.8e-6	7.0e-5	3.9e-4
B	3.0	0.25	0.010	0.8	6.6e-6	4.1e-5	2.0e-4
C	5.0	0.14	0.050	0.0	1.9e-6	-	-
Worst case: Assumed minimum $\Delta^2 p_F$ :					1.0e-6	1.0e-5	1.0e-4

If  $\Delta p_F$  in the year before the threshold is reached is calculated by MCS as  $\Delta \hat{p}_{F,1}$ , then  $\Delta p_{F,1}$  is described by the cdf  $F_{\Delta p_{F,1}} \sim N(\Delta \hat{p}_{F,1}, S[\Delta \hat{p}_{F,1}])$ , where  $S[\Delta \hat{p}_{F,1}]$  is evaluated from Equation (C-4).  $\Delta p_F$  in the year after the threshold is reached is denoted by  $\Delta p_{F,2}$ , it is equivalently modelled by  $F_{\Delta p_{F,2}} \sim N(\Delta \hat{p}_{F,2}, S[\Delta \hat{p}_{F,2}])$ . The probability of an error in the determination of the inspection time can then be written as

$$\begin{aligned} P(\varepsilon_{t_{insp}} | \Delta \hat{p}_{F,1}, \Delta \hat{p}_{F,2}, \Delta p_F^T, n_{MC}) &= P(\Delta p_F^T < \Delta p_{F,1} \cup \Delta p_F^T > \Delta p_{F,2}) \\ &= (1 - F_{\Delta p_{F,1}}(\Delta p_F^T)) + F_{\Delta p_{F,2}}(\Delta p_F^T) \end{aligned} \quad (C-6)$$

The summation of the probabilities of the two individual failure events, namely that the inspection is demanded too early or too late, is based on the fact that the two events are mutually exclusive.

Equation (C-6) can be applied to estimate the probability of an error in the determination of the inspection years after the calculations have been performed. However, for practical applications it is generally of interest to determine the error probability for a specific  $n_{MC}$  before the calculations are performed, i.e. when  $\Delta \hat{p}_{F,1}$  and  $\Delta \hat{p}_{F,2}$  are unknown. This is facilitated by the following considerations: Assuming that the values of  $\Delta p_{F,1}$  and  $\Delta p_{F,2}$  are known, the outcomes of the MCS are predicted as normal distributed around the true values with standard deviations given as

$$\sigma_{\Delta \hat{p}_{F,i}} = \frac{E[\Delta p_{F,i}] - E^2[\Delta p_{F,i}]}{n_{MC}} \quad (C-7)$$

For given  $\Delta p_{F,1}$  and  $\Delta p_{F,2}$ , the probability that the MCS correctly predicts the required inspection time can thus be calculated by Equation (C-8), as illustrated in Figure C.2.

$$\begin{aligned} P(\varepsilon_{t_{insp}} | \Delta p_{F,1}, \Delta p_{F,2}, \Delta p_F^T, n_{MC}) &= P(\Delta p_F^T < \Delta \hat{p}_{F,1} \cup \Delta p_F^T > \Delta \hat{p}_{F,2}) \\ &= (1 - F_{\Delta \hat{p}_{F,1}}(\Delta p_F^T)) + F_{\Delta \hat{p}_{F,2}}(\Delta p_F^T) \end{aligned} \quad (C-8)$$

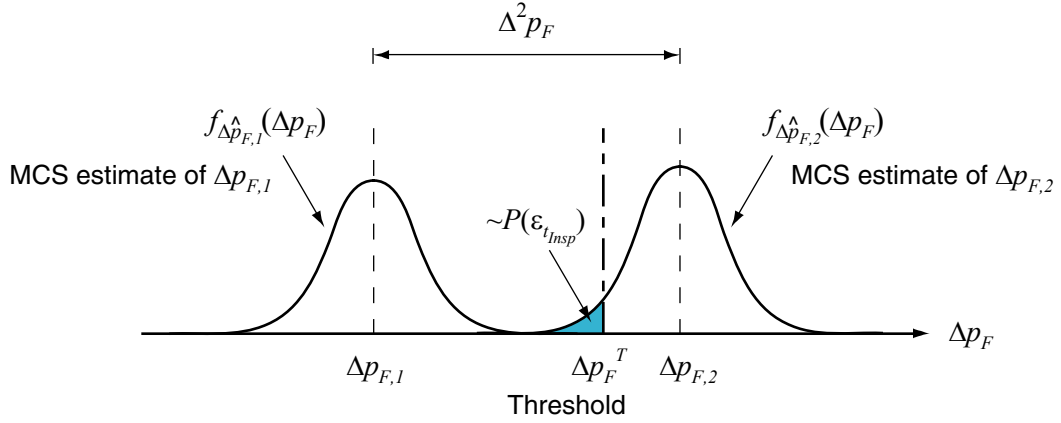


Figure C.2 - Illustration of Equation (C-8).

In practice,  $\Delta p_{F,1}$  and  $\Delta p_{F,2}$  are not known, but, with  $\Delta^2 p_F = \Delta p_{F,2} - \Delta p_{F,1}$ , they are limited to

$$\begin{aligned} \Delta p_F^T - \Delta^2 p_F &\leq \Delta p_{F,1} \leq \Delta p_F^T \\ \Delta p_F^T &\leq \Delta p_{F,2} \leq \Delta p_F^T + \Delta^2 p_F \end{aligned} \tag{C-9}$$

Within these boundaries, they can lie everywhere with equal probability. This can be accounted for by integrating over this range, which leads to the final estimation of the error probability as a function of  $n_{MC}$  and  $\Delta^2 p_F$ :

$$P(\varepsilon_{t_{insp}} | \Delta^2 p_F, \Delta p_F^T, n_{MC}) \approx \frac{1}{\Delta^2 p_F} \int_{\Delta p_F^T - \Delta^2 p_F}^{\Delta p_F^T} P(\varepsilon_{t_{insp}} | \Delta p_F, \Delta p_F + \Delta^2 p_F, \Delta p_F^T, n_{MC}) d\Delta p_F \tag{C-10}$$

Figure C.3 and Figure C.4 show the application of Equation (C-10) based on the  $\Delta^2 p_F$  values from Table C.1.

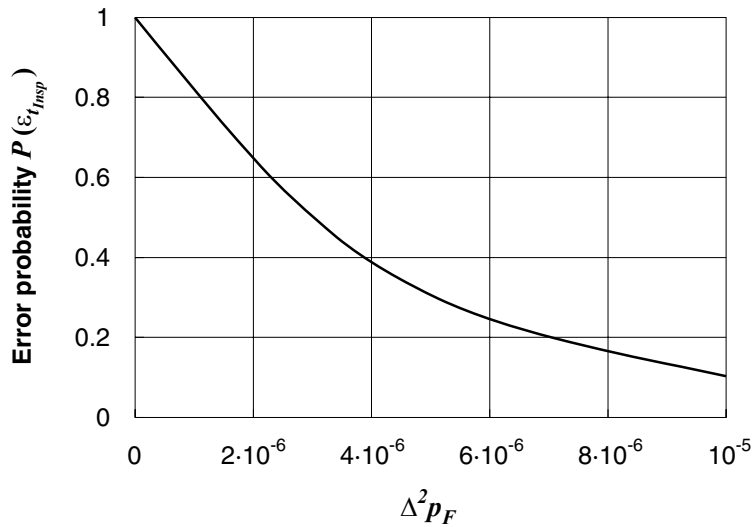


Figure C.3 - Probability of demanding the inspection in the wrong year for a threshold  $p_F^{th} = 10^{-5}$  and  $n_{MC} = 2 \cdot 10^6$  simulations as a function of  $\Delta^2 p_F$ , the annual increase in  $\Delta p_F$ .

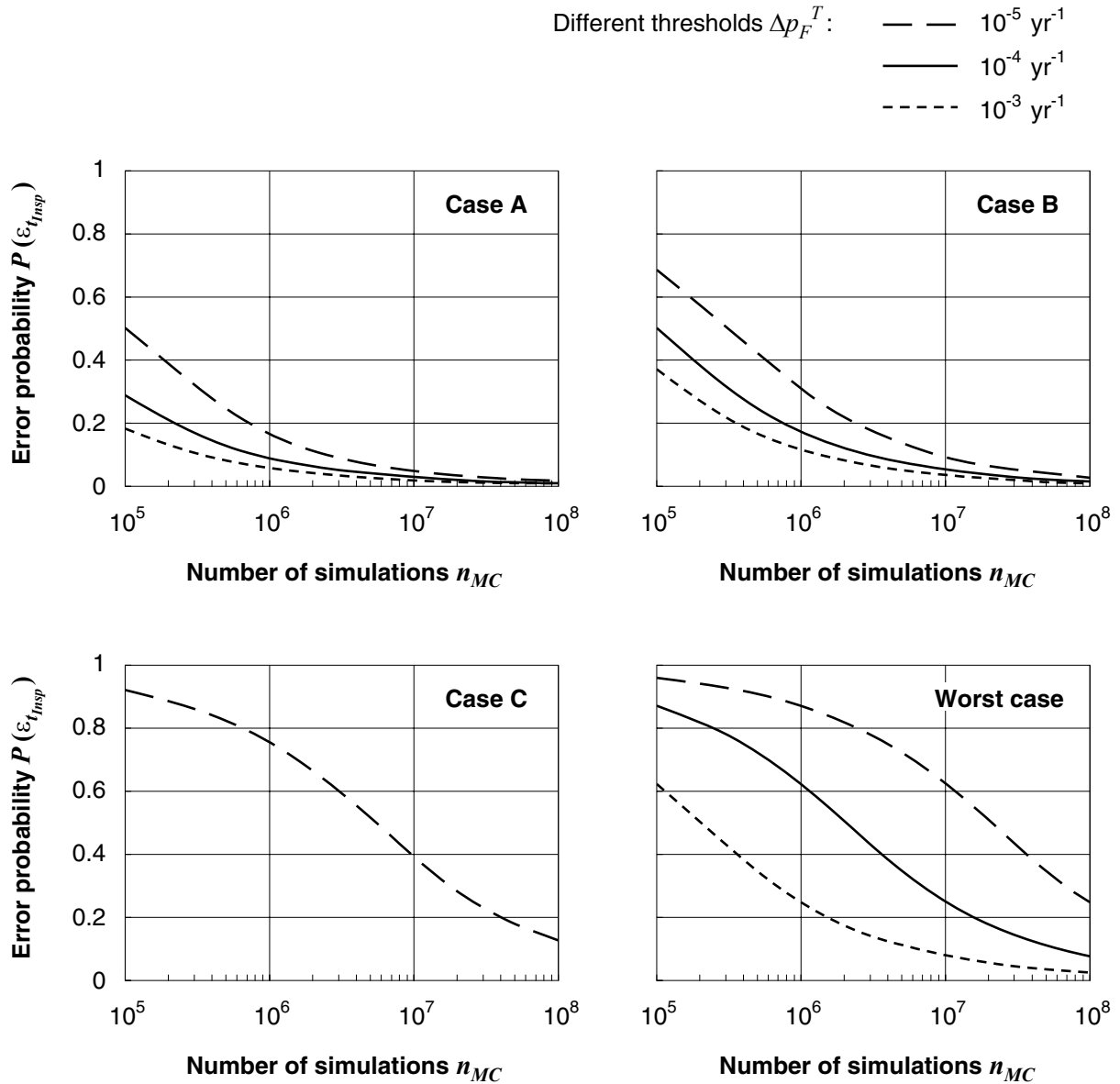


Figure C.4 - Probability of prescribing the inspection in a wrong year for the cases from Table C.1.

### C.3 Discussion

In this work, all calculations which are performed by means of MCS are performed with  $n_{MC} = 2 \cdot 10^6$  simulations. Figure C.3 and Figure C.4 indicate that the probability of an error in the inspection plans is considerable for this value of  $n_{MC}$ . However, it should be borne in mind that the computation time increases linearly with  $n_{MC}$ , whereas the accuracy increases only approximately linearly with  $\sqrt{n_{MC}}$ . Regarding the large computation times, a substantial increase in the accuracy through increasing  $n_{MC}$  is not feasible. Fortunately, the error probability is larger for cases with smaller  $\Delta^2 p_F$ , i.e. for the cases where the inspections are required at later times. The lowest accuracy is achieved for the situations where an inspection is required in the last year of service. Inspections in the distant future have a smaller impact

on the total expected cost than those in the near future; consequently the impact of an error is inverse proportional to its occurrence probability.

Note that an error is defined as not prescribing the correct inspection year, which is not necessarily serious. By means of the presented equations also the probability of an error of more than one year or more than two years can be calculated by changing  $\Delta^2 p_F$  accordingly:  $\Delta t$  in Equation (C-5) is simply set equal to the considered time period.

The presented results are the estimation of the accuracy before the calculations are performed. Once the inspection plans are obtained, the probability of an error can be determined exactly by means of Equation (C-6). Table C.2 shows the effectively observed  $P(\varepsilon_{t_{insp}})$  evaluated with the values of  $\Delta \hat{p}_{F,1}$  and  $\Delta \hat{p}_{F,2}$  obtained during the calculations. It is observed that the effective errors in this example are in most cases smaller than those predicted before the calculations are performed.

Table C.2 – Observed probabilities of an error in the inspection times ( $N_{MC} = 2 \cdot 10^6$ ).

Case	Observed $P(\varepsilon_{t_{insp}})$ for different $\Delta p_F^T$		
	$\Delta p_F^T = 10^{-5}$	$\Delta p_F^T = 10^{-4}$	$\Delta p_F^T = 10^{-3}$
A	$5.8 \cdot 10^{-2}$	$1.5 \cdot 10^{-4}$	$7.4 \cdot 10^{-3}$
B	0.32	$5.4 \cdot 10^{-2}$	$1.2 \cdot 10^{-3}$
C	0.67	-	-

An aspect which that has not been considered so far is that the number of simulations  $n_{MC}$  decreases as the time in the simulation advances, especially if several inspections are performed. This is because the annual probability of failure  $\Delta p_F$  is conditional on survival in the previous years and conditional on no-indication at previous inspections. With each conditional event, some simulations are excluded from the calculations and  $n_{MC}$  is reduced. This effect is illustrated in Figure C.5, showing the increased scattered in the calculations with advancing time and number of inspections.

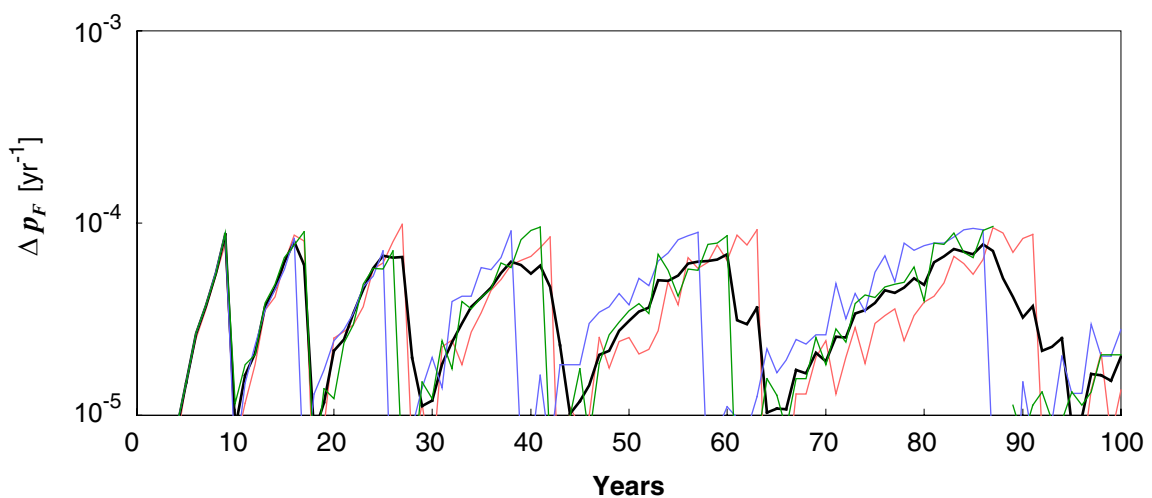


Figure C.5 –  $\Delta p_F$  of the reference case from Section 5.5 for a threshold  $\Delta p_F^T = 10^{-4} \text{ yr}^{-1}$ , calculated in different runs, each with  $2 \cdot 10^6$  simulations. The bold line indicates the average.

## D iPlan.xls

The generic database is provided in the form of an Excel workbook named *iPlan.xls*. This annex gives an overview on *iPlan.xls* as developed in Section 5.5 for fatigue subjected structures. The design of the generic database for the application to corrosion subjected structures, as introduced in Section 5.6, is similar.

### D.1 Concept

The generic inspection plans are stored in hidden worksheets in *iPlan.xls* according to the database scheme outlined in Section 5.3.2. Visual Basic for Application (VBA) is used for the computation of the routines that perform the evaluation of the expected costs, the interpolation of the inspection plans for the specific hot spots and the presentation of the final results<sup>a</sup>. Although this software layout is not optimised for computational speed, it ensures greatest flexibility for both the designer and the user of the database. All the options of Excel are available for the user to illustrate the results and full compatibility with the common software applied for reporting purposes is ensured. If desired, it is furthermore possible to uncover the database and the codes to the user.

### D.2 Input and calculation options

The input/output is organised in different worksheets. All input is entered in the “Parameter Input” worksheet shown in Figure D.3. This includes a project name, the service life period  $T_{SL}$ , the year of installation and the parameters of the specific hot spots in the structure. These include an identifier (index), the specific values of the generic parameters, the cost model and an acceptance criterion  $\Delta p_F^{max}$ , which is defined in accordance with Chapter 7. The program requires that all hot spots are entered in successive lines. If an empty line is encountered, the program stops the execution. The input sheet furthermore provides an additional option: For structures, where inspection campaigns are carried out only every other year, the option “bi-yearly inspections” is available. The resulting inspection plans are then automatically rearranged.

In the iPlan menu, presented in Figure D.1, additional options and information are available. When “iPlan options” is selected, a window opens that provides the different options in regard to the calculation of the expected costs. This window is shown in Figure D.2, which illustrates the default values for these options. It can be chosen whether false indications are to be considered (by use of the *PFI*) or not ( $PFI = 0$ ). Furthermore, in accordance with Annex

---

<sup>a</sup> The computation of inspection plans thus requires that the use of *macros* in Excel is allowed. This depends on the settings in the Tools/Options→Security→Macro Security menu.

It must be decided whether to apply the linear or the logarithmic interpolation algorithm. Following the discussion in Section 5.5.9.3 the logarithmic interpolation is used by default. Finally it can be selected which simplification rule to apply, (a) or (b), which are defined in accordance with Section 2.4 and which concern the assumptions regarding the behaviour of the hot spots after a repair. Note that the speed of the calculations is dependent on the chosen simplification rule: If rule (a) is chosen, the calculations may become very slow, depending on the required number of inspections and on the number of generic parameters. Therefore, if only the inspection times are of interest, simplification rule (b) should be activated. In case rule (a) is selected and the computation time is too large, the evaluation of the inspection plans can be interrupted by pressing the “Esc” key.

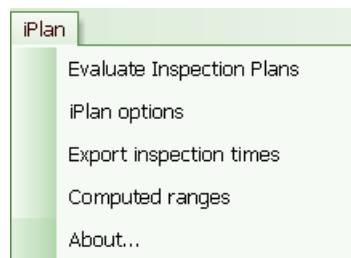


Figure D.1 - The iPlan menu in the worksheet.

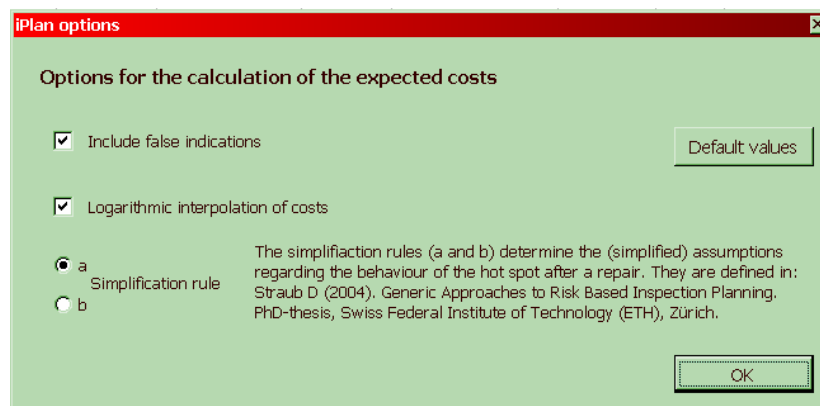


Figure D.2 – The “iPlan options” window.

The “Computed ranges” and the “About...” function in the iPlan menu (Figure D.1) provide information about iPlan.xls. The “Export inspection times” function in the iPlan menu (Figure D.1) allows exporting the resulting inspection times, which are provided in a graphical format, into a numerical format. Thereby only the inspection times of the active worksheet are exported.

The evaluation of the inspection plans is initiated by selecting the “Evaluate Inspection Plans” function in the iPlan menu.



iPlan PhD\_1.xls

**iPlan PhD**

Input sheet

Project name: Test Jacket

Date: 2004-01-24  
Prepared by: DS  
Checked by:  
Approved by:

Bi-Yearly Inspections  
 Odd Years  
 Even Years

Platform installation year: 0  
Service life [Yrs]: 40

Index	Median			λ	ΔS	V [Yr-1]	Thickness		DoB	Fatigue		RIF	Cost Model				
	BS	COV	BS				[m]	Initiation Model		Life [Yrs]	Inspection model		Threshold [pf/yr]	Comments	Inspection Repair	Failure	Interest
Case 1	1.00	0.30	1.00	0.70	3.00E+06	3.00E+06	1.00E-02	2.00E-01	Lassens_Model	200	MPI_Tubular_ICON	1.0E-04	0.75	0.001	0.01	1	0.05
Case 2	1.00	0.35	1.00	0.90	3.00E+06	3.00E+06	4.00E-02	3.00E-01	Lassens_Model	135	MPI_Tubular_ICON	1.0E-04	0.75	0.001	0.01	1	0.05
Case 3	1.00	0.33	1.00	1.10	3.00E+06	2.00E-02	2.00E-02	4.00E-01	Lassens_Model	83	MPI_Tubular_ICON	1.0E-04	0.75	0.001	0.01	1	0.05
Case 4	1.00	0.30	1.00	1.30	3.00E+06	1.30E-02	1.30E-02	5.00E-01	Lassens_Model	64	MPI_Tubular_ICON	1.0E-04	0.75	0.001	0.01	1	0.05
Case 5	1.00	0.40	1.00	1.50	3.00E+06	5.00E-02	5.00E-02	6.00E-01	Lassens_Model	175	MPI_Tubular_ICON	1.0E-04	0.75	0.001	0.01	1	0.05
Case 6	1.00	0.35	1.00	1.00	3.00E+06	3.00E-02	7.00E-01	7.00E-01	Lassens_Model	302	MPI_Tubular_ICON	1.0E-04	0.75	0.001	0.01	1	0.05
Case 7	1.00	0.35	1.00	1.00	3.00E+06	8.00E-03	8.00E-01	8.00E-01	Lassens_Model	79	MPI_Tubular_ICON	1.0E-04	0.75	0.001	0.01	1	0.05
Case 8	1.00	0.30	1.00	0.60	3.00E+06	1.20E-02	0.00E+00	0.00E+00	Lassens_Model	160	MPI_Tubular_ICON	1.0E-04	0.75	0.001	0.01	1	0.05
Case 9	1.00	0.30	1.00	0.80	3.00E+06	4.50E-02	4.00E-01	4.00E-01	Lassens_Model	400	MPI_Tubular_ICON	1.0E-04	0.75	0.001	0.01	1	0.05
Case 10	1.00	0.35	1.00	0.90	3.00E+06	1.00E-02	3.00E-01	3.00E-01	Lassens_Model	300	MPI_Tubular_ICON	1.0E-04	0.75	0.001	0.01	1	0.05

Parameter Input / Total Cost / Inspection Plans / Inspection Plans Threshold E-2 / Inspection Plans Threshold E-3 / Inspection Plans Threshold

Figure D.3 - The input worksheet in iPlan.xls.

### **D.3 Output**

The final results are provided in different worksheets. The worksheet “Total cost” includes all results related to the expected costs of the inspection plans for the different hot spots. It is presented in Figure D.4. The results consist of expected cost of failure, of repair, of inspection and the total expected cost. A graph illustrates the expected costs; when a hot spot is selected, the graph automatically changes to the values for this hot spot.

The inspection times for the chosen thresholds are provided in the worksheet “Inspection Plans” shown in Figure D.5. The inspection times are presented in a graphical form, but they can be exported for further editing in a numerical format by means of the “Export inspection times” function in the iPlan menu. A grey cell with an “X” indicates that an inspection is required in this year using the NDE technique specified in the input worksheet. If a cell is red, such as for case 5 and year 1 in Figure D.5, then in principle more than one inspection are required to comply with the respective threshold. An alternative is to apply a different inspection method with higher accuracy.

The inspection times for all thresholds for which expected costs are calculated, are provided in additional worksheets similar to the one shown in Figure D.5.



Figure D.4 - The output worksheet providing the expected costs for all hot spots and thresholds.

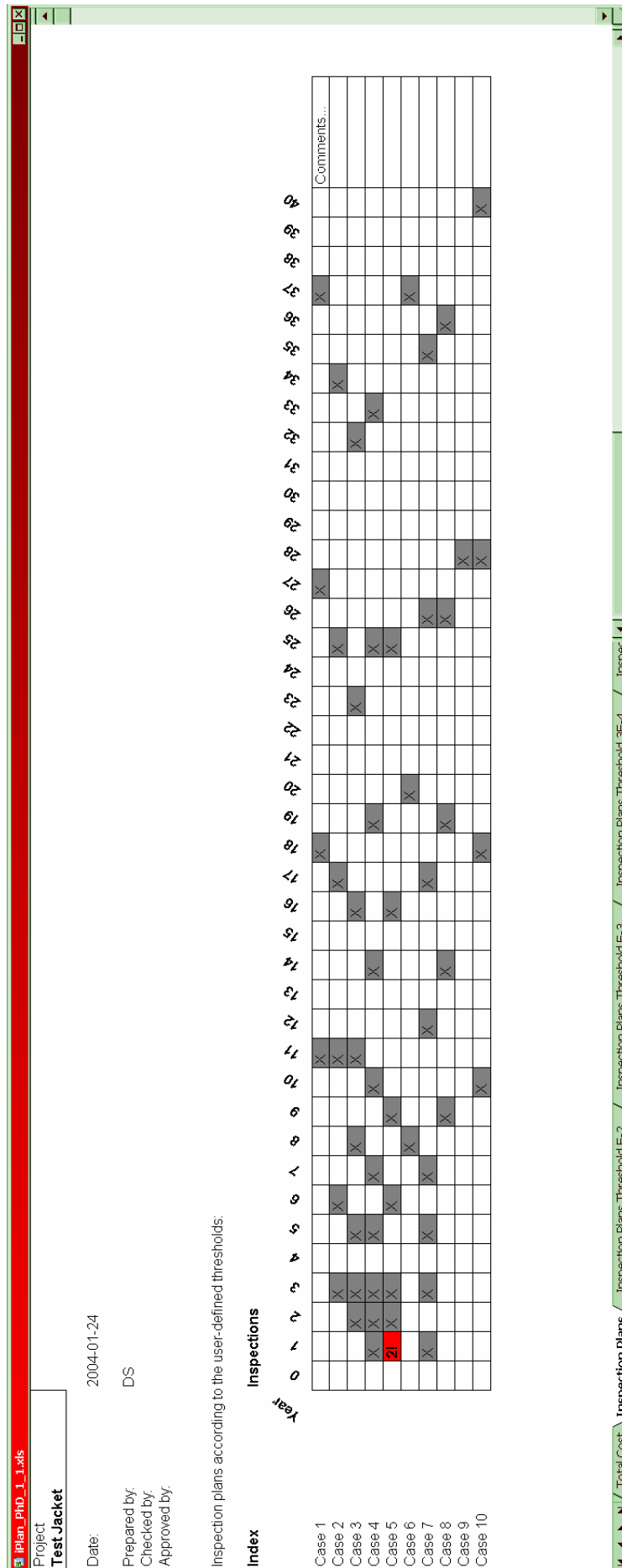


Figure D.5 - The output worksheet providing the inspection times for all hot spots and the chosen thresholds.

## E Interpolation of inspection plans

From the set of generic inspection plans, inspection plans for the specific hot spots are evaluated by interpolation, as first described in Faber et al. (2000) for the case with one single generic parameter and in Goyet et al. (2002b) for the case with two generic parameters. Inspection plans, in accordance with Section 5.2, consist of inspection times and probabilities of occurrence of the different branches in the decision tree describing the inspection planning problem. From these probabilities, expected costs (of failure, inspection and repair) are computed for each generic inspection plan based on the specific cost model. Whereas the interpolation of these expected costs is straightforward according to the multi-dimensional interpolation procedure described in Section E.2, the interpolation of inspection times requires some additional rules, due to the fact that the individual plans may contain different numbers of inspections. This is treated in Section E.3.

### E.1 Types of generic parameters

There are three different types of generic parameters with respect to the interpolation:

1. Fixed parameters
2. Parameters that allow interpolation
3. Parameters that allow interpolation and extrapolation

Fixed parameters are typically qualitative parameters, such as the inspection type. There cannot be an interpolation between two different inspection methods, it is either one or the other. The set of generic plans is thus first restricted to those that are identical to the considered specific hot spot with respect to all fixed generic parameters.

All quantitative generic parameters, such as the  $FDF$ , allow for interpolation. Notionally, for all these parameters also extrapolation is possible. Considering that the procedure is purely empirical based, however, extrapolation with respect to any generic parameter should not be allowed<sup>a</sup>; therefore only interpolation is considered hereafter.

---

<sup>a</sup> For some generic parameters physical reasoning can show that the required inspection efforts will always decrease with either increasing or decreasing parameter values. For such generic parameters a (conservative) extrapolation procedure is allowable: The inspection efforts for all parameter values either larger or smaller than that for which a generic inspection plan is available are set equal to the available generic inspection plan. Such a parameter is e.g. the member thickness for fatigue subjected hot spots, see Section 5.5.7.2 for further details.

## E.2 Multi-dimensional interpolation

The problem of multi-dimensional interpolation is treated in the general mathematical literature; some references are given by Press et al (1989). Here only interpolation on a Cartesian mesh is considered, i.e. the case where generic inspection plans are available for all combinations of the different generic representations, in accordance with Equation (5-1). With this restriction, the subsequent discussion follows closely Press et al. (1989).

In Figure E.1 the problem is shown for two dimensions, e.g. if the inspection plan is only interpolated between different *FDF* and thickness *d*. These generic parameters are here denoted by  $x_1$  and  $x_2$ . The function value to interpolate, which is e.g. the first inspection time, is named  $y$ . Figure E.1 illustrates the concept of the grid square, in which the searched specific hot spot (with the generic parameters equal to  $x_{1,hs}$  and  $x_{2,hs}$ ) falls.  $x_{iL}$  is thereby the closest generic representation of  $x_i$  with a value lower than  $x_{i,hs}$ ,  $x_{iU}$  the closest one with a higher value. The same nomenclature is valid for the second parameter  $x_2$ .  $y_{UL}$  is the value the interpolated function at the intersection of the two generic representations  $x_{1U}$  and  $x_{2L}$ , the nomenclature of the other function values follows accordingly.

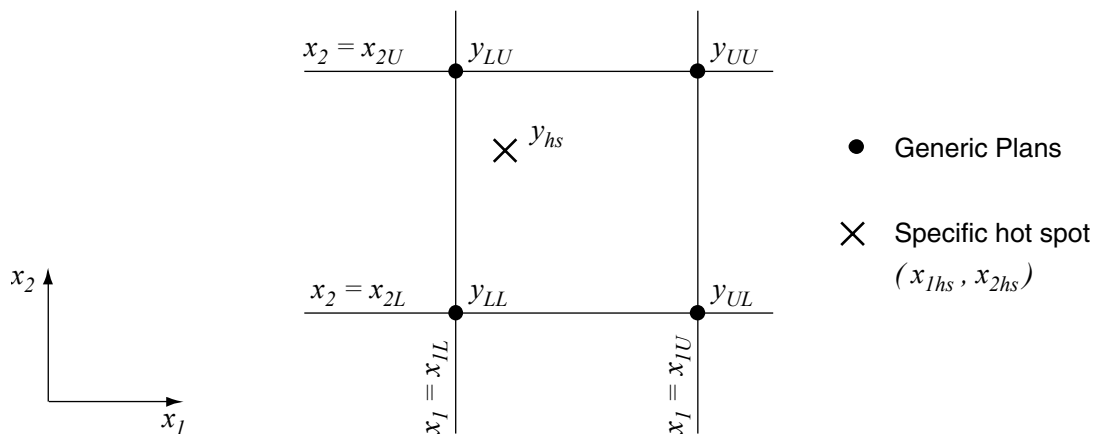


Figure E.1 – The grid square in two-dimensional interpolation

Linear (1<sup>st</sup> order) interpolation is used. For the considered 2-dimensional case the interpolated value  $y_{hs}$  is then given by

$$y_{hs} = (1-r_1)(1-r_2)y_{LL} + r_1(1-r_2)y_{UL} + (1-r_1)r_2y_{LU} + r_1r_2y_{UU} \quad (\text{E-1})$$

with

$$r_i = \frac{x_{i,hs} - x_{iL}}{x_{iU} - x_{iL}}, \quad i = 1, 2 \quad (\text{E-2})$$

For problems with  $n$  dimensions, Equation (E-2) is applied for  $i = 1 \dots n$ . Equation (E-1) then changes accordingly: It consists of  $2^n$  additive terms, corresponding to the  $2^n$  generic plans.

The algorithm implemented in iPlan solves the problem recursively by splitting it into a sequence of one-dimensional interpolations.

It is also possible to perform an interpolation of higher order if more than two representations of a generic parameter are available, see Press et al. (1989). Due to the empirical nature of the relationship between inspection times (or expected cost) and the generic parameters, it appears questionable to relate a specific hot spot to a generic plan with parameters far from those of the considered hot spot. Instead it is decided to guarantee the linear behaviour of the  $y$  between two points in the mesh (two generic representations) by an appropriate design of the generic database (i.e. the choice of the generic representations). This is ensured by means of the preliminary investigations as presented in Section 5.5.7.

### E.2.1 Logarithmic interpolation of the expected costs

For some of the considered generic parameters, it is the logarithm of the expected costs that varies approximately linearly with the generic parameter, instead of the expected costs directly. As a consequence, it is found (see Section 5.5.9) that the interpolation procedure is improved if the linear interpolation described above is applied with the log-transformed values of the expected costs. The interpolation procedure is thus as presented above, with the  $y$ -values being equal to the logarithm of the costs. This is named the *logarithmic interpolation scheme*, as opposed to the *linear interpolation scheme* above, although it is actually a linear interpolation of the logarithm of the function values.

## E.3 Rules for the interpolation of inspection times

If inspection times are interpolated, not all generic plans will contain the same number of inspections. This problem is circumvented by extrapolating inspection times beyond the time for which inspections are calculated,  $T_{SL,max}$ . The idea is to introduce “fictive” inspection times so that all generic inspection plans have the maximal number of inspections encountered, namely  $n_{insp}$ . Based on these fictive inspection times, the interpolation is then performed separately for the first inspection, for the second inspection and for all inspections until the  $n_{insp}^{\text{th}}$  inspection.

### E.3.1 Determination of the fictive inspection times

The following three situations with respect to the extrapolation may occur: The generic inspection plan with less inspection times contains

1. no inspection;
2. exactly one inspection;
3. more than one inspection, namely  $i_{insp}$  inspections.

The fictive inspection times are evaluated for the three cases as:

1.  $t_{Insp,i} = i \cdot (T_{SL,max} + 1yr)$ ,  $i = 1 \dots n_{Insp}$ , conservatively assuming that the first inspection is in the first year after  $T_{SL,max}$ ;
2.  $t_{Insp,2} = \begin{cases} 2 \cdot t_{Insp,1}, & t_{Insp,1} \cdot 2 > T_{SL,max} \\ T_{SL,max} + 1yr, & \text{else} \end{cases}$ ,  $t_{Insp,i} = 2 \cdot t_{Insp,(i-1)} - t_{Insp,(i-2)}$ ,  $i = 3 \dots n_{Insp}$ ;
3.  $t_{Insp,i} = 2 \cdot t_{Insp,(i-1)} - t_{Insp,(i-2)}$ ,  $i = i_{Insp} \dots n_{Insp}$ .

These cases are illustrated in Figure E.2.

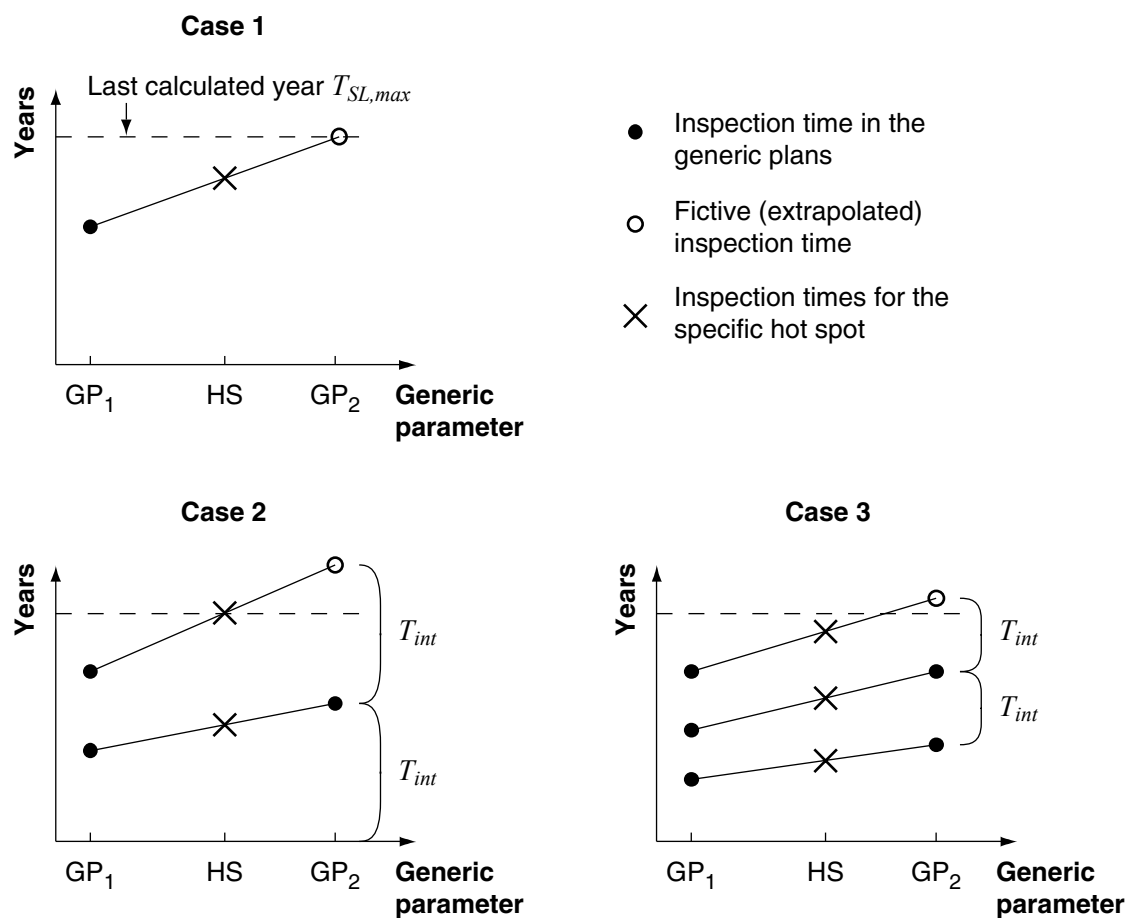


Figure E.2 – Illustration of the different interpolation cases.



## F Nomenclature

The symbols in this work are generally explained when first introduced. In addition to the list below, arbitrary variables may be specified locally to exemplify a description. Because this work covers several specialist fields, in some instances deviations from the symbols commonly applied in the literature are required to avoid ambiguities.

Some general conventions followed in this work:

- All time intervals are indicated by a capital  $T$ , all points in time by a small  $t$ ;
- The values given in square braces following a distribution denotation are the mean values and the standard deviation of the distribution:  $[\mu, \sigma]$ ;
- Probabilities (of an event  $E$ ) are either written as  $P(E)$  or equivalently as  $p_E$ ;
- Random variables are denoted by an upper case letter, their realisations by the corresponding lower case letters.

### F.1 Roman symbols

$a$	Terminal action in decision theory; crack depth;	$D_0$	SN damage at the time of a load modification $t_{Mod}$ ;
$a_c$	Critical crack size;	$D_p$	Pipe diameter;
$a_D$	Detectable crack depth;	$D_{tot}$	SN damage indicator;
$a_m$	Measured crack depth;	$DoB$	Degree of bending;
$a_R$	Repair criterion for the crack depth;	$DSR$	Damaged Strength Ratio;
$a_0$	Initial crack depth;	$d$	Decision rule (repair policy), wall thickness;
$B$	Model uncertainty in the collapse LSF for fixed offshore platforms;	$d(e, z)$	Decision rule as a function of the inspection $e$ and the outcome $z$ ;
$B_S$	Error in the calculated stress;	$d_0$	Reference thickness (factor in the thickness correction of SN diagrams);
$b$	Plate width;	$d_2$	Decision rule on additional inspections;
$C_1$	Parameter of the SN diagram;	$d_{crit}$	Critical member thickness;
$C_1^D$	Characteristic value of $C_1$ ;	$d_C$	Corrosion depth;
$C_F$	Cost of failure;	$d_{LC}$	Depth of the localized corrosion;
$C_{Insp}$	Cost of inspection;	$d_{lim}$	Limiting corrosion depth measurement;
$C_P$	Crack growth parameter (in Paris' law);	$d_m$	Measured corrosion depth;
$C_{P,a}, C_{P,c}$	Crack growth parameter in the depth respectively length direction;	$d_R$	Repair criterion for corrosion depth;
$C_R$	Cost of repair;	$d_{UC}$	Depth of the uniform corrosion;
$C_T$	Total cost;	$E$	Event;
$COL$	Event of structural collapse;	$E[X]$	Expected value of $X$ ;
$CoV$	Coefficient of variation;	EXP	Exponential distribution;
$c$	Half the crack length;	$E_X[y(X)]$	Expected value of $y$ with respect to $X$ ;
$c_0$	Half the initial crack length;	$e, e_2, \underline{e}$	Inspections or experiments;
$c_p$	Pit growth parameter;		
$D$	Event of detection at the inspection;		

Annex F - Nomenclature

$F$	Event of failure, event of hot spot failure;	$K_{min}$	Minimal stress intensity factor;
$F_X(x)$	Probability distribution function of $X$ ;	$K_{op}$	Stress intensity factor at which the crack opens;
$FA$	Event of a fatality;	$k_{\Delta S}$	Scale parameter of the Weibull distribution describing the (long term) stress ranges;
$FAR$	Fatal accident rate;	$L$	Likelihood function, Event of defect size $s$ larger than $s_m$ ;
$FAR^{max}$	Acceptable $FAR$ value;	LN	Lognormal distribution;
$FAR_{OS}$	$FAR$ value from all accident scenarios other than those caused by deterioration;	$l$	Defect length;
$FDF$	Fatigue Design Factor;	$l_{LC}$	Length of the localised corrosion defect;
$FDF_{Mod}$	Fatigue Design Factor in the period after a modification;	$M$	Measurement event;
$FI$	Event of false indication at the inspection;	$M_k$	Weld magnification factor;
$f_{CO_2}$	CO <sub>2</sub> fugacity;	$M_P$	Folias factor;
$f_{FA}$	Fatigue analysis resulting in the $FDF$ ;	$\tilde{m}$	Median;
$f_X(x)$	Probability density function of $X$ ;	$m_1, m_2$	Exponential parameters of the SN diagram;
$f'_X(x)$	Prior probability density function of $X$ ;	$m_{FM}$	Exponential parameter in the crack growth law;
$f''_X(x)$	Posterior probability density function of $X$ ;	$m_f$	Factor relating the flow stress to the yield stress;
$g$	Limit state function (LSF);	$N$	Number of stress cycles;
$g_E$	LSF describing the event $E$ ;	$N$	Normal distribution;
$g_{a_c}$	LSF for fatigue failure described by the critical crack depth;	$N^+(T)$	Number of out-crossings in the period $T$ ;
$g_C$	LSF for leakage due to corrosion;	$N_0$	Parameter of the SN diagram (cut off level);
$g_{C,p}$	LSF for rupture in a pressurised system;	$N_F$	Number of cycles to fatigue failure;
$g_{COL}$	LSF for collapse of a fixed offshore structure due to wave overload;	$N_I$	Number of cycles to fatigue crack initiation;
$g_D$	LSF describing the detection event;	$N_{I_0}$	Parameter in Lassen's fatigue crack initiation model;
$g_I$	LSF describing the indication event;	$N_P$	Number of cycles in the fatigue crack propagation phase;
$g_M$	LSF describing the measurement event;	$N_q$	Parameter in the SN diagram defining the change of slope;
$g_{fracture}$	Fracture LSF;	$n_a$	Number of different mitigation actions after the inspection;
$g_{SN}$	Fatigue LSF;	$n_b$	Number of branches in the decision tree;
$H$	Maximum annual wave height;	$n_{GIP}$	Number of generic inspection plans;
$H$	Heaviside step function;	$n_{GP}$	Number of generic parameters;
$I$	Event of indication at the inspection;	$n_{GR}$	Number of generic representations;
$I_F$	Indicator function;	$n_{HS}$	Number of hot spots in the structure;
$I_L$	Event of indication of a defect larger than $s_m$ ;	$n_{Insp}$	Number of inspections;
$I_S$	Event of indication of the largest defect;	$n_{MC}$	Number of simulations in the MCS;
$K$	Stress intensity factor;	$n_{OP}$	Number of considered values of the optimization parameter;
$K_a$	Stress intensity factor in the depth direction (mode I);	$n_{CO_2}$	Fraction of CO <sub>2</sub> in the gas phase;
$K_c$	Stress intensity factor in the length direction (mode I);	$P_0$	Parameter of the exponential threshold $PoD$ model;
$K_{I, NR}$	Newman-Raju approximation to the mode I stress intensity factor;	$P_{CO_2}$	Partial pressure of CO <sub>2</sub> ;
$K_{IC}$	Fracture toughness;	$P_o$	Operating pressure;
$K_{max}$	Maximal stress intensity factor;	$PFI$	Probability of false indication;

$PoD$	Probability of detection;	$s$	Defect size;
$PoD_S$	System probability of detection;	$\mathbf{s}$	Vector of defect size;
$PoI$	Probability of indication;	$\underline{\mathbf{s}}_0$	Vector of the initial defect (crack) size;
$p_F$	Probability of failure;	$s_D$	Detectable defect size;
$p_I$	Probability of indication;	$s_m$	Measured size of the largest defect;
$p_{MC}$	Monte Carlo estimate of the true probability $p$ ;	$s_O$	Measured size of an indicated defect;
$p_R$	Resistance of a pressure vessel;	$T$	Time period;
$p_S$	Loading in a pressure vessel;	$T_D$	Time period before failure during which a growing defect is detectable;
$\underline{\mathbf{Q}}$	Vector containing all the slowly varying ergodic processes;	$T_{FL}$	Design fatigue life;
$q$	Decision parameter in the adaptive strategy;	$T_{FL,fict}$	Fictive design fatigue life;
$\underline{\mathbf{q}}$	Vector of the inspection parameters;	$T_{FL,Mod}$	Design fatigue life after a load modification;
$q_d$	Factor in the thickness correction of SN diagrams;	$T_o$	Operating temperature;
$R$	Resistance; repair event;	$T_{o,e}$	Equivalent operating temperature;
$\underline{\mathbf{R}}$	Vector of all time invariant random variables;	$T_{SL}$	Service life period;
$R_S$	Stress ratio;	$T_{SL,max}$	Number of years for which an inspection plan is evaluated;
$R_t$	Resistance at time $t$ ;	$T_{SL,Mod}$	Residual service life period after a load modification;
$RRC$	Risk reduction cost;	$t$	Point in time;
$RSR$	Reserve strength ratio;	$t_{FIY}$	Fictive installation time;
$RSR_{F_i}$	Reserve strength ratio of the structure after failure of hot spot $i$ ;	$t_{Mod}$	Time of a modification in the fatigue loading;
$RSR_{intact}$	Reserve strength ratio of the intact structure;	$t_{n_{INSP}}$	Time of the last inspection;
$r$	Interest rate;	$u$	Utility;
$r_{aspect}$	Initial aspect ratio of the crack size;	$u_{max}$	Parameter describing the growth of the maximal corrosion pit;
$r_{CO_2}$	CO <sub>2</sub> corrosion rate;	$u_s$	Sample utility;
$S$	Stress, loads;	$u_t$	Terminal utility, parameter of the Gumbel distribution for the maximal corrosion pit;
$S^2[X]$	Sample variance of $X$ ;	$V_X$	Variance of $X$ ;
$S_b$	Outer-fiber stress from bending;	$V_{XY}$	Covariance of $X$ and $Y$ ;
$S_{b,0}$	Initial outer-fiber stress from bending;	$X_M$	Model uncertainty of the CO <sub>2</sub> corrosion rate;
$S_f$	Flow stress;	$Y_G$	Stress intensity factor correction function;
$S_{HS}$	Hot spot stress;	$Y_{NR}$	Stress intensity factor correction function to the Newman-Raju approximation;
$S_i$	Maximum defect size at hot spot $i$ ;	$Z, Z_2$	Inspection outcomes.
$S_{max}$	Maximal load / stress;		
$S_{min}$	Minimal stress;		
$S_N$	Nominal stress;		
$S_n$	Notch stress;		
$S_t$	Uniform tension stress;		
$S_y$	Yield stress;		

## F.2 Greek symbols

$\alpha$	Sensitivity factor of a random variable in SRA;	$\Delta p_F^{max}$	Maximal acceptable annual probability of failure;
$\alpha_D$	Parameter of the log-logistics <i>PoD</i> model;	$\Delta p_F^T$	Threshold on the annual probability of failure;
$\alpha_{2D}$	Parameter of the two-dimensional log-logistics <i>PoD</i> model;	$\Delta p_{F,1}, \Delta p_{F,2}$	$\Delta p_F$ in the year before, respectively after the inspection;
$\alpha_{LC}$	Parameter for localised corrosion growth;	$\hat{\Delta p}_{F,1}, \hat{\Delta p}_{F,2}$	MCS estimate of $\Delta p_F$ in the year before, respectively after the inspection;
$\alpha_{max}$	Parameter describing the growth of the maximal corrosion pit;	$\Delta S$	Stress range;
$\alpha_t$	Parameter of the Gumbel distribution for the maximal corrosion pit size at time $t$ ;	$\Delta S_0$	Cut off in the SN diagram;
$\alpha_{UC}$	Parameter for uniform corrosion growth;	$\Delta S_{calc}$	Calculated stress range;
$\beta$	Reliability index;	$\Delta S_e$	Equivalent stress range;
$\beta_D$	Parameter of the log-logistics <i>PoD</i> model;	$\Delta S_q$	Parameter of the SN diagram defining the change of slope;
$\beta_{D,a}, \beta_{D,l}$	Parameter of the two-dimensional log-logistics <i>PoD</i> model;	$\Delta^2 p_F$	Yearly increase in the annual failure probability;
$\beta_{FM}$	Reliability against fatigue as evaluated with the FM model;	$\delta$	Dirac's delta function;
$\beta_{LC}$	Exponential parameter for localised corrosion growth;	$\delta$	Exponential factor in the collapse LSF for fixed offshore platforms;
$\beta_{SN}$	Reliability against fatigue as evaluated with the SN model;	$\varepsilon_m$	Measurement error;
$\beta_{UC}$	Exponential parameter for uniform corrosion growth;	$\varepsilon_{t_{insp}}$	Error in the determination of the inspection times;
$\Gamma(x)$	Gamma function;	$\Phi$	Standard normal distribution function;
$\Gamma(x, s)$	(Upper) incomplete gamma function	$\varphi$	Standard normal probability density function;
$\gamma$	Inspection coverage;	$\eta_S$	Bending-to-membrane stress ratio;
$\Delta$	Criteria for fatigue failure in the SN model;	$\Theta$	State of nature;
$\Delta D_i$	SN fatigue damage increment in one stress cycle;	$\theta$	One realisation of the state of nature;
$\Delta K$	Stress intensity range;	$\theta_R$	Repair criterion;
$\Delta K_{eff}$	Effective stress intensity range;	$\lambda_D$	Parameter of the exponential threshold <i>PoD</i> model;
$\Delta K_{th}$	Threshold on the stress intensity range;	$\lambda_{\Delta S}$	Shape parameter of the Weibull distribution describing the (long term) stress ranges;
$\Delta p_{COL}$	Annual probability of structural collapse;	$\mu_X$	Mean value of $X$ ;
$\Delta p_{COL}^{max}$	Maximal acceptable annual probability of structural collapse;	$\nu$	Stress cycle rate;
$\Delta p_{COL,F}^{max}$	Maximal acceptable annual probability of structural collapse due to deterioration failures at the hot spots;	$\nu_e$	Equivalent stress cycle rate;
$\Delta p_F$	Annual probability of failure (failure rate);	$\rho$	Correlation coefficient;
		$\rho_S$	Correlation between the defect sizes at different hot spots;
		$\sigma_X$	Standard deviation of $X$ ;
		$u_t$	Conditional value of perfect information;
		$u_{tz}$	Conditional value of sample information;
		$\psi$	Deterioration importance factor for the risk acceptance criteria related to structural collapse.

### F.3 Abbreviations

API	American Petroleum Institute;	LSF	Limit state function;
cdf	(Cumulative) probability distribution function;	MCS	Monte Carlo simulation;
CVPI	Conditional value of perfect information;	MPI	Magnetic Particle Inspection;
CVSI	Conditional value of sample information;	NDE	Non-destructive evaluation;
DoE	Department of Energy, UK;	pdf	Probability density function;
EVPI	Expected value of perfect information;	QRA	Quantitative risk analysis;
EVSI	Expected value of sample information;	RAC	Risk acceptance criteria;
FEM	Finite element methods;	RBI	Risk based inspection planning;
FORM	First order reliability methods;	rv	Random variable;
FPSO	Floating Production, Storage and Offloading Unit;	SCC	Stress corrosion cracking;
GNP	Gross National Product;	SCF	Stress concentration factor;
HSE	Health and Safety Executive, UK;	SN	Fatigue stress range vs. number of cycles to failure;
IIW	International Institute of Welding;	SORM	Second order reliability methods;
JCCS	Joint Committee on Structural Safety;	SIA	Swiss Society of Engineers and Architects;
LEFM	Linear elastic fracture mechanics;	SRA	Structural reliability analysis;
LQI	Life quality index;	SSC	Ship Structure Committee;
		VBA	Visual Basic for Applications;
		VOI	Value of information.



## References

- Aaghaakouchak A., Glinka G., Dharmavasan S. (1989). A Load Shedding Model for Fracture Mechanics Analysis of Fatigue Cracks in Tubular Joints. *Proc. 8<sup>th</sup> Offshore Mechanics and Arctic Engineering Conference*, Vol. II, pp. 159-165.
- Ahammed M., Melchers R.E. (1996). Reliability estimation of pressurized pipelines subject to localized corrosion defects. *International Journal of Pressure Vessels & Piping*, **96**(3), pp. 267-272.
- Aker Engineering (1990). *Probabilistic in-service inspection planning*. Report, Rev. 1.1.
- Almar-Næss A. (ed) (1984). *Fatigue Handbook for Offshore Steel Structures*. Tapir Publishers, Trondheim.
- Anderson T.L. (1995). *Fracture Mechanics*. 2<sup>nd</sup> edition, CLC Press.
- Ang A.H.S., Tang W.H. (1975). *Probability Concepts in Engineering Planning and Design*. Vol. I and II, John Wiley & Sons.
- Apostolakis G. (1990). The Concept of Probability in Safety Assessments of Technological Systems. *Science*, **250**, pp.1359-1364.
- Aven T. (1992). *Reliability and Risk Analysis*. Elsevier Applied Science.
- B31G (1984). *Manual for Determining the Remaining Strength of Corroded Pipelines*. American National Standards Institute (ANSI) & American society of Mechanical Engineers (ASME).
- Banon H., Bea R.G., Bruen F.J., Cornell C.A., Krieger W.F., Stewart D.A. (1994). Assessing Fitness for Purpose of Offshore Platforms. I: Analytical Methods and Inspections. *Journal of Structural Engineering*, **120**(12), pp. 3595 - 3612.
- Benjamin J.R., Cornell C.A. (1970). *Probability, statistics and decision for civil engineers*. McGraw-Hill, New York.
- Berens A.P. (1989). NDE Reliability Data Analysis. *Metals Handbook*, 9<sup>th</sup> edition, American Society of Materials ASM, pp. 679-701.
- Berens A.P., Hovey P.W. (1983). Statistical Methods for Estimating Crack Detection Probabilities. in *Probabilistic Fracture Mechanics and Fatigue Methods: Applications for Structural Design and Maintenance*, ASTM STP 798, J.M.Bloom and J.C.Ekevall (Eds.), pp. 79 – 94.
- Bloch A., Sørensen J.D., Faber M.H. (2000). Simplified Approach to Inspection Planning. *Proc. 8<sup>th</sup> ASCE Specialty Conference on Probabilistic Mechanics and Structural Reliability*, Notre Dame, USA.
- Bokalrud T., Karlsen A. (1981). Probabilistic fracture mechanics evaluation of fatigue failure from weld defects in butt welded joints. *Proceedings, Conference on Fitness for Purpose Validation of Welded Constructions*, Paper #28, London.
- Bolotin V.V., Babkin A.A., Belousov I.L. (1998). Probabilistic model of early fatigue crack growth. *Probabilistic Engineering Mechanics*, **13**(3), pp. 227-232.
- Broek D. (1986). *Elementary Engineering Fracture Mechanics*. 4<sup>th</sup> revised edition, Kluwer Academic Publishers.
- Bureau Veritas rules (2000). *BV Rules for the Classification of Steel Ships*. Bureau Veritas, Marine Department, Paris.
- BV NI 393 (1998). *Fatigue Strength of Welded Ship Structures*. Guidance Note, Bureau Veritas, Marine Division, Paris.

## References

- Byers W.G., Marley M.J., Mohammadi J., Nielsen R.J., Sarkani S. (1997b). Fatigue Reliability Reassessment Applications: State-of-the-Art Paper. *Journal of Structural Engineering*, **123**(3), pp. 277-285.
- Cole I.S. (2002). Recent Progress in Modelling Atmospheric Corrosion. *Corrosion Reviews*, **20**(4-5), pp.317-337.
- Committee on Fatigue and Fracture Reliability of the Committee on Structural Safety and Reliability of the Structural Division (1982). Fatigue and Fracture Reliability: A State-of-the-Art Review. *Journal of the Structural Division*, ASCE, **108**(1), pp. 3-88.
- Cramer E.H., Friis-Hansen P. (1994). Reliability-Based Optimization of Multi-Component Welded Structures. *Journal of Offshore Mechanics and Arctic Engineering*, **116**, pp. 233 – 238.
- CRIS (2004). *Corrosion Reliability Inspection Scheduling JIP - Final report*. TSC Inspection Systems, UK.
- De Souza G.F.M., Ayyub B.M. (2000). Probabilistic Fatigue Life Prediction for Ship Structures Using Fracture Mechanics. *Naval Engineers Journal*, **112**(4), pp. 375-397.
- Der Kiureghian A., Liu P.-L. (1986). Structural Reliability under Incomplete Probability Information. *Journal of Engineering Mechanics*, **112**(1), pp. 85 – 104.
- DeWaard C., Lotz U., Dugstad A. (1995). Influence of Liquid Flow Velocity on CO<sub>2</sub> Corrosion: A Semi-empirical Model. *Proc. Corrosion95*, NACE, paper #65.
- DeWaard C., Lotz U., Milliams D.E. (1991). Predictive Model for CO<sub>2</sub> Corrosion Engineering in Wet Natural Gas Pipelined. *Corrosion*, **47**(12), pp.976-985.
- DeWaard C., Milliams D.E. (1975). Carbonic Acid Corrosion of Steel. *Corrosion*, **31**(5), pp. 177-181.
- Dickie R.A. (1992). Toward a Unified Strategy of Service Life Prediction. *Journal of Coatings Technology*, **64**(809), pp. 61-65.
- Ditlevsen O. (2003). Decision modeling and acceptance criteria. *Structural Safety*, **65**, pp. 165-191.
- Ditlevsen O., Madsen H.O. (1996). *Structural Reliability Methods*. John Wiley & Sons. Also available online: <http://www.mek.dtu.dk/staff/od/books.htm>.
- Dowling N.E. (1972). Fatigue Failure Predictions for Complicated Stress-Strain Histories. *Journal of Materials*, **7**(1), pp. 71-87.
- ECCS (1985). Recommendations for the fatigue design of steel structures. European Convention for Constructional Steel, Report #43.
- Elber W. (1971). The Significance of Fatigue Crack Closure. *Damage Tolerance in Aircraft Structures*, ASTM STP 486, American Society for Testing and Materials, pp. 230-242.
- Engelund S., Rackwitz R., Lange C. (1995). Approximations of first-passage times for differentiable processes based on higher-order threshold crossings. *Probabilistic Engineering Mechanics*, **10**, pp.53-60.
- Etube L.S., Brennan F.P., Dover W.D. (2000). A new method for predicting stress intensity factors in cracked welded tubular joints. *International Journal of Fatigue*, **22**, pp. 447-456.
- Eurocode 3 (1992). *Design of Steel Structures*. ENV 1993-1-1, April 1992.
- Faber M.H. (2000). Reliability Based Assessment of Existing Structures. *Journal of Progress in Structural Engineering and Materials*, **2**(2), pp.247-253.
- Faber M.H. (2003a). *Risk and Safety in Civil Engineering*. Lecture Notes, Institute of Structural Engineering, Swiss Federal Institute Of Technology.
- Faber M.H. (2003b). Uncertainty Modelling and Probabilities in Engineering Decision Analysis. *Proc. 22<sup>nd</sup> Offshore Mechanics and Arctic Engineering Conference*, Cancun, Mexico, paper #37217.
- Faber M.H., Engelund S., Sørensen J.D., Bloch A. (2000). Simplified and Generic Risk Based Inspection Planning. *Proc. 19<sup>th</sup> Offshore Mechanics and Arctic Engineering Conference*, New Orleans.



- Faber M.H., Sørensen J.D. (1999). Aspects of Inspection Planning – Quality and Quantity. *Proc. ICASP8*, Sydney, pp. 739-746.
- Faber M.H., Sørensen J.D. (2002). Indicators for inspection and maintenance planning of concrete structures. *Structural Safety*, **24**(4), pp. 377 – 396.
- Faber M.H., Sørensen J.D., Kroon I.B. (1992a). Optimal Inspection Strategies for Offshore Structural Systems. *Proc. 11<sup>th</sup> Offshore Mechanics and Arctic Engineering Conference*, Calgary, pp. 145-151.
- Faber M.H., Sørensen J.D., Rackwitz R., Thoft-Christensen P., Bryla P. (1992b). Reliability Analysis of an Offshore Structure: A Case Study - I. *Proc. 11th Offshore Mechanics and Arctic Engineering Conference*, Vol. II, Calgary, pp. 449-455.
- Faber M.H., Straub D. (2003). *Reliability and Risk Based Inspection Planning for Jacket Structures in the Gulf of Mexico*. Confidential report, Swiss Federal Institute of Technology, ETH.
- Faber M.H., Straub D., Goyet J. (2003a). Unified Approach to Risk Based Inspection Planning for Offshore Production Facilities. *Journal of Offshore Mechanics and Arctic Engineering*, **125**(2). pp. 126-131.
- Faber M.H., Straub D., Sørensen J.D., Tychsen J. (2003b). Field Implementation of RBI for Jacket Structures. *Proc. 22<sup>nd</sup> Offshore Mechanics and Arctic Engineering Conference*, Cancun, Mexico, paper #37304.
- Faller M., Richner P. (2003). Material selection of safety-relevant components in indoor swimming pools. *Materials and Corrosion*, **54**(5), pp. 331–38.
- Feliu S., Morcillo M., Feliu S. Jr. (1993a). The Prediction of Atmospheric Corrosion from Meteorological and Pollution Parameters – Annual Corrosion. *Corrosion Science*, **34**(3), pp. 403-414.
- Feliu S., Morcillo M., Feliu S. Jr. (1993b). The Prediction of Atmospheric Corrosion from Meteorological and Pollution Parameters – Long-Term Forecasts. *Corrosion Science*, **34**(3), pp. 415-422.
- Finley H.F. (1967). An Extreme-Value Statistical Analysis of Maximum Pit Depths and Time to First Perforation. *Corrosion*, **23**(4), pp. 83-87.
- Folsø R., Otto S., Parmentier G. (2002). Reliability-based calibration of fatigue design guidelines for ship structures. *Marine Structures*, **15**, pp. 627-651.
- Forman R.G., Kearney V.E., Engle, R.M. (1967). Numerical Analysis of Crack Propagation in cyclic-Loaded Structures. *Journal of Basic Engineering*, **89**, Series D, pp. 459-464.
- Francois M., Mo O., Fricke W., Mitchell K., Healy B. (2000). FPSO Integrity: Comparative Study of Fatigue Analysis Methods, *Proc. Offshore Technology Conference*, Houston, paper #12148.
- Freudenthal A.M. (1947). The safety of structures. *Transactions of the ASCE*, **112**, pp. 125-159.
- Fricke W. (2003). Fatigue analysis of welded joints: state of development. *Marine Structures*, **16**, pp. 185-200.
- Fricke W., Cui W., Kierkegaard H. et al. (2002). Comparative fatigue strength assessment of a structural detail in a containership using various approaches of classification societies. *Marine Structures*, **15**, pp. 1-13.
- Friis Hansen P. (1994). *Reliability Analysis of a Midship Section*. PhD thesis, Technical University of Denmark DTU.
- Fujita M., Schall G., Rackwitz R. (1989). Adaptive Reliability-Based Inspection Strategies for Structures Subject to Fatigue. *Proc. 5<sup>th</sup> ICOSSAR*, Vol. 2, San Francisco, pp. 1619-1626.
- Goyet J., Faber M.H., Paygnard J.C., Maroini A. (1994). Optimal Inspection and Repair Planning: Case Studies using IMREL software. *Proc. 13<sup>th</sup> Offshore Mechanics and Arctic Engineering Conference*, Vol. II, pp. 325-333.
- Goyet J., Rouhan A., Faber M.H. (2004). Industrial Implementation of Risk Based Inspection Planning Methods – Lessons Learnt from Experience: The Case of FPSO's. *Proc. 23<sup>th</sup> Offshore Mechanics and Arctic Engineering Conference*, Vancouver.
- Goyet J., Straub D., Faber M.H. (2002a). Risk Based Inspection Planning for Offshore Installations. *Structural Engineering International*, **12**(3), pp. 200-208.

## References

- Goyet J., Straub D., Faber M.H. (2002b). Risk Based Inspection Planning - Methodology and Application to an Offshore Structure. *Revue française de Génie civil*, **6**(3), pp. 489-503.
- Guedes Soares C., Garbatov Y. (1996a). Fatigue reliability of the ship hull girder accounting for inspection and repair. *Reliability Engineering and System Safety*, **51**, pp. 341-351.
- Guedes Soares C., Garbatov Y. (1996b). Reliability of Maintained Ship Hulls Subjected to Corrosion. *Journal of Ship Research*, **40**(3), pp.235-243.
- Guedes Soares C., Garbatov Y. (1999). Reliability of maintained, corrosion protected and plates subjected to non-linear corrosion and compressive loads. *Marine Structures*, **12**, pp. 425-455.
- Gurney T.R. (1978). *An analysis of some recent fatigue crack propagation data for steels subjected to pulsating tension loading*. Report 1978E, The Welding Institute TWI, UK.
- Hagen O., Sigurdsson G. (1994). Fatigue and Final Fracture: Combined Failure Modes. *Proc. 13<sup>th</sup> Offshore Mechanics and Arctic Engineering Conference*, Vol. II, pp. 161-171.
- Harlow D.G., Wei R.P. (1994). Probability Approach for Prediction of Corrosion and Corrosion Fatigue Life. *AIAA Journal*, **32**(10), pp. 2073-2079.
- Harlow D.G., Wei R.P. (1999). Probabilities of occurrence and detection of damage in airframe materials. *Fatigue and Fracture of Engineering Materials & Structures*, **22**, pp. 427-436.
- Hasofer A.M., Lind N.C. (1974). Exact and Invariant Second-Moment Code Format. *Journal of Engineering Mechanics*, ASCE, **100**, pp. 111-121.
- Hellevik S.G., Langen I., Sørensen J.D. (1999). Cost optimal reliability based inspection and replacement planning of piping subjected to CO<sub>2</sub> corrosion. *International Journal of Pressure Vessels and Piping*, **76**, pp. 527-538.
- Hirt M.A., Bez R. (1998). *Stahlbau – Grundbegriffe und Bemessungsverfahren*. Ernst & Sohn Verlag, Berlin.
- Hobbacher A. (1983). Schadenuntersuchungen zum Unglück des Halbtäuchers “Alexander L. Kielland”. *Der Maschinenschaden*, **56**(2), pp. 42-48.
- Hohenbichler M., Rackwitz R. (1981). Non-Normal Dependent Vectors in Structural Safety. *Journal of Engineering Mechanics*, **107**(6), pp.1227-1238.
- Hong H.P. (1997). Reliability analysis with nondestructive inspection. *Structural Safety*, **19**(4), pp. 383 – 395.
- Hong H.P. (1999). Inspection and maintenance planning of pipeline under external corrosion considering generation of new defects. *Structural Safety*, **21**, pp. 203-222.
- Horn D., Mayo W.R. (2000). NDE reliability gains from combining eddy-current and ultrasonic testing. *NDT & E International*, **33**, pp. 351-362.
- HSE (1998). *A Review of Fatigue Crack Growth Rates in Air and Seawater*. Offshore Technology Report, Health & Safety Executive, UK. Available online: [www.hse.gov.uk/research](http://www.hse.gov.uk/research).
- HSE (2001). *Comparison of fatigue provision in codes and standards*. Offshore Technology Report, 2001/083, Health & Safety Executive, UK, available online: [www.hse.gov.uk/research](http://www.hse.gov.uk/research).
- HSE (2002a). *Target levels for reliability-based assessment of offshore structures during design and operation*. Offshore Technology Report #60, Health & Safety Executive, UK. Available online: [www.hse.gov.uk/research](http://www.hse.gov.uk/research).
- HSE (2002b). *Validation of inspection planning methods*. Offshore Technology Report #059, Health & Safety Executive, UK. Available online: [www.hse.gov.uk/research](http://www.hse.gov.uk/research).
- IIW (1996). *Fatigue design of welded joints and components*. International Institute of Welding, Abington Publishing, Cambridge, UK.
- IMSL (1997). *Fortran Subroutines for Mathematical Applications*. Visual Numerics, [www.vni.com](http://www.vni.com).

- Irving P.E., McCartney L.N. (1977). Prediction of fatigue crack growth rates: theory, mechanisms and experimental results. *Metal Science*, pp. 351-360.
- JCSS (2001) *Probabilistic Assessment of Existing Structures*. Joint Committee on Structural Safety JCSS, published by RILEM Publications.
- JCSS (2002). *Probabilistic Model Code*. Joint Committee on Structural Safety JCSS, internet publication: [www.jcss.ethz.ch](http://www.jcss.ethz.ch).
- Kaesche H. (1990). *Die Korrosion der Metalle*. 3<sup>rd</sup> edition, Springer-Verlag.
- Kiefener J.F., Maxey W.A., Eiber R.J., Duffy A.R. (1973). Failure stress levels of flaws in pressurized cylinders. In *Progress in Flaw Growth and Fracture Toughness Testing*, ASTM STP 536. American Society for Testing and Materials, pp. 461-481.
- Kirkemo F (1990). Probabilistic strategy increases jacket in-service inspection efficiency. *Offshore*, **50**(12), pp. 46-47
- Koch G.H., Brongers M.P.H., Thompson N.G., Virmani Y.P., Payer J.H. (2001). *Corrosion Cost and Preventive Strategies in the United States*. Report FHWA-RD-01-156, Federal Highway Administration, USA. Available online: [www.corrosioncost.com](http://www.corrosioncost.com).
- Kondo Y. (1989). Prediction of Fatigue Crack Growth Initiation Life Based on Pit Growth. *Corrosion*, **45**(1), pp. 7-11.
- Koppen G. (1998). Development of Risk Based Inspection. *Proc. First International Conference on NDE in Relation to Structural Integrity for Nuclear and Pressurised Components*, Rotterdam, The Netherlands.
- Kountouris I.S., Baker M.J. (1989). *Defect Assessment. Analysis of defects detected by MPI in an Offshore Structure*. CESLIC Report #OR6, Dept. Civil Engineering, Imperial College, London.
- Kübler O., Faber M.H. (2002). Optimality and Acceptance Criteria in Offshore Design. *Proc. 21<sup>st</sup> Offshore Mechanics and Arctic Engineering Conference*, Oslo, paper S&R-28427.
- Lassen T. (1997). *Experimental Investigation and Stochastic Modelling of the Fatigue Behaviour of Welded Steel Joints*. PhD Thesis, Dept. of Building Technology and Structural Engineering, University of Aalborg, Denmark.
- Lawrence F.V., Mattos R.J., Higashidei Y., Burk J.D. (1978). Estimation of the Fatigue Crack Initiation Life of Welds. *ASTM, STP 648*, American Society for Testing and Materials, pp. 134-158.
- Laycock P.J., Cottis R.A., Scarf P.A. (1990). Extrapolation of Extreme Pit Depths in Space and Time. *Journal of the Electrochemical Society*, **137**(1), pp. 64-69.
- Lindley D.V. (1965). *Introduction to Probability and Statistics from a Bayesian Viewpoint*. Vol. 1 & 2. Cambridge University Press.
- Lotsberg I., Sigurdsson G., Wold P.T. (1999). Probabilistic Inspection Planning of the Åsgard A FPSO Hull Structure with Respect to Fatigue. *Proc. 18<sup>th</sup> Offshore Mechanics and Arctic Engineering Conference*, New Foundland, Canada, paper S&R-6040, pp. 259-266.
- Luce R.D., Raiffa H. (1957). *Games and Decisions*. John Wiley & Sons.
- Lutes L.D., Corazao M., Hu S.J., Zimmermann J. (1984). Stochastic Fatigue Damage Accumulation, *Journal of Structural Engineering*, **110**(11), pp. 2585-2601.
- Maddox S.J. (1991). *Fatigue strength of welded structures*. 2<sup>nd</sup> edition, Abington Publishing, Cambridge, UK.
- Madsen H.O. (1987). Model Updating in Reliability Theory. *Proc. ICASP5*, Vancouver, Canada, pp. 565-577.
- Madsen H.O., Krenk, S., Lind N.C. (1986). *Methods of Structural Safety*. Prentice Hall, New Jersey.
- Madsen H.O., Skjong R., Kirkemo F. (1987). Probabilistic Fatigue Analysis of Offshore Structures – Reliability Updating Through Inspection Results. in *Integrity of Offshore Structures 3*, edited by Faulkner D, Cowling MJ, Incecik A, Elsevier Applied Science.

## References

- Madsen H.O., Sørensen J.D., Olesen R. (1989). Optimal Inspection Planning for Fatigue Damage of Offshore Structures. *Proc. 5<sup>th</sup> ICOSSAR*, Vol. 3, pp. 2099-2106.
- Marley M.J., Moan T. (1992). Time variant formulation for fatigue reliability. *Proc. 11<sup>th</sup> Offshore Mechanics and Arctic Engineering Conference*, ASME, Vol. II, pp. 161-168.
- Mathisen J., Larsen K. (2002). Risk Based Inspection Planning for Mooring Chain. *Proc. 21<sup>st</sup> Offshore Mechanics and Arctic Engineering Conference*, Oslo, paper S&R-28409.
- Maxey W.A., Kiefener J.F., Eiber R.J., Duffy A.R. (1972). Ductile fracture initiation, propagation and arrest in cylindrical vessels. *Fracture toughness, Proc. National Symposium on Fracture Mechanics*, Part II, ASTM STP 536, American Society for Testing and Materials, pp. 70-81.
- McCartney L.N., Irving P.E. (1977). Comments on: "A Correlation for Fatigue Crack Growth". *Scripta Metallurgica*, **11**(3), pp. 181-183.
- Melchers R.E. (1994). *Pitting Corrosion in Marine Environments – A Review*. Research Report, Dept. of Civil Engineering, University of Newcastle, Australia.
- Melchers R.E. (1999a). Corrosion uncertainty modelling for steel structures. *Journal of Constructional Steel Research*, **52**, pp. 3-19.
- Melchers R.E. (1999b). *Structural Reliability Analysis and Prediction*. Second edition, John Wiley & Sons.
- Melchers R.E. (2003a). Modeling of Marine Immersion Corrosion for Mild and Low-Alloy Steels – Part 1: Phenomenological Model. *Corrosion*, **59**(4), pp. 319-334.
- Melchers R.E. (2003b). Modeling of Marine Immersion Corrosion for Mild and Low-Alloy Steels – Part 2: Uncertainty Estimation. *Corrosion*, **59**(4), pp. 335-344.
- Miner M.A. (1945). Cumulative Damage in Fatigue. *Journal of Applied Mechanics*, ASME, **12**, pp. A159-A164.
- Moan T., Song R. (1998). Implication of Inspection Updating on System Fatigue Reliability of Offshore Structures. *Proc. 17<sup>th</sup> Offshore Mechanics and Arctic Engineering Conference*, paper S&R-1214.
- Moan T., Vårdal O.T. (2001). Probabilistic assessment of fatigue reliability of existing offshore platforms. *Proc. ICOSSAR 2001*, Newport Beach, California.
- Moan T., Vårdal O.T., Hellevig N.C., Skjoldli K. (2000a). Initial Crack Depth and POD Values Inferred From In-Service Observations of Cracks in North Sea Jackets. *Journal of Offshore Mechanics and Arctic Engineering*, **122**, pp. 157 - 162.
- Moan T., Vårdal O.T., Johannesen J.M. (2000b). Probabilistic inspection planning of fixed offshore structures. *Proc. ICASP8*, Sydney, pp. 191-200.
- Nathwani J.S., Lind N.C., Pandey M.D. (1997). *Affordable Safety by Choice: The Life Quality Method*. Institute for Risk Research, University of Waterloo, Canada.
- Newman J.C. (1998). The merging of fatigue and fracture mechanics concepts: a historical perspective. *Progress in Aerospace Science*, **34**, pp.347-39.
- Newman J.C., Raju I.S. (1981). An empirical stress intensity factor equation for surface cracks. *Engineering Fracture Mechanics*, **15**, pp. 185-192.
- NORSOK (1998). *Design of Steel Structures*. Standard N-004, Revision 1, available online: [www.nts.no/norsok](http://www.nts.no/norsok).
- Palmgren A. (1924). Die Lebensdauer von Kugellagern. *Zeitschrift des Vereins deutscher Ingenieure*, **68**(14), pp.339-341.
- Paris P., Erdogan F. (1963). A Critical Analysis of Crack Propagation Laws. *Journal of Basic Engineering*, **85**, pp. 528-534.
- Paté-Cornell E. (1994). Quantitative safety goals for risk management of industrial facilities. *Structural Safety* **13**, pp. 145-157.

- PD 6493 (1991). *Guidance on methods for assessing the acceptability of flaws in fusion welded structures*. British Standards.
- Pedersen C., Nielsen J.A., Riber J.P., Madsen H.O., Krenk S. (1992). Reliability Based Inspection Planning for the Tyra Field. *Proc. 11<sup>th</sup> Offshore Mechanics and Arctic Engineering Conference*, Vol. 2, pp. 255-263.
- Phillips E.P., Newman J.C. (1989). Impact of Small-crack Effects on Design-life Calculations. *Experimental Mechanics*, **29**(2), pp. 221-225.
- Press W.H., Flannery B.P., Teukolsky S.A., Vetterling W.T. (1989). *Numerical recipes – Fortran version*. Cambridge University Press.
- Pugsley A.G. (1942). *A philosophy of aeroplane strength factors*. Reports and Memoranda no. 1906, Aeronautical Research Council, London.
- RACH (1999). *Reliability Assessment for Containers of Hazardous materials on offshore structures - Final Report*. Available from TSC Inspection Systems, www.tscinspectionssystem.com.
- Rackwitz R (2000). Optimization – the basis for code-making and reliability verification. *Structural Safety* **22**, pp. 27-60.
- Rackwitz R. (2002). Optimization and risk acceptability based on the Life Quality Index. *Structural Safety*, **24**, pp.297-331.
- Radaj D. (1995). *Ermüdungsfestigkeit*. Springer-Verlag, Berlin.
- Radaj D., Sonsino C.M. (2000). *Ermüdungsfestigkeit von Schweißverbindungen nach lokalen Konzepten*. DVS-Verlag, Düsseldorf.
- Raiffa H., Schlaifer R. (1961). *Applied Statistical Decision Theory*. Cambridge University Press, Cambridge, Mass.
- Roberge P.R. (1999). *Handbook of Corrosion Engineering*. McGraw-Hill.
- Roberge P.R., Klassen R.D., Haberecht P.W. (2002). Atmospheric corrosivity modeling – a review. *Materials and Design*, **23**, pp.321-330.
- Rosenblueth E., Mendoza E. (1971). Reliability Optimization in Isostatic Structures. *Journal of the Engineering Mechanics Division*, ASCE, **97**(6), pp. 1625-1642.
- Rouhan A., Goyet J., Faber M.H. (2004). Industrial Implementation of Risk Based Inspection Planning Methods – Lessons Learnt from Experience: The Case of Fixed Steel Structures. *Proc. 23<sup>th</sup> Offshore Mechanics and Arctic Engineering Conference*, Vancouver.
- Rouhan A., Schoefs F. (2003). Probabilistic modeling of inspection results for offshore structures. *Structural Safety*, **25**, pp. 379-399.
- Rudlin J.R., Dover W.D. (1996). The ICON Project – Data for Underwater Inspection. *Insight*, **38**(6), pp. 412 – 414.
- Rudlin J.R., Wolfenstein L.C. (1992). Development of Statistical Probability of Detection Models Using Actual Trial Inspection Data. *British Journal of Non-Destructive Testing*, **34**( 12), pp. 583-589.
- Ryan M.P., Williams D.E., Chater R.J., Huton B.M., McPhail D.S. (2002). Why stainless steel corrodes. *Nature*, **415**, pp. 770-774.
- Savage L.J. (1972). *The Foundations of Statistics*. 2<sup>nd</sup> revised edition, Dover publications.
- Scarf P.A., Cottis R.A., Laycock P.J. (1992). Extrapolation of Extreme pit Depths in space and Time Using the *r* Deepest Pit Depths. *Journal of the Electrochemical Society*, **139**(9), pp. 2621-2627.
- Schall G., Faber M.H., Rackwitz R. (1991). The Ergodicity Assumption for Sea States in the Reliability Estimation of Offshore Structures. *Journal of Offshore Mechanics and Arctic Engineering*, ASME, **113**, pp.241-246.

## References

- Schijve J. (1979). Four Lectures on Fatigue Crack Growth. *Engineering Fracture Mechanics*, **11**, pp. 167 – 221.
- Schijve J. (1994). Fatigue Predictions and Scatter. *Fatigue and Fracture of Engineering Materials & Structures*, **17**(4), pp. 381-396.
- Schindler H.J. (2002). *Grundlagen der technischen Bruchmechanik*. Lecture Notes, Institute of Mechanics, ETH Zürich.
- Schütz W. (1979). The Prediction of Fatigue Life in the Crack Initiation and Propagation Stages – A State of the Art Survey. *Engineering Fracture Mechanics*, **11**, pp. 405-421.
- Sharp J.V., Billingham J., Robinson M.J. (2001). The risk management of high-strength steels in jack-ups in seawater. *Marine Structures*, **14**, pp. 537-551.
- Shi P., Mahadevan S. (2003). Corrosion fatigue and multiple site damage reliability analysis. *International Journal of Fatigue*, **25**, pp. 457-469.
- Shibata T. (1996). Statistical and Stochastic Approaches to Localized Corrosion. *Corrosion*, **52**(11), pp. 813-830.
- Shooman ML (1968). *Probabilistic Reliability: An Engineering Approach*. McGraw-Hill, New York.
- SIA 161 (1990). *Stahlbauten*. Norm SIA 161, Schweizerischer Ingenieur- und Architektenverein, Zürich.
- Sigurdsson G., Torhaug R. (1993). Discussion of the Fatigue Crack Growth Model Used as a Decision Basis for Probabilistic Inspection Planning. *Proc. 12<sup>th</sup> Offshore Mechanics and Arctic Engineering Conference*, Vol. 2, pp. 79-87.
- Sindel R, Rackwitz R (1996). *Calculation of the Failure Probability and Inspection Optimization for Cracks in Ships*. Technische Universität München, Institut für Tragwerksbau.
- Singh R., Koenke C. (2000). Simulation framework for risk assessment of damage tolerant structures. *Computer & Structures*, **77**, pp. 101-115.
- Skjong R. (1985). Reliability Based Optimization of Inspection Strategies. *Proc. ICOSSAR 85*, Vol. III, Kobe, Japan, pp. 614-618.
- Skjong R., Gregersen E.B., Cramer E., et al. (1995). *Guideline for Offshore Structural Reliability Analysis*. Det Norske Veritas, Report #95-2018.
- Slovic P. (2000). *The Perception of Risk*. Earthscan Publications.
- Smith I.J., Hurworth S.J. (1984). *The effect of geometry changes upon the predicted fatigue strength of welded joints*. Welding Institute Report # 244, Cambridge, UK.
- Sørensen J.D., Faber M.H., Kroon I.B. (1995). Optimal Reliability-Based Planning of Experiments for POD curves. *Proc. 5<sup>th</sup> International Offshore and Polar Engineering Conference*, Vol. IV, Den Haag, pp. 339-345.
- Sorensen J.D., Faber M.H., Rackwitz R., Thoft-Christensen P., Lebas G. (1992). Reliability Analysis of an Offshore Structure: A Case Study - II. *Proc. 11th Offshore Mechanics and Arctic Engineering Conference, Vol. II*, Calgary, pp. 457-463.
- Sørensen J.D., Faber M.H., Rackwitz R., Thoft-Christensen P.T. (1991). Modelling in Optimal Inspection and Repair. *Proc. 10<sup>th</sup> Offshore Mechanics and Arctic Engineering Conference*, Stavanger, Norway, pp. 281-288.
- SSC (1996). *Probability Based Ship Design: Implementation of Design Guidelines*. Ship Structure Committee, Report #392.
- Stadelmann M. (2003). *Katalogisierung der Einflussparameter bei der Ermüdung von Eisenbahnbrücken*. Diploma Thesis, Institute of Structural Engineering IBK, ETH Zürich.
- Stephens R.I., Fatemi A., Stephens R.R., Fuchs H.O. (2001). *Metal Fatigue in Engineering*. 2<sup>nd</sup> edition, John Wiley and Sons.

- Stewart G., Klever F.J., Ritchie D. (1994). An Analytical Model to Predict the Burst Capacity of Pipelines. *Proc. 13<sup>th</sup> Offshore Mechanics and Arctic Engineering Conference*, Houston, Vol. 5, pp. 177-188.
- Straub D. (2001). *Detailed Risk Based Inspection Planning for FPSO Components Subject to Fatigue*. Bureau Veritas, Technical Note #2682, ATA 818A.
- Straub D. (2002). Probabilistic Modeling of Non-Destructive Testing of Steel Structures. *Proc. 4th International Ph.D. Symposium in Civil Engineering*, Munich, Vol.2, pp. 311-320.
- Straub D. (2003). Accounting for Dependencies in Inspection Planning for Steel Structures. *Proc. Workshop on Risk-Based Maintenance*, TU Delft,
- Straub D., Faber M.H. (2000). Generic Risk Based Inspection Planning for Components Subject to Corrosion. *Proc. ESRA Workshop on Risk Based Inspection Planning*, Zürich, pp. 129-138.
- Straub D., Faber M.H. (2002a). On the Relation between Inspection Quality and Quantity. *Proc. European-American Workshop on Reliability of NDE*, Berlin.
- Straub D., Faber M.H. (2002b). System Effects in Generic Risk Based Inspection Planning. Accepted for publication in *Journal of Offshore Mechanics and Arctic Engineering*, *Trans. ASME*. Presented at the 21<sup>st</sup> *Offshore Mechanics and Arctic Engineering Conference*, Oslo, 2002.
- Straub D., Faber M.H. (2003a). Modeling Dependency in Inspection Performance. *Applications of Statistics and Probability in Civil Engineering*, Der Kiureghian, Madanat & Pestana (eds), Millpress, pp. 1123 - 1130.
- Straub D., Faber M.H. (2003b). Risk Based Acceptance Criteria for Joints Subject to Fatigue Deterioration. *Proc. 22<sup>nd</sup> Offshore Mechanics and Arctic Engineering Conference*, Cancun, Mexico, paper #37224.
- Streicher H., Rackwitz R. (2003). Objective functions for reliability-oriented structural optimization. *Proc. Workshop on Reliability-based Optimization*, Warsaw.
- Struel (1999). *Structural reliability analysis program system, Comrel 7.0 & Sysrel 9.6*. RCP Consulting, Munich.
- Strutt J.E. (1998). *Development of Probabilistic Corrosion Risk Analysis Techniques for Offshore Pipelines and Risers*. Centre of Industrial Safety and Reliability, Cranfield University, UK.
- Sydberger T., Edwards J.D., Mørk KJ (1995). A Probabilistic Approach to Prediction of CO<sub>2</sub>-Corrosion and its Application to Life Cycle Cost Analysis of Oil and Gas Equipment. *Proc. Corrosion95*, NACE, paper #65.
- Tait N.R.S. (1993). The use of probability in engineering design – an historical survey. *Reliability Engineering and System Safety*, **40**, pp.119-132.
- Tang W.H. (1973). Probabilistic Updating of Flaw Information. *Journal of Testing and Evaluation*, **1**(6), pp. 459-467.
- Thoft-Christensen P., Sørensen J.D. (1987). Optimal strategy for inspection and repair of structural systems. *Civil Engineering Systems*, **4**, pp. 94-100.
- Turnbull A. (1993). Review of Modelling of Pit Propagation Kinetics. *British Corrosion Journal*, **28**(4), pp. 297-308.
- Uhlig H.H. (1949). The Cost of Corrosion to the US. *Chemical and Engineering News*, **27**(39), pp. 2764-2767.
- Van Wingerde A.M., Packer J.A., Wardenier J. (1995). Criteria for the Fatigue Assessment of Hollow Structural Section Connections. *Journal of Constructional Steel Research*, **35**, pp. 71-115.
- Vinnem J.E. (1998). Evaluation of methodology for QRA in offshore operations. *Reliability Engineering and System Safety*, **61**(1), pp. 39 – 52.
- Von Neumann J., Morgenstern O. (1947). *Theory of games and economical behaviour*. 2<sup>nd</sup> edition, Princeton University Press.
- Vrouwenvelder A.C.W.M. (2002). Developments towards full probabilistic design codes. *Structural Safety*, **24**, pp. 417-432.

## References

- Vrouwenvelder A.C.W.M. (2004). Spatial correlation aspects in deterioration models. *Proceedings, 2<sup>nd</sup> International Conference on Lifetime-Oriented Design Concepts*, Bochum, Germany.
- Waarts P.H., Vrouwenvelder A.C.W.M. (1992). *Traffic Loads on Bridges*. TNO report B-92-011, Delft, The Netherlands.
- Wall M., Wedgwood F.A. (1994). NDT – Value for Money. *Insight*, **36**( 10), pp. 782-790.
- Wall M., Wedgwood F.A. (1998). Economic Assessment of Inspection – the Inspection Value Method. *e-Journal of Nondestructive Testing*, **3**(12), available online: [www.ndt.net/journal/archive.htm](http://www.ndt.net/journal/archive.htm).
- Walter G.W. (1986). A Critical Review of the Protection of Metals by Paints. *Corrosion Science*, **26**(1), pp. 27-38.
- Winterstein S.R. (1984). Non-Normal Responses and Fatigue Damage. *Journal of Engineering Mechanics*, ASCE, **111**(10), pp. 1291-1295.
- Winterstein S.R., Lange C.H. (1996). Load Models for Fatigue Reliability From Limited Data. *Journal of Solar Energy Engineering*, ASME, **118**, pp. 64-68.
- Winterstein S.R., Veers P.S. (2000). *A Numerical Analysis of the Fatigue and Reliability of Wind Turbine Components*. Sandia National Laboratories, Report #SAND94-2459.
- Wirsching P.H. (1984). Fatigue Reliability for Offshore Structures. *Journal of Structural Engineering*, ASCE, **110**(10), pp. 2340-2356.
- Wirsching P.H., Chen Y.N. (1988). Probability-based design for marine structures. *Marine Structures*, **1**(1), pp. 23-45.
- Wirsching P.H., Light M.C. (1980). Fatigue under Wide Band Random Stresses. *Journal of the Structural Division*, ASCE, **106**(7), pp. 1593-1607.
- Yamamoto N., Ikegami K. (1996). A Study on the Degradation of Coating and Corrosion of Ship's Hull Based on the Probabilistic Approach. *Proc. 15<sup>th</sup> Offshore Mechanics and Arctic Engineering Conference*, Vol. 2, pp. 159-166.
- Yang J.N. (1994). Application of reliability methods to fatigue, quality assurance and maintenance. *Proc. 6th ICOSSAR*, Vol. 1, pp. 3 – 20.
- Yang J.N., Donath R.C. (1983). Improving NDE reliability through multiple inspections. *Review of Progress in Quantitative NDE*, **1**, pp. 69-78.
- Yang J.N., Trapp W.J. (1974). Reliability Analysis of Aircraft Structures under Random Loading and Periodic Inspection. *AIAA Journal*, **12**(12), pp. 1623-1630.
- Yang J.N., Trapp W.J. (1975). Inspection frequency optimization for aircraft structures based on reliability analysis. *Journal of Aircraft*, AIAA, **12**(5), pp. 494-496.
- Zhang R., Mahadevan S. (2001). Fatigue Reliability Analysis Using Nondestructive Inspection. *Journal of Structural Engineering*, **127**(8), pp. 957 – 965.
- Zhang R., Mahadevan S. (2001). Reliability-based reassessment of corrosion fatigue life. *Structural Safety*, **23**, pp. 77-91.
- Zhao W., Stacey A. (2002). Review of Defect Distributions for Probabilistic Structural Integrity Assessment. *Proc. 21<sup>st</sup> Offshore Mechanics and Arctic Engineering Conference*, Oslo, paper S&R-28616.
- Zhao Z., Haldar A. (1996). Bridge fatigue damage evaluation and updating using non-destructive inspections. *Engineering Fracture Mechanics*, **53**(5), pp. 775-788.



# Curriculum Vitae

Daniel Straub

born 30 November 1975 in Schlieren (Switzerland)

citizen of Switzerland

## Education

1995	Matura Kantonschule Zürich-Oerlikon
1995-2000	Diploma in Civil Engineering Swiss Federal Institute of Technology, ETH Zürich
since 2000	PhD studies Swiss Federal Institute of Technology, ETH Zürich

## Professional activities

since 2000	Research and teaching assistant with Prof. Faber Institute of Structural Engineering, ETH Zürich
2001	Research and development activities related to the PhD project Bureau Veritas, Paris
since 2002	Involvement in several industrial projects related to the PhD research